UNIVERSITY OF CALIFORNIA

Santa Barbara

Novel Conjugation Strategies Using the Diels–Alder Reaction

A dissertation submitted in partial satisfaction of the

requirements for the degree Doctor of Philosophy in Chemistry

by

Andre Henri St. Amant

Committee in charge:

Professor Javier Read de Alaniz, Chair

Professor Gabriel Ménard

Professor R. Daniel Little

Professor Armen Zakarian

December 2018

The dissertation of Andre Henri St. Amant is approved.

_____

Gabriel Ménard

_____

R. Daniel Little

_____

Armen Zakarian

_____

Javier Read de Alaniz, Committee Chair

December 2018

Novel Conjugation Strategies Using the Diels–Alder Reaction

by

Andre Henri St. Amant

ACKNOWLEDGEMENTS

The last 5 years have been some of the best of my life. There are so many people that have helped me along the way, it's hard to know where to begin!

Let me start before my PhD. My entire chemistry career started with Dr. Robert H.E. Hudson encouraging me to apply to a summer program in his lab. Through his help (and David W Dodd, Filip Wojciechowski, Mojmír Suchý) I learned the basics of organic chemistry, they got me excited about it as a career, and I thank them for that. This is also where I began my streak of picking amazing PIs. The second PI I'd like to thank is Leonard G. Luyt for hiring me after my MSc and being supportive of my choice to leave for a PhD.

Thank you to all of the chemists from my year – it was great making so many new friends when I moved here. I'll never forget sitting around grading (playing cookie clicker), trivia (Will and Alisa), and many pint nights.

I have to thank all of the people of Javier's lab (and the Hawker/Liming/Zakarian labs and others). Emre, Ngan (Shay), and Shelby – you are so talented, it's been a pleasure working with all of you and being your friend. D Fish – late nights dancing at the hood with you are some of my best memories. My officemates Clarky-fresh, Jaaaamie, Meggo, Seven and so many more that I don't have the space to list (you know who you are!).

I would like to thank both the government of California and the United States for funding international students like me. Also a huge thank you to NSERC and my own government of Canada for funding me – allowing me to spend more time in the lab, and less time grading! Lastly thanks to R. James (Jim) Christie and MedImmune for funding the ADC project in my 3rd year – that began my love for the Diels–Alder reaction!

Sometimes, in our academic bubble, we forget that chemists are just a small part of the world. There is so much support staff has been essential to this achievement: the

administrative staff, technical staff, facilities, shipping/receiving, the custodians and grounds staff that make this campus so beautiful, and the people at Subway and Yoshinoya. I'd also like to thank the content creators that kept me sane: Josh and Chuck (SYSK), my local NPR station KCLU, Brandon Sanderson, and George RR Martin.

I'd like to thank all of my friends back in Canada. Leaving my you for 5 years was tough, but it was made easier knowing that you're my friends for life. Thanks for all the memes. Thank you Shunyao, you've made the last year of my PhD the best one!

I'd now like to thank the third amazing PI I've worked for – Javier Read de Alaniz. You've been supportive of me through the good times and the bad. Thanks to you, I've grown so much these last 5 years as a scientist and as a person. You're a great mentor and friend – your lab will be a hard one to follow.

Most of all I'd like to thank my family. You have been so supportive of me and I treasure trips home to see you all. Thank you to Sparky and Charlie for being good bois. My dear sister Danielle, who has been excited and supportive of me to move to faaabulous California! I love our phone chats, it always makes me feel better when I'm stressed. And most of all, mom and dad. I don't think anybody could ask for a better upbringing than the one you provided. I was always encouraged to follow my passion and I felt secure knowing that you would support me unconditionally. Dad, you've always been there for me with great advice. Mom, you've said that you're proud of me – we both know that your support helped me through this.

I'm so thankful for everyone that has helped me along the way. I hope to continue to grow as a scientist and that my research will make the world a better place for everybody.

VITA OF ANDRE HENRI ST. AMANT

September 2018

EDUCATION

Honors Bachelor of Science in Chemistry and Biochemistry, The University of Western Ontario, August 2009
Master of Science in Chemistry, The University of Western Ontario, August 2011
Doctor of Philosophy in Chemistry, University of California, Santa Barbara, December 2018 (expected)

PROFESSIONAL EMPLOYMENT

2011-13: Laboratory Manager, London Regional Cancer Program

PUBLICATIONS

St. Amant, A. H. and Hudson, R. H. E. (2012). "Synthesis and Oligomerization of Fmoc/Boc-Protected PNA Monomers of 2,6-Diaminopurine, 2-Aminopurine and Thymine." Organic and Biomolecular Chemistry 10(4): 876.

St. Amant, A. H., Bean, L. A., Hudson, R. H. E. (2012). "Click fleximers: a modular approach to purine base-expanded ribonucleoside analogues." Organic & Biomolecular Chemistry 10(32): 6521.

St. Amant, A. H., Engbers, C., Hudson, R. H. E. (2013). "A Solid-Phase CuAAC Strategy for the Synthesis of PNA Containing Nucleobase Surrogates." Artificial DNA: PNA & XNA 4(1): 4.

Azad, B. B., Rota, V., Yu, L., McGirr, R., St. Amant, A. H., Lee, T. Y., Dhanvantari, S., Luyt, L. G. (2015). “Synthesis and Evaluation of Optical and PET GLP-1 Peptide Analogues for GLP-1R Imaging.” Molecular Imaging 14: 1.

Veits, G. K., Wenz, D. R., Palmer, L. I., St. Amant, A. H., Hein, J. E., Read de Alaniz, J. (2015). “Cascade rearrangement of furylcarbinols with hydroxylamines: practical access to densely functionalized cyclopentane derivatives.” Organic and Biomolecular Chemistry 13(31): 8465.

Gavin, C. T., Ali, S. N., Tailly, T., Olvera-Posada, D., Alenezi, H., Power, N. E., Hou, J. Q., St. Amant, A. H., Luyt, L. G., Wood, S., Wu, C., Razvi, H., Leong, H. S. (2016). “Alternative Methods in Determining Calculi Composition: Petrographic Thin Sectioning of Calculi and Nanoscale Flow Cytometry Urinalysis.” Scientific Reports 6: 19328.

St. Amant, A. H., Frazier, C. P., Newmeyer, B., Fruehauf, K. R., Read de Alaniz, J. (2016). "Direct synthesis of anilines and nitrosobenzenes from phenols." Organic and Biomolecular Chemistry 14(24): 5520.

Discekici, E. H.,* St. Amant, A. H.,* Nguyen, N., Lee, I. H., Hawker, C. J., Read de Alaniz, J. (2018). "Endo and Exo Diels–Alder Adducts: Temperature Tunable Building Blocks for Efficient Polymer Modification." Journal of the American Chemical Society 140(15): 5009.

St. Amant, A. H., Lemen, D., Florinas, S., Mao, S., Fazenbaker, C., Zhong, H., Wu, H., Gao, C., Christie, R. J., Read de Alaniz, J. (2018). "Tuning the Diels–Alder Reaction for Bioconjugation to Maleimide Drug-Linkers." Bioconjugate Chemistry 29(7): 2406.

Ali, S. N., Dayarathna, T. K., Ali, A. N., Osumah, T., Ahmed, M., Cooper, T. T., Power, N. E., Zhang, D, Kim, D., Kim, R., St. Amant, A., Hou, J., Tailly, T., Yang, J., Luyt, L., Spagnuolo, P. A., Burton, J. P., Razvi H., Leong, H. S. (2018). "Drosophila melanogaster as a function-based high-throughput screening model for anti-nephrolithiasis agents in kidney stone patients" Disease Models & Mechanisms, Accepted.

"Building the Next Generation "Click" Chemistry for Functional Polymer Synthesis Using a Masked Cyclopentadiene" in progress.

"A Reactive Antibody Platform Enables One-Step Conjugation Through a Diels–Alder Reaction with Maleimide" in progress.

"A Cyclic Diene Non-Canonical Amino Acid Enables Homogenous and Heterogeneous Diels-Alder Reactions Following Incorporation into Antibodies" in progress.

AWARDS

Undergraduate Student Research Award (USRA), 2007 & 2008

Dean's Honor Roll, 2005-06 & 2008-09

Phi Lambda Upsilon Award, 2013-14

Robert H. DeWolfe Teaching Fellowship in Organic Chemistry, 2016-17

Postgraduate Scholarships-Doctoral (PGS D), 2015-17

FIELDS OF STUDY

Major Field: Organic Chemistry with Professor Javier Read de Alaniz

Studies in Organic Chemistry with Professor Robert H. E. Hudson

ABSTRACT

Novel Conjugation Strategies Using the Diels–Alder Reaction

by

Andre Henri St. Amant

The development of new functional materials requires reliable conjugation chemistry for coupling molecular fragments under mild reaction conditions. The Diels–Alder (DA) reaction has been used in organic synthesis extensively over the past 90 years, but only recently has its ability to form fast and stable linkages been explored. New developments in small molecule DA reactivity have led to advances in protecting group chemistry and conjugation strategies. During my graduate studies, we developed novel diene-linkers, attached them onto antibodies, and conjugated maleimide-drugs to form DA antibody–drug conjugates. While exploring these adducts, we were able to exploit the lower retro-DA temperature of *endo* furan–maleimide adducts towards a new protecting group for maleimides in polymer synthesis. We also developed norbornadiene-containing polymers as a new "protected" form of cyclopentadiene that can be unmasked at room temperature with readily available reagents. These three conjugation strategies have enabled facile preparation of functional materials with more stable bonds and greater architectural complexity.

TABLE OF CONTENTS

LIST OF FIGURES

ABBREVIATIONS

ADC	Antibody–Drug Conjugate
ATRP	Atom transfer radical polymerization
BnMA	Benzyl methacrylate
CHO	Chinese hamster ovary
Cp	Cyclopentadiene
DA	Diels–Alder
DA-ADC	Diels–Alder Antibody–Drug Conjugate
DAR	Drug-antibody ratio
DCM	Dichloromethane
DEAD	Diethyl azodicarboxylate
DMAD	Dimethyl acetylenedicarboxylate
DMP	Dess–Martin periodinane
DMSO	Dimethyl sulfoxide
DpTz	Dipyridyltetrazine
HOMO	Highest occupied molecular orbital
IEDDA	Inverse electron-demand Diels–Alder
LAH	Lithium aluminum hydride
LAR	Linker-antibody ratio
LUMO	Lowest unoccupied molecular orbital
MMA	Methyl methacrylate
NBD	Norbornadiene
OM	Omacetaxine mepesuccinate
PEG	Poly(ethyleneglycol)
PIDA	Phenyliodine(III) diacetate
PLA	Polylactic acid
PMMA	Poly(methyl methacrylate)
PnBMA	Poly(n-butyl methacrylate)
PyrM	N-(1-pyrenyl)maleimide
RAFT	Reversible addition−fragmentation chain-transfer
rDA	Retro Diels–Alder
ROMP	Ring-opening metathesis polymerisation
ROMP	Ring opening metathesis polymerization
SAR	Structure activity relationship
SAXS	Small-angle x-ray scattering
SMCC	Succinimidyl-4-(N-maleimidomethyl)cyclohexane-1-carboxylate
THF	Tetrahydrofuran

1 Introduction

1.1 Synthetic Organic Chemistry

Chemistry is sometimes called the "central science" in the physical sciences, as it connects and overlaps with both physics and biology. Within chemistry, the subdiscipline organic chemistry has had arguably the greatest impact (both positive and negative) on humanity. Organic chemistry as a general field is the study of the structure, properties, and reactivity of molecules containing carbon – an element essential to life.

Although an oversimplification, synthetic organic chemists can be divided into three general subdisciplines: total synthesis/medicinal chemistry, methods development, and materials chemistry. Total synthesis chemists develop synthetic pathways to molecules often produced by Nature and their derivatives to enable access to quantities not easily accessible from Nature, allowing for the study of their biological properties. Medicinal chemists synthesize focused libraries to improve the properties of biologically active compounds. Methods researchers develop new chemical reactions to improve the synthesis of target compounds. Materials chemists apply synthetic organic chemistry to develop polymers, plastics, and other materials with specific desired properties. These subdisciplines have one thing in common – the knowledge and application of chemical reactions can be used to produce value-added molecules from simpler starting materials.

1.2 Click Chemistry

The development of new functional materials requires reliable conjugation chemistry for coupling molecular fragments under mild reaction conditions. These highly efficient reactions are often grouped under the general umbrella of "click chemistry", a term first coined by

Sharpless; some of the criteria necessary to be considered a "click reaction" are: use of readily available starting materials, modularity, functional group tolerance, react in near quantitative yield, and use of simple reaction conditions.[1]

1.3 The Azide–Alkyne Cycloaddition

The criteria for a reaction to be "click" are subjective, but there are several reactions that fit the broad definition associated with "click" reactions, with the quintessential example being Sharpless' copper-catalyzed azide–alkyne cycloaddition (CuAAC, **Figure 1.1**).

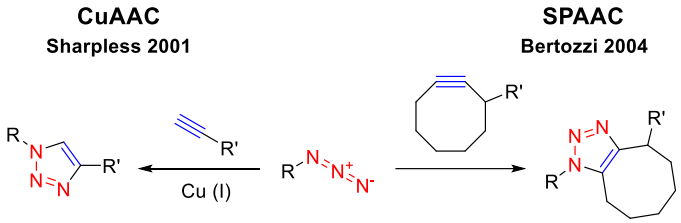

Figure 1.1 The copper-catalyzed and strain-promoted azide–alkyne cycloadditions.

The thermal 1,3-dipolar cycloaddition between azides and alkyne was studied by Huisgen,[2,3] but it wasn't considered a "click reaction" until the Cu(I)-catalyzed variant was disclosed by Sharpless.[1] The CuAAC reaction rate is greatly accelerated, ~200 $M^{-1}s^{-1}$, and has been an indispensable tool for conjugation chemistry. We have used the CuAAC reaction in the synthesis of "click fleximers"[4] and conjugation of fluorophores to peptide nucleic acid.[5]

Despite the advantages of this reaction (fast rates, simple starting materials) there are several undesirable properties – its dependence on toxic/explosive azides, and the toxic copper catalyst.[6] To avoid the copper toxicity and allow for this reaction, a strain-promoted azide-alkyne cycloaddition (SPAAC) was developed by Bertozzi.[7] This allowed the conjugation to be performed within a living cell, a class of reactions that are bioorthogonal.[8] The SPAAC reaction has been utilized in conjugations to avoid copper, but it still relies on azides. Overall, the reaction rate is slower (~1 $M^{-1}s^{-1}$) than the CuAAC reaction. In addition, the cyclooctynes

are large and challenging to synthesize. Given these drawbacks, several new metal-free "click reactions" have been developed, including the inverse-electron demand Diels–Alder (IEDDA) reaction.

1.4 The Inverse-Electron Demand Diels–Alder Reaction

The Diels–Alder (DA) reaction, a [4+2] cycloaddition between a diene and a dienophile, was first disclosed 90 years ago by Otto Diels and Kurt Alder.[9] The IEDDA reaction, where the reaction partners are an electron-poor diene (such as 1,2,4,5-tetrazine) and an electron-rich dienophile, was later developed.[10,11] The IEDDA reaction fulfills many of the criteria of "click" reactions. Recently, the Fox group has developed a new conjugation approach based on the IEDDA reaction using trans-cyclooctenes as powerful diene reaction partners that react with tetrazines at extremely fast rates (up to 22,000 $M^{-1}s^{-1}$, **Figure 1.2**).[12]

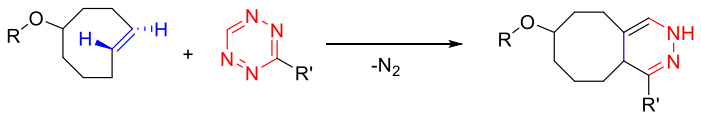

Figure 1.2 The inverse-electron demand Diels–Alder reaction.

Given the metal-free reaction conditions, compatibility with biological processes, and rapid rates, the IEDDA reaction is considered the gold standard of bioorthogonal chemistry.[13] Due to these favourable properties, several groups have genetically incorporated IEDDA reaction partners to synthesize protein adducts.[14–16] While the IEDDA reaction has several advantages over other conjugation reactions, there are few commercially available tetrazines/dienophiles, the reaction partners are large and hydrophobic, and the synthesis can be challenging.[17] As such, there is a need to develop new conjugation chemistry that is metal-free and takes advantage of simple, commercially available reaction partners.

1.5 The Normal-Electron Demand Diels–Alder Reaction

The normal-electron DA reaction is a pericyclic reaction that occurs in one cyclic transition state and relies on orbital symmetry. The highest occupied molecular orbital (HOMO) of an electron-rich diene will react with the lowest unoccupied molecular orbital (LUMO) of an electron-deficient dienophile (**Figure 1.3**). By increasing the interaction between these orbitals, such as by raising the HOMO with electron-density or lowering the LUMO with a Lewis acid,[18] the reaction kinetics can be improved.

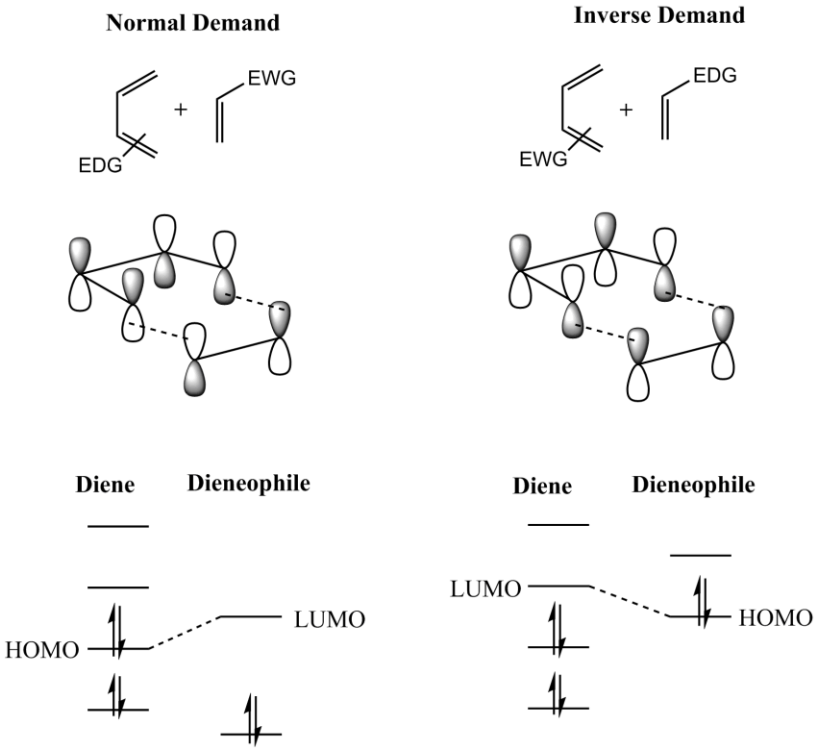

Figure 1.3 Frontier-molecular orbital diagram of the DA and IEDDA reactions. Image by Chrito23 is licensed under CC-BY-SA-3.0.

The normal-electron demand DA reaction has been used in organic synthesis extensively over the past 90 years, but only recently has its ability to form fast and stable linkages for bioconjugation been explored. Compared to the IEDDA reaction, conjugation using the DA reaction has several challenges. Firstly, the DA reaction is not bioothogonal – it requires electron-poor dienophiles that can also react with nucleophiles through the Michael reaction

within cells. Secondly, the rates are much slower than the IEDDA.[13] Finally, the use of electron-rich dienes required for fast kinetics suffer from potential side reactions that arise due to their high reactivity.[19]

Despite these potential challenges with the normal demand DA reaction, we hypothesized that synthetic modifications to the electron-rich dienes could be used to control their reactivity and enable them to be used in new conjugation strategies. The successful realization of this goal would also enable the use of electron-rich dienes in material science which could streamline the synthesis of functional polymer materials.

1.6 Thesis Outline

Given our long-standing interest in the development of practical, user friendly transformations for small molecule synthesis and polymer functionalization, we sought to explore the use of the cycloaddition reaction with maleimide and electron-rich dienes as a new platform for conjugation in biological and material applications.

In this context, this dissertation focuses on a range of synthetic organic chemistry projects that draws inspiration from small molecule reaction development, targeted drug therapy, and materials. By exploiting reactivity disclosed in small molecule chemistry, and applying it to bioconjugation, we were able to develop Diels–Alder antibody–drug conjugates which is described in **Chapter 2**. While attempting a new bioconjugation, we uncovered an interesting kinetic property of the retro-Diels–Alder, and exploited this reactivity to produce temperature-controlled polymer architectures, **Chapter 3**. Building on our work with electron-rich dienes and maleimides, we employed a new strategy using a "protected" form of cyclopentadiene to produce complex polymer conjugates, **Chapter 4**. Continuing with the theme of developing practical and user-friendly reaction conditions, we also developed a new methodology to

produce anilines from phenols (a feedstock chemical), **Chapter 5**. Finally, **Chapter 6** of this dissertation focuses on our efforts towards a synthesis of desmethoxy cephalotaxine.

1.7 References

(1) Kolb, H. C.; Finn, M. G.; Sharpless, K. B. Click Chemistry: Diverse Chemical Function from a Few Good Reactions. *Angew. Chemie Int. Ed.* **2001**, *40* (11), 2004–2021.

(2) Michael, A. Ueber Die Einwirkung von Diazobenzolimid Auf Acetylendicarbonsäuremethylester. *J. für Prakt. Chemie* **1893**, *48* (1), 94–95.

(3) Huisgen, R. Proceedings of the Chemical Society. October 1961. *Proc. Chem. Soc.* **1961**, No. October, 357–396.

(4) St. Amant, A. H.; Bean, L. A.; Guthrie, J. P.; Hudson, R. H. E. Click Fleximers: A Modular Approach to Purine Base-Expanded Ribonucleoside Analogues. *Org. Biomol. Chem.* **2012**, *10* (32), 6521–6525.

(5) St. Amant, A. H.; Engbers, C.; Hudson, R. H. E. A Solid-Phase CuAAC Strategy for the Synthesis of PNA Containing Nucleobase Surrogates. *Artif. DNA PNA XNA* **2013**, *4* (1), 4–10.

(6) Kennedy, D. C.; McKay, C. S.; Legault, M. C. B.; Danielson, D. C.; Blake, J. A.; Pegoraro, A. F.; Stolow, A.; Mester, Z.; Pezacki, J. P. Cellular Consequences of Copper Complexes Used To Catalyze Bioorthogonal Click Reactions. *J. Am. Chem. Soc.* **2011**, *133* (44), 17993–18001.

(7) Agard, N. J.; Prescher, J. A.; Bertozzi, C. R. A Strain-Promoted [3 + 2] Azide−Alkyne Cycloaddition for Covalent Modification of Biomolecules in Living Systems. *J. Am. Chem. Soc.* **2004**, *126* (46), 15046–15047.

(8) Sletten, E. M.; Bertozzi, C. R. From Mechanism to Mouse: A Tale of Two

Bioorthogonal Reactions. *Acc. Chem. Res.* **2011**, *44* (9), 666–676.

(9) Diels, O.; Alder, K. Synthesen in Der Hydroaromatischen Reihe. *Justus Liebigs Ann. Chem.* **1928**, *460* (1), 98–122.

(10) Carboni, R. A.; Lindsey, R. V. Reactions of Tetrazines with Unsaturated Compounds. A New Synthesis of Pyridazines. *J. Am. Chem. Soc.* **1959**, *81* (16), 4342–4346.

(11) Sauer, J.; Lang, D. Diels-Alder-Reaktionen Der 1.2.4.5-Tetrazine. *Angew. Chemie* **1964**, *76* (13), 603.

(12) Taylor, M. T.; Blackman, M. L.; Dmitrenko, O.; Fox, J. M. Design and Synthesis of Highly Reactive Dienophiles for the Tetrazine–trans-Cyclooctene Ligation. *J. Am. Chem. Soc.* **2011**, *133* (25), 9646–9649.

(13) Knall, A.-C.; Slugovc, C. Inverse Electron Demand Diels-Alder (IEDDA)-Initiated Conjugation: A (High) Potential Click Chemistry Scheme. *Chem. Soc. Rev.* **2013**, *42* (12), 5131–5142.

(14) Seitchik, J. L.; Peeler, J. C.; Taylor, M. T.; Blackman, M. L.; Rhoads, T. W.; Cooley, R. B.; Refakis, C.; Fox, J. M.; Mehl, R. A. Genetically Encoded Tetrazine Amino Acid Directs Rapid Site-Specific in Vivo Bioorthogonal Ligation with Trans-Cyclooctenes. *J. Am. Chem. Soc.* **2012**, *134* (6), 2898–2901.

(15) Lang, K.; Davis, L.; Torres-Kolbus, J.; Chou, C.; Deiters, A.; Chin, J. W. Genetically Encoded Norbornene Directs Site-Specific Cellular Protein Labelling via a Rapid Bioorthogonal Reaction. *Nat. Chem.* **2012**, *4*, 298.

(16) Lang, K.; Davis, L.; Wallace, S.; Mahesh, M.; Cox, D. J.; Blackman, M. L.; Fox, J. M.; Chin, J. W. Genetic Encoding of Bicyclononynes and Trans-Cyclooctenes for Site-Specific Protein Labeling in Vitro and in Live Mammalian Cells via Rapid Fluorogenic

Diels–Alder Reactions. *J. Am. Chem. Soc.* **2012**, *134* (25), 10317–10320.

(17) Blackman, M. L.; Royzen, M.; Fox, J. M. Tetrazine Ligation: Fast Bioconjugation Based on Inverse-Electron-Demand Diels−Alder Reactivity. *J. Am. Chem. Soc.* **2008**, *130* (41), 13518–13519.

(18) Pindur, U.; Lutz, G.; Otto, C. Acceleration and Selectivity Enhancement of Diels-Alder Reactions by Special and Catalytic Methods. *Chem. Rev.* **1993**, *93* (2), 741–761.

(19) Wilson, P. J.; Wells, J. H. The Chemistry and Utilization of Cyclopentadiene. *Chem. Rev.* **1944**, *34* (1), 1–50.

2 The Normal-Electron Demand Diels–Alder Reaction for Bioconjugation with Maleimide

Portions of this chapter were originally published in *Bioconjugate Chemistry,*[1] two manuscripts under preparation[2,3] and the U.S. Patent 62/511,415 (submitted May 26, 2017). Reproduced (or 'Reproduced in part') with permission from *Bioconjugate Chem.*, **2018**, *29* (7), pp 2406–2414.

2.1 Introduction

Bioconjugation reactions have a unique and essential role in life science research and drug development, due to their ability to couple biomolecules with drugs, reporter molecules, polymers, surfaces, and other biologically active compounds.[4,5] In particular, bioconjugation technologies are used for production of antibody–drug conjugates (ADCs) that provide a delivery platform for selectively targeting anticancer drugs to tumor cells.[6,7] The impact of this approach has been validated with four ADCs that have been approved by the US Food and Drug Administration (FDA), as well as more than 65 that are under clinical evaluation.[8] Among the classes of available bioconjugation methods, the Michael addition reaction between thiols and maleimides (**Figure 2.1A**) is one of the most widely used; two FDA-approved ADCs (brentuximab vedotin and trastuzumab emtansine) utilize this chemistry for attaching drugs to antibodies.

Of the various reactive groups that are available for coupling drugs to antibodies, maleimide holds unique potential. The use of maleimides for bioconjugation is routine in the laboratory and in certain clinical drugs; as a result, many compounds bearing a maleimide group are commercially available. For example, the maleimide–drug maleimidocaproyl-

valine-citrulline-*p*-aminobenzyloxy-carbonyl-monomethyl-auristatin-E (vedotin or **vcMMAE**) is synthesized on an industrial scale to produce brentuximab vedotin and several other vedotin ADCs in clinical trials. Additionally, maleimide compounds are routinely used for labeling biomolecules with fluorophores,[9] metal chelators,[10,11] and polymers.[12] Despite the widespread use of maleimide in bioconjugation chemistries, a significant challenge is to identify conjugation strategies that leverage the properties of maleimide without relying on the thiol-maleimide Michael reaction, which suffers from several limitations. For instance, conjugation to maleimide requires a free thiol that is produced through a partial reduction of native disulfide bonds or introduction of cysteine residues by protein engineering.[13,14] Although maleimide conjugation to antibody thiols is an efficient reaction, preparation of antibody for conjugation can be a cumbersome process. For example, reducing agents such as tris(2-carboxyethyl)phosphine (TCEP) or dithiothreitol (DTT) used to activate cysteines also inactivate maleimide and so must be removed before conjugation.[15] Site-specific maleimide–thiol conjugation to engineered cysteines (non-hinge) allows for controlled drug:antibody ratios (DAR), but the conjugation process requires an additional oxidation step to re-form native disulfides in the antibody hinge region.[14]

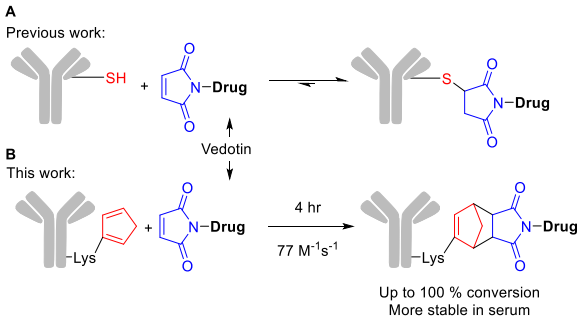

Figure 2.1 (A) Brentuximab vedotin: reduced hinge-region thiols reacted with maleimide–drug (Michael addition) (B) Conjugation approach with randomly-distributed electron-rich dienes which takes advantage of available maleimide–drugs. The DA conjugation is fast and results in adducts stable in serum.

Furthermore, thiosuccinimide adducts often undergo a site-dependent retro-Michael reaction, leading to deconjugation in vivo with a half-life of approximately 4-5 days in rats[16] which decreases the efficacy of an ADC.[17] To overcome challenges, several innovative strategies have been developed to increase the stability of the thiol-maleimide linkage; for example, engineering antibodies with cysteine residues in stable conjugation positions[17] or designing a thiosuccinimide that undergoes a stabilizing succinimide hydrolysis.[16,18–21] Additionally, new reagents for thiol specific conjugation have also been developed; however, these new linkages for in vivo applications remain relatively unexplored and do not harness the proven applications of maleimide compounds.[22–24] One appealing solution would be to develop new maleimide-linkage strategies for antibody-drug conjugation that are stable regardless of location, while simultaneously using a simplified conjugation protocol.

The DA reaction offers unrealized potential in this context.[25] Maleimide is an excellent dienophile due to its electron-deficient and sterically-unhindered π-system. As a result, maleimide is one of the most commonly used dienophiles in DA reactions; it has been used to chemically tag proteins,[26] oligonucleotides,[27] oligosaccharides,[28] and nanoparticles.[29] Because of synthetic ease, these reactions typically rely on furan and electron-rich 2,4-hexadiene derivatives that can be readily incorporated and used for a given application. Although these results clearly demonstrate the potential of the DA-maleimide bioconjugation, the sluggish reaction rates constitute a serious drawback for production of ADCs. For example, reactions between furans and maleimide typically have a second order rate constant on the order of 10^{-5} $M^{-1}s^{-1}$.[30] These rate constants can be offset by high concentrations of the maleimide, long reaction times, or elevated temperatures.[31] Although this is feasible for materials chemistry or organic synthesis, such reaction conditions for ADC production are prohibitive due to

antibody sensitivity, stability, and cost. High concentrations cannot be used to overcome slow conjugation, as antibodies can undergo aggregation, and many maleimide-drugs have low water solubility. Furthermore, sophisticated drug-linker molecules used for conjugation to antibodies are expensive and minimizing equivalents is desirable.[6,7,32] Thus, fast kinetics are needed to overcome limitations.

Improved kinetics for the DA reaction with maleimide have been achieved by modifying the diene component or the reaction solvent. For example, a study of the DA reaction of maleic anhydride (which has similar reactivity to maleimide) has shown that the electron-rich and cyclic cyclopentadiene has about a 1,300-fold rate enhancement compared to unsubstituted butadiene.[33] In conjugation studies, Barner-Kowollik,[34] our group,[35] and others[36–40] have also reported examples of highly efficient and rapid DA or hetero-DA cycloadditions with substituted cyclopentadienes. The DA reaction rate also depends on the solvent, as rates are accelerated in water due to hydrophobic aggregation and hydrogen-bonding.[41,42] For instance, Grandas used an aqueous DA reaction to produce peptide-oligonucleotide conjugates with good efficiency.[43] We envisioned developing an ADC system utilizing electron-rich dienes that, although historically considered a liability due to their high reactivity, could be incorporated onto an antibody and then reacted with a commercially available maleimide–drug to form stable ADCs (**Figure 2.1B**). Such a system would allow properties of the DA reaction (reaction rate, selectivity, stability, and synthetic ease) to be exploited in the context of antibodies and clinically validated drug-linkers.

This dissertation chapter discusses our progress to address the above challenges using the normal electron-demand DA. This conjugation approach takes advantage of widely available maleimide–drugs with established manufacturing processes. In addition, design of the

conjugation strategy is centered on the drug–linkers typically used for ADC production. Antibodies were modified with electron-rich and cyclic dienes and subsequently reacted with the therapeutically relevant maleimide drug-linker **vcMMAE**. Reaction rates were found to be 2.6–77 $M^{-1}s^{-1}$, which is suitable for ADC production. The DA cycloadducts are more stable in serum than are thiol–maleimide linkages formed with the same maleimide–drug. The resulting Diels-Alder antibody–drug conjugates (DAADCs) produced using trastuzumab exhibited potencies similar to analogous thiol–maleimide conjugates in vitro and in vivo, demonstrating that this conjugation approach maintains drug potency.

These DAADCs produced through lysine conjugation are a proof-of-concept for the next generation of ADCs using site-specific drug conjugation. In comparison to ADCs prepared by stochastic conjugation to lysines or native hinge thiols, site-specific ADCs have improved therapeutic index, stability, and *in vivo* efficacy.[44–48] Site-specific conjugation of drugs to antibodies via a chemical approach can be achieved with engineered cysteine residues (commonly referred to as THIOMAB antibodies[14]), modification of glycans, use of peptide tags, or ncAA engineering.[47,49] In this chapter, after validation of the DA reaction as a conjugation method, we genetically encode dienes to produce site-specific DAADCs.

2.2 Design and Synthesis of Electron-Rich and Cyclic Diene Compounds

The DA reaction rate and the stability of both diene and DA adducts are crucial for efficient production of DAADCs. The diene must be highly reactive in conditions suitable for antibodies (ie, aqueous solution, ≤37°C) and yet avoid dimerization or polymerization during synthesis, storage, and conjugation with maleimide. Identification of such a diene is challenging because reagents that incorporate this functional group into antibodies are not readily available. To develop a general and practical synthetic approach to evaluating DA

reactions with highly reactive, electron-rich and cyclic dienes on antibodies, we designed a modular approach that could be systematically investigated. We synthesized heterobifunctional linkers incorporating a range of diene functionality for reaction with maleimide and an *N*-hydroxysuccinimide (NHS) ester to react with antibody lysine amines. We focused on furan and cyclopentadiene-containing linkers, for which the sterics and electronics could be easily tuned (**Figure 2.2**).

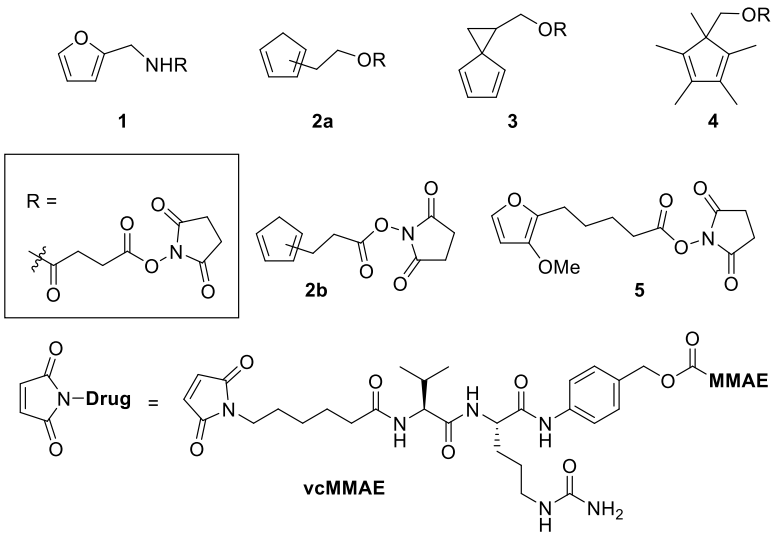

Figure 2.2. Overview of diene-NHS esters and dienophile compounds used to investigate stability and reactivity. Compounds 2a and 2b are obtained as an interconverting mixture of 1- and 2-substituted cyclopentadienes.

We began with NHS-ester **1**, using a strategy similar to that described for the conjugation of furan-containing nanoparticles with maleimide-containing antibodies;[29,50,51] Furan NHS-esters have been widely utilized in bioconjugation approaches, and therefore this strategy provides an easy way to evaluate and compare the reactivity to known systems. The reactivity of **1** with maleimide was low under typical antibody conjugation conditions (1.3% conjugation, 20 h, 2.7 mg/mL antibody, pH 5.5, room temperature), which motivated us to explore other more reactive dienes. We designed **2a** to take advantage of cyclopentadiene's fast kinetics in the DA reaction.[33] In addition, the *endo* DA adduct does not undergo a retro-

DA until reaching approximately 275°C.[52,53] This feature increases the thermal stability of the DA conjugate and distinguishes it from the DA adduct between **1** and maleimide, which yields a mixture of *endo* and *exo* adducts, with the retro-DA occurring at approximately 50°C for the *endo* adduct.[54,55] The synthesis of **2a** was obtained with an interconverting mixture of 1- and 2-cyclopentadiene isomers, as monosubstituted cyclopentadienes undergo a facile [1,5]-hydride shift.[56] Like many monosubstituted cyclopentadienes with a low molecular weight, **2a** was found to dimerize at room temperature (approximately 55% dimer after 5 days) and required storage at -20°C, where it was stable for several months. To provide access to dienes with enhanced stability while maintaining similar reactivity, spiroheptadiene **3**[57] and pentamethylcyclopentadiene **4**[58,59] were synthesized; these electron-rich dienes have not been reported to dimerize at room temperature,[60] thus simplifying the synthesis and handling of the material. In addition to cyclopentadienes **2**–**4**, we designed the more reactive furan derivative, 3-methoxyfuran **5**.[61] Compared to 3*H* furan, the DA reaction of 3-alkoxyfuran with maleimide is reported to have a lower kinetic barrier due to reduced aromaticity.[62] Altogether, the synthesis of a series of diene-NHS bifunctional linkers was straightforward and provided a means for incorporating various diene functionalities onto antibodies for evaluation of the DA reaction with maleimide–drugs.

2.3 Production of Diene-Functionalized Antibodies

With a series of dienes bearing NHS-esters in hand, we next sought to functionalize antibodies through the well-known reaction between lysine amines and NHS-activated esters. A typical IgG1 molecule bears approximately 40 surface-exposed reactive lysine residues,[63] thus, lysine modification in solution or on solid support[64] is random, and the distribution of product obtained is controlled by the antibody:NHS-ester ratio used in the reaction.

Conjugation of **1**, **2a**, **3**, **4**, and **5** to antibody lysine amines was confirmed and quantified by mass spectrometry, yielding antibody-dienes **mAb-1** to **mAb-5** with average linker-to-antibody ratios (LARs) between 2 and 4. A distribution of products were obtained ranging from one to eight modified amines per antibody.

In all cases examined, there was no observed antibody aggregation or dimerization for the diene after antibody conjugation. Of note, this includes **mAb-2a**, the conjugate formed with the dimerization-prone cyclopentadiene **2a** (**Figure 2.3**). Antibody species with high LAR values are the most susceptible to deleterious properties such as aggregation and/or dimerization of diene functional groups, which were not observed. Ester cleavage of **2a** was observed following incubation at pH 7.4 and 37°C for several days (data not shown); this is likely to have occurred via reaction with water or a neighboring lysine ε-amine. We designed cyclopentadiene **2b**, which lacks an internal ester**,** for production of ADCs for use in vivo and in vitro (vide infra).

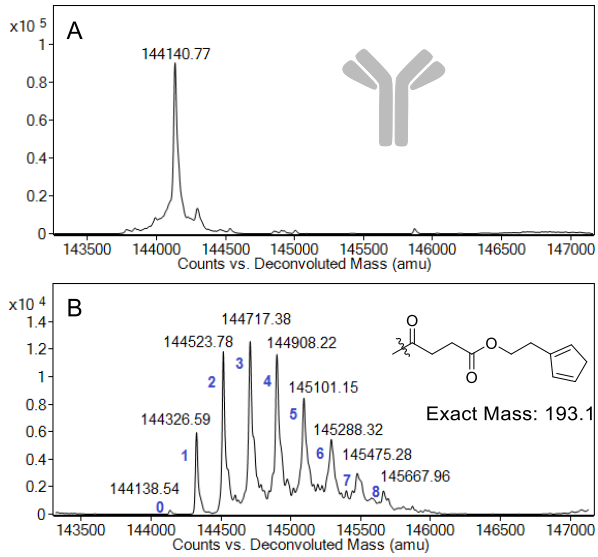

Figure 2.3 Mass spectrometry analysis of (A) mAb and (B) mAb-2a conjugate. Antibodies were deglycosylated with EndoS and analyzed intact. Peak masses and linker to antibody ratio (LAR) are indicated (average LAR for this sample is 3.7). Only one isomer of cyclopentadiene is shown.

2.4 Diels–Alder Reaction

To examine whether mAb-dienes **mab-1** to **mAb-5** were amenable to facile DA cycloaddition, we reacted them with an excess of the therapeutically relevant maleimide-containing drug **vcMMAE**. For the initial studies, 15 equivalents of **vcMMAE** was added to the diene-functionalized antibody (note that the diene:maleimide ratio was from 4.5:1 to 6.5:1 due to variable LAR values, see below). Reaction conversion was monitored by mass spectrometry, which can be used to quantify drug conjugated to antibodies.[65,66] Dimethyl sulfoxide (DMSO) was added to all reaction mixtures to solubilize **vcMMAE** and ensure homogenous reaction conditions. The DA reaction of **mAb-1** with **vcMMAE** (6 equivalents relative to diene) produced **mAb-1-MMAE** in a very low yield (<2%, **Table 2.1**). With extended reaction times and elevated temperature (20 h, 37°C), the yield was not improved and ~1% nonselective conjugation (ie, conjugation to a heavy or light chain that does not contain diene) was observed. As expected for the production of DAADCs, 3*H* furan does not react at sufficient rates for practical use. In contrast to **mAb-1**, the antibody-dienes **mAb-2a**, **mAb-4**, and **mAb-5** underwent complete conversion after 4 h at both room temperature and 37°C when reacted with 4–6 equivalents of **vcMMAE** per diene (**Figure 2.4**), indicating promising reaction kinetics for these more reactive dienes. Although spiroheptadiene **mAb-3**'s conversion was lower under these conditions (73% at room temperature or 88% at 37°C), nearly quantitative conversion could be obtained with longer reaction times (48 h, **Figure 2.5**). No non-selective conjugation was observed for **mAb-2a** to **mAb-5**, indicating high specificity for the diene. Importantly, other than slow ester hydrolysis observed while DAADCs of **2a**, **3**, and **4** were incubated, the DAADCs were found to be stable over the course of the reaction, during purification, and upon storage in buffer (phosphate-buffered saline

(PBS), pH 7.4). The DA reaction was further measured at a stoichiometric ratio of 1:1 diene:maleimide to determine second order rate constants (see below).

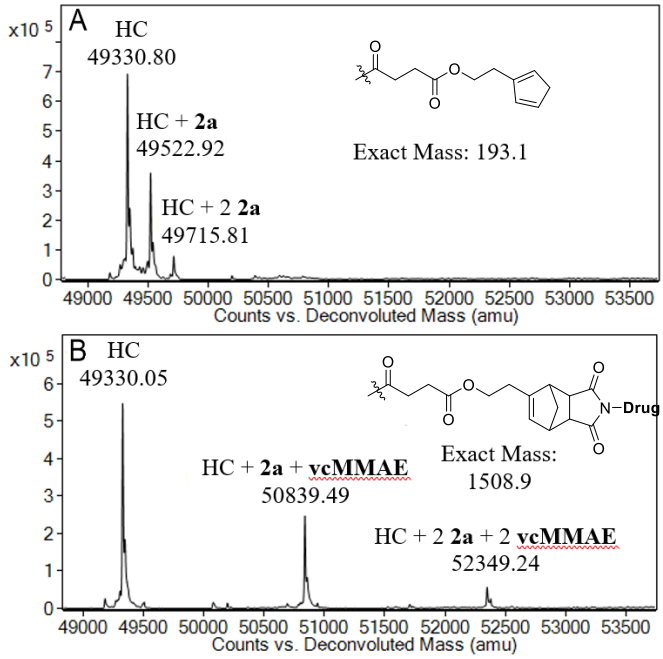

Figure 2.4 Mass spectrometry analysis of mAb-2a before (A) and after (B) reaction with vcMMAE (15 equivalents relative to mAb, 22°C, 4 h). Samples were deglycosylated and reduced prior to analysis, spectra are zoomed to show the heavy chain (HC) species only. Only one isomer of cyclopentadiene is shown.

Table 2.1 Diels–Alder conjugation of mAb-dienes with an excess of vcMMAE[a,b]

mAb-Diene	LAR	Reaction time (h)		Conversion (%)[c]
		22°C	37°C	
mAb-1[d]	2.5	20	-	1.3[e]
mAb-2a	2.3	4	100	100
mAb-3	3.3	4	73	88
mAb-4	3.04	4	100	100
mAb-5	2.95	4	100	99

[a]All conjugation reactions were performed in PBS supplemented with 100 mM sodium phosphate monobasic, 20% DMSO, pH 5.5. The antibody used was R347. [b]All reactions were performed with 15 molar equivalents vcMMAE relative to mAb. mAb concentration was 2.7 mg/mL (18 µM) for all reactions. Diene concentration for each reaction can be obtained by multiplying LAR by 18 µM. [c]Conversion was calculated from disappearance of mAb-diene peaks following deglycosylated, reduced mass spectrometry analysis. Both heavy and light chains were analyzed. [d]Antibody used was 5T4. [e]An additional 1.1% nonspecific conjugation was observed.

2.5 Kinetics of the DA Reaction

To discern differences in diene reactivity and understand the effects of solvent on the DA reaction, we measured the conjugation rate in aqueous solution (with diene-modified mAbs) and in organic solvent (with the NHS-esters). The rate of aqueous conjugation reactions is a critical feature for the development of ADCs. If a reaction is too slow, large quantities of drug-linker or long reaction times must be used to drive the reaction to completion. However, this can be cost prohibitive, can lead to aggregation, and may not be possible for drug-linkers with low solubility in aqueous buffer. We began by monitoring the rates in organic solvent to evaluate the reactivity trend. Second-order rate constants in organic conditions for the DA reaction between dienes **1**, **2b**, **3**, **4**, and **5** and *N*-ethylmaleimide were determined in deuterated chloroform (**Table 2.2**).

Table 2.2 Kinetic data for the Diels–Alder reaction in water and deuterated chloroform.

mAb-Diene Reaction with **vcMMAE** in Water[a,b]					NHS-Diene Reaction with *N*-Ethylmaleimide in $CDCl_3$[c]		Aqueous Rate Acceleration $k_2(H_2O)$ / $k_2(CDCl_3)$
mAb-Diene	LAR	[Diene] (μM)	$k_2(H_2O)$ $(M^{-1}s^{-1})$[d,e]	Half-life (min)	$k_2(CDCl_3)$ $(1000 \times M^{-1}s^{-1})$[f]	Half-life (days)[h]	
mAb-1	-	-	ND	ND	0.0491 ± 0.0005	7873	ND
mAb-2a	3.4 ± 0.3	31 ± 2	77 ± 7	7.0 ± 0.4	97 ± 7[g]	4	794
mAb-3	2.9 ± 0.4	27 ± 3	2.6 ± 0.2	237 ± 50	8.7 ± 0.6	44	299
mAb-4	2.9 ± 0.2	27 ± 2	18 ± 8	34 ± 20	12.1 ± 0.1	32	1488
mAb-5	3.0 ± 0.1	26 ± 1	4 ± 2	160 ± 108	12.6 ± 0.7	31	317

[a]All conjugation reactions were performed in PBS supplemented with 100 mM sodium phosphate monobasic, 20% DMSO, pH 5.5, at 22°C. [b]All reactions were performed with 1 equivalents vcMMAE relative to diene. mAb concentration was 1.3 mg/mL for all reactions. [c]Reactions were performed in $CDCl_3$ with 2b, 3, 4, or 5 (0.01 M) and *N*-ethylmaleimide (0.01 M) at room temperature. 1 was performed at 0.05 M. [d]$k_2(H_2O)$ was calculated from the concentration of unreacted mAb-diene peaks (deglycosylated and reduced mass spectrometry analysis). Both heavy and light chains were analyzed. [e]Errors reported for k_2 values were derived from the best fit line of the inverse concentration plot, n=3 for mAb-2a and mAb-3, n=2 for mAb-4 and mAb-5. [f]$k_2(CDCl_3)$ was calculated from the integration of diagnostic peaks in ^{1}H NMR spectra, n=3. [g]2b was used. [h]Half-life calculated from the $k_2(CDCl_3)$ at 30 μM.

Reactions were monitored using ^{1}H nuclear magnetic resonance (NMR), which provides a rapid way to screen the dienes. Furan **1**'s second-order rate at room temperature was the slowest in the series with 4.9×10^{-5} $M^{-1}s^{-1}$, with a calculated half-life of 7,873 days (30 μM at room temperature, conditions in the range commonly used for ADC conjugation). The reactivity of 3-methoxyfuran **5** was markedly greater than that of 3*H* furan, with a half-life of 31 days. The half-lives of cyclopentadiene derivatives **3** and **4** are 44 and 32 days respectively. The least sterically hindered cyclopentadiene in our series, **2b**, reacted the fastest, having a calculated half-life of 4 days. Although the reaction rates in organic solvent are unacceptable for ADC production, the reactivity trend is important and the DA reaction would be accelerated in aqueous buffer.[41,42]

Diene–maleimide DA reaction rates were further evaluated in aqueous conditions using mAb-dienes and **vcMMAE**. Cycloaddition reactions showed reaction rates ranging from 2.6 to 77 $M^{-1}s^{-1}$ (**Figure 2.5**, **Table 2.2**). The second-order rate constant for **mAb-2a** at 22°C was the fastest at k_2 = 77 $M^{-1}s^{-1}$, whereas cycloadditions rates for **mAb-3**, **mAb-4**, and **mAb-5** were slightly slower with rate constants from 2.6 to 18 $M^{-1}s^{-1}$. Enhanced reactivity for **mAb-2a** is probably due to reduced steric interactions compared to dienes **3** and **4.** Although **4** is more sterically hindered than **3**, the rate of cycloaddition benefits from five electron-donating methyl groups and greater hydrophobic aggregation than **3**. Analyses of the cycloaddition reaction also revealed that dienophiles based on furan could be tuned to increase their rate of cycloaddition. Furan **5** bearing the electron donating methyl ether group in the 3 position dramatically increased the rate compared to unsubstituted furan **1**.[62] In fact, the rate constant for **mAb-1** was not determined because the rate was prohibitively slow. Note that reaction rates reported here cannot discern the potential effect of antibody position on DA reaction rate due to the random nature of lysine modification. It is currently unknown if antibody position affects DA reaction rate; thus, the reaction rates reported here should be considered average values.

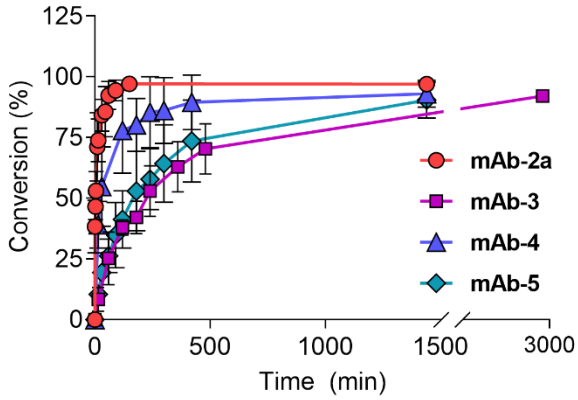

Figure 2.5 Kinetic analysis of the reaction of mAb-diene (1 equivalents of diene) with vcMMAE (1 equivalents). All reactions were performed at 22°C, unreacted diene concentration was determined by mass spectrometry. Data are plotted as the average value ± standard deviation, n=3, for mAb-2a and mAb-3 samples. Data are plotted as the average value ± absolute error, n=2, for mAb-4 and mAb-5 samples. Kinetic experiments were repeated with independent samples.

Overall, the diene-maleimide cycloaddition rates for **mAb-2a** to **mAb-5** enable nearly quantitative conversion of diene groups in a time frame of hours, with one equivalent of maleimide:diene, at antibody concentrations that could be used for routine conjugations. Although slower than the thiol-maleimide Michael addition (k_2 ~ 730 $M^{-1}s^{-1}$),[67] this DA strategy avoids the challenges of selectively reducing and handling thiols. The normal electron-demand DA reaction is slower than the inverse electron-demand DA reaction (k_2 up to 2.8 × 10^6 $M^{-1}s^{-1}$ with *trans*-cyclooctene and tetrazine),[68–70] but it uses a commercially available maleimide–drug, and the cyclopentadiene-NHS ester **2b** can be readily synthesized in three steps. Overall, the DA reaction rate is comparable to that of other commonly used ligation chemistries such as the strain-promoted azide–alkyne cycloaddition (k_2 ~ 10^{-2} to 1 $M^{-1}s^{-1}$) or the copper-catalyzed version (k_2 ~ 10 to 200 $M^{-1}s^{-1}$).[71] This DAADC strategy may have been overlooked for ADC production because reported organic reaction rates were too slow at concentrations typically encountered for bioconjugation to antibodies, as well as the propensity of electron-rich and cyclic dienes to undergo self-dimerization. However, our

findings demonstrate that maleimide–diene aqueous reaction rates are accelerated approximately 300–1500 fold and the dienes are stable, allowing efficient conjugation at diene concentrations in the micromolar range. The rate acceleration is consistent with previous literature reports demonstrating acceleration of the DA reaction in aqueous phase up to 10,000-fold.[72,73]

2.6 Evaluation of Trastuzumab DAADCS

Two DA dienes, the cyclopentadiene and furan with fastest reaction rates (**2b** and **5** respectively), were further evaluated in functional DAADCs using trastuzumab (**T**). DAADCs were prepared by functionalizing the antibody with NHS-linkers **2b** or **5**, followed by reaction with **vcMMAE** (as described in **Table 2.1**) with DARs of approximately 3–4 as determined by mass spectrometry and rRP-HPLC (**Table 2.3**). Reaction of **vcMMAE** with **T**-diene resulted in nearly quantitative conversion of the diene groups. Monomer content in the DAADCs remained high, indicating that diene functionalization, DA reaction, and purification did not cause aggregation. As a control, ADCs were also prepared by Michael addition to reduced native hinge thiols (**T-Cys-MMAE**), with DARs targeted to be the same as the DAADCs (DAR = 3–4).

Table 2.3 Summary of Trastuzumab ADCs.

mAb-Linker-Druga	DAR		EC50 (ng/mL)		
	(MS)	(rRP-HPLC)	Monomer (%)	N87	SKBr3
T-2b-MMAE	3.9	3.5	98.7	1.98	1.98
mAb-2b-MMAE	3.2	3.4	98.4	8230	1811
T-5-MMAE	3.5	4.5	97.7	3.02	1.57
mAb-5-MMAE	3.2	3.5	98.1	9990	~2000
T-Cys-MMAEb	3.2	3.5	97.4	3.61	2.78
mAb-Cys-MMAEb	2.9	3.1	98.5	8177	>2000

[a]ADCs were prepared using trastuzumab (T) or a control antibody (mAb). [b]Prepared using the thiol-maleimide reaction of native hinge cysteines.

In vitro, the ADCs **T-2b-MMAE** and **T-5-MMAE** exhibited similar potency to **T-Cys-MMAE** in gastric carcinoma N87 and adenocarcinoma SKBr3 cell lines (**Table 2.3**). ADCs produced with non-binding control antibody (**mAb**, R347) had very low inhibition, indicating low non-specific activity. Overall, *in vitro* cytotoxicity values were in the expected range for a vedotin ADC and the DA conjugation approach did not result in lower potency.

2.7 Serum Stability of DAADCs

The stability of the ADCs prepared via DA linkage or thiosuccinimide linkage was evaluated *ex vivo* in both rat and mouse serum (**Figure 2.6**, 7 days at 37°C). Total human antibody was recovered from serum by immunocapture and analyzed by mass spectrometry to determine the amount of drug remaining on ADCs.[74] We did not expect the DAADCs to deconjugate in serum through the retro-DA reaction because the adduct of cyclopentadiene and maleimide does not undergo a retro-DA reaction until temperatures exceed 275°C,[52,53] and the 3-alkoxyfuran–maleimide adducts are reported to be irreversible.[62] Indeed, both DAADCs **mAb-2b-MMAE** and **mAb-5-MMAE** were stable in rat serum (**Figure 2.6A**), having 90% and 94% drug retention respectively. In mouse serum there was significant loss

of drug through cleavage of the Val-Cit linker; however, the DA linkage remained intact. Enzymatic cleavage of the Val-Cit dipeptide is a known property of mouse plasma, and is especially prevalent for ADCs prepared by conjugation to solvent-exposed positions.[75] By combining the intact DAADCs and the Val-Cit cleaved species that retained the DA-adduct, the stability of the DA linkage in mouse serum was confirmed (**Figure 2.6B**).

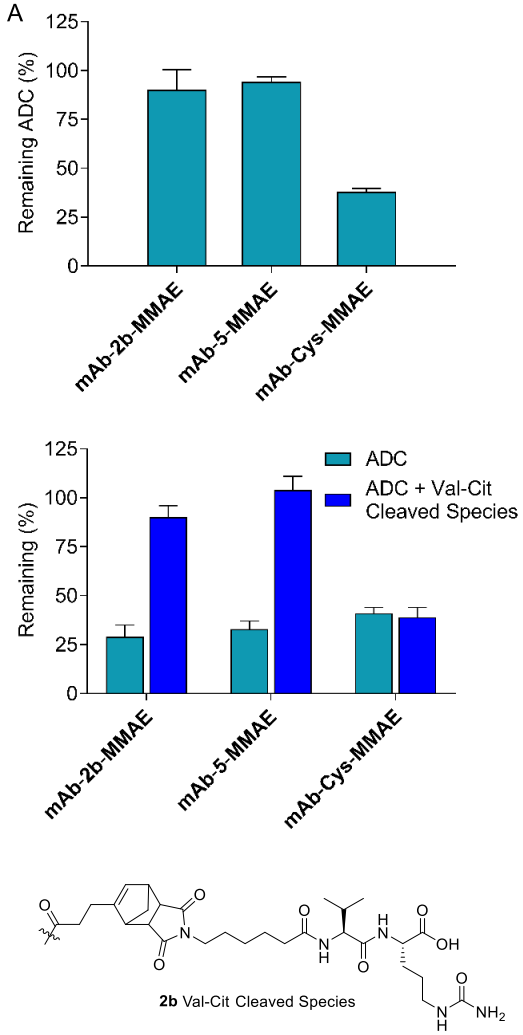

Figure 2.6 Serum stability of ADCs. Samples were added to normal rat (A) or mouse (B) serum and maintained at 37°C for 7 d prior to analysis. Samples were recovered from serum by immunocapture, reduced, deglycosylated and analyzed by mass spectrometry. Quantification of intact ADC (including stable thiosuccinimide-hydrolyzed species) or intact DA adduct only (C, ADC + the Val-Cit cleaved species) was determined from relative peak heights of mass spectra. Intact linker in mouse serum was calculated as the sum of intact ADC and the valine-citrulline cleaved species. Each analysis is reported as the average value ± standard deviation, n=3.

Thiol-conjugated drug in **mAb-Cys-MMAE** incurred significant deconjugation in both rat and mouse serum (38% and 41% respectively), with remaining drug connected through a hydrolyzed thiosuccinimide linkage. The amount of drug loss observed here for thiol-linked ADCs is consistent with previous reports, and highlights the potential liability of stability for ADCs produced through thiol–maleimide coupling.[17,22,76] Drug loss for thiosuccinimide-linked ADCs occurs via the retro-Michael reaction, in which regenerated maleimide can subsequently react with endogenous thiols in serum such as serum albumin.[19,22] The amount of drug loss for thiosuccinimide-linked ADCs is position dependent, with solvent-exposed positions typically undergoing higher deconjugation; in contrast, positions that are buried or that promote thiosuccinimide hydrolysis can be highly stable.[77] Thiosuccinimide linkage stability is also influenced by linker properties, such that hydrophilic and/or cationic linkers capable of promoting thiosuccinimide hydrolysis yield stable thiol-linked constructs.[16,20] Interestingly, **mAb-Cys-MMAE** did not undergo significant Val-Cit cleavage in mouse serum, possibly due to the sheltered nature of the thiols in the hinge region.

Effective stabilization of the drug–mAb linkage in ADCs prepared with maleimide drug–linkers using the DA conjugation strategy represents an alternative approach to current methods. To date, most strategies for stabilizing maleimide–mAb conjugates involve identifying stable antibody conjugation positions or altering chemistry in the drug-linker reaction partner to promote thiosuccinimide hydrolysis. In the DA conjugation strategy, the maleimide conjugate stability was improved by using an antibody-diene as the reaction partner, which to date has not been demonstrated.

2.8 In Vivo Study

Functional ADCs **T-2b-MMAE**, **T-5-MMAE**, and **T-Cys-MMAE** and control ADC **mAb-2b-MMAE** were evaluated for antitumor activity *in vivo* using mice bearing N87 xenograft tumor models (**Figure 2.7**). The dose of 3 mg/kg was chosen based on a recent literature report for a trastuzumab-MMAE ADC that showed a durable tumor response for a DAR 3.8 Cys-ADC dosed at 5 mg/kg and partial tumor growth inhibition and complete regrowth after 35 days when dosed at 1 mg/kg in a NCI-N87 model.[78] Thus, at 3 mg/kg dose, a clear tumor response is expected, and a drastic loss in ADC potency should also be evident. As seen in **Figure 2.7**, all functional ADCs evaluated in this work resulted in complete tumor regression for 30 days after a single injection of ADC. **T-Cys-MMAE** and **T-5-MMAE** ADCs showed continued strong tumor growth inhibition for up to 40 days, whereas tumors treated with **T-2b-MMAE** ADC grew slightly from days 30 to 40; however, tumor volume did not exceed the tumor volume at the beginning of treatment and the differences at day 40 were not statistically significant ($p > 0.05$). Considering the ex vivo mouse serum stability results, both DAADCs and Cys-linked ADCs are expected to lose approximately the same amount of drug 7 days after injection, albeit through different mechanisms (Val-Cit linker cleavage and retro-Michael addition respectively). Thus, current results suggest that DA conjugation does not lead to deleterious loss of drug function *in vivo* compared to cysteine-based ADCs. Avoiding Val-Cit linker cleavage by incorporating the diene at non-exposed positions or by use of other maleimide–drugs could yield ADCs with higher potency than cysteine-based surrogates, which is a focus of our future studies. Altogether, randomly lysine-conjugated DAADCs have similar potency to hinge Cys-linked ADCs *in vitro* and *in vivo*, resulting in ADCs with potent anti-tumor activity.

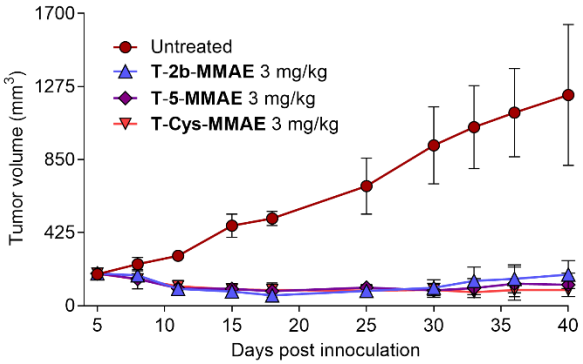

Figure 2.7 NCI-N87 tumor growth inhibition by ADCs. Treated mice received a single dose (IV) of T-Cys-MMAE (3 mg/kg), T-2b-MMAE (3 mg/kg), or T-5-MMAE (3 mg/kg) 5 days after tumor inoculation. Tumor volumes are plotted as the average volume ± SD, n=5.

2.9 Site-Specific Antibody–Drug Conjugates using the Diels–Alder Reaction

With the DAADCs proof-of-concept demonstrated using random lysine conjugation proven, we wanted to use this technology for "next generation" ADCs. With a DAR of 0–8, the hydrophobicity and pharmacokinetics of stochastic ADCs are highly variable; the next generation ADCs use a DAR of 2 and the drug is attached site-selectively. The overarching goal of this project in collaboration with MedImmune has been to synthesize a diene amino acid that can be genetically encoded for site-selective DAADCs.

The ability to perform specific chemical transformations with complex biological reaction partners has enabled development of new classes of biotherapeutics[79] and tools to study the life sciences.[4] Key to advances in these areas has been strategies that exploit orthogonal pairs of non-natural reagents to enable reactions within complex biological milieu such as cell culture media, within live cells, and even *in vivo*. These "bioorthogonal" chemistries, such as the Staudinger ligation,[80] strain-promoted azide-alkyne cycloaddition,[81] and inverse electron-demand Diels-Alder reaction[82] have enabled great advancements in production of bioconjugates and also provided valuable insight into metabolic processes. Incorporation of

these reagents into proteins has been achieved by genetic code expansion to deliver non-canonical amino acids (ncAAs) containing the reactive functionality at desired positions in the protein.[83] This approach results in production of reactive biomolecules that can be further manipulated by chemical modification in a site-specific manner.[84]

Currently, many ADC candidates employ the fast and selective Michael reaction to attach maleimido drug-linkers to antibody thiols, forming a thiosuccinimide linkage (**Figure 2.8**). Thiol-maleimide conjugation does have drawbacks, however, including instability of resulting thiosuccinimides and the need to manipulate antibodies prior to conjugation. Thiosuccinimides are susceptible to the retro-Michael reaction, resulting in drug-linker deconjugation in serum that can reduce on-target ADC potency and increase off-target cytotoxicity. Instability of ADCs in circulation may be overcome using self-hydrolyzing maleimides[16,18,85] and cysteine engineering strategies, however the latter approach is highly position dependenant.[17,86] Drug attachment to cysteine is a cumbersome process, requiring a multistep procedure that involves reduction, oxidation, conjugation, and purification of intermediates. Given that at least ten unique maleimide drug-linkers[44] have been produced on scale and accompanied by quality-control processes to support drug manufacturing, new site-specific conjugation strategies that take advantage of these already developed maleimides would facilitate the production of modern ADCs. Additionally, considering the abundance of off-the-shelf maleimide reagents available for a range of applications, from dye-labelling[87] and metal chelation,[11] to polymer conjugation,[88] the production of reactive proteins that access currently available reaction partners would grant immediate access to compounds and applications outside the scope of ADCs.

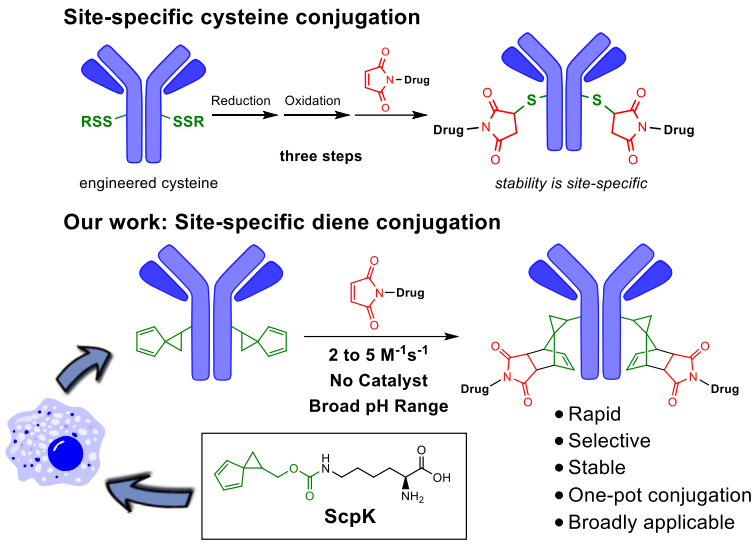

Figure 2.8 Current method for ADC production with maleimide drug-linkers using an engineered cysteine (top) and our method with an engineered diene (bottom).

Synergistic combinations of new bioconjugation chemistry[1] and ncAA (non-canonical amino acid) engineering[89–92] offers a general approach to site-specific production of ADCs with maleimide-based warheads. To date, three strategies have been reported in which ncAAs in antibodies have been used for drug bioconjugation to produce site-specific ADCs. The Schultz group has incorporated a ketone functional group to produce an oxime linker;[93] however, this reaction requires acidic conditions (pH ~4.5) and is slow (60 h) without an aniline catalyst. Azide-alkyne click chemistry has also been used, but this approach relies on either copper(I) catalysis,[94] large, hydrophobic cyclooctyne payloads,[95,96] or ncAAs with low antibody titers (0.5 mg/L).[97] Recently, the Chin group has reported the incorporation of a cyclopropene derivative into an antibody that undergoes a rapid and efficient inverse-electron demand Diels–Alder (IEDDA) reaction with tetrazine derivatives to construct ADCs.[98] In many cases the ADCs prepared using an ncAA approaches were more efficacious *in vivo* than conjugates generated using conventional or THIOMAB methods,[99] however, none enable the use of clinically available maleimide-based drug-linkers[100] and thus forfeit the many practical advantages of maleimide chemistry.

We have described a Diels–Alder bioconjugation that enables selective and rapid attachment of maleimide-based drugs to antibodies in a single-step process using the genetically encoded spirocyclopentadiene-containing ncAA, **ScpK** (**Figure 2.9**). **ScpK** was incorporated into antibody heavy chain positions S239, K274, or N297 (Kabat numbering) to yield reactive antibodies with titers of 42–82 mg/L. **ScpK** was genetically encoded into the antibody sequence using an amber stop codon at the desired position in the plasmid and the *Methanosarcina mazei* pyrrolysine tRNA synthetase (PylRS)/tRNA(Pyl) pair in a transient Chinese hamster ovary (CHO) cell expression system. Our results showed, for the first time, that the electron-rich diene component of the normal demand DA reaction was stable throughout the 10-day antibody expression process and that the isolated antibody product was homogeneous and retained reactivity. To highlight the potential generalizability of this method, **ScpK**-containing monoclonal antibodies (mAbs) were conjugated to three commercially available maleimide-containing ADC drug-linkers with high efficiency. In contrast to thiol-maleimide conjugation reactions with the same drug-linkers, which required activation of the cysteine residues, simply adding the maleimide drug-linker to **ScpK**-containing mAb in buffer resulted in efficient conjugation (room temperature, 5–24 h). Although the actual coupling reaction of maleimide drug-linker to cysteine is much faster than the DA-based approach (requiring minutes instead of hours), the overall process of activating the antibody for site-specific attachment of drug to engineered cysteines is a multi-step process. Finally, the resulting DA adducts were stable in rat serum (*ex vivo*) for at least 1 week at 37 °C, and ADC potency was demonstrated both *in vitro* and *in vivo*. Preparation of ADCs by conjugation to **ScpK** represents an attractive route for straightforward production of

homogeneous and stable ADCs and demonstrates practical utility of the classic DA reaction outside of the context of traditional organic synthesis schemes.

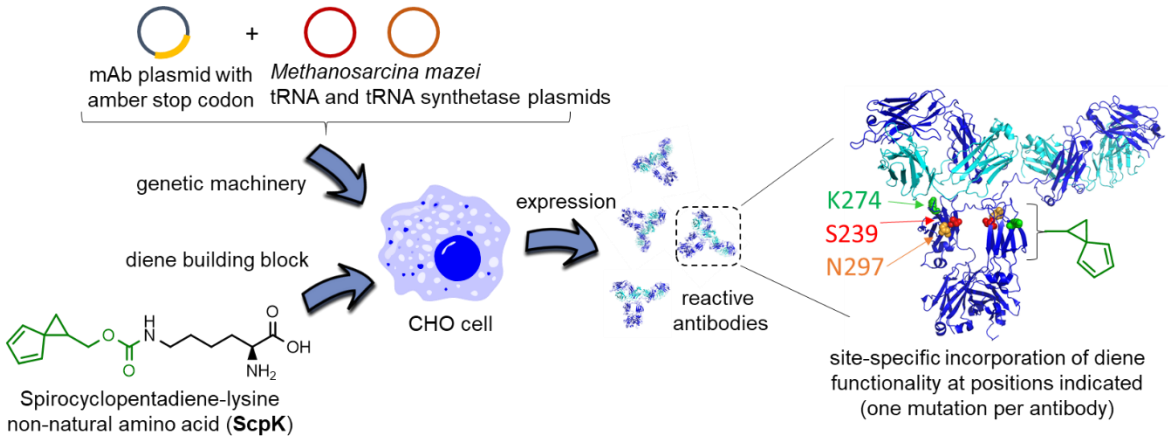

Figure 2.9 Overview of ScpK incorporation into mAbs.

2.10 Design of the Diene ncAA ScpK

Our study of cyclic dienes and their reaction with maleimides for ADC production[1] led to our selection of spiroheptadiene for incorporation into an ncAA because of its reaction kinetics, ease of synthesis, and relative stability.[60] ncAAs with large functional groups are typically attached to lysine through a carbamate linkage and are incorporated into proteins using PylRS mutants.[101] Using spiro[2.4]hepta-4,6-diene-1-methanol[102,103] as the starting material, **ScpK** was synthesized in four steps with an overall yield of 37% on a 3.7 gram scale as a mixture of diastereomers. Stock solutions of **ScpK** were prepared (260 mM in 0.2 M NaOH) and the stock solution was stable in the freezer for at least several months.

2.11 ScpK Incorporation into Antibodies

ScpK was incorporated in response to amber stop codons encoded in antibody heavy chain positions using amber stop-codon suppression technology that replaces native amino acids at the desired positions in the antibody gene sequence (**Figure 2.9**).[94,101,104] Expression of antibodies containing **ScpK** was performed by transient transfection of CHO cells with three

plasmids encoding (1) target mAb containing an amber stop codon at the desired site, (2) nine copies of the tRNA(Pyl) under control of the U6 snRNA promoter,[105] and (3) the *Methanosarcina mazei* PylRS under control of the cytomegalovirus promoter. moeit cells were cultured in media supplemented with **ScpK** (0.5 mM) for 10 days under standard antibody expression conditions. **ScpK** was incorporated at positions S239, K274, or N297 of an anti-EphA2 (named 1C1) antibody heavy chain (in separate antibodies). Antibody positions for **ScpK** incorporation were chosen for comparison with analogous cysteine-based linked ADCs and to identify any position-dependent differences between DA-ADCs and cysteine-based ADCs (i.e. in conjugation, stability, and potency). In that regard, cysteine-linked ADCs produced with S239C are known to be stable and homogeneous,[106] K274C produces homogeneous and unstable ADCs,[17] and N297C produces heterogeneous and unstable ADCs (Ohri et al.[86] and unpublished observations). For some studies, **ScpK** was introduced into a non-binding isotype control IgG1 antibody at the above-mentioned positions to evaluate on-target/off-target activity of ADCs.

Some ncAAs may present challenges for antibody production due to potential reactions with cellular metabolites (eg. cyclooctynes can react with thiols),[107] which can produce cytotoxic effects or undesirable antibody–metabolite conjugates. Given that cyclopentadienes are highly reactive and known to react with oxygen, polymerize with acid, and dimerize,[108] we were extremely gratified to observe that **ScpK** did not appear to appear to succumb to the above-mentioned processes or react with endogenous dienophiles throughout the 10-day culture period in CHO cell medium as confirmed by mass spectrometry (MS) analysis of antibody products. Additionally, the presence of **ScpK** in media did not have an impact on cell viability up to a concentration of 2 mM after 10 days of exposure, indicating acceptable

biocompatibility. Antibody titers after recovery by protein A chromatography were 42–82 mg/L and MS analysis showed **ScpK** incorporation was successful, as a single antibody species was observed for each construct corresponding to the calculated mass change after mutation of natural amino acids to **ScpK** (**Figure 2.10A**). Furthermore, MS analysis of reduced antibodies confirmed that **ScpK** incorporation was specific to the antibody heavy chain as designed, as no mass change was observed in the antibody light chain. Analysis of **ScpK**-mAbs by sodium dodecyl sulfate–polyacrylamide gel electrophoresis (SDS-PAGE) indicated typical profiles under both nonreducing and reducing conditions (**Figure 2.10B**). N297ScpK showed moderate aggregation (21%) that may have had an impact on recovery, as this construct also exhibited the lowest yield (**Table 2.4**). Incorporation of **ScpK** at positions S239 and K274 resulted in higher yields (54–82 mg/L) and high monomer content (92–99%). Overall, we observed expression levels that were similar to those achieved with other ncAA systems,[98] but **ScpK** antibody expression levels were lower than those of cysteine-engineered antibodies prepared under standard antibody expression conditions which were several-fold higher. In general, this decreased antibody expression is currently a limitation of ncAA technology for antibody production; increasing titers of ncAA-containing antibodies and proteins expressed in mammalian systems is an area of active research.[109]

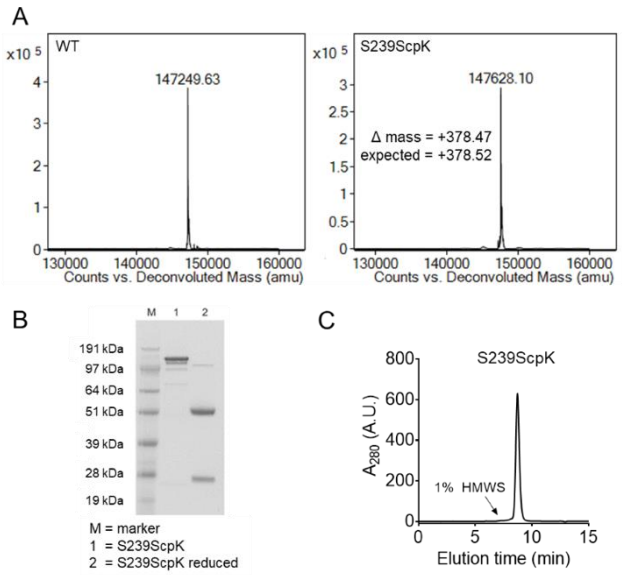

Figure 2.10 Characterization of ScpK-containing antibody S239ScpK. (A) Intact, deglycosylated (EndoS) mass spectrometry of wild-type (WT) and S239ScpK. (B) SDS-PAGE analysis of S239ScpK. (C) Size exclusion chromatography analysis of S239ScpK (high-molecular-weight species are indicated).

Table 2.4 Summary of ScpK-mAb properties and second order rate kinetics with AZ1508

mAb	Titer (mg/L)	Monomer (%)	Reaction Rate ($M^{-1}s^{-1}$)
S239ScpK	76-82[a]	99	2.6 ± 0.5
K274ScpK	54-69[a]	92	1.8 ± 0.4
N297ScpK	42	79	5.4 ± 1.1

[a]Reported as the range obtained from four experiments.

2.12 Reaction of ScpK Antibodies with Maleimido-Drugs

ScpK-mAbs were reacted with Val-Cit-linked monomethyl auristatin E (vcMMAE), AZ1508, or SG3249 (**Figure 2.11**) to produce DA-ADCs. Nearly quantitative conversion of diene to the corresponding DA adduct was observed at 5 equivalents maleimide to diene after overnight reaction at room temperature, with conversion half-lives of 27–146 min. Conversion of ScpK-mAbs to DA-ADCs was confirmed by mass spectrometry, hydrophobic interaction chromatography (HIC), and reduced reverse-phase high-performance liquid chromatography (rRP-HPLC), and all methods confirmed the drug-antibody ratio (DAR) as ~2, the theoretical

yield (**Table 2.5**). Analysis of recovered DA-ADCs by mass spectrometry confirmed that diene-maleimide conjugation occurred on the heavy chain as expected, with nearly complete consumption of **ScpK**-containing heavy chain (**Figure 2.12**). High conjugation efficiency was also confirmed by HIC, which indicated an increase in hydrophobicity after attachment of drug. rRP-HPLC confirmed drug attachment to the antibody heavy chain and corroborated the mass spectrometry results as well. SDS-PAGE analysis of DA-ADCs revealed typical running patterns for antibodies under nonreduced and reduced conditions after conjugation of drug-linker. Finally, coupling drug-linker to antibodies via DA reaction with **ScpK** did not increase their propensity to aggregate, as >90% monomer was obtained for all ADCs.

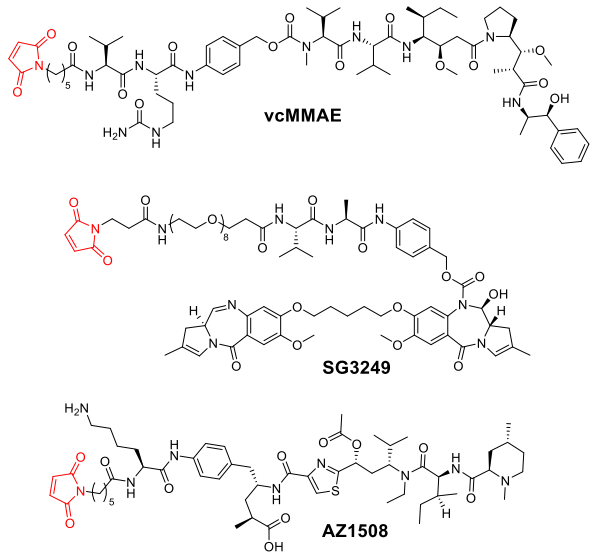

Figure 2.11 Maleimido drug-linkers used in this study.

Table 2.5 Summary of DA and cysteine-linked ADC properties.

ADC	DAR			ADC Monomer (%)	EC50 (ng/mL)[a]
	MS	HIC	rRP-HPLC		
S239ScpK-vcMMAE	1.94	1.90	1.94	>99	35
C239i-vcMMAE[b]	1.90	1.90	1.90	ND	23
S239ScpK-SG3249	1.95	1.63	1.90	>99	7
C239i-SG3249[b]	1.74	1.60	1.82	99	5
S239ScpK-AZ1508	1.96	ND	ND	97	9
S239C-AZ1508	1.96	ND	ND	97	7
K274ScpK-vcMMAE	1.96	1.94	1.83	98	13
K274ScpK-AZ1508	1.96	1.87	ND	>99	7
K274C-AZ1508	1.88	1.84	ND	97	8
K274ScpK-SG3249	1.98	1.80	1.72	98	4
K274C-SG3249	1.81	1.84	1.83	98	4
N297ScpK-AZ1508	1.96	ND	ND	>99[c]	10
N297C-AZ1508	1.60	ND	ND	86[c]	4
N297ScpK-SG3249	1.98	1.92	1.78	97[c]	13
N297C-SG3249	1.57	1.9	1.74	93[c]	14

[a]PC3 cells. [b]Antibodies were produced through cysteine insertion.[110] [c]Aggregate was removed from N297ScpK and N297C samples prior to conjugation. EC_{50} = 50% effective concentration in cell cytotoxicity assays; ND = not determined.

Reaction kinetics between antibodies incorporating **ScpK** and maleimide drug-linkers were explored by reaction with 1 molar equivalent of AZ1508 (relative to **ScpK**), and the progress of the reaction was monitored by MS in a manner similar to previously described methods.[18,65,111] Second-order rate constants were consistently fast at each antibody position studied (1.8–5.4 $M^{-1}s^{-1}$; **Table 2.4**), placing this normal electron-demand DA reaction on par with reported reaction rates for strain-promoted azide–alkyne coupling ($k_2 \approx 1.4$ $M^{-1}s^{-1}$),[96] *p*-phenylenediamine-catalyzed oxime ligation ($k_2 = 4.7$ $M^{-1}s^{-1}$),[112] and the bioorthogonal IEDDA ($k_2 = 7$ $M^{-1}s^{-1}$).[113] However, these reaction rates are slower than those achieved with the thiol–maleimide Michael addition (~500–700 $M^{-1}s^{-1}$).[18,67] Finally, conversion was nearly

quantitative with only one equivalent of maleimide:diene, which is attractive from the perspective of ADC manufacturing because drug-linker can be minimized if desired.

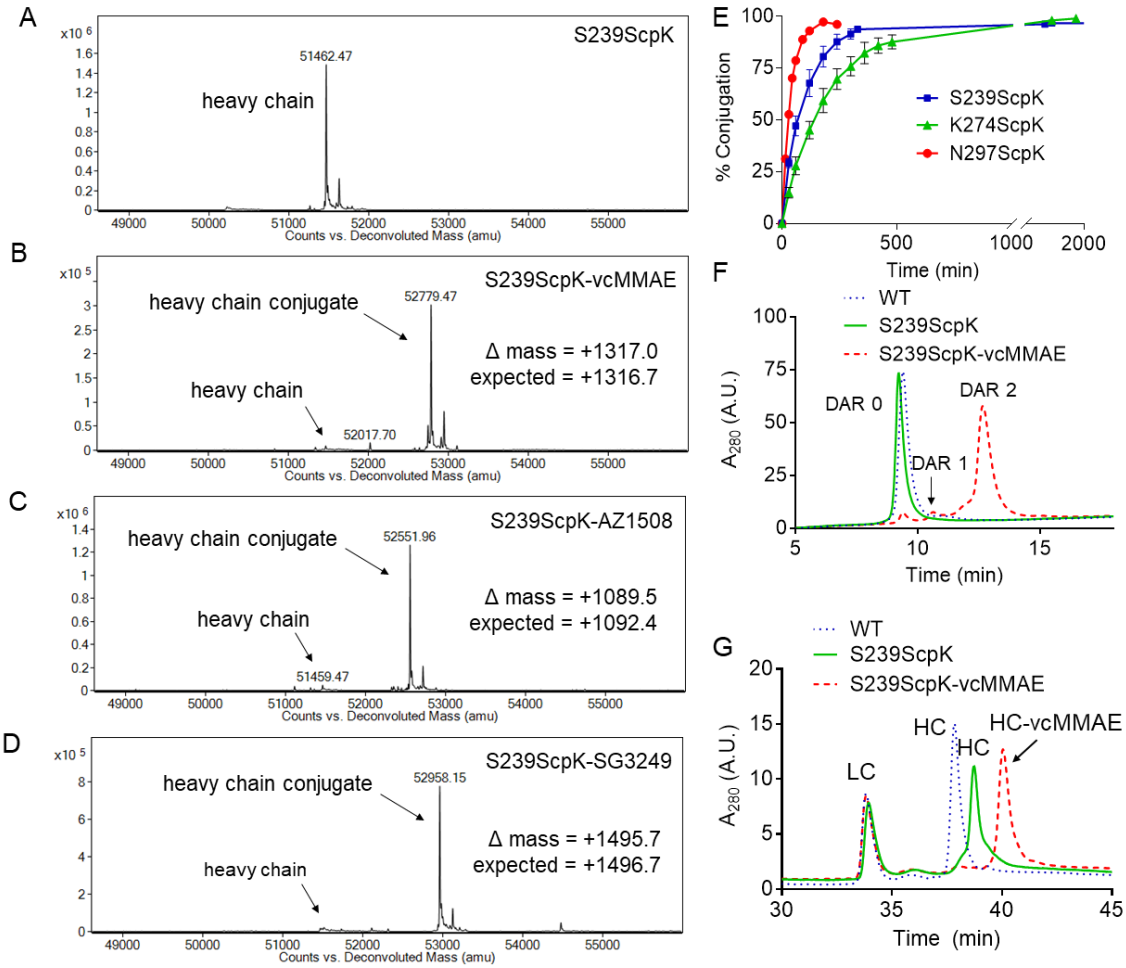

Figure 2.12 Characterization of DA-linked ADCs. (A–D) Reduced MS analysis of S239ScpK antibody and ADCs. (E) Conversion of ScpK-mAbs to DA-ADCs with 5 equivalents of AZ1508 (1.3 mg/mL antibody [17.4 µM diene] in 0.1 M PBS; 0.15 M NaCl; 20% v/v DMSO, pH 5.5; room temperature). Data are plotted as the average ± absolute error (n = 2). (F) HIC analysis of WT mAb, S239ScpK mAb, and S239ScpK-vcMMAE. (G) rRP-HPLC analysis of WT mAb, S239ScpK mAb, and S239ScpK-vcMMAE. DAR = drug–antibody ratio; HC = heavy chain; LT = light chain; WT = wild type

Reaction kinetics were found to be nearly identical in pH 5.5 phosphate-buffered saline (PBS) (with or without 20% v/v DMSO) and pH 7.4 PBS. Performing the reaction in water results in second order kinetics that are significantly accelerated compared to those achieved with organic solvents, owing to increased hydrophobic aggregation and hydrogen bonding.[41,42] We have previously shown that the reaction between spirocyclopentadiene and

maleimide is ~300 times faster in aqueous buffer than in an organic solvent ($CDCl_3$).[1] This property of the DA reaction is critical for production of DA-ADCs at the concentrations required for antibody chemistry (micromolar). If the antibody reaction proceeded at the organic solvent reaction rate (without aqueous acceleration) it would take >30 days to go to completion under our reaction conditions.

To compare this new DA bioconjugation method with the traditional engineered-cysteine approach, ADCs were also prepared via thiol-Michael addition at the same positions used to produce DA-ADCs. Conjugation of maleimide–drugs to analogous cysteine-engineered antibodies produced results similar to those achieved with **ScpK** antibodies for positions S239 and K274, but position N297 revealed a difference between the two conjugation methods. First, HIC analysis indicated that N297ScpK-AZ1508 was less hydrophobic than unconjugated N297ScpK. This is interesting because conjugation of drug to antibodies typically increases the hydrophobicity of the molecule. One possible explanation for this observation is that the DA adduct formed with **ScpK** allows AZ1508 to occupy the space normally taken by sugars, thus minimizing its exposure to solvent and decreasing the apparent hydrophobicity of the molecule. Furthermore, N297C did not produce homogeneous ADCs, as observed by SDS-PAGE analysis of intact antibodies, which indicated a heavy chain–light chain dimer (~75 kDa). The presence of this band indicates that native interchain disulfides are not correctly formed, likely due to scrambling with the engineered cysteine. This finding was corroborated with reduced mass spectrometry results for N297C ADCs, which showed under- and over-conjugated heavy chains. Position N297 also revealed differences in propensity to aggregate, where N297ScpK DA-ADCs retained high monomer content after drug attachment whereas N297C ADCs slowly aggregated upon storage (4°C in PBS; data

not shown). Thus, position N297 represents a limitation of cysteine engineering to produce homogeneous ADC product that can be overcome by conjugating drug through **ScpK**.

2.13 Stability of Site-Specific DA-ADCs in Serum

Arguably, one of the most important features of an ADC is conjugate stability, where a stable linker can improve its pharmacological properties.[16] Stability of DA-ADCs was evaluated by incubation in reconstituted rat serum for 7 days at 37°C, followed by recovery by immunocapture, and analysis by mass spectrometry to determine the amount of drug attached to the antibody (**Figure 2.13**). Analogous cysteine-engineered ADCs were subjected to the same procedure for comparison of the DA adduct and thiosuccinimide linkages. Rat serum was selected due to the presence of enzymes in mouse serum that cleave peptide linkers[75] and deacetylate tubulysin,[114] which complicates the tracking of drug deconjugation. DA-ADCs prepared at all sites (S239ScpK, K274ScpK, and N297ScpK) with all three maleimide-drugs (AZ1508, vcMMAE, and SG3249) exhibited no detectable drug loss after incubation in rat serum. In contrast, cysteine-linked ADCs prepared with AZ1508 and subjected to the same conditions exhibited variable stability that was dependent on amino acid position. S239C-AZ1508 was the most stable ADC, exhibiting ~10% drug loss. This was probably due to the cysteine's high apparent thiol pK_a, which causes a stabilizing thiosuccinimide hydrolysis, and/or to the buried nature of this position.[115] The other sites examined (K274C-AZ1508 and N297C-AZ1508) lost 30–40% of the drug after 7 days. These results highlight a possible advantage of ADCs prepared with **ScpK**, as conjugate stability appears to be high regardless of the conjugation position.

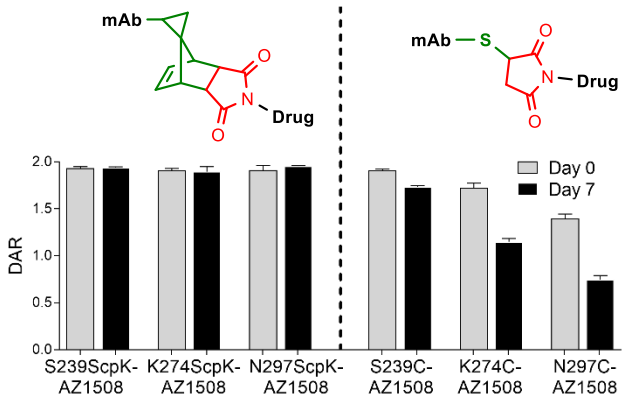

Figure 2.13 Stability of DA- and cysteine-linked ADCs of AZ1508 in rat serum after incubation at 37°C for 7 days.

2.14 Activity of Site-Specific DA-ADCs in vitro and in vivo

Cell-killing activities of ADCs were assessed *in vitro* using EphA2 receptor-positive PC3 cells. ADCs prepared and evaluated in this study include drug-linkers with two different mechanisms of action: vcMMAE and AZ1508 act to prevent tubulin polymerization,[75,116] and SG3249 crosslinks DNA.[117] Regardless of the drug's mechanism of action, DA-ADCs performed similarly to cysteine-linked ADCs and had low 50% effective concentrations (EC_{50}s) (**Table 2.5**). DA-linked ADCs produced with a non-binding isotype control antibody (R347) showed very low activities (EC_{50} = 2,748 to >64,000 ng/mL; data not shown), confirming target-specific activity. These promising ADC activities observed *in vitro* led us to investigate DA-ADC activity *in vivo*.

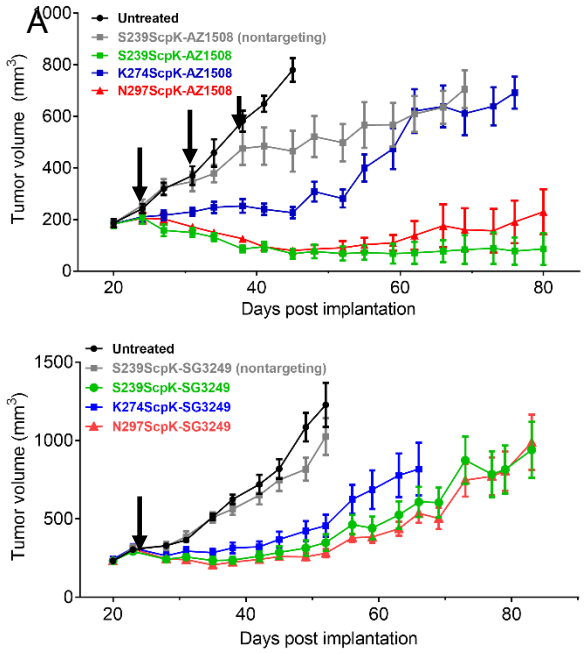

Figure 2.14 Activity of DA-ADCs in PC3 xenograft tumor models in vivo. (A) AZ1508 DA-ADCs (3 mg/kg, three doses), (B) SG3249 DA-ADCs (1 mg/kg, one dose). Data are plotted as the average ± standard deviation, n = 8 (AZ1508) or n = 10 (SG3249). Dosing time points are indicated by black arrows.

DA-ADC activity *in vivo* was assessed in mice bearing solid-tumor xenograft models generated with PC3 cells and animals were dosed with DAR-2 ADCs prepared with AZ1508 or SG3249 drug-linkers (**Figure 2.14**). For AZ1508 ADCs, drug was dosed once weekly at 3 mg/kg for 3 weeks,[118] which resulted in complete tumor regression for positions S239 and N297 but not K274. Further investigation of ADC stability in mouse serum indicated that antitumor activity correlated with the extent of deacetylation in mouse serum. In the mouse serum stability study, K274ScpK-AZ1508 was completely deacetylated after 7 days, whereas N297ScpK-AZ1508 and S239ScpK-AZ1508 showed 65% and 35% deacetylation, respectively. This deacetylation likely reduced the potency of the ADC *in vivo*.[114,119] Tubulysin deacetylation is caused by a mouse serum-specific enzyme and impacts drug-linkers conjugated at solvent-exposed positions (i.e., K274).[114] SG3249 DA-ADCs were evaluated in the same PC3 tumor model after a single dose of 1 mg/kg, which resulted in

tumor regression for ~50 days for S239ScpK-SG3249 and N297ScpK-SG3249 and tumor stasis for ~40 days for K274ScpK-SG3249. As with AZ1508 DA-ADCs, the K274ScpK-SG3249 was less potent than the other sites examined. Reduced activity was probably due to cleavage of the Val-Ala dipeptide in mouse serum, which reduced ADC activity in a similar study evaluating SG3249 ADCs prepared at the exposed position T289C.[85] Altogether, DA-ADCs prepared with two different classes of drug–linkers were potent inhibitors of tumor growth in receptor-positive cells *in vivo*.

2.15 Synthesis of Cyclopentadiene-Containing ncAA, CpK

The cyclopentadiene NHS ester **2b** was the diene we examined with the fastest DA reaction with maleimide. Cyclopentadiene is a sword without a hilt – there is no safe way to grasp it. Monosubstituted Cp are obtained as a mixture of interconverting isomers[56] that may have different reactivity, and they are able to dimerize at room temperature. They also pose a synthetic challenge when selecting protecting groups, as Cp is not stable to acidic conditions or hydrogenation. Nevertheless, with faster kinetics than **ScpK**, a Cp-containing ncAA (**CpK, Figure 2.15**) would be a desirable diene to genetically encode into antibodies.

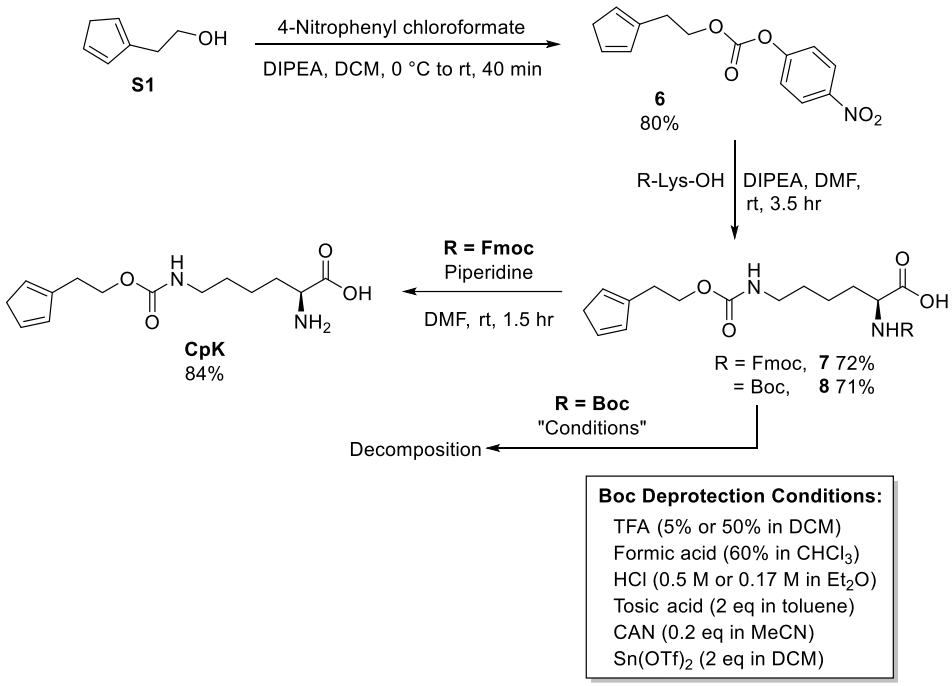

Figure 2.15 Synthesis of cyclopentadiene-containing ncAA CpK. Only the 2-substituted isomer of cyclopentadiene is shown.

We began the synthesis of **CpK** with the alcohol **S1**. Direct coupling of the alcohol with triphosgene to Boc-Lys-OH only proceeded low yield (38%). To avoid the toxicity of phosgene-derivatives, when scaling up and optimizing the reaction we decided to synthesize the activated carbonate **6**, as this synthetic route would allow its purification using column chromatography. **6** was produced in good yield and can be stored for several weeks at -20 °C with no signs of dimerization.

With the activated carbamate in hand, a coupling with a copper lysinate complex was attempted, but isolation of **CpK** after treatment with 8-hydroxyquinoline or EDTA was not fruitful. This reaction was not pursued further because of concerns of copper impurities in the ncAA. The reaction of **6** with Boc-Lys-OH provided the Boc-protected **8** in 71% yield, but efforts to remove the Boc group led to decomposition of the Cp ring.

With the copper- and Boc-protected lysine derivatives unsuccessful, another protecting group had to be selected. The Cp ring is not stable to acid or hydrogenation, and the carbamate

is not stable to reduction or basic hydrolysis. The Fmoc-protected lysine derivative was selected as it can be cleaved with mild base and it is commercially available. The reaction of **6** with Fmoc-Lys-OH produces the **8** in 72% yield. Many column chromatography conditions were attempted to separate p-nitrophenol from **8**, and Hexane:EtOAc 3:1 was found to selectively elute this impurity. After column chromatography and removal of solvent it was found that the product was contaminated with DMF and AcOH. Many attempts at azeotropically removing the residual solvent under high vacuum failed and we chose to use the material directly in the next step.

The Fmoc protecting group can be deprotected using piperidine in DMF to obtain **CpK** in 84% yield. Using DCM rather than DMF led to significant contamination of DCM-piperidine substitution products.[120] CpK has poor solubility in commonly used deuterated solvents – a drop of TFA can be added to increase solubility, but leads to decomposition after several hours. All 5 Cp protons in **CpK** exchange with deuterium when dissolved in a strongly basic D_2O solution; if performed in basic tritiated water, a radiolabelled ^{3}H-**CpK** could theoretically be obtained.

The successful incorporation of the carbamate **CpK** encouraged us to synthesize the amide-derivative **CpbK** (**Figure 2.16**). The synthesis is essentially the same as CpK, but rather than using the carbonate **6**, we used the NHS-ester **2b**.

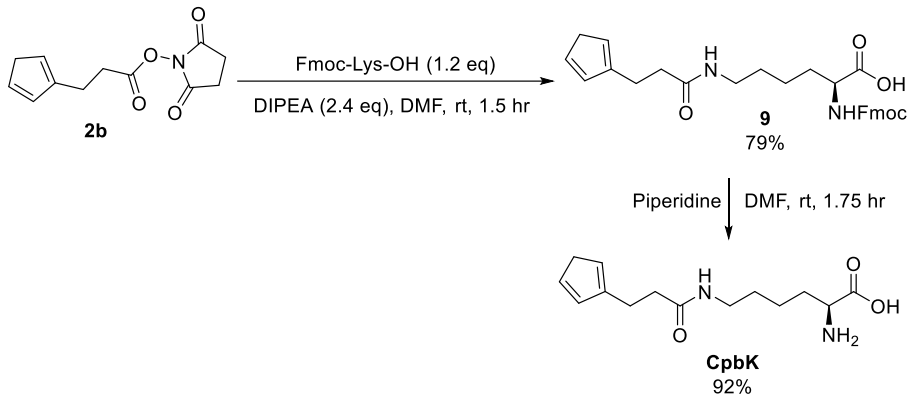

Figure 2.16 Synthesis of the amide derivative of cyclopentadiene-containing ncAA CpbK. Only the 2-substituted isomer of cyclopentadiene is shown.

Preliminary results indicate that the genetic encoding of **CpbK** was not successful. The majority of ncAAs that are successfully incorporated contain a lysine with a carbamate linkage[101] – these results confirmed that trend and **CpbK** was not pursued further.

2.16 Genetically Encoded Cyclopentadiene CpK

The incorporation of **CpK** into antibodies proceeds in a similar fashion to **ScpK**. Preliminary results have shown that the stability of the Cp is highly position-dependent (**Figure 2.17**). Because antibodies are symmetrical species composed of two heavy chains and two light chains, two dienes are incorporated in each antibody.

The mutation site K274 (Kabat numbering) was well-behaved and produced antibodies with two **CpK** incorporated. These K274CpK antibodies reacted with maleimide at ~70 $M^{-1}s^{-1}$, approximately 21 times faster than our **ScpK** diene (~3.3 $M^{-1}s^{-1}$). This represents a substantial improvement over our spirocyclopentadiene and will facilitate the production of DA-ADCs faster and with fewer equivalents of expensive maleimide-drug payload.

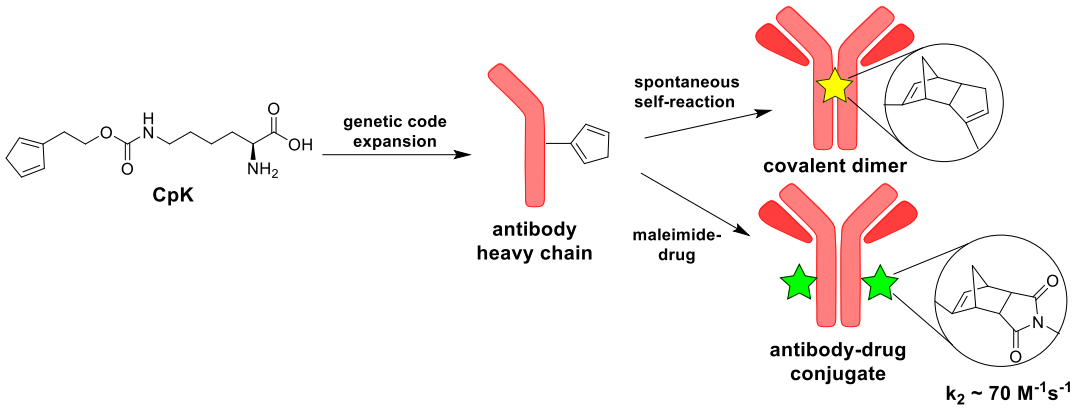

Figure 2.17 Overview of CpK incorporation into mAbs. The Cp can undergo self-stapling or be used in the DA reaction with maleimide–drugs.

Surprisingly, we found that the mutation site S239 (Kabat numbering) produced heavy chain-heavy chain dimers that are unreactive with maleimide. This occurs through dimerization of Cp[121] producing strong bonds that undergo a rDA at 210 °C.[122] The distance between the alpha carbons of S239 is approximately 20 Å, bringing the two dienes in close proximity. The rate of dimerization, the effect of water, and the effects of acidic/basic residues is currently under investigation. Investigations are underway to apply this ligation to stabilize single-chain variable fragment–fragment crystallizable (scFv-FC) fusion protein.

In summary, we have described the synthesis and genetic incorporation of the Cp ncAA **CpK**. With judicious selection of mutation site, we have access to two unique DA reactivities: conjugation with maleimide, or self-stapling. The conjugation with maleimide–drugs produces DA-ADCs quickly, forming a stable linkage with commercially available and clinically relevant payloads. To our knowledge, CpK is the first example of a proximity-driven self-stapling of a ncAA.

2.17 Synthesis of Pentamethylcyclopentadiene-Containing ncAA, Cp*K

With the successful synthesis and genetic incorporation of ncAA derivatives of compounds **2b** and **3** (**ScpK** and **CpK**), we also wanted to explore a ncAA based on

pentamethylcyclopentadiene (Cp*), **Cp*K**. We began the synthesis with (1,2,3,4,5-pentamethylcyclopenta-2,4-dienyl)methanol, forming the activated carbonate **10** (**Figure 2.18**). After coupling to Fmoc-Lys-OH and deprotection in a similar fashion to our other ncAAs, Cp*K was obtained in a somewhat lower yield. We believe this to be due to the greasy nature of the Cp* – the increased solubility in diethyl ether caused much of the **Cp*K** to be washed away during purification.

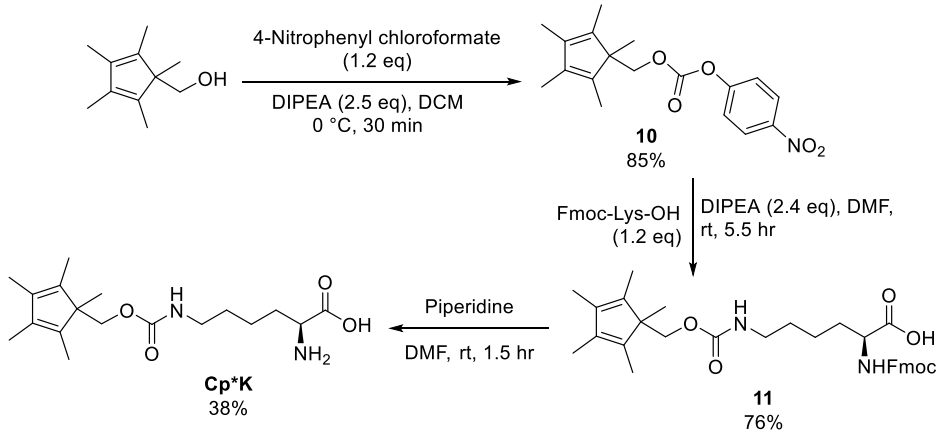

Figure 2.18 Synthesis of the pentamethylcyclopentadiene-containing ncAA Cp*K.

Next the genetic incorporation of **Cp*K** was attempted; the compound's insolubility in acidic or basic buffer made the preparation of stock solutions challenging. Attempts to produce antibodies containing **Cp*K** resulted in no incorporation, with no whole antibodies being produced. Other large and greasy ncAAs have been successfully genetically encoded in *E. coli*,[123,124] but they have not yet been applied to the production of antibodies. **Cp*K** may genetically encode proteins in *E. coli*, but this ncAA was not pursued further.

2.18 Strain-Promoted DA Reaction of Cyclopropene and Cyclopentadiene

Cyclopentadiene is a privileged structure for the DA reaction[33] due to its sterically unhindered, electron-rich, strained diene with geometry near the DA reaction transition state.[125] Cyclopentadiene's reaction partner is typically electron-withdrawn (maleimides,

acrylates, etc), but a less explored reactivity is with cyclopropenes.[126] The reaction between unsubstituted cyclopentadiene and 1,2-unsubstituted cyclopropene[127,128] and 1-methylcyclopropene[129] are known (**Figure 2.19**).

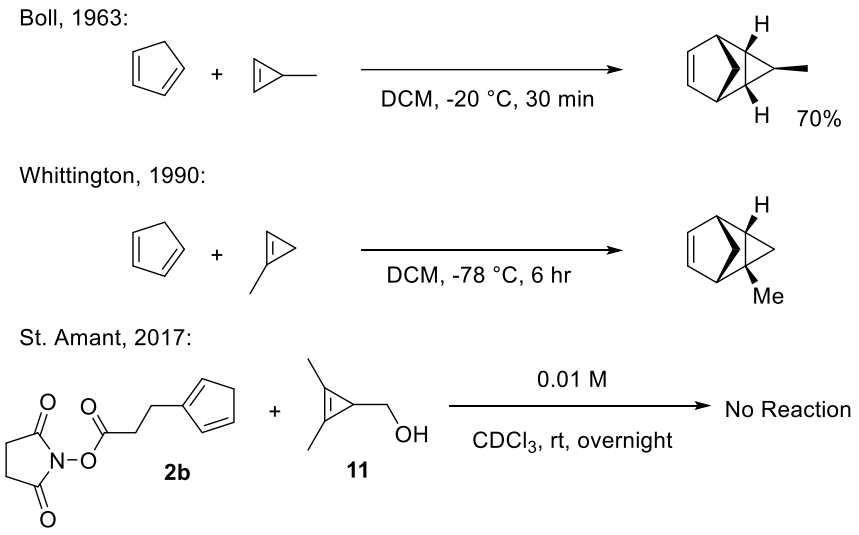

Figure 2.19 Reaction of 1,2-unsubstituted, monomethyl, and dimethyl cyclopropenes with cyclopentadienes

We hypothesized that because Whittington's 1-methylcyclopropene reacted with cyclopentadiene at a lower temperature than Boll's 1,2-unsubstituted cyclopropene (–78 vs –20 °C), a 1,2-dimethylcyclopropene would react with kinetics sufficient for bioconjugation. To test this idea, we synthesized **11** from the rhodium(II) acetate catalyzed reaction of ethyl diazoacetate with dimethyl acetylene, followed by DIBAL reduction.[130] With **11** in hand, we attempted to measure reaction kinetics with our monosubstituted cyclopentadiene **2b** but found no reaction at the concentrations examined. The reaction rates for cyclopropene–cyclopentadiene conjugation are not reported;[131] the synthesis and screening of a library of small molecule cyclopropenes would aid in the development of this relatively unexplored chemistry. The successful realization of this desired reactivity with a cyclopropene partner in combination with **ScpK** or **CpK** could enable a new bioorthogonal ligations through the

strain-promoted DA reaction. The incorporation of this cyclopropene into a ncAA[132] would enable its incorporation site selectively.

2.19 Reaction of Cyclopentadiene with Fullerene

With a family of electron-rich dienes in hand, we also wanted to explore their use in other potentially valuable areas. For example, the 1996 Nobel Prize in Chemistry was awarded to Kroto, Curl and Smalley for the discovery of the C_{60} allotrope of carbon, fullerene. Fullerene has been explored in materials for its interesting electronic and optical properties such as in solar cells. To selectively functionalize fullerene, a chemical handle such as an ester group is added; the most common mono-functionalized fullerene was developed by the Wudl group using a cyclopropanation reaction with a diazo-containing ester.[133] The DA reaction between fullerene and cyclopentadiene has been known since the 90s as well, where an olefin in C_{60} acts as a dienophile.[134,135] This strategy has been applied to C_{60}-PEG conjugates by the Barner-Kowollik group to increase the solubility of the notoriously insoluble fullerene.[136] The preparation of NHS-esters of fullerene for bioconjugation is of interest to probe its biological activity; these compounds are typically synthesized in 3 steps from fullerene (cyclopropanation, ester hydrolysis, and NHS-ester formation).[137] With Cp-NHS ester **2b** in hand we wanted to explore a one-step mono-functionalization of fullerene (**Figure 2.20**).

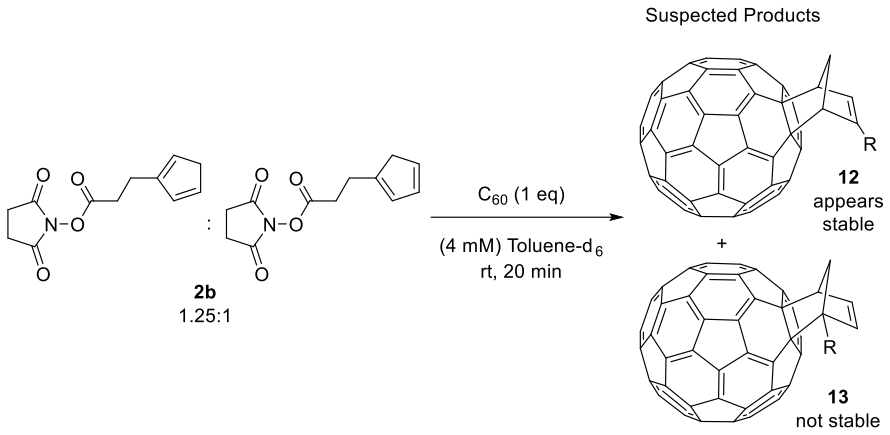

Figure 2.20 Reaction of cyclopentadiene to produce fullerene-NHS esters through the DA reaction.

We performed a preliminary NMR study to examine the feasibility of this strategy. The reaction was fast in deuterated toluene (~50% conversion of **2b** after 20 min), but several products were obtained. After 3 hr, one of the DA adducts that we observed at 20 min (we suspect **13**) was completely consumed. It may be possible that more complicated rearrangements or dimerization may be occurring, and further optimization is required.

2.20 Conclusion

In summary, we have developed the first systematic investigation of a normal-demand DA reaction to produce ADCs. This method involves easily synthesized diene compounds, facile antibody incorporations, and was studied both *in vitro* and *in vivo*. Of the five electron-rich dienes that were incorporated onto mAbs, four underwent conjugation with maleimide with rates viable for ADC production. To our knowledge, this is the first systematic investigation of normal-demand DA reaction rates on the surface of antibodies. In general, cycloaddition rates for these reactions were found to be comparable with those of ligation reactions such as the strain-promoted or copper-catalyzed azide–alkyne cycloaddition. It was also demonstrated that enhancement of the DA reaction rate in water is a key factor for bringing this reaction into the realm of practical application. An approximately 300–1,500 fold rate acceleration was

determined for the aqueous maleimide–diene reaction, which supports the potential for the application of this ligation approach to a wide range of bioconjugation strategies. DAADCs produced with cyclopentadiene **2b** and 3-methoxyfuran **5** are more stable to deconjugation than is the classic thiol–maleimide linkage in serum, which is desirable for production of clinical compounds that require predictable properties. Functional DAADCs of trastuzumab have activities in vitro and in vivo that are comparable to those of thiol–maleimide ADCs, demonstrating that attaching drugs to antibodies through a DA linkage does not lead to drastic loss of drug function.

A key design feature of the DA conjugation strategy as compared with other methodologies is its capitalization on the large number of commercially available maleimide compounds, such as maleimide–drugs, fluorophores, and chelators. This avoids the need to develop new entities to facilitate bioconjugation reactions and represents a key step toward a general DA bioconjugation method with maleimide. Moreover, in comparison with the thiol-maleimide Michael addition reaction, which is the most widely used reaction with maleimides, the DA reaction avoids the technical challenges associated with generating free thiols. Overall, we have shown that the normal-demand DA reaction strategy can serve as a useful bioconjugation platform when fast kinetics and high conjugate stability are required.

The ncAA work demonstrates the feasibility of applying the classic DA reaction for production of therapeutically relevant bioconjugates under mild aqueous conditions. Evaluation of diene chemistry in the context of ncAAs and ADCs allowed insight into the biocompatibility, stability, reactivity with maleimide, and ultimately translation of the technology *in vivo* using an anti-cancer drug. Incorporation of **ScpK** into antibodies using genetic code expansion technology demonstrated that the electron-rich diene was stable in

mammalian cells and produced proteins capable of rapid and selective coupling with maleimides in a one-step conjugation protocol. This "plug-and-play" approach is attractive for production of next-generation, site-specific ADCs and other protein conjugates with widely available maleimide compounds. In the case of ADCs, developing reactive ncAAs to match current drug-linker chemistries could potentially simplify the path to commercialization without redevelopment of drug–payloads. Furthermore, changing the maleimide reaction partner from a cysteine thiol to **ScpK** resulted in irreversible conjugates that were consistently stable in serum. This represents an improvement over thiosuccinimide chemistry that exhibits variable stability. Finally, we demonstrated that linking maleimide–drugs through conjugation with **ScpK** yields DA-ADCs that are potent both *in vitro* and *in vivo*, suggesting that advantages in production and stability do not come at the cost of reduced activity.

We also explored the potential of the mono-substituted cyclopentadiene ncAA **CpK**. The DA reaction rate with maleimide was accelerated compared to **ScpK**, but its incorporation was site-dependent. When two **CpK** amino acids are in close proximity on the antibody they undergo a self-stapling dimerization, making **CpK** the first self-stapling ncAA; this reactivity is currently being explored to stabilize antibody mimetics. Moreover, we described the synthesis of the ncAAs **CpbK** and **Cp*K**, which are an amide- and pentamethyl-derivatives of **CpK**. Unfortunately, these were not successfully incorporated into proteins through genetic encoding. Finally, we briefly screened cyclopropene and fullerene as reaction partners for cyclopentadiene. Overall, the DA conjugation strategies described here could be widely utilized across the life sciences to produce stable stochastic or homogeneous bioconjugates using readily available maleimide-payloads.

2.21 Experimental

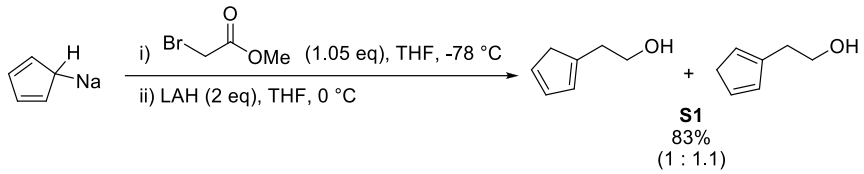

2-(Cyclopenta-1,3-dienyl)ethanol & 2-(cyclopenta-1,4-dienyl)ethanol (**S1**):

A solution of methyl bromoacetate (6.0 mL, 63 mmol, 1.05 equiv) in THF (60 mL) was cooled to -78 °C. A sodium cyclopentadienylide solution (2 M in THF, 30 mL, 60 mmol, 1 equiv) was added dropwise over 10 min and the reaction was stirred a further 2 h at -78 °C. The reaction was quenched with H_2O (6 mL) and silica gel (6 g) then allowed to warm to rt. The reaction mixture was filtered through a plug of silica with DCM (100 mL) and the solvent removed to yield the methyl ester which was used directly in the next reaction. A solution of lithium aluminum hydride (4.55 g, 120 mmol, 2 equiv) in THF (300 mL) was cooled to 0 °C. The crude methyl ester (~60 mmol) was dissolved in THF (10 mL) and added dropwise in 4 portions over 1 h at 0 °C then stirred for a further 2 h at rt. The reaction mixture was cooled to 0 °C and carefully quenched with H_2O (20 mL), NaOH (4 M in H_2O, 5 mL), then H_2O (20 mL). The reaction mixture was filtered, rinsed with Et_2O (100 mL), then transferred to a separatory funnel. Brine (100 mL) was added then extracted with Et_2O (3 x 100 mL). The organic layers were combined, washed with brine (100 mL), dried over $MgSO_4$, filtered, and the solvent removed. The residue was filtered through a silica plug (EtOAc:Hexane, 2:1, 200 mL) and the solvent removed to yield **S1** (5.45 g, 83% over two steps) as an amber oil. Dimerization of the cyclopentadiene occurs slowly when stored at -20 °C, for long term storage **S1** was frozen in a matrix of benzene. Spectral data matched that of literature reported data.[138] **S1**: Rf (Hexane:EtOAc, 4:1): 0.14; ^{1}H NMR (400 MHz, $CDCl_3$) δ 6.52 - 6.10 (m, 3 H), 3.88 - 3.71 (m, 2 H), 3.07 - 2.89 (m, 2 H), 2.77 - 2.57 (m, 2 H), 1.52 (br.s., 2 H) ppm; ^{13}C

NMR (100 MHz, $CDCl_3$) δ 145.3, 143.2, 134.5, 134.2, 132.4, 131.5, 128.7, 128.4, 62.2, 61.6, 43.4, 41.6, 34.0, 33.2 ppm.

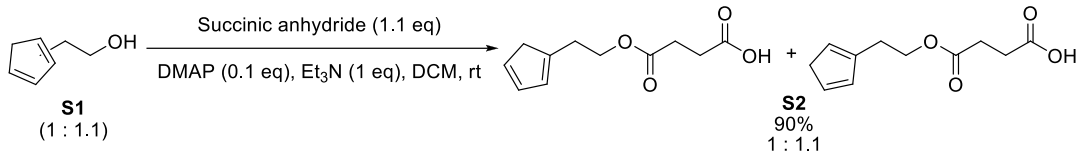

4-(2-(Cyclopenta-1,3-dienyl)ethoxy)-4-oxobutanoic acid & 4-(2-(cyclopenta-1,4-dienyl)ethoxy)-4-oxobutanoic acid (**S2**):

To a solution of **S1** (0.33 g, 3.0 mmol, 1 equiv) in DCM (1.5 mL) in a vial was added Et_3N (0.42 mL, 3.0 mmol, 1 equiv), 4-dimethylaminopyridine (37 mg, 0.3 mmol, 0.1 equiv), and succinic anhydride (0.33 g, 3.3 mmol, 1.1 equiv). The reaction was capped under an atmosphere of air and stirred at rt for 1 h, then transferred to a separatory funnel with DCM (50 mL). The organic layer was washed with HCl (1 M in H_2O, 50 mL) then H_2O (50 mL). The organic layer was dried over $MgSO_4$, filtered, and the solvent removed to yield **S2** (0.57 g, 90%) as a tan powder. **S2**: Rf (EtOAc): 0.67; ^{1}H NMR (400 MHz, $CDCl_3$) δ 11.49 (br.s., 1 H), 6.48 - 6.05 (m, 3 H), 4.33 - 4.21 (m, 2 H), 2.98 - 2.89 (m, 2 H), 2.83 - 2.52 (m, 6 H) ppm; ^{13}C NMR (100 MHz, $CDCl_3$) δ 178.4, 172.0, 144.3, 142.3, 134.2, 134.0, 132.2, 131.4, 128.3, 127.9, 64.3, 63.9, 43.4, 41.4, 29.7, 29.0, 28.8, 28.8 ppm; IR (ATR) 2934, 2671, 2568, 1720, 1706, 1693, 1418, 1358, 1235, 1178 cm^{-1}; HRMS (CI) Exact mass cald. for $C_{11}H_{13}O_4$ $[M-H]^+$: 209.0814, found: 209.0815.

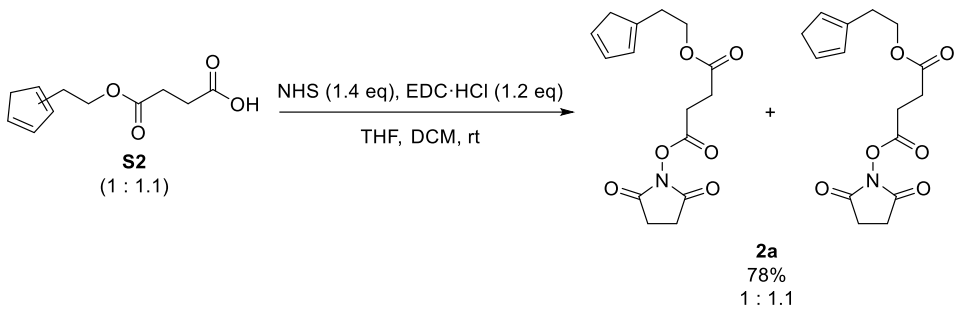

2-(Cyclopenta-1,3-dienyl)ethyl 2,5-dioxopyrrolidin-1-yl succinate & 2-(cyclopenta-1,4-dienyl)ethyl 2,5-dioxopyrrolidin-1-yl succinate (**2a**):

To a solution of **S2** (0.42 g, 2.0 mmol, 1 equiv) in THF (10 mL) in a vial was added *N*-hydroxysuccinimide (0.32 g, 2.8 mmol, 1.4 equiv), *N*-(3-dimethylaminopropyl)-*N*′-ethylcarbodiimide hydrochloride (0.46 g, 2.4 mmol, 1.2 equiv) and DCM (5 mL). The reaction was capped under an atmosphere of air and stirred at rt overnight. The solvent was removed and the residue was subjected to flash column chromatography (Hexane:EtOAc, 1:1) to yield **2a** (0.48 g, 78%) as a clear, viscous oil. At room temperature **2a** will dimerize, but it is stable for several months when stored at -20 °C. **2a**: Rf (Hexane:EtOAc, 1:1): 0.33; ^{1}H NMR (400 MHz, $CDCl_3$) δ 6.49 - 6.06 (m, 3 H), 4.37 - 4.25 (m, 2 H), 3.03 - 2.90 (m, 4 H), 2.85 (br.s., 4 H), 2.80 - 2.68 (m, 4 H) ppm; ^{13}C NMR (125 MHz, $CDCl_3$) δ 170.8, 168.9, 167.6, 144.3, 142.3, 134.2, 134.1, 132.3, 131.4, 128.4, 128.0, 64.5, 64.2, 43.5, 41.4, 29.7, 29.0, 28.7, 26.2, 25.5 ppm; IR (ATR) 2953, 1814, 1783, 1731, 1362, 1201, 1068, 993 cm^{-1}; HRMS (CI) Exact mass cald. for $C_{15}H_{16}NO_6$ $[M-H]^+$: 306.0978, found: 306.0981.

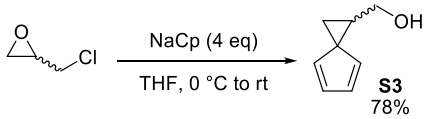

Spiro[2.4]hepta-4,6-dien-1-ylmethanol (**S3**):

Sodium cyclopentadienide (2 M solution in THF, 10 mL, 20 mmol, 4 equiv) was added to THF (40 mL) and cooled to 0 °C. (±)-Epichlorohydrin (0.39 mL, 5.0 mmol, 1 equiv) was added dropwise and the reaction was stirred at 0 °C for 1.5 h then a further 2 h at rt. The

reaction was quenched with H_2O (40 mL) then transferred to a separatory funnel. A saturated solution of $NaHCO_3$ in H_2O (40 mL) was added then extracted with Et_2O (40 mL). The organic layer was washed with brine (40 mL), dried over $MgSO_4$, filtered, and the solvent removed. The residue was subjected to flash column chromatography (Hexane:EtOAc, 2:1) to yield **S3** (0.48 g, 78%) as a brown oil. Spectral data matched that of literature reported data.[139] **S3**: Rf (Hexane:EtOAc, 2:1): 0.22; ^{1}H NMR (500 MHz, $CDCl_3$) δ 6.64 (td, *J* = 1.6, 5.1 Hz, 1 H), 6.57 - 6.43 (m, 1 H), 6.34 - 6.21 (m, *J* = 1.0, 1.0, 5.2 Hz, 1 H), 6.12 (td, *J* = 1.7, 5.1 Hz, 1 H), 4.08 - 3.88 (m, 1 H), 3.59 (dd, *J* = 8.8, 11.7 Hz, 1 H), 2.51 - 2.37 (m, *J* = 6.0, 7.3, 8.6, 8.6 Hz, 1 H), 1.87 (dd, *J* = 4.3, 8.7 Hz, 1 H), 1.69 (dd, *J* = 4.4, 7.0 Hz, 1 H), 1.57 (br.s., 1 H) ppm; ^{13}C NMR (125 MHz, $CDCl_3$) δ 139.4, 133.9, 131.7, 128.6, 64.9, 41.9, 30.0, 17.6 ppm.

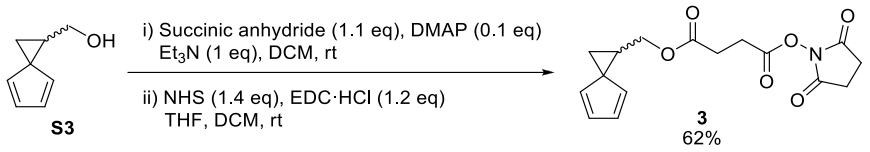

2,5-Dioxopyrrolidin-1-yl spiro[2.4]hepta-4,6-dien-1-ylmethyl succinate (**3**):

DCM (1.5 mL) was added to a vial containing **S3** (0.37 g, 3.0 mmol, 1 equiv). Et_3N (0.42 mL, 3.0 mmol, 1 equiv), 4-dimethylaminopyridine (37 mg, 0.30 mmol, 0.1 equiv) and succinic anhydride (0.33 g, 3.3 mmol, 1.1 equiv) were added, the reaction capped under an atmosphere of air, and stirred at rt 1.75 h. The reaction mixture was poured into a separatory funnel with DCM (50 mL) and washed with aqueous HCl (1 M, 50 mL). The aqueous layer was extracted with DCM (50 mL), the organic layers combined, dried over Na_2SO_4, filtered, and the solvent removed to yield acid **S4** which was used directly in the next reaction. **S4**: Rf (EtOAc): 0.56; ^{1}H NMR (400 MHz, $CDCl_3$) δ 10.60 (br.s., 1 H), 6.57 (td, *J* = 1.9, 5.3 Hz, 1 H), 6.50 (td, *J* = 1.8, 5.1 Hz, 1 H), 6.21 (td, *J* = 1.7, 5.2 Hz, 1 H), 6.07 (td, *J* = 1.8, 5.1 Hz, 1 H), 4.37 (dd, *J* = 7.4, 11.7 Hz, 1 H), 4.20 (dd, *J* = 7.0, 11.7 Hz, 1 H), 2.74 - 2.57 (m, 4 H), 2.42 (quin, *J* = 7.8

Hz, 1 H), 1.85 (dd, *J* = 4.5, 8.4 Hz, 1 H), 1.69 (dd, *J* = 4.3, 7.0 Hz, 1 H) ppm. THF (10 mL) was added to a vial containing **S4** (~3 mmol). *N*-hydroxysuccinimide (0.48 g, 4.2 mmol, 1.4 equiv), *N*-(3-dimethylaminopropyl)-*N′*-ethylcarbodiimide hydrochloride (0.69 g, 3.6 mmol, 1.2 equiv) and DCM (5 mL) were added, the reaction capped under an atmosphere of air, and stirred at rt overnight. The solvent was removed and the residue was subjected to flash column chromatography (Hexane:EtOAc, 1:1) to yield **3** (0.59 g, 62% over two steps) as a colorless, viscous oil. **3**: Rf (Hexane:EtOAc, 1:1): 0.34; ^{1}H NMR (400 MHz, $CDCl_3$) δ 6.56 (td, J = 1.8, 5.1 Hz, 1 H), 6.48 (td, J = 1.8, 5.1 Hz, 1 H), 6.21 (td, J = 1.6, 3.4 Hz, 1 H), 6.06 (td, J = 1.6, 3.4 Hz, 1 H), 4.36 (dd, J = 7.4, 11.7 Hz, 1 H), 4.21 (dd, J = 7.4, 11.7 Hz, 1 H), 2.93 (t, J = 7.0 Hz, 2 H), 2.83 (s, 4 H), 2.73 (t, J = 7.4 Hz, 2 H), 2.42 (quin, J = 7.6 Hz, 1 H), 1.83 (dd, J = 4.3, 8.6 Hz, 1 H), 1.68 (dd, J = 4.5, 6.8 Hz, 1 H) ppm; ^{13}C NMR (100 MHz, $CDCl_3$) δ 170.8, 168.9, 167.6, 138.8, 134.3, 131.2, 129.0, 66.6, 41.5, 28.6, 26.2, 25.5, 25.1, 17.3 ppm; IR (ATR) 2945, 1814, 1783, 1732, 1366, 1202, 1068 cm^{-1}; HRMS (EI) Exact mass cald. for $C_{16}H_{17}NO_6$ $[M]^+$: 319.1056, found: 319.1051.

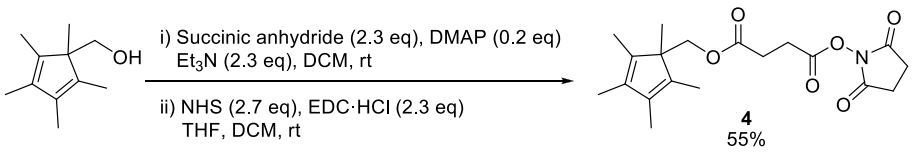

2,5-Dioxopyrrolidin-1-yl (1,2,3,4,5-pentamethylcyclopenta-2,4-dienyl)methyl succinate (**4**):

DCM (8 mL) was added to a vial containing (1,2,3,4,5-pentamethylcyclopenta-2,4-dienyl)methanol[140] (0.33 g, 2.0 mmol, 1 equiv). Et_3N (0.64 mL, 4.6 mmol, 2.3 equiv), 4-dimethylaminopyridine (46 mg, 0.38 mmol, 0.2 equiv) and succinic anhydride (0.46 g, 4.6 mmol, 2.3 equiv) were added, the reaction capped under an atmosphere of air, and stirred at rt overnight. The reaction was quenched with H_2O (1 mL) then poured into a separatory

funnel. HCl (1 M, 50 mL) was added and extracted with DCM (2 x 50 mL). The organic layers were combined, washed with brine (50 mL), dried over Na_2SO_4, filtered, and the solvent removed to yield the acid **S5** which was used directly in the next reaction. **S5**: Rf (EtOAc): 0.24; ^{1}H NMR (400 MHz, $CDCl_3$) δ 3.98 (s, 2 H), 2.64 - 2.59 (m, 2 H), 2.59 - 2.54 (m, 2 H), 1.76 (s, 6 H), 1.74 (s, 6 H), 0.95 (s, 3 H) ppm. THF (10 mL) was added to a vial containing **S5** (~2 mmol). *N*-hydroxysuccinimide (0.61 g, 5.3 mmol, 2.7 equiv), *N*-(3-dimethylaminopropyl)-*N′*-ethylcarbodiimide hydrochloride (0.87 g, 4.6 mmol, 2.3 equiv) and DCM (6 mL) were added, the reaction capped under an atmosphere of air, and stirred at rt overnight. The solvent was removed and the residue was subjected to flash column chromatography (Hexane:EtOAc, 3:1 → 2:1) to yield **4** (0.39 g, 55% over two steps) as a white solid. **4**: Rf (Hexane:EtOAc, 7:3): 0.27; ^{1}H NMR (400 MHz, $CDCl_3$) δ 4.00 (s, 2 H), 2.89 (t, *J* = 6.7 Hz, 2 H), 2.85 (br.s., 4 H), 2.67 (t, *J* = 7.8 Hz, 2 H), 1.77 (s, 6 H), 1.74 (s, 6 H), 0.95 (s, 3 H) ppm; ^{13}C NMR (100 MHz, $CDCl_3$) δ 170.7, 168.9, 167.6, 138.4, 135.0, 68.2, 55.3, 28.6, 26.2, 25.5, 16.8, 11.0, 10.1 ppm; IR (ATR) 2973, 2935, 1815, 1782, 1729, 1208, 1089, 1069, 967 cm^{-1}; HRMS (EI) Exact mass cald. for $C_{19}H_{25}NO_6$ $[M]^+$: 363.1682, found: 363.1676.

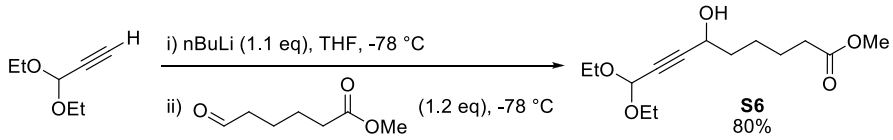

Methyl 9,9-diethoxy-6-hydroxynon-7-ynoate (**S6**):

3,3-Diethoxyprop-1-yne (0.72 mL, 5.0 mmol, 1 equiv) was added to THF (15 mL) then cooled to -78 °C. nBuLi (2.33 M in hexanes, 2.4 mL, 5.5 mmol, 1.1 equiv) was added dropwise then the reaction mixture stirred a further 30 min at -78 °C. Methyl 6-oxohexanoate (0.87 g, 6.0 mmol, 1.2 equiv) dissolved in THF (5 mL) was added dropwise, then the reaction mixture stirred at -78 °C for 1 h. The reaction mixture was poured into a separatory funnel containing

a saturated aqueous solution of sodium bicarbonate (100 mL) then extracted with Et_2O (2 x 50 mL). The combined organic layers were washed with brine (50 mL), dried over $MgSO_4$, filtered, the solvent removed, and the residue subjected to flash column chromatography (Hexane:EtOAc, 2:1) to yield **S6** (1.1 g, 80%) as a clear and colorless oil. **S6**: Rf (Hexane:EtOAc, 6:4): 0.41; ^{1}H NMR (400 MHz, $CDCl_3$) δ 5.28 (d, *J* = 1.6 Hz, 1 H), 4.47 - 4.36 (m, *J* = 3.5 Hz, 1 H), 3.76 - 3.67 (m, 2 H), 3.67 - 3.63 (m, 3 H), 3.56 (qd, *J* = 7.0, 9.4 Hz, 2 H), 2.34 - 2.27 (m, 3 H), 1.76 - 1.59 (m, 4 H), 1.54 - 1.42 (m, 2 H), 1.21 (t, *J* = 7.0 Hz, 6 H) ppm; ^{13}C NMR (100 MHz, $CDCl_3$) δ 174.0, 91.2, 86.2, 80.0, 61.8, 60.8, 60.8, 51.5, 36.9, 33.8, 24.6, 24.4, 15.0 ppm; IR (ATR) 3451, 2932, 1736, 1437, 1328, 1135, 1051, 1012 cm^{-1}; HRMS (EI) Exact mass cald. for $C_{14}H_{23}O_5$ $[M-H]^+$: 271.1545, found: 271.1546.

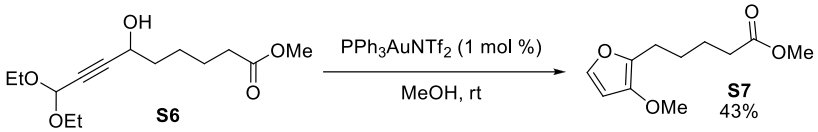

Methyl 5-(3-methoxyfuran-2-yl)pentanoate (**S7**):

MeOH (3.9 mL) was added to a vial containing **S6** (1.06 g, 3.89 mmol, 1 equiv). PPh_3AuNTf_2 (29 mg, 0.039 mmol, 0.01 equiv) was added, the reaction capped under an atmosphere of air, and stirred at rt overnight. The reaction mixture was poured into a separatory funnel containing brine (50 mL) then extracted with DCM (2 x 50 mL). The combined organic layers were washed with brine (50 mL), dried over Na_2SO_4, filtered, the solvent removed, and the residue subjected to flash column chromatography (Hexane:EtOAc, 15:1 → 9:1) to yield **S7** (0.35 g, 43%) as a clear and colorless oil. **S7**: Rf (Hexane:EtOAc, 9:1): 0.35; ^{1}H NMR (400 MHz, $CDCl_3$) δ 7.11 (d, *J* = 2.0 Hz, 1 H), 6.27 (d, *J* = 2.0 Hz, 1 H), 3.72 (s, 3 H), 3.66 (s, 3 H), 2.61 (t, *J* = 6.8 Hz, 2 H), 2.33 (t, *J* = 7.2 Hz, 2 H), 1.69 - 1.60 (m, 4 H) ppm; ^{13}C NMR (100 MHz, $CDCl_3$) δ 174.1, 143.3, 139.2, 138.9, 102.9, 59.4, 51.4, 33.7,

27.5, 24.5, 24.3 ppm; IR (ATR) 2950, 1734, 1662, 1600, 1230, 1179, 1111 cm^{-1}; HRMS (EI) Exact mass cald. for $C_{11}H_{16}O_4$ $[M]^+$: 212.1049, found: 212.1045.

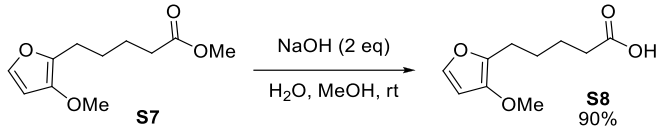

5-(3-Methoxyfuran-2-yl)pentanoic acid (**S8**):

To a vial containing **S7** (0.331 g, 1.56 mmol, 1 equiv) dissolved in MeOH (4 mL) was added a solution of NaOH (0.125 g, 3.12 mmol, 2 equiv) in H_2O (4 mL). The reaction was capped under an atmosphere of air, and stirred at rt for 30 min. The reaction mixture was poured into a separatory funnel containing H_2O (50 mL), and HCl (1 M in H_2O) was added to pH 2-3 (~4 mL). The aqueous layer was extracted with DCM (2 x 50 mL). The combined organic layers were washed with brine (50 mL), dried over Na_2SO_4, filtered, the solvent removed to yield **S8** (0.280 g, 90%) as a clear and colorless oil. **S8**: Rf (Hexane:EtOAc, 1:1): 0.55; ^{1}H NMR (400 MHz, $CDCl_3$) δ 10.37 (br.s., 1 H), 7.12 (d, *J* = 2.0 Hz, 1 H), 6.28 (d, *J* = 2.0 Hz, 1 H), 3.73 (s, 3 H), 2.62 (t, *J* = 6.5 Hz, 2 H), 2.38 (t, *J* = 6.5 Hz, 2 H), 1.73 - 1.61 (m, 4 H) ppm; ^{13}C NMR (100 MHz, $CDCl_3$) δ 179.8, 143.4, 139.1, 139.0, 102.9, 59.4, 33.7, 27.4, 24.4, 24.0 ppm; IR (ATR) 3133, 2940, 1706, 1662, 1454, 1411, 1279, 1236, 1109 cm^{-1}; HRMS (EI) Exact mass cald. for $C_{10}H_{14}O_4$ $[M]^+$: 198.0892, found: 198.0890.

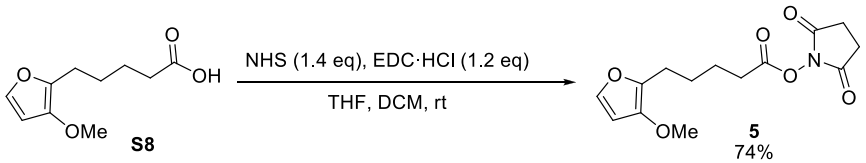

2,5-Dioxopyrrolidin-1-yl 5-(3-methoxyfuran-2-yl)pentanoate (**5**):

THF (5 mL) was added to a vial containing **S8** (0.265 g, 1.34 mmol, 1 equiv). *N*-hydroxysuccinimide (0.216 g, 1.87 mmol, 1.4 equiv), *N*-(3-dimethylaminopropyl)-*N*′-ethylcarbodiimide hydrochloride (0.308 g, 1.61 mmol, 1.2 equiv) and DCM (3 mL) were

added, the reaction capped under an atmosphere of air, and stirred at rt overnight. The solvent was removed and the residue was subjected to flash column chromatography (Hexane:EtOAc, 2:1 → 1:1) to yield **5** (0.293 g, 74%) as a colourless, viscous oil. **5**: Rf (Hexane:EtOAc, 2:1): 0.33; ^{1}H NMR (400 MHz, $CDCl_3$) δ 7.11 (d, *J* = 2.0 Hz, 1 H), 6.27 (d, *J* = 2.0 Hz, 1 H), 3.72 (s, 3 H), 2.82 (br.s., 4 H), 2.69 - 2.54 (m, 4 H), 1.81 - 1.60 (m, 4 H) ppm; ^{13}C NMR (100 MHz, $CDCl_3$) δ 169.1, 168.5, 143.5, 139.1, 138.7, 102.8, 59.3, 30.5, 27.0, 25.5, 24.2, 23.8 ppm; IR (ATR) 2948, 1814, 1735, 1638, 1413, 1206, 1058, 1046 cm^{-1}; HRMS (EI) Exact mass cald. for $C_{14}H_{17}NO_6$ $[M]^+$: 295.1056, found: 295.1062.

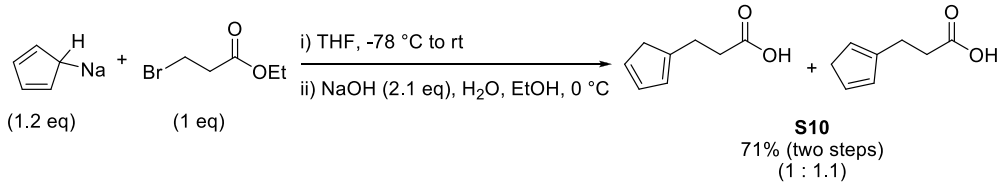

3-(Cyclopenta-1,3-dienyl)propanoic acid & 3-(cyclopenta-1,4-dienyl)propanoic acid (**S10**):

Sodium cyclopentadienide (2 M solution in THF, 30 mL, 60 mmol, 1.2 equiv) was added to THF (100 mL) and cooled to -78 °C. Ethyl 3-bromopropionate (6.41 mL, 50 mmol, 1 equiv) was added dropwise and the reaction was stirred at -78 °C for 3 h, removed from the cooling bath, and stirred a further 1 h. Water (6 mL) and silica gel (6 g) were added and the suspension stirred 5 min. The reaction mixture was filtered through silica gel with DCM (50 mL) and the solvent removed to yield **S9** as a yellow oil which was used directly in the next reaction. Spectral data matched that of literature reported data.[141] **S9**: Rf (Hexane:EtOAc, 9:1): 0.45; ^{1}H NMR (400 MHz, $CDCl_3$) δ 6.47 - 6.02 (m, 3 H), 4.17 - 4.11 (m, 2 H), 2.96 (s, 0.31 H), 2.91 (d, *J* = 1.4 Hz, 1.69 H), 2.78 - 2.68 (m, *J* = 1.7 Hz, 2 H), 2.59 - 2.53 (m, 2 H), 1.26 (t, *J* = 7.1 Hz, 3 H). A solution of **S9** (~50 mmol) dissolved in EtOH (36 mL) was cooled to 0 °C. A solution of NaOH (3.63 g, 90.72 mmol, 2.1 equiv) in H_2O (36 mL) was added and the

reaction stirred at 0 °C for 1.5 h. The reaction mixture was poured into a separatory funnel containing HCl (1 M in H_2O, 100 mL) and extracted with DCM (3 x 50 mL). The combined organic layers were washed with brine (50 mL), dried over Na_2SO_4, filtered, the solvent removed to yield **S10** (4.90 g, 71% two steps) as a yellow solid that decomposes at room temperature. **S10**: Rf (Hexane:EtOAc, 1:2): 0.69; ^{1}H NMR (400 MHz, $CDCl_3$) δ 10.57 (br.s., 1 H), 6.49 - 6.02 (m, 3 H), 2.97 (d, *J* = 1.6 Hz, 1.07 H), 2.92 (d, *J* = 1.2 Hz, 0.93 H), 2.82 - 2.68 (m, 2 H), 2.68 - 2.58 (m, 2 H) ppm; ^{13}C NMR (100 MHz, $CDCl_3$) δ 179.7, 179.7, 147.1, 144.9, 134.2, 134.1, 132.3, 131.1, 127.0, 126.4, 43.3, 41.3, 33.9, 33.3, 25.5, 24.7 ppm; IR (ATR) 3070, 2926, 1705, 1412, 1283, 1205, 913 cm^{-1}; HRMS (EI) Exact mass cald. for $C_8H_{10}NO_2$ $[M]^+$: 138.0681, found: 138.0678.

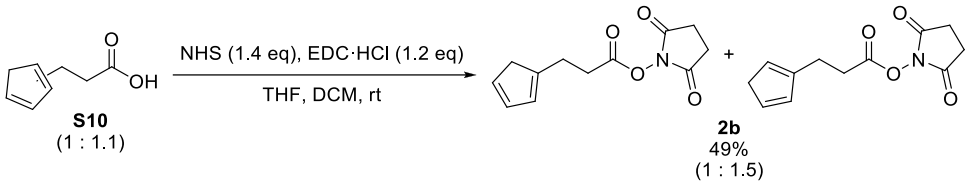

2,5-Dioxopyrrolidin-1-yl 3-(cyclopenta-1,3-dienyl)propanoate & 2,5-dioxopyrrolidin-1-yl 3-(cyclopenta-1,4-dienyl)propanoate (**2b**):

S10 (4.90 g, 35.5 mmol, 1 equiv) was dissolved in THF (50 mL). *N*-hydroxysuccinimide (5.71 g, 49.7 mmol, 1.4 equiv), N-(3-dimethylaminopropyl)-N′-ethylcarbodiimide hydrochloride (8.17 g, 42.6 mmol, 1.2 equiv) and DCM (50 mL) were added, the reaction capped under an atmosphere of air, and stirred 2 h. The reaction mixture was filtered through a silica plug with DCM (100 mL) and the solvent removed. The residue was subjected to flash column chromatography (Hexane:EtOAc, 2:1 → 1:1) to yield **2b** (4.00 g, 49%) as an eggshell powder that must be stored in the freezer to prevent dimerization. **2b** dimerizes much more slowly than **2a**, this may be due to it being a solid. **2b** is stable for over 2 years in the freezer, although the ratio 2-cyclopentadiene to 1-cyclopentadiene increases to ~3:1. **2b**: Rf

(Hexane:EtOAc, 2:1): 0.29; ^{1}H NMR (400 MHz, $CDCl_3$) δ 6.47 - 6.08 (m, 3 H), 2.97 (d, *J* = 1.2 Hz, 1.2 H), 2.92 (d, *J* = 1.6 Hz, 0.8 H), 2.90 - 2.75 (m, 8 H); ^{13}C NMR (100 MHz, $CDCl_3$) δ 169.1, 168.2, 168.1, 145.7, 143.9, 134.4, 133.8, 132.2, 131.4, 127.7, 127.1, 43.2, 41.4, 30.8, 30.2, 25.5, 25.3, 24.5; IR (ATR) 2947, 1810, 1779, 1735, 1420, 1366, 1204, 1062, 1046 cm^{-1}; HRMS (EI) Exact mass cald. for $C_{12}H_{13}NO_4$ $[M]^+$: 235.0845, found: 235.0848.

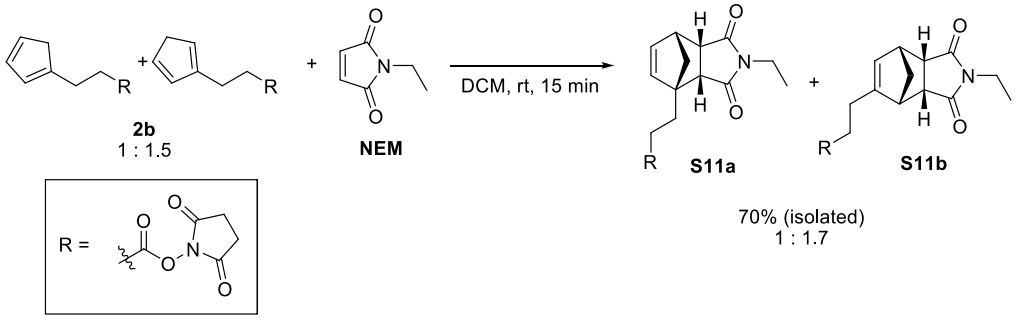

***Endo* Diels–Alder adducts of 2,5-Dioxopyrrolidin-1-yl 3-(cyclopenta-1,3-dienyl)propanoate (S11a) & 2,5-dioxopyrrolidin-1-yl 3-(cyclopenta-1,4-dienyl)propanoate (S11b)**:

To a solution of **2b** (105 mg, 0.446 mmol, 1 equiv) dissolved in DCM (5 mL) was added **NEM** (75 mg, 0.60 mmol, 1.3 equiv) and the solution was stirred for 15 min. The solvent was removed and the residue was subjected to flash column chromatography (Hexane:EtOAc, 1:2) to yield **S11a** and **S11b** (1:1.7, 112 mg, 70%) as a white foam. **S11a** & **S11b**: Rf (Hexane:EtOAc, 1:2): 0.33; ^{1}H NMR (400 MHz, $CDCl_3$) δ 6.11 (dd, *J* = 2.2, 5.7 Hz, 0.38 H, **S11a**), 5.92 (d, *J* = 5.9 Hz, 0.38 H, **S11a**), 5.73 (d, *J* = 1.2 Hz, 0.62 H, **S11b**), 3.41 - 2.54 (m, 12 H, **S11a** & **S11b**), 2.53 - 2.36 (m, 1.24 H, **S11b**), 2.28 (ddd, *J* = 6.5, 8.9, 14.8 Hz, 0.38 H, **S11a**), 1.79 (d, *J* = 8.6 Hz, 0.62 H, **S11b**), 1.67 (d, *J* = 8.6 Hz, 0.38 H, **S11a**), 1.52 (d, *J* = 9.0 Hz, 0.62 H, **S11b**), 1.44 (d, *J* = 8.6 Hz, 0.38 H, **S11a**), 1.01 (t, *J* = 7.2 Hz, 3 H, **S11a** & **S11b**); ^{13}C NMR (100 MHz, $CDCl_3$) δ 177.5, 177.2, 177.1, 176.8, 169.1, 169.0, 168.3, 167.6, 146.7, 136.1, 135.4, 126.9, 57.5, 55.0, 52.4, 48.8, 47.8, 47.4, 46.8, 45.7, 45.3, 44.7, 33.2, 33.1, 28.7,

27.9, 26.2, 25.5, 25.5, 25.3, 13.0, 13.0; IR (ATR) 2984, 2941, 1812, 1780, 1727, 1684, 1443, 1399, 1339, 1208, 1139, 1064 cm^{-1}; HRMS (CI) Exact mass cald. for $C_{18}H_{21}N_2O_6$ $[M+H]^+$: 361.1400, found: 361.1398.

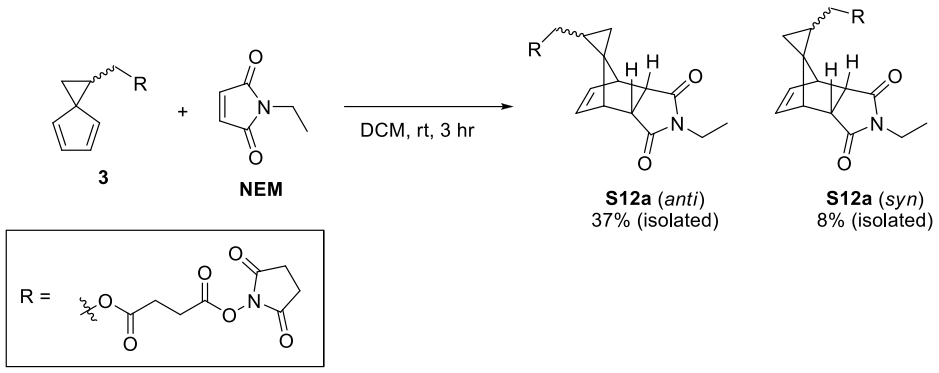

Endo **Diels–Alder adducts of 2,5-Dioxopyrrolidin-1-yl spiro[2.4]hepta-4,6-dien-1-ylmethyl succinate** (**S12a**, *anti*) **&** (**S12b**, *syn*):

To a solution of **3** (116 mg, 0.364 mmol, 1 equiv) dissolved in DCM (5 mL) was added **NEM** (64 mg, 0.51 mmol, 1.4 equiv) and the solution was stirred for 3 h. The solvent was removed and the residue was subjected to flash column chromatography (Hexane:EtOAc, 1:2 → 1:3) to yield **S12a** (59.9 mg, 37%) and **S12b** (13.3 mg, 8%) as a white foams. Note: The conversion for the DA reaction is high, but significant amount of material is not recovered due to hydrolysis of the NHS-ester on silica gel. The isomers were assigned through the ^{13}C NMR shift of the cyclopropane methylene (*syn* = 10.2 ppm, *anti* = 12.5 ppm).[142] **S12a**: Rf (Hexane:EtOAc, 1:2): 0.26; ^1H NMR (400 MHz, $CDCl_3$) δ 6.15 (t, *J* = 2.0 Hz, 2 H), 4.11 (dd, *J* = 7.2, 11.5 Hz, 1 H), 3.87 (dd, *J* = 8.2, 11.3 Hz, 1 H), 3.39 (q, *J* = 7.0 Hz, 2 H), 3.36 - 3.33 (m, 2 H), 3.04 - 2.98 (m, 1 H), 2.97 - 2.88 (m, 2 H), 2.84 (s, 4 H), 2.80 - 2.75 (m, 1 H), 2.70 (t, *J* = 6.7 Hz, 2 H), 1.38 (dq, *J* = 5.3, 8.0 Hz, 1 H), 1.04 (t, *J* = 7.2 Hz, 3 H), 0.76 (dd, *J* = 5.9, 9.0 Hz, 1 H), 0.47 (t, *J* = 5.5 Hz, 1 H); ^{13}C NMR (100 MHz, $CDCl_3$) δ 177.0, 176.9, 170.7, 168.9, 167.6, 134.3, 133.9, 66.3, 52.3, 50.3, 46.2, 45.7, 45.3, 33.3, 28.7, 26.3, 25.5, 17.8, 13.0,

12.5; IR (ATR) 2991, 2954, 1820, 1783, 1731, 1686, 1399, 1375, 1346, 1203, 1137, 1088, 1066 cm^{-1}; HRMS (CI) Exact mass cald. for $C_{22}H_{25}N_2O_8$ $[M+H]^+$: 445.1611, found: 445.1630. **S12b**: Rf (Hexane:EtOAc, 2:1): 0.39; ^1H NMR (400 MHz, $CDCl_3$) δ 6.21 - 6.13 (m, 2 H), 4.42 (dd, *J* = 5.5, 11.7 Hz, 1 H), 3.67 (dd, *J* = 9.8, 11.7 Hz, 1 H), 3.48 - 3.30 (m, 4 H), 3.06 - 3.02 (m, 1 H), 2.96 (dt, *J* = 3.7, 6.6 Hz, 2 H), 2.86 (br.s., 4 H), 2.79 - 2.72 (m, 3 H), 1.35 - 1.29 (m, 1 H), 1.05 (t, *J* = 7.0 Hz, 3 H), 0.82 (dd, *J* = 6.1, 9.2 Hz, 1 H), 0.47 (t, *J* = 5.5 Hz, 1 H); ^{13}C NMR (100 MHz, $CDCl_3$) δ 177.2, 170.8, 169.0, 167.6, 134.0, 133.9, 77.2, 66.2, 52.6, 50.4, 46.2, 45.8, 45.6, 33.3, 28.9, 26.5, 25.6, 19.0, 13.0, 10.2; IR (ATR) 2986, 2941, 1815, 1783, 1732, 1687, 1399, 1375, 1351, 1203, 1137, 1068 cm^{-1}; HRMS (CI) Exact mass cald. for $C_{22}H_{25}N_2O_8$ $[M+H]^+$: 445.1611, found: 445.1631.

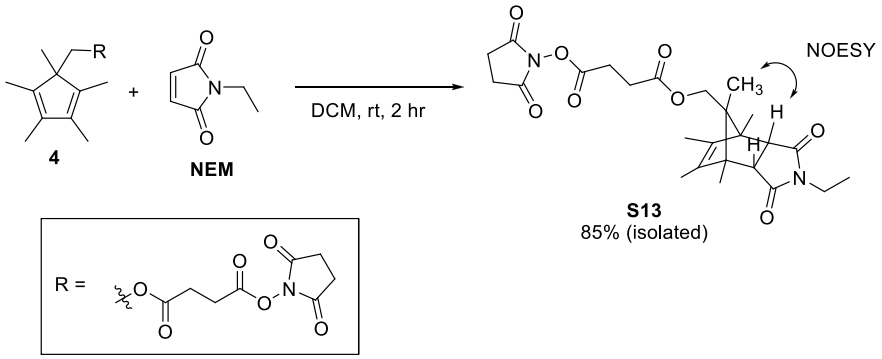

***Endo* Diels–Alder adduct of 2,5-Dioxopyrrolidin-1-yl (1,2,3,4,5-pentamethylcyclopenta-2,4-dienyl)methyl succinate** (**S13**, *anti*):

To a solution of **4** (108 mg, 0.297 mmol, 1 equiv) dissolved in DCM (5 mL) was added **NEM** (52 mg, 0.42 mmol, 1.4 equiv) and the solution was stirred for 2 h. The solvent was removed and the residue was subjected to flash column chromatography (Hexane:EtOAc, 2:3) to yield **S13** (72.7 mg, 50%) as a white foam. The *anti* configuration of the Diels-Alder adduct was assigned through the NOESY signal of the methyl group indicated.[59] **S13**: Rf (Hexane:EtOAc, 1:1): 0.21; ^1H NMR (400 MHz, $CDCl_3$) δ 3.97 (s, 2 H), 3.35 (q, *J* = 7.2 Hz, 2 H), 2.94 (t, *J* = 7.0 Hz, 2 H), 2.91 (s, 2 H), 2.84 (s, 4 H), 2.72 (t, *J* = 7.0 Hz, 2 H), 1.52 (s, 6

H), 1.30 (s, 6 H), 0.98 (t, *J* = 7.0 Hz, 3 H), 0.88 (s, 3 H); ^{13}C NMR (100 MHz, $CDCl_3$) δ 177.2, 170.9, 168.8, 167.6, 135.1, 77.2, 67.4, 66.4, 59.1, 51.1, 32.8, 28.7, 26.2, 25.5, 13.1, 12.6, 12.4, 11.3; IR (ATR) 2965, 2938, 1815, 1785, 1733, 1686, 1441, 1401, 1380, 1347, 1224, 1202, 1142, 1088, 1068 cm^{-1}; HRMS (CI) Exact mass cald. for $C_{25}H_{33}N_2O_8$ $[M+H]^+$: 489.2237, found: 489.2239.

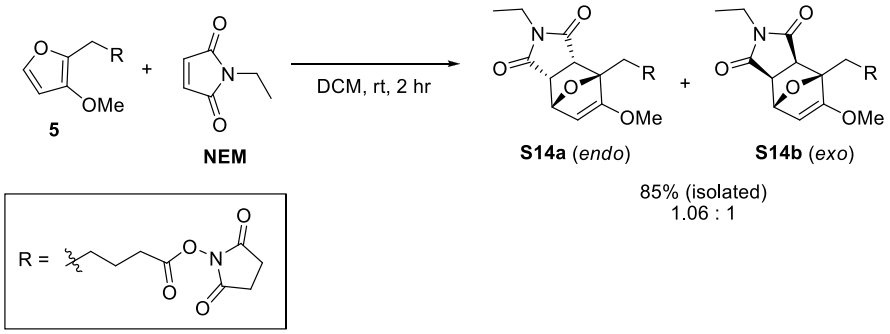

Diels–Alder adducts of 2,5-dioxopyrrolidin-1-yl 5-(3-methoxyfuran-2-yl)pentanoate (**S14a**, *endo*) **&** (**S14b**, *exo*):

To a solution of **5** (100. mg, 0.339 mmol, 1 equiv) dissolved in DCM (5 mL) was added **NEM** (59 mg, 0.47 mmol, 1.4 equiv) and the solution was stirred for 2 h. The solvent was removed and the residue was subjected to flash column chromatography (Hexane:EtOAc, 1:2) to yield **S14a** and **S14b** (1.06:1, 121 mg, 85%) as a white foam. The *endo* and *exo* isomers were assigned through analogy with Sheppard's work.[62] **S14a** & **S14b**: Rf (Hexane:EtOAc, 1:1): 0.33; ^{1}H NMR (400 MHz, $CDCl_3$) δ 5.15 - 5.09 (m, 3 H), 4.99 (d, *J* = 2.0 Hz, 1 H, **S14a**), 3.66 - 3.60 (m, 4 H), 3.54 - 3.46 (m, 5 H), 3.39 (q, *J* = 7.0 Hz, 2 H, **S14a**), 3.17 (d, *J* = 7.8 Hz, 1 H, **S14a**), 3.07 (d, *J* = 6.7 Hz, 1 H, **S14b**), 2.86 - 2.78 (m, 8 H), 2.62 (q, *J* = 7.4 Hz, 4 H), 2.31 - 2.20 (m, 1 H), 2.11 - 1.53 (m, 12 H), 1.13 (t, *J* = 7.2 Hz, 3 H, **S14b**), 1.06 (t, *J* = 7.0 Hz, 3 H, **S14a**); ^{13}C NMR (100 MHz, $CDCl_3$) δ; IR (ATR) 2942, 1813, 1783, 1733, 1689, 1627, 1442, 1401, 1347, 1203, 1135, 1065 cm^{-1}; HRMS (CI) Exact mass cald. for $C_{12}H_{13}NO_4$ $[M+H]^+$: 421.1611, found: 421.1607.

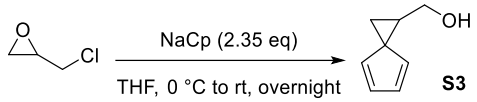

Large Scale Synthesis of Spiro[2.4]hepta-4,6-dien-1-ylmethanol (**S3**):

Sodium cyclopentadienide (2 M solution in THF, 40 mL, 80 mmol, 2.35 eq) was added to THF (250 mL) and cooled to 0 °C. Epichlorohydrin (2.66 mL, 34 mmol, 1 eq) was added dropwise over 20 min and the reaction was stirred overnight allowing the ice bath to expire. The reaction was quenched with H_2O (250 mL) then transferred to a separatory funnel containing a saturated solution of $NaHCO_3$ in H_2O (150 mL) and ether (250 mL) and the layers separated. The aqueous layer was extracted again with ether (150 mL). The organic layers were combined, washed with brine (200 mL), dried over $MgSO_4$, filtered, and then the solvent removed. The residue was filtered through a plug of silica gel with DCM (100 mL) and the solvent removed to yield **S3** (3.82 g) as a brown oil which was used directly in the next reaction.

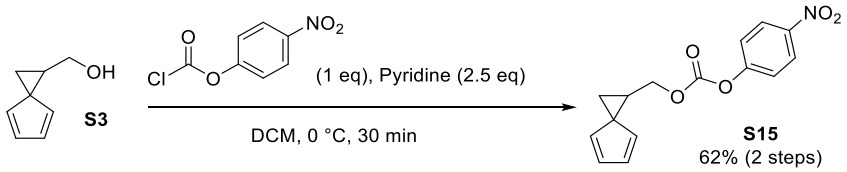

4-Nitrophenyl spiro[2.4]hepta-4,6-dien-1-ylmethyl carbonate (S15):

Crude **S3** (3.82 g) was added to DCM (150 mL) and cooled to 0 °C. Pyridine (6.38 mL, 78.3 mmol) was added, followed by 4-nitrophenyl chloroformate (6.30 g, 31.3 mmol). The reaction was stirred at 0 °C until consumption of the starting material (TLC, 30 min). The reaction was poured into a separatory funnel containing a saturated solution of NH_4Cl in H_2O (150 mL) and the layers separated. The aqueous layer was extracted with DCM (100 mL). The organic layers were combined, washed with brine (50 mL), dried over Na_2SO_4, filtered, and the solvent removed. The residue was subjected to flash column chromatography (Hexane:EtOAc, 6:1 to 4:1) to yield **S15** (6.05 g, 62% over two steps) as an amber oil that

solidified on storage in the freezer. **S15**: Rf (Hexane:EtOAc, 4:1): 0.45; ^{1}H NMR (400 MHz, $CDCl_3$) δ 8.28 (d, *J* = 9.0 Hz, 2 H), 7.37 (d, *J* = 9.0 Hz, 2 H), 6.62 (td, *J* = 1.7, 5.2 Hz, 1 H), 6.53 (td, *J* = 1.7, 4.8 Hz, 1 H), 6.25 (td, *J* = 1.8, 5.5 Hz, 1 H), 6.11 (td, *J* = 1.6, 5.1 Hz, 1 H), 4.53 (dd, *J* = 7.6, 11.5 Hz, 1 H), 4.40 (dd, *J* = 7.4, 11.3 Hz, 1 H), 2.52 (quin, *J* = 7.6 Hz, 1 H), 1.92 (dd, *J* = 4.7, 8.6 Hz, 1 H), 1.76 (dd, *J* = 4.7, 6.7 Hz, 1 H) ppm; ^{13}C NMR (100 MHz, $CDCl_3$) δ 155.4, 152.3, 145.3, 138.6, 133.8, 131.7, 129.4, 125.2, 121.7, 70.9, 41.5, 24.6, 16.9 ppm; IR (ATR) 3119, 3084, 3008, 2963, 2901, 2862, 1760, 1522, 1491, 1345, 1204, 1162, 858, 716 cm^{-1}; HRMS (CI) Exact mass cald. for $C_{15}H_{14}NO_5$ $[M+H]^+$: 288.0866, found: 288.0862.

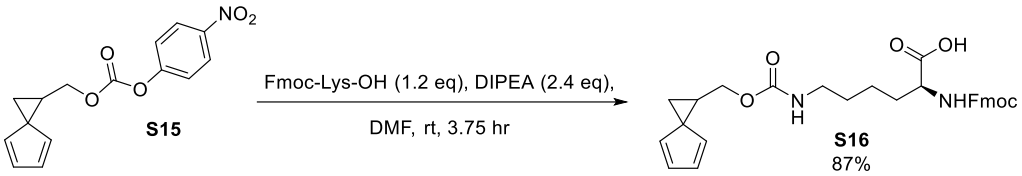

Fmoc-Lys(spiro[2.4]hepta-4,6-dien-1-ylmethyl carbonate)-OH (S16):

S15 (6.05 g, 21.1 mmol, 1 eq) was added to DMF (50 mL), followed by Fmoc-Lys-OH (9.31 g, 25.3 mmol, 1.2 eq) and DIPEA (8.80 mL, 50.5 mmol, 2.4 eq). The reaction was stirred at rt until consumption of the starting material (NMR, 3.75 hr), then poured into EtOAc (150 mL) and H_2O (150 mL). The aqueous layer was acidified to pH ~2 with HCl (1 M, 100 mL), poured into a separatory funnel, and the layers separated. The aqueous layer was extracted with EtOAc (2 x 100 mL). The organic layers were combined, washed with brine (100 mL), dried over Na_2SO_4, filtered, and the solvent removed. The residue was subjected to flash column chromatography (Hexane:EtOAc 3:1, then DCM:MeOH:AcOH 89:10:1) and the solvent removed. The residue was dissolved in benzene and the solvent removed (3 times) then repeated with DCM (3 times). The product is a thick foam with residual solvent that does not affect the next reaction. Drying the compound under vacuum yielded **S16** (10.2 g, purity

93% (NMR), 87%) as a sticky eggshell foam. **S16**: Rf (DCM:MeOH, 9:1): 0.39; ^{1}H NMR (400 MHz, $CDCl_3$) δ 10.20 (br. s., 1 H), 7.75 (d, *J* = 7.4 Hz, 2 H), 7.65 - 7.53 (m, 2 H), 7.39 (t, *J* = 7.0 Hz, 2 H), 7.30 (t, *J* = 7.4 Hz, 2 H), 6.54 (br. s., 1 H), 6.46 (d, *J* = 3.5 Hz, 1 H), 6.29 - 6.17 (m, 1 H), 6.03 (br. s., 1 H), 5.72 (major rotamer, d, *J* = 7.4 Hz, 1 H), 4.91 (major rotamer, t, *J* = 5.1 Hz, 1 H), 4.60 - 3.95 (m, 6 H), 3.22 - 3.00 (m, 2 H), 2.50 - 2.27 (m, 1 H), 1.98 - 1.58 (m, 4 H), 1.58 - 1.25 (m, 4 H) ppm; ^{13}C NMR (125 MHz, $CDCl_3$) δ 175.4, 156.6, 156.2, 143.8, 143.7, 141.2, 138.9, 134.5, 130.9, 128.9, 127.6, 127.0, 125.1, 119.9, 67.0, 66.4, 53.5, 47.1, 41.6, 40.4, 31.8, 29.2, 25.8, 22.2, 17.1 ppm; IR (ATR) 3412, 3324, 3068, 2937, 2865, 1698, 1520, 1448, 1335, 1240, 1046, 738 cm^{-1}; HRMS (CI) Exact mass cald. for $C_{30}H_{32}N_2NaO_6$ $[M+Na]^+$: 539.2153, found: 539.2173.

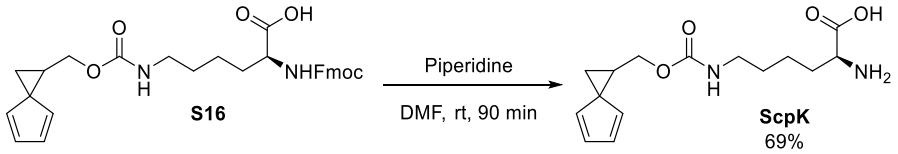

N^6-((spiro[2.4]hepta-4,6-dien-1-ylmethoxy)carbonyl)-*L*-lysine (ScpK):

Piperidine (30 mL) was added to a solution of **S16** (10.2 g, purity 93%, 18.4 mmol) in DMF (250 mL). The reaction was stirred at rt until consumption of the starting material (TLC, 90 min) then the solvent was removed. The residue was dissolved in DMF (50 mL) then the solvent was removed. The residue was suspended in Et_2O (100 mL), filtered, then rinsed sequentially with Et_2O (100 mL), H_2O (2 x 100 mL), and Et_2O (100 mL). The solid was suspended in MeOH (40 mL) then Et_2O (100 mL) was added. The suspension was filtered, rinsed with Et_2O (100 mL), and dried to yield **ScpK** (3.72 g, 69%) as an eggshell powder. **ScpK**: Rf (DCM:MeOH, 85:15): 0.20; ^{1}H NMR (400 MHz, DMSO-d_6 + 1 drop TFA) δ 8.20 (br. s., 3 H), 7.16 (t, J = 5.5 Hz, 1 H), 6.48 (td, J = 1.8, 5.1 Hz, 1 H), 6.40 (d, J = 5.1 Hz, 1 H), 6.32 (d, J = 5.1 Hz, 1 H), 6.12 (td, J = 1.9, 4.9 Hz, 1 H), 4.24 (dd, J = 6.7, 11.7 Hz, 1 H), 3.99

(dd, J = 7.6, 11.5 Hz, 1 H), 3.88 (d, J = 5.1 Hz, 1 H), 2.94 (d, J = 5.9 Hz, 2 H), 2.37 (quin, J = 7.5 Hz, 1 H), 1.83 - 1.63 (m, 4 H), 1.44 - 1.19 (m, 4 H) ppm; ^{13}C NMR (100 MHz, DMSO-d_6 + 1 drop TFA): 171.2, 156.2, 139.3, 135.2, 130.4, 128.3, 65.3, 51.9, 42.0, 39.8, 29.7, 28.9, 25.7, 21.6, 16.4; IR (ATR) 3334, 3069, 2939, 2864, 2609, 1688, 1580, 1515, 1409, 1321, 1270, 1239, 1049, 748 cm^{-1}; MS (EI) Exact mass cald. for $C_{15}H_{22}N_2O_4$ $[M]^+$: 294.1580, found: 294.1571.

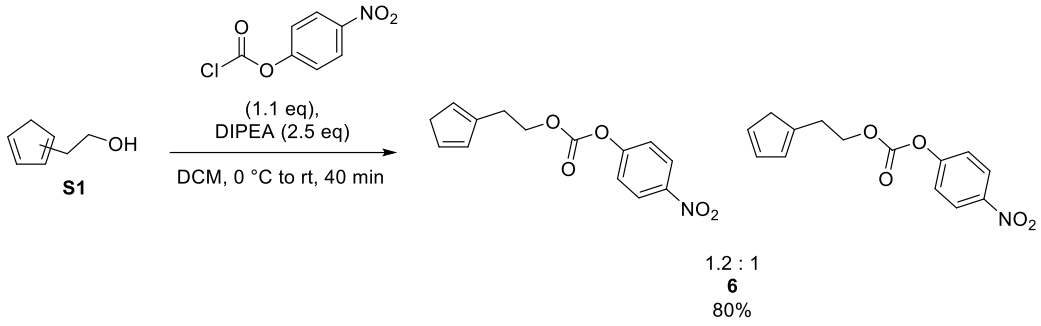

2-(Cyclopenta-1,4-dien-1-yl)ethyl (4-nitrophenyl) carbonate and 2-(cyclopenta-1,3-dien-1-yl)ethyl (4-nitrophenyl) carbonate (6):

S1 (2.86 g, 26.0 mmol, 1 eq) was added to DCM (100 mL) and cooled to 0 °C. Pyridine (5.2 mL, 65 mmol, 2.5 eq) was added followed by 4-nitrophenyl chloroformate (5.76 g, 28.6 mmol, 1.1 eq) in 2 portions over 10 min. The ice bath was removed and the reaction was stirred until consumption of the starting material (TLC, 40 min). The reaction was poured into a separatory funnel and washed with a saturated NH_4Cl in H_2O (100 mL). The aqueous layer was extracted with DCM (100 mL). The organic layers were combined, washed with brine (50 mL), dried over Na_2SO_4, filtered, and the solvent removed. The residue was subjected to flash column chromatography (Hexane:EtOAc, 6:1) to yield **6** (5.69 g, 80 %) as a yellow oil that solidifies in the freezer. **6**: Rf (Hexane:EtOAc, 4:1): 0.43; ^{1}H NMR (400 MHz, $CDCl_3$) δ 8.34 - 8.24 (m, 2 H), 7.40 - 7.34 (m, 2 H), 6.56 - 6.13 (m, 3 H), 4.47 (td, *J* = 6.8, 10.2 Hz, 2 H), 3.02 (d, *J* = 0.8 Hz, 1 H), 2.98 (d, *J* = 1.2 Hz, 1 H), 2.88 (dtd, *J* = 1.0, 6.9, 16.1 Hz, 2 H)

ppm; ; ^{13}C NMR (100 MHz, $CDCl_3$) δ 155.5, 155.4, 152.4, 145.3, 143.2, 141.5, 134.4, 133.9, 132.3, 131.8, 129.0, 128.5, 125.2, 121.7, 68.7, 68.3, 43.5, 41.6, 29.7, 29.0 ppm; IR (ATR) 3133, 2966, 2854, 1757, 1593, 1519, 1341, 1255, 1211, 1162, 1109, 955, 854, 746 cm^{-1}; HRMS (ES+) Exact mass cald. for $C_{28}H_{26}N_2NaO_{10}$ $[2M+Na]^+$: 573.1480, found: 573.1478.

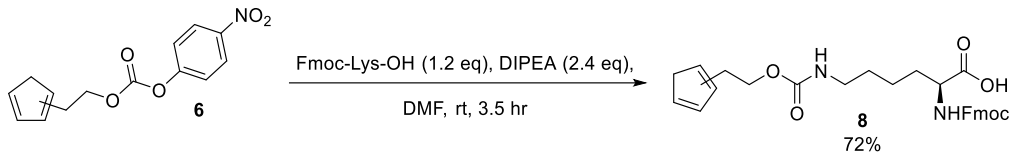

N2-(((9H-fluoren-9-yl)methoxy)carbonyl)-N6-((2-(cyclopenta-1,4-dien-1-yl)ethoxy)carbonyl)-L-lysine and N2-(((9H-fluoren-9-yl)methoxy)carbonyl)-N6-((2-(cyclopenta-1,3-dien-1-yl)ethoxy)carbonyl)-L-lysine (8):

6 (3.60 g, 13.1 mmol, 1 eq) was added to DMF (30 mL), followed by Fmoc-Lys-OH (5.78 g, 15.7 mmol, 1.2 eq) and DIPEA (5.4 mL, 32 mmol, 2.4 eq). The reaction was stirred until consumption of the starting material (NMR, 3.5 hr), then poured into EtOAc (100 mL) and H_2O (140 mL). The aqueous layer was acidified with HCl (1 M, 60 mL), poured a separatory funnel, and the layers separated. The aqueous layer was extracted with EtOAc (2 x 100 mL). The organic layers were combined, washed with brine (100 mL), dried over Na_2SO_4, filtered, and the solvent removed. The residue was subjected to flash column chromatography (Hexane:EtOAc, 3:1, then DCM:MeOH:AcOH, 89:10:1) and the solvent removed. Residual AcOH and DMF was removed by coevaporating the product in benzene (3 times) then DCM (3 times). The product is a thick foam that may still have residual solvent that does not affect the next reaction. Drying the compound under high vacuum yielded **8** (4.73 g, 72%) as a white foam. **8**: Rf (DCM:MeOH:AcOH, 89:10:1): 0.50; ^{1}H NMR (400 MHz, $CDCl_3$) δ 7.76 (d, *J* = 7.4 Hz, 2 H), 7.66 - 7.56 (m, 2 H), 7.39 (t, *J* = 7.4 Hz, 2 H), 7.31 (t, *J* = 7.2 Hz, 2 H), 6.57 - 5.96 (m, 3 H), 5.85 - 5.54 (m, 1 H), 4.84 - 4.11 (m, 7 H), 3.27 - 2.61 (m, 6 H), 1.99 - 1.11 (m,

6 H) ppm; IR (ATR) 3325, 3055, 2931, 1697, 1528, 1450, 1251, 1102, 1048, 740 cm^{-1}; HRMS (ES+) Exact mass cald. for $C_{29}H_{32}N_2NaO_6$ $[M+Na]^+$: 527.2153, found: 527.2165.

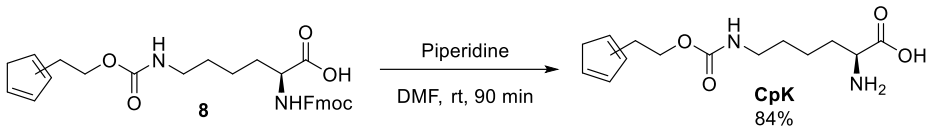

N6-((2-(cyclopenta-1,4-dien-1-yl)ethoxy)carbonyl)-L-lysine and N6-((2-(cyclopenta-1,3-dien-1-yl)ethoxy)carbonyl)-L-lysine (CpK):

8 (4.61 g, 9.13 mmol, 1 eq) was added to DMF (130 mL), followed by piperidine (14.4 mL). The reaction was stirred until consumption of the starting material (TLC, 90 min), then the solvent was removed. Et_2O (100 mL) was added to the residue, and the suspension was sonicated for 5 min. The suspension was filtered and rinsed with Et_2O (100 mL). The solid was suspended in MeOH (10 mL), stirred for 10 min, Et_2O (40 mL) was added, the suspension filtered and rinsed with Et_2O (50 mL). The compound was dried under vacuum to yield **CpK** (2.15 g, 84%) as a tan powder. **CpK**: ^{1}H NMR (400 MHz, Methanol-d4 + one drop TFA) δ 6.53 - 6.07 (m, 3 H), 4.29 - 4.11 (m, 2 H), 3.96 (t, J = 6.3 Hz, 1 H), 3.11 (t, J = 1.0 Hz, 2 H), 3.01 - 2.62 (m, 3 H), 2.02 - 1.81 (m, 2 H), 1.62 - 1.35 (m, 4 H) ppm; IR (ATR) 3336, 3061, 2942, 2863, 1686, 1580, 1517, 1410, 1323, 1269, 1239, 1143, 1025 cm^{-1}; HRMS (ES+) Exact mass cald. for $C_{14}H_{22}N_2NaO_4$ $[M+Na]^+$: 305.1472, found: 305.1478.

2.22 References

(1) St Amant, A. H.; Lemen, D.; Florinas, S.; Mao, S.; Fazenbaker, C.; Zhong, H.; Wu, H.; Gao, C.; Christie, R. J.; Read De Alaniz, J. Tuning the Diels-Alder Reaction for Bioconjugation to Maleimide Drug-Linkers. *Bioconjug. Chem.* **2018**, *29* (7), 2406–2414.

(2) St. Amant, A. H.; Huang, F.; Lin, J.; Lemen, D.; Chakiath, C.; Mao, S.; Fazenbaker,

C.; Zhong, H.; Harper, J.; Xu, W.; Patel, N.; Adams, L.; Vijayakrishnan, B.; Howard, P. W.; Marelli, M.; Wu, H.; Gao, C.; Read de Alaniz, J.; Christie, R. J. A Reactive Antibody Platform Enables One-Step Conjugation Through a Diels–Alder Reaction with Maleimide.

(3) St. Amant, A. H.; Huang, F.; Lin, J.; Lemen, D.; Chakiath, C.; Mao, S.; Fazenbaker, C.; Zhong, H.; Harper, J.; Xu, W.; Patel, N.; Adams, L.; Vijayakrishnan, B.; Howard, P. W.; Marelli, M.; Wu, H.; Gao, C.; Read de Alaniz, J.; Christie, R. J. A Cyclic Diene Non-Canonical Amino Acid Enables Homogenous and Heterogeneous Diels-Alder Reactions Following Incorporation into Antibodies.

(4) Hermanson, G. T. *Bioconjugate Techniques*, 3rd ed.; Academic press: Boston, 2013.

(5) Kalia, J.; Raines, R. T. Advances in Bioconjugation. *Curr. Org. Chem.* **2010**, *14* (2), 138–147.

(6) Lu, J.; Jiang, F.; Lu, A.; Zhang, G. Linkers Having a Crucial Role in Antibody–Drug Conjugates. *International Journal of Molecular Sciences* . 2016.

(7) Tsuchikama, K.; An, Z. Antibody-Drug Conjugates: Recent Advances in Conjugation and Linker Chemistries. *Protein Cell* **2016**.

(8) Polakis, P. Antibody Drug Conjugates for Cancer Therapy. *Pharmacol. Rev.* **2016**, *68* (1), 3–19.

(9) Handbook, M. P. A Guide to Fluorescent Probes and Labeling Technologies. 11th. Carlsbad, CA: Invitrogen Life Sciences.

(10) Banerjee, S. R.; Schaffer, P.; Babich, J. W.; Valliant, J. F.; Zubieta, J. Design and Synthesis of Site Directed Maleimide Bifunctional Chelators for Technetium and Rhenium. *Dalt. Trans.* **2005**, No. 24, 3886–3897.

(11) Ahlgren, S.; Orlova, A.; Rosik, D.; Sandström, M.; Sjöberg, A.; Baastrup, B.; Widmark, O.; Fant, G.; Feldwisch, J.; Tolmachev, V. Evaluation of Maleimide Derivative of DOTA for Site-Specific Labeling of Recombinant Affibody Molecules. *Bioconjug. Chem.* **2008**, *19* (1), 235–243.

(12) Goodson, R. J.; Katre, N. V. Site-Directed Pegylation of Recombinant Interleukin-2 at Its Glycosylation Site. *Nat Biotech* **1990**, *8* (4), 343–346.

(13) Sun, M. M. C.; Beam, K. S.; Cerveny, C. G.; Hamblett, K. J.; Blackmore, R. S.; Torgov, M. Y.; Handley, F. G. M.; Senter, P. D.; Alley, S. C. Reduction-Alkylation Strategies for the Modification of Specific Monoclonal Antibody Disulfides. *Bioconjug. Chem.* **2005**, *16* (5), 1282–1290.

(14) Junutula, J. R.; Raab, H.; Clark, S.; Bhakta, S.; Leipold, D. D.; Weir, S.; Chen, Y.; Simpson, M.; Tsai, S. P.; Dennis, M. S.; et al. Site-Specific Conjugation of a Cytotoxic Drug to an Antibody Improves the Therapeutic Index. *Nat Biotech* **2008**, *26* (8), 925–932.

(15) Getz, E. B.; Xiao, M.; Chakrabarty, T.; Cooke, R.; Selvin, P. R. A Comparison between the Sulfhydryl Reductants Tris(2-Carboxyethyl)Phosphine and Dithiothreitol for Use in Protein Biochemistry. *Anal. Biochem.* **1999**, *273* (1), 73–80.

(16) Lyon, R. P.; Setter, J. R.; Bovee, T. D.; Doronina, S. O.; Hunter, J. H.; Anderson, M. E.; Balasubramanian, C. L.; Duniho, S. M.; Leiske, C. I.; Li, F.; et al. Self-Hydrolyzing Maleimides Improve the Stability and Pharmacological Properties of Antibody-Drug Conjugates. *Nat Biotech* **2014**, *32* (10), 1059–1062.

(17) Shen, B.-Q.; Xu, K.; Liu, L.; Raab, H.; Bhakta, S.; Kenrick, M.; Parsons-Reponte, K. L.; Tien, J.; Yu, S.-F.; Mai, E.; et al. Conjugation Site Modulates the in Vivo Stability

and Therapeutic Activity of Antibody-Drug Conjugates. *Nat Biotech* **2012**, *30* (2), 184–189.

(18) Christie, R. J.; Fleming, R.; Bezabeh, B.; Woods, R.; Mao, S.; Harper, J.; Joseph, A.; Wang, Q.; Xu, Z.-Q.; Wu, H.; et al. Stabilization of Cysteine-Linked Antibody Drug Conjugates with N-Aryl Maleimides. *J. Control. Release* **2015**, *220*, *Part*, 660–670.

(19) Baldwin, A. D.; Kiick, K. L. Tunable Degradation of Maleimide–Thiol Adducts in Reducing Environments. *Bioconjug. Chem.* **2011**, *22* (10), 1946–1953.

(20) Fontaine, S. D.; Reid, R.; Robinson, L.; Ashley, G. W.; Santi, D. V. Long-Term Stabilization of Maleimide–Thiol Conjugates. *Bioconjug. Chem.* **2015**, *26* (1), 145–152.

(21) Dovgan, I.; Kolodych, S.; Koniev, O.; Wagner, A. 2-(Maleimidomethyl)-1,3-Dioxanes (MD): A Serum-Stable Self-Hydrolysable Hydrophilic Alternative to Classical Maleimide Conjugation. *Sci. Rep.* **2016**, *6*, 30835.

(22) Alley, S. C.; Benjamin, D. R.; Jeffrey, S. C.; Okeley, N. M.; Meyer, D. L.; Sanderson, R. J.; Senter, P. D. Contribution of Linker Stability to the Activities of Anticancer Immunoconjugates. *Bioconjug. Chem.* **2008**, *19* (3), 759–765.

(23) Koniev, O.; Leriche, G.; Nothisen, M.; Remy, J.-S.; Strub, J.-M.; Schaeffer-Reiss, C.; Van Dorsselaer, A.; Baati, R.; Wagner, A. Selective Irreversible Chemical Tagging of Cysteine with 3-Arylpropiolonitriles. *Bioconjug. Chem.* **2014**, *25* (2), 202–206.

(24) Badescu, G.; Bryant, P.; Swierkosz, J.; Khayrzad, F.; Pawlisz, E.; Farys, M.; Cong, Y.; Muroni, M.; Rumpf, N.; Brocchini, S.; et al. A New Reagent for Stable Thiol-Specific Conjugation. *Bioconjug. Chem.* **2014**, *25* (3), 460–469.

(25) J., B. R.; K., D. N. Diels–Alder and Inverse Diels–Alder Reactions. *Chemoselective*

and Bioorthogonal Ligation Reactions. March 3, 2017.

(26) de Araújo, A. D.; Palomo, J. M.; Cramer, J.; Köhn, M.; Schröder, H.; Wacker, R.; Niemeyer, C.; Alexandrov, K.; Waldmann, H. Diels–Alder Ligation and Surface Immobilization of Proteins. *Angew. Chemie Int. Ed.* **2006**, *45* (2), 296–301.

(27) Borsenberger, V.; Howorka, S. Diene-Modified Nucleotides for the Diels–Alder-Mediated Functional Tagging of DNA. *Nucleic Acids Res.* **2009**, *37* (5), 1477–1485.

(28) Petrelli, A.; Samain, E.; Pradeau, S.; Halila, S.; Fort, S. Efficient Conjugation of Oligosaccharides to Polymer Particles through Furan/Maleimide Diels–Alder Reaction: Application to the Capture of Carbohydrate-Binding Proteins. *ChemBioChem* **2017**, *18* (2), 206–212.

(29) Shi, M.; Wosnick, J. H.; Ho, K.; Keating, A.; Shoichet, M. S. Immuno-Polymeric Nanoparticles by Diels–Alder Chemistry. *Angew. Chemie Int. Ed.* **2007**, *46* (32), 6126–6131.

(30) Gandini, A.; Coelho, D.; Silvestre, A. J. D. D. Reversible Click Chemistry at the Service of Macromolecular Materials. Part 1: Kinetics of the Diels–Alder Reaction Applied to Furan–maleimide Model Compounds and Linear Polymerizations. *Eur. Polym. J.* **2008**, *44* (12), 4029–4036.

(31) Gandini, A. The Furan/Maleimide Diels–Alder Reaction: A Versatile Click–unclick Tool in Macromolecular Synthesis. *Prog. Polym. Sci.* **2013**, *38* (1), 1–29.

(32) Chudasama, V.; Maruani, A.; Caddick, S. Recent Advances in the Construction of Antibody-Drug Conjugates. *Nat Chem* **2016**, *8* (2), 114–119.

(33) Sauer, J.; Lang, D.; Mielert, A. The Order of Reactivity of Dienes towards Maleic Anhydride in the Diels-Alder Reaction. *Angew. Chemie Int. Ed. English* **1962**, *1* (5),

268.

(34) Inglis, A. J.; Sinnwell, S.; Stenzel, M. H.; Barner-Kowollik, C.; Andrew J., I.; Sebastian, S.; Martina H., S.; Christopher, B. Ultrafast Click Conjugation of Macromolecular Building Blocks at Ambient Temperature. *Angew. Chemie Int. Ed.* **2009**, *48* (13), 2411–2414.

(35) Samoshin, A. V; Hawker, C. J.; Read de Alaniz, J. Nitrosocarbonyl Hetero-Diels–Alder Cycloaddition: A New Tool for Conjugation. *ACS Macro Lett.* **2014**, *3* (8), 753–757.

(36) Boger, D. L.; Weinreb, S. M. *Hetero Diels-Alder Methodology in Organic Synthesis*; Elsevier, 2012; Vol. 47.

(37) Blond, G.; Gulea, M.; Mamane, V. Recent Contributions to Hetero Diels-Alder Reactions. *Current Organic Chemistry*. pp 2161–2210.

(38) Sun, X.-L.; Yang, L.; Chaikof, E. L. Chemoselective Immobilization of Biomolecules through Aqueous Diels–Alder and PEG Chemistry. *Tetrahedron Lett.* **2008**, *49* (16), 2510–2513.

(39) Yousaf, M. N.; Mrksich, M. Diels−Alder Reaction for the Selective Immobilization of Protein to Electroactive Self-Assembled Monolayers. *J. Am. Chem. Soc.* **1999**, *121* (17), 4286–4287.

(40) Levandowski, B. J.; Gamache, R. F.; Murphy, J. M.; Houk, K. N. Readily Accessible Ambiphilic Cyclopentadienes for Bioorthogonal Labeling. *J. Am. Chem. Soc.* **2018**.

(41) Otto, S.; Engberts Jan, B. F. N. Diels_Alder Reactions in Water. *Pure and Applied Chemistry*. 2000, p 1365.

(42) Rideout, D. C.; Breslow, R. Hydrophobic Acceleration of Diels-Alder Reactions. *J. Am. Chem. Soc.* **1980**, *102* (26), 7816–7817.

(43) Marchán, V.; Ortega, S.; Pulido, D.; Pedroso, E.; Grandas, A. Diels-Alder Cycloadditions in Water for the Straightforward Preparation of Peptide–oligonucleotide Conjugates. *Nucleic Acids Res.* **2006**, *34* (3), e24–e24.

(44) Beck, A.; Goetsch, L.; Dumontet, C.; Corvaïa, N. Strategies and Challenges for the next Generation of Antibody–drug Conjugates. *Nat. Rev. Drug Discov.* **2017**, *16*, 315.

(45) Behrens, C. R.; Liu, B. Methods for Site-Specific Drug Conjugation to Antibodies. *MAbs* **2014**, *6* (1), 46–53.

(46) Hallam, T. J.; Wold, E.; Wahl, A.; Smider, V. V. Antibody Conjugates with Unnatural Amino Acids. *Mol. Pharm.* **2015**, *12* (6), 1848–1862.

(47) Agarwal, P.; Bertozzi, C. R. Site-Specific Antibody–Drug Conjugates: The Nexus of Bioorthogonal Chemistry, Protein Engineering, and Drug Development. *Bioconjug. Chem.* **2015**, *26* (2), 176–192.

(48) Lucas, A. T.; Price, L. S. L.; Schorzman, A. N.; Storrie, M.; Piscitelli, J. A.; Razo, J.; Zamboni, W. C. Factors Affecting the Pharmacology of Antibody–Drug Conjugates. *Antibodies* **2018**, *7* (1).

(49) Kumar, A.; White, J.; James Christie, R.; Dimasi, N.; Gao, C. Chapter Twelve - Antibody-Drug Conjugates. In *Platform Technologies in Drug Discovery and Validation*; Goodnow, R. A. B. T.-A. R. in M. C., Ed.; Academic Press, 2017; Vol. 50, pp 441–480.

(50) Chan, D. P. Y.; Owen, S. C.; Shoichet, M. S. Double Click: Dual Functionalized Polymeric Micelles with Antibodies and Peptides. *Bioconjug. Chem.* **2013**, *24* (1), 105–113.

(51) Shi, M.; Ho, K.; Keating, A.; Shoichet, M. S. Doxorubicin-Conjugated Immuno-

Nanoparticles for Intracellular Anticancer Drug Delivery. *Adv. Funct. Mater.* **2009**, *19* (11), 1689–1696.

(52) Wong, A. C.; Ritchey, W. M. The Endo-Exo Isomerization of N-Phenyl-5-Norbornene-2,3-Dicarboximide. *Spectrosc. Lett.* **1980**, *13* (7), 503–508.

(53) Rulíšek, L.; Šebek, P.; Havlas, Z.; Hrabal, R.; Čapek, P.; Svatoš, A. An Experimental and Theoretical Study of Stereoselectivity of Furan−Maleic Anhydride and Furan−Maleimide Diels−Alder Reactions. *J. Org. Chem.* **2005**, *70* (16), 6295–6302.

(54) Froidevaux, V.; Borne, M.; Laborbe, E.; Auvergne, R.; Gandini, A.; Boutevin, B. Study of the Diels-Alder and Retro-Diels-Alder Reaction between Furan Derivatives and Maleimide for the Creation of New Materials. *RSC Adv.* **2015**, *5* (47), 37742–37754.

(55) Discekici, E. H.; St. Amant, A. H.; Nguyen, S. N.; Lee, I. H.; Hawker, C. J.; Read De Alaniz, J. Endo and Exo Diels-Alder Adducts: Temperature-Tunable Building Blocks for Selective Chemical Functionalization. *J. Am. Chem. Soc.* **2018**, *140* (15), 5009–5013.

(56) Mironov, V. A.; Sobolev, E. V; Elizarova, A. N. Some General Characteristic Properties of Substituted Cyclopentadienes. *Tetrahedron* **1963**, *19* (12), 1939–1958.

(57) Starr, J. T.; Koch, G.; Carreira, E. M. Enantioselective Synthesis of the Cyclopentyl Core of the Axinellamines. *J. Am. Chem. Soc.* **2000**, *122* (36), 8793–8794.

(58) Masaru, I.; Shingo, T.; Minako, S.; Satoshi, I. Highly Syn π-Facial Preference in the Diels-Alder Reactions of 1,2,3,4,5-Pentamethylcyclopentadienes Having Carboxy, Ethoxycarbonyl, and Cyano Substituents at 5-Positions. *Chem. Lett.* **1995**, *24* (8), 739–740.

(59) Letourneau, J. E.; Wellman, M. A.; Burnell, D. J. Diels−Alder Reactions of 5-Alkyl-

1,3-Cyclopentadienes. *J. Org. Chem.* **1997**, *62* (21), 7272–7277.

(60) Froese, R. D. J.; Organ, M. G.; Goddard, J. D.; Stack, T. D. P.; Trost, B. M. Theoretical and Experimental Studies of the Diels-Alder Dimerizations of Substituted Cyclopentadienes. *J. Am. Chem. Soc.* **1995**, *117* (44), 10931–10938.

(61) Pennell, M. N.; Foster, R. W.; Turner, P. G.; Hailes, H. C.; Tame, C. J.; Sheppard, T. D. Gold Catalysed Synthesis of 3-Alkoxyfurans at Room Temperature. *Chem. Commun.* **2014**, *50* (11), 1302–1304.

(62) Foster, R. W.; Benhamou, L.; Porter, M. J.; Bučar, D.-K.; Hailes, H. C.; Tame, C. J.; Sheppard, T. D. Irreversible Endo-Selective Diels–Alder Reactions of Substituted Alkoxyfurans: A General Synthesis of Endo-Cantharimides. *Chemistry* **2015**, *21* (16), 6107–6114.

(63) Wang, L.; Amphlett, G.; Blättler, W. A.; Lambert, J. M.; Zhang, W. Structural Characterization of the Maytansinoid–monoclonal Antibody Immunoconjugate, HuN901–DM1, by Mass Spectrometry. *Protein Sci.* **2005**, *14* (9), 2436–2446.

(64) Arlotta, K. J.; Gandhi, A. V; Chen, H.-N.; Nervig, C. S.; Carpenter, J. F.; Owen, S. C. In-Depth Comparison of Lysine-Based Antibody-Drug Conjugates Prepared on Solid Support Versus in Solution. *Antibodies* **2018**, *7* (1).

(65) Valliere-Douglass, J. F.; McFee, W. A.; Salas-Solano, O. Native Intact Mass Determination of Antibodies Conjugated with Monomethyl Auristatin E and F at Interchain Cysteine Residues. *Anal. Chem.* **2012**, *84* (6), 2843–2849.

(66) Tumey, L. N.; Charati, M.; He, T.; Sousa, E.; Ma, D.; Han, X.; Clark, T.; Casavant, J.; Loganzo, F.; Barletta, F.; et al. Mild Method for Succinimide Hydrolysis on ADCs: Impact on ADC Potency, Stability, Exposure, and Efficacy. *Bioconjug. Chem.* **2014**,

25 (10), 1871–1880.

(67) Saito, F.; Noda, H.; Bode, J. W. Critical Evaluation and Rate Constants of Chemoselective Ligation Reactions for Stoichiometric Conjugations in Water. *ACS Chem. Biol.* **2015**, *10* (4), 1026–1033.

(68) Taylor, M. T.; Blackman, M. L.; Dmitrenko, O.; Fox, J. M. Design and Synthesis of Highly Reactive Dienophiles for the Tetrazine–trans-Cyclooctene Ligation. *J. Am. Chem. Soc.* **2011**, *133* (25), 9646–9649.

(69) Rossin, R.; van den Bosch, S. M.; ten Hoeve, W.; Carvelli, M.; Versteegen, R. M.; Lub, J.; Robillard, M. S. Highly Reactive Trans-Cyclooctene Tags with Improved Stability for Diels–Alder Chemistry in Living Systems. *Bioconjug. Chem.* **2013**, *24* (7), 1210–1217.

(70) Patterson, D. M.; Nazarova, L. A.; Prescher, J. A. Finding the Right (Bioorthogonal) Chemistry. *ACS Chem. Biol.* **2014**, *9* (3), 592–605.

(71) Lang, K.; Chin, J. W. Bioorthogonal Reactions for Labeling Proteins. *ACS Chem. Biol.* **2014**, *9* (1), 16–20.

(72) Otto, S.; Blokzijl, W.; Engberts, J. B. F. N. Diels-Alder Reactions in Water. Effects of Hydrophobicity and Hydrogen Bonding. *J. Org. Chem.* **1994**, *59* (18), 5372–5376.

(73) Engberts, J. B. F. N. Diels-Alder Reactions in Water: Enforced Hydrophobic Interaction and Hydrogen Bonding. *Pure and Applied Chemistry*. 1995, p 823.

(74) Xu, K.; Liu, L.; Saad, O. M.; Baudys, J.; Williams, L.; Leipold, D.; Shen, B.; Raab, H.; Junutula, J. R.; Kim, A.; et al. Characterization of Intact Antibody–drug Conjugates from Plasma/Serum in Vivo by Affinity Capture Capillary Liquid Chromatography–mass Spectrometry. *Anal. Biochem.* **2011**, *412* (1), 56–66.

(75) Doronina, S. O.; Toki, B. E.; Torgov, M. Y.; Mendelsohn, B. A.; Cerveny, C. G.; Chace, D. F.; DeBlanc, R. L.; Gearing, R. P.; Bovee, T. D.; Siegall, C. B.; et al. Development of Potent Monoclonal Antibody Auristatin Conjugates for Cancer Therapy. *Nat Biotech* **2003**, *21* (7), 778–784.

(76) Lin, D.; Saleh, S.; Liebler, D. C. Reversibility of Covalent Electrophile−Protein Adducts and Chemical Toxicity. *Chem. Res. Toxicol.* **2008**, *21* (12), 2361–2369.

(77) Tumey, L. N.; Li, F.; Rago, B.; Han, X.; Loganzo, F.; Musto, S.; Graziani, E. I.; Puthenveetil, S.; Casavant, J.; Marquette, K.; et al. Site Selection: A Case Study in the Identification of Optimal Cysteine Engineered Antibody Drug Conjugates. *AAPS J.* **2017**, 1–13.

(78) Jackson, D.; Atkinson, J.; Guevara, C. I.; Zhang, C.; Kery, V.; Moon, S.-J.; Virata, C.; Yang, P.; Lowe, C.; Pinkstaff, J.; et al. In Vitro and In Vivo Evaluation of Cysteine and Site Specific Conjugated Herceptin Antibody-Drug Conjugates. *PLoS One* **2014**, *9* (1), e83865.

(79) Gunnoo, S. B.; Madder, A. Bioconjugation - Using Selective Chemistry to Enhance the Properties of Proteins and Peptides as Therapeutics and Carriers. *Org. Biomol. Chem.* **2016**, *14* (34), 8002–8013.

(80) Saxon, E.; Armstrong, J. I.; Bertozzi, C. R. A "Traceless" Staudinger Ligation for the Chemoselective Synthesis of Amide Bonds. *Org. Lett.* **2000**, *2* (14), 2141–2143.

(81) Agard, N. J.; Prescher, J. A.; Bertozzi, C. R. A Strain-Promoted [3 + 2] Azide−Alkyne Cycloaddition for Covalent Modification of Biomolecules in Living Systems. *J. Am. Chem. Soc.* **2004**, *126* (46), 15046–15047.

(82) Blackman, M. L.; Royzen, M.; Fox, J. M. Tetrazine Ligation: Fast Bioconjugation

Based on Inverse-Electron-Demand Diels−Alder Reactivity. *J. Am. Chem. Soc.* **2008**, *130* (41), 13518–13519.

(83) Hohsaka, T.; Sisido, M. Incorporation of Non-Natural Amino Acids into Proteins. *Curr. Opin. Chem. Biol.* **2002**, *6* (6), 809–815.

(84) de Graaf, A. J.; Kooijman, M.; Hennink, W. E.; Mastrobattista, E. Nonnatural Amino Acids for Site-Specific Protein Conjugation. *Bioconjug. Chem.* **2009**, *20* (7), 1281–1295.

(85) Christie, R. J.; Tiberghien, A. C.; Du, Q.; Bezabeh, B.; Fleming, R.; Shannon, A.; Mao, S.; Breen, S.; Zhang, J.; Zhong, H.; et al. Pyrrolobenzodiazepine Antibody-Drug Conjugates Designed for Stable Thiol Conjugation. *Antibodies* **2017**, *6* (4).

(86) Ohri, R.; Bhakta, S.; Fourie-O'Donohue, A.; dela Cruz-Chuh, J.; Tsai, S. P.; Cook, R.; Wei, B.; Ng, C.; Wong, A. W.; Bos, A. B.; et al. High-Throughput Cysteine Scanning To Identify Stable Antibody Conjugation Sites for Maleimide- and Disulfide-Based Linkers. *Bioconjug. Chem.* **2018**.

(87) Renault, K.; Fredy, J. W.; Renard, P.-Y.; Sabot, C. Covalent Modification of Biomolecules through Maleimide-Based Labeling Strategies. *Bioconjug. Chem.* **2018**.

(88) Dolci, E.; Froidevaux, V.; Joly-Duhamel, C.; Auvergne, R.; Boutevin, B.; Caillol, S. Maleimides As a Building Block for the Synthesis of High Performance Polymers. *Polym. Rev.* **2016**, *56* (3), 512–556.

(89) Torres, J. *Synthesis of Unnatural Amino Acids for Protein Labeling and Activation*; North Carolina State University, 2014.

(90) Liu, C. C.; Schultz, P. G. Adding New Chemistries to the Genetic Code. *Annu. Rev. Biochem.* **2010**, *79* (1), 413–444.

(91) Chin, J. W. Expanding and Reprogramming the Genetic Code of Cells and Animals. *Annu. Rev. Biochem.* **2014**, *83* (1), 379–408.

(92) Chin, J. W. Expanding and Reprogramming the Genetic Code. *Nature* **2017**, *550*, 53.

(93) Axup, J. Y.; Bajjuri, K. M.; Ritland, M.; Hutchins, B. M.; Kim, C. H.; Kazane, S. A.; Halder, R.; Forsyth, J. S.; Santidrian, A. F.; Stafin, K.; et al. Synthesis of Site-Specific Antibody-Drug Conjugates Using Unnatural Amino Acids. *Proc. Natl. Acad. Sci.* **2012**, *109* (40), 16101–16106.

(94) VanBrunt, M. P.; Shanebeck, K.; Caldwell, Z.; Johnson, J.; Thompson, P.; Martin, T.; Dong, H.; Li, G.; Xu, H.; D'Hooge, F.; et al. Genetically Encoded Azide Containing Amino Acid in Mammalian Cells Enables Site-Specific Antibody–Drug Conjugates Using Click Cycloaddition Chemistry. *Bioconjug. Chem.* **2015**, *26* (11), 2249–2260.

(95) Yin, G.; Stephenson, H. T.; Yang, J.; Li, X.; Armstrong, S. M.; Heibeck, T. H.; Tran, C.; Masikat, M. R.; Zhou, S.; Stafford, R. L.; et al. RF1 Attenuation Enables Efficient Non-Natural Amino Acid Incorporation for Production of Homogeneous Antibody Drug Conjugates. *Sci. Rep.* **2017**, *7* (1), 3026.

(96) Zimmerman, E. S.; Heibeck, T. H.; Gill, A.; Li, X.; Murray, C. J.; Madlansacay, M. R.; Tran, C.; Uter, N. T.; Yin, G.; Rivers, P. J.; et al. Production of Site-Specific Antibody–Drug Conjugates Using Optimized Non-Natural Amino Acids in a Cell-Free Expression System. *Bioconjug. Chem.* **2014**, *25* (2), 351–361.

(97) Koehler, C.; Sauter, P. F.; Wawryszyn, M.; Girona, G. E.; Gupta, K.; Landry, J. J. M.; Fritz, M. H.-Y.; Radic, K.; Hoffmann, J.-E.; Chen, Z. A.; et al. Genetic Code Expansion for Multiprotein Complex Engineering. *Nat. Methods* **2016**, *13*, 997.

(98) Benjamí, O.; Gene, K.; W., C. J. Rapid and Efficient Generation of Stable Antibody–

Drug Conjugates via an Encoded Cyclopropene and an Inverse-Electron-Demand Diels–Alder Reaction. *Angew. Chemie Int. Ed.* **2018**, *57* (11), 2831–2834.

(99) Zhou, Q. Site-Specific Antibody Conjugation for ADC and Beyond. *Biomedicines* **2017**, *5* (4).

(100) J., S. M.; Daniel, S. Red-Light-Controlled Protein–RNA Crosslinking with a Genetically Encoded Furan. *Angew. Chemie Int. Ed.* **2013**, *52* (17), 4690–4693.

(101) Wan, W.; Tharp, J. M.; Liu, W. R. Pyrrolysyl-TRNA Synthetase: An Ordinary Enzyme but an Outstanding Genetic Code Expansion Tool. *Biochim. Biophys. Acta - Proteins Proteomics* **2014**, *1844* (6), 1059–1070.

(102) Schaltegger, H. Über Die Reaktion Zwischen Epichlorhydrin Und Cyclopentadienyl-Natrium. *Helv. Chim. Acta* **1962**, *45* (4), 1368–1375.

(103) Bangert, K.; Boekelheide, V. On the Reaction of Cyclopentadienylsodium and Epichlorohydrin. *Tetrahedron Lett.* **1963**, *4* (17), 1119–1121.

(104) Robin, B.; A., F. M. Pyrrolysine Amber Stop-Codon Suppression: Development and Applications. *ChemBioChem* **2017**, *18* (20), 1973–1983.

(105) Mukai, T.; Kobayashi, T.; Hino, N.; Yanagisawa, T.; Sakamoto, K.; Yokoyama, S. Adding L-Lysine Derivatives to the Genetic Code of Mammalian Cells with Engineered Pyrrolysyl-TRNA Synthetases. *Biochem. Biophys. Res. Commun.* **2008**, *371* (4), 818–822.

(106) Jeffrey, S. C.; Burke, P. J.; Lyon, R. P.; Meyer, D. W.; Sussman, D.; Anderson, M.; Hunter, J. H.; Leiske, C. I.; Miyamoto, J. B.; Nicholas, N. D.; et al. A Potent Anti-CD70 Antibody–Drug Conjugate Combining a Dimeric Pyrrolobenzodiazepine Drug with Site-Specific Conjugation Technology. *Bioconjug. Chem.* **2013**, *24* (7), 1256–

1263.

(107) van Geel, R.; Pruijn, G. J. M.; van Delft, F. L.; Boelens, W. C. Preventing Thiol-Yne Addition Improves the Specificity of Strain-Promoted Azide–Alkyne Cycloaddition. *Bioconjug. Chem.* **2012**, *23* (3), 392–398.

(108) Wilson, P. J.; Wells, J. H. The Chemistry and Utilization of Cyclopentadiene. *Chem. Rev.* **1944**, *34* (1), 1–50.

(109) Tian, F.; Lu, Y.; Manibusan, A.; Sellers, A.; Tran, H.; Sun, Y.; Phuong, T.; Barnett, R.; Hehli, B.; Song, F.; et al. A General Approach to Site-Specific Antibody Drug Conjugates. *Proc. Natl. Acad. Sci. U. S. A.* **2014**, *111* (5), 1766–1771.

(110) Dimasi, N.; Fleming, R.; Zhong, H.; Bezabeh, B.; Kinneer, K.; Christie, R. J.; Fazenbaker, C.; Wu, H.; Gao, C. Efficient Preparation of Site-Specific Antibody–Drug Conjugates Using Cysteine Insertion. *Mol. Pharm.* **2017**, *14* (5), 1501–1516.

(111) He, J.; Su, D.; Ng, C.; Liu, L.; Yu, S.-F.; Pillow, T. H.; Del Rosario, G.; Darwish, M.; Lee, B.-C.; Ohri, R.; et al. High-Resolution Accurate-Mass Mass Spectrometry Enabling In-Depth Characterization of in Vivo Biotransformations for Intact Antibody-Drug Conjugates. *Anal. Chem.* **2017**, *89* (10), 5476–5483.

(112) Wendeler, M.; Grinberg, L.; Wang, X.; Dawson, P. E.; Baca, M. Enhanced Catalysis of Oxime-Based Bioconjugations by Substituted Anilines. *Bioconjug. Chem.* **2014**, *25* (1), 93.

(113) Yang, J.; Šečkutė, J.; Cole, C. M.; Devaraj, N. K. Live-Cell Imaging of Cyclopropene Tags with Fluorogenic Tetrazine Cycloadditions. *Angew. Chemie Int. Ed.* **2012**, *51* (30), 7476–7479.

(114) Tumey, L. N.; Leverett, C. A.; Vetelino, B.; Li, F.; Rago, B.; Han, X.; Loganzo, F.;

Musto, S.; Bai, G.; Sukuru, S. C. K.; et al. Optimization of Tubulysin Antibody–Drug Conjugates: A Case Study in Addressing ADC Metabolism. *ACS Med. Chem. Lett.* **2016**, *7* (11), 977–982.

(115) Vollmar, B. S.; Wei, B.; Ohri, R.; Zhou, J.; He, J.; Yu, S.-F.; Leipold, D.; Cosino, E.; Yee, S.; Fourie-O'Donohue, A.; et al. Attachment Site Cysteine Thiol PKa Is a Key Driver for Site-Dependent Stability of THIOMAB Antibody–Drug Conjugates. *Bioconjug. Chem.* **2017**, *28* (10), 2538–2548.

(116) Parker, J. S.; McCormick, M.; Anderson, D. W.; Maltman, B. A.; Gingipalli, L.; Toader, D. The Development and Scale-Up of an Antibody Drug Conjugate Tubulysin Payload. *Org. Process Res. Dev.* **2017**, *21* (10), 1602–1609.

(117) Tiberghien, A. C.; Levy, J.-N.; Masterson, L. A.; Patel, N. V; Adams, L. R.; Corbett, S.; Williams, D. G.; Hartley, J. A.; Howard, P. W. Design and Synthesis of Tesirine, a Clinical Antibody–Drug Conjugate Pyrrolobenzodiazepine Dimer Payload. *ACS Med. Chem. Lett.* **2016**, *7* (11), 983–987.

(118) Lewis Phillips, G. D.; Li, G.; Dugger, D. L.; Crocker, L. M.; Parsons, K. L.; Mai, E.; Blättler, W. A.; Lambert, J. M.; Chari, R. V. J.; Lutz, R. J.; et al. Targeting HER2-Positive Breast Cancer with Trastuzumab-DM1, an Antibody–Cytotoxic Drug Conjugate. *Cancer Res.* **2008**, *68* (22), 9280 LP-9290.

(119) Staben, L. R.; Yu, S.-F.; Chen, J.; Yan, G.; Xu, Z.; Del Rosario, G.; Lau, J. T.; Liu, L.; Guo, J.; Zheng, B.; et al. Stabilizing a Tubulysin Antibody–Drug Conjugate To Enable Activity Against Multidrug-Resistant Tumors. *ACS Med. Chem. Lett.* **2017**, *8* (10), 1037–1041.

(120) Kyran, S. J.; Sanchez, S. G.; Arp, C. J.; Darensbourg, D. J. Syntheses and Structures of

[CH2(NCnH2n)2]Mo(CO)4 (n = 4,5) Complexes with Bis(Cycloamine) Ligands Easily Prepared from CH2Cl2. *Organometallics* **2015**, *34* (14), 3598–3602.

(121) CSICSERY, S. M. Methylcyclopentadiene Isomers. *J. Org. Chem.* **1960**, *25* (4), 518–521.

(122) Darkwa, J.; Giolando, D. M.; Murphy, C. J.; Rauchfuss, T. B.; Müller, A. Bis(H5-Methylcyclopentadienyl)Titanium Pentasulfide, Bis(μ-Methylcyclopentadienyl)-Divanadium Pentasulfide, and Bis(M5-Methylcyclopentadienyl)Divanadium Tetrasulfide. *Inorganic Syntheses*. January 5, 2007.

(123) Plass, T.; Milles, S.; Koehler, C.; Schultz, C.; Lemke, E. A. Genetically Encoded Copper-Free Click Chemistry. *Angew. Chemie Int. Ed.* **2011**, *50* (17), 3878–3881.

(124) Borrmann, A.; Milles, S.; Plass, T.; Dommerholt, J.; Verkade, J. M. M.; Wießler, M.; Schultz, C.; van Hest, J. C. M.; van Delft, F. L.; Lemke, E. A. Genetic Encoding of a Bicyclo[6.1.0]Nonyne-Charged Amino Acid Enables Fast Cellular Protein Imaging by Metal-Free Ligation. *ChemBioChem* **2012**, *13* (14), 2094–2099.

(125) Levandowski, B. J.; Houk, K. N. Theoretical Analysis of Reactivity Patterns in Diels–Alder Reactions of Cyclopentadiene, Cyclohexadiene, and Cycloheptadiene with Symmetrical and Unsymmetrical Dienophiles. *J. Org. Chem.* **2015**, *80* (7), 3530–3537.

(126) Liu, F.; Paton, R. S.; Kim, S.; Liang, Y.; Houk, K. N. Diels–Alder Reactivities of Strained and Unstrained Cycloalkenes with Normal and Inverse-Electron-Demand Dienes: Activation Barriers and Distortion/Interaction Analysis. *J. Am. Chem. Soc.* **2013**, *135* (41), 15642–15649.

(127) Closs, G. L.; Closs, L. E.; Boll, W. A. The Base-Induced Pyrolysis of Tosylhydrazones of α,β-Unsaturated Aldehydes and Ketones. A Convenient Synthesis of Some

Alkylcyclopropenes. *J. Am. Chem. Soc.* **1963**, *85* (23), 3796–3800.

(128) Yan, N.; Liu, X.; Pallerla, M. K.; Fox, J. M. Synthesis of Stable Derivatives of Cycloprop-2-Ene Carboxylic Acid. *J. Org. Chem.* **2008**, *73* (11), 4283–4286.

(129) Coxon, J. M.; Steel, P. J.; Whittington, B. I. Trajectory of Electrophilic Attack on Trisubstituted Cyclopropanes. *J. Org. Chem.* **1990**, *55* (13), 4136–4144.

(130) Patterson, D. M.; Nazarova, L. A.; Xie, B.; Kamber, D. N.; Prescher, J. A. Functionalized Cyclopropenes As Bioorthogonal Chemical Reporters. *J. Am. Chem. Soc.* **2012**, *134* (45), 18638–18643.

(131) Ravasco, J. M. J. M.; Monteiro, C. M.; Trindade, A. F. Cyclopropenes: A New Tool for the Study of Biological Systems. *Org. Chem. Front.* **2017**, *4* (6), 1167–1198.

(132) Yu, Z.; Pan, Y.; Wang, Z.; Wang, J.; Lin, Q. Genetically Encoded Cyclopropene Directs Rapid, Photoclick Chemistry-Mediated Protein Labeling in Mammalian Cells. *Angew. Chem. Int. Ed. Engl.* **2012**, *51* (42), 10600–10604.

(133) Hummelen, J. C.; Knight, B. W.; LePeq, F.; Wudl, F.; Yao, J.; Wilkins, C. L. Preparation and Characterization of Fulleroid and Methanofullerene Derivatives. *J. Org. Chem.* **1995**, *60* (3), 532–538.

(134) Wudl, F.; Hirsch, A.; Khemani, K. C.; Suzuki, T.; Allemand, P.-M.; Koch, A.; Eckert, H.; Srdanov, G.; Webb, H. M. Survey of Chemical Reactivity of C_{60}, Electrophile and Dieno—polarophile Par Excellence. In *Fullerenes*; ACS Symposium Series; American Chemical Society, 1992; Vol. 481, pp 11–161.

(135) Rotello, V. M.; Howard, J. B.; Yadav, T.; Conn, M. M.; Viani, E.; Giovane, L. M.; Lafleur, A. L. Isolation of Fullerene Products from Flames: Structure and Synthesis of the C60-Cyclopentadiene Adduct. *Tetrahedron Lett.* **1993**, *34* (10), 1561–1562.

(136) Nebhani, L.; Barner-Kowollik, C. Functionalization of Fullerenes with Cyclopentadienyl and Anthracenyl Capped Polymeric Building Blocks via Diels–Alder Chemistry. *Macromol. Rapid Commun.* **2010**, *31* (14), 1298–1305.

(137) Tsumoto, H.; Takahashi, K.; Suzuki, T.; Nakagawa, H.; Kohda, K.; Miyata, N. Preparation of C60-Based Active Esters and Coupling of C60 Moiety to Amines or Alcohols. *Bioorg. Med. Chem. Lett.* **2008**, *18* (2), 657–660.

(138) Rubner, G.; Bensdorf, K.; Wellner, A.; Bergemann, S.; Ott, I.; Gust, R. [Cyclopentadienyl]Metalcarbonyl Complexes of Acetylsalicylic Acid as Neo-Anticancer Agents. *Eur. J. Med. Chem.* **2010**, *45* (11), 5157–5163.

(139) Ledford, B. E.; Carreira, E. M. Total Synthesis of (+)-Trehazolin: Optically Active Spirocycloheptadienes as Useful Precursors for the Synthesis of Amino Cyclopentitols. *J. Am. Chem. Soc.* **1995**, *117* (47), 11811–11812.

(140) Peterson, G. I.; Church, D. C.; Yakelis, N. A.; Boydston, A. J. 1,2-Oxazine Linker as a Thermal Trigger for Self-Immolative Polymers. *Polymer (Guildf).* **2014**, *55* (23), 5980–5985.

(141) Honzíček, J.; Mukhopadhyay, A.; Santos-Silva, T.; Romão, M. J.; Romão, C. C. Ring-Functionalized Molybdenocene Complexes. *Organometallics* **2009**, *28* (9), 2871–2879.

(142) Reynaud, C.; Giorgi, M.; Doucet, H.; Santelli, M. Stereoselective Synthesis of Spiro Tricyclic Polyoxygenated Compounds: Solvolytic Behavior of 1-(Tosyloxymethyl)Spiro[2.4]Hepta-4,6-Diene. *Synthesis (Stuttg).* **2011**, *2011* (04), 674–680.

3 *Endo* Diels–Alder Adducts with Furan as a New Protecting Group for Maleimide

Portions of this chapter were originally published in the *Journal of the American Chemical Society*.[1] Reproduced (or 'Reproduced in part') with permission from *J. Am. Chem. Soc.*, **2018**, *140* (15), pp 5009–5013.

3.1 Introduction

The development of 'click' chemistry has had a profound impact on applications ranging from small molecule bioconjugation to the synthesis of complex and multifunctional macromolecular systems.[2] From the myriad of available 'click' reactions, maleimides represent one of the most versatile building blocks, as they offer two distinct and highly efficient reaction pathways for secondary functionalization. The first is a facile [4 + 2] Diels–Alder (DA) cycloaddition between electron-deficient maleimides and dienes. The second is a thiol-Michael reaction where a nucleophilic thiol adds across the maleimide double bond.[3] Both pathways proceed quantitatively under equimolar conditions from a wide variety of starting materials. While the high reactivity of maleimides is desirable for post-polymerization functionalization, direct incorporation into polymers prepared through conventional free radical and controlled radical polymerization (CRP) is precluded.[4–6] In previous work, Haddleton and coworkers developed an *exo* furan-protected maleimide atom transfer radical polymerization (ATRP) initiator for incorporation of a masked maleimide moiety at the α chain-end.[7] The furan protecting group could then be removed via a *retro*-DA (rDA) process upon heating at elevated temperatures (~110 °C). Coupled with the facile thiol-Michael addition, this strategy has significantly impacted the preparation of polymer-protein

bioconjugates.[8] Maynard and coworkers expanded this work, demonstrating successful incorporation of *exo* furan-protected maleimides in reversible addition fragmentation chain-transfer (RAFT) polymerization processes.[9] Dove and Sanyal also demonstrated successful utility in ring opening polymerization (ROP) systems.[10,11] Despite the importance of maleimide addition to the field of functional polymer synthesis, only the *exo* isomer has been explored as a functionalization platform. As such, the inherently high deprotection temperature is problematic for thermally unstable systems, such as bioconjugates and supramolecular assemblies.[12] To address this challenge, we hypothesized that the *endo* isomer, which undergoes rDA at considerably lower temperatures,[13,14] would afford a new functional building block with the added benefit of temperature tunability (**Figure 3.1**).

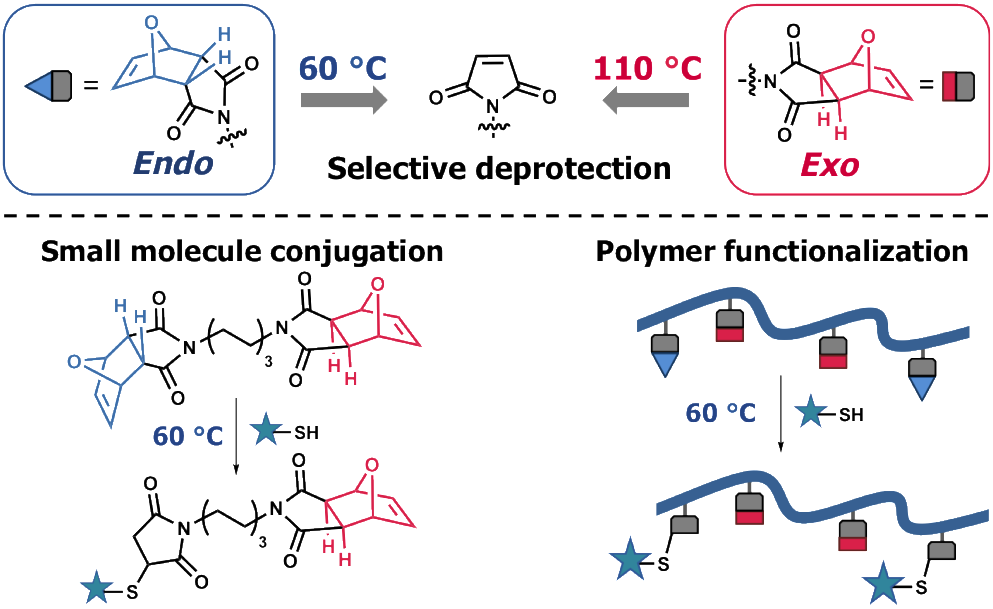

Figure 3.1 Graphical depiction of *endo* and *exo* isomers of furan-protected maleimide for temperature dependent deprotection and selective functionalization of small molecules and synthetic polymers.

3.2 Results and Discussion

Our initial exploration focused on a scalable and straightforward synthesis of the *endo* adduct, **1**. Using inexpensive and readily available starting materials (furan and maleimide),

a mixture of DA adducts enriched with **1** can be obtained when the cycloaddition reaction is performed at room temperature. From this mixture, the *endo* isomer, **1**, is selectively recrystallized from dichloromethane on up to a 4-gram scale (23% yield). The reaction of **1** with the *exo* isomer, **2,**[15] results in the *endo/exo* heterodimer model compound (**3**), which offers the possibility of selective deprotection and separate/successive thiol-Michael addition steps. Significantly, when **3** was heated at 60 °C, deprotection of only the *endo* adduct was observed. While extended reaction time for complete deprotection is necessary, nucleophilic addition with *n*-dodecanethiol enables exclusive monofunctionalization of the heterodimer to give **3-mono** in good yield (**Figure 3.2**). Subsequent deprotection of the *exo* adduct at 100 °C followed by reaction with 4-trifluorobenzyl mercaptan furnished the final di-substituted compound **3-di** (**Figure 3.3**), confirmed by ^{1}H, ^{13}C, ^{19}F NMR and electrospray ionization - mass spectrometry (ESI-MS) analysis.

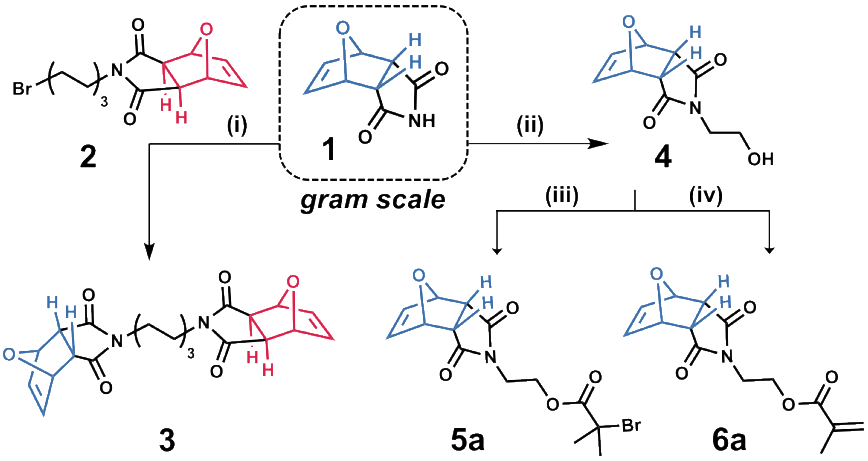

Figure 3.2 Synthesis of *endo/exo* heterodimer (3) and *endo* polymer building blocks (5a – initiator; 6a – monomer). (i) K_2CO_3, MeCN, RT, 56%. (ii) 2-bromothanol, K_2CO_3, MeCN, RT, 73%. (iii) BIBB, Et_3N, DCM, 0 °C to RT, 84%. (iv) Methacryloyl chloride, Et_3N, DCM, 0 °C to RT, 80%.

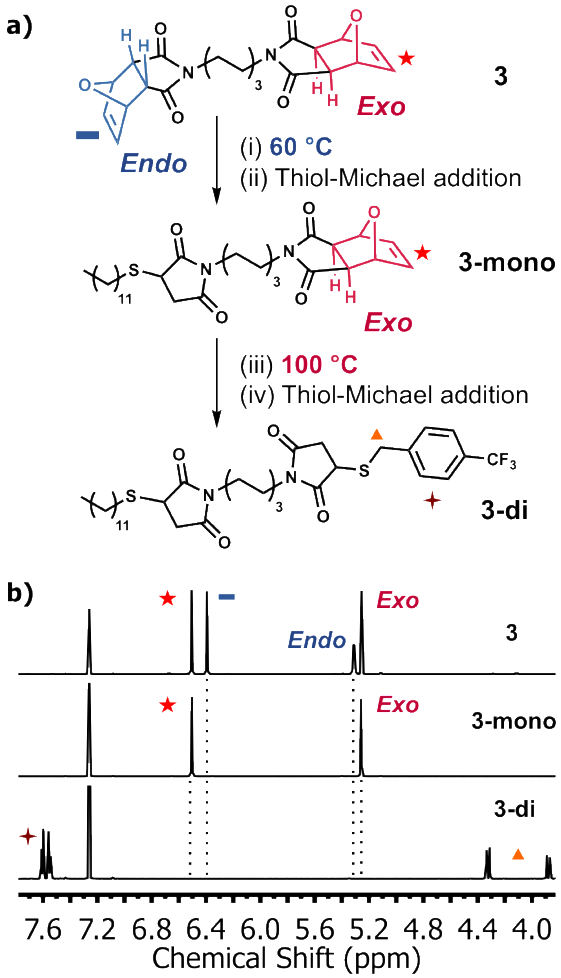

Figure 3.3 (a) Scheme and (b) ^{1}H NMR overlay of orthogonal deprotection and thiol-maleimide coupling reactions using small molecule *endo*/*exo* heterodimer, 3: (i) DMF, 60 °C, 22 h; (ii) *n*-$C_{12}H_{25}SH$, TEA, $CHCl_3$, RT, 15 h, column chromatography, (93%, two steps); (iii) Toluene, 100 °C, 17 h, >95% conversion of *exo* (iv) *p*-CF_3BnSH, TEA, $CHCl_3$, RT, 4 h, column chromatography (81%, two steps).

With selective conjugation achieved on a small molecule heterodimer, our efforts focused on adapting this chemistry to facilitate orthogonal post-functionalization of synthetic polymers. To obtain the necessary polymeric building blocks, a key hydroxyethyl precursor (**4**) was synthesized in one step from **1** (**Figure 3.2**) with single crystal X-ray analysis confirming the *endo* conformation of **4**. A traditional ATRP initiator (**5a**) and methacrylate monomer (**6a**) bearing the *endo* isomer could then be obtained from **4** using 2-bromoisobutyryl bromide and methacryloyl chloride, respectively.

Given the lower deprotection temperature of the *endo* isomer and the associated incompatibility with traditional thermally-driven radical polymerization techniques, our attention was drawn to ATRP systems that operate under ambient temperatures. Initial investigation of the viability of **5a** for Cu(0) polymerization[16] reveals a bimodal distribution at moderate to high conversions. This is in agreement with previous reports that suggest protected maleimides can still participate in copolymerizations[7] when using Cu-ATRP. To address this issue, we turned to light-mediated CRP techniques, namely metal-free ATRP[17–21] and photoinduced electron transfer-RAFT (PET-RAFT),[22–24] for direct incorporation of temperature sensitive functionalities into polymeric scaffolds.

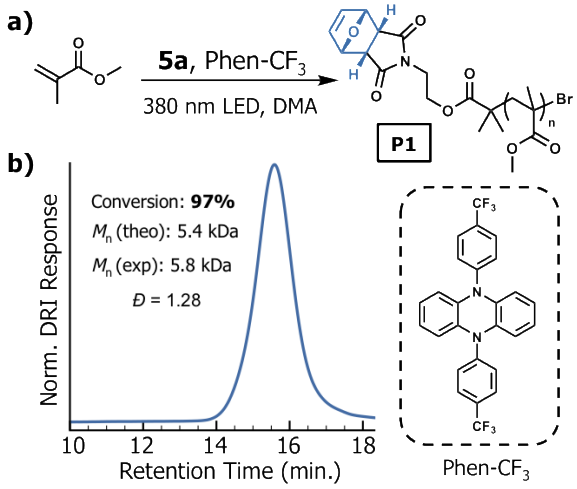

Figure 3.4 (a) Scheme of metal-free ATRP of MMA using the *endo* ATRP initiator, 5a (b) Size exclusion chromatography (SEC) confirming unimodal distribution with low *Đ*.

Implementation of metal-free ATRP with purified *endo*- and *exo*-monomers would therefore allow the development of multifunctional polymers that leverage the selective deprotection temperatures of the *endo* and *exo* building blocks, opening up the range of functionalization chemistries available in synthetic polymer systems. Significantly, metal-free ATRP using Phen-CF_3 yielded a unimodal distribution with low *Đ* for the *endo*-initiator (**Figure 3.4**), while PhenO allows **6a** (*endo* adduct) to be successfully copolymerized with **6b** (*exo* adduct), methyl methacrylate (MMA) and benzyl methacrylate (BnMA). The choice of

photocatalyst was based on optimal compatibility with the initiator-type as demonstrated in previous reports.[20,21] This represents the first copolymer (**P2**) to contain both *endo* and *exo* isomers (**Figure 3.5**). The addition of BnMA serves as a covalently bound internal ^{1}H NMR reference to facilitate reliable determination of the efficiency of selective deprotection. One of the most attractive features of a CRP is the ability to impart site-specific control over a desired functionality. Heating the copolymer in DMF-d_7 at 60 °C results in complete deprotection of the *endo* isomer. *In situ* addition of 4-trifluoromethyl benzyl mercaptan and characterization by ^{19}F NMR confirmed the fidelity of deprotection to maleimide and the associated reactivity toward thiols. Importantly, subsequent heating to 110 °C after *endo* functionalization resulted in quantitative deprotection of the remaining *exo*-isomer to furnish the reactive maleimide.

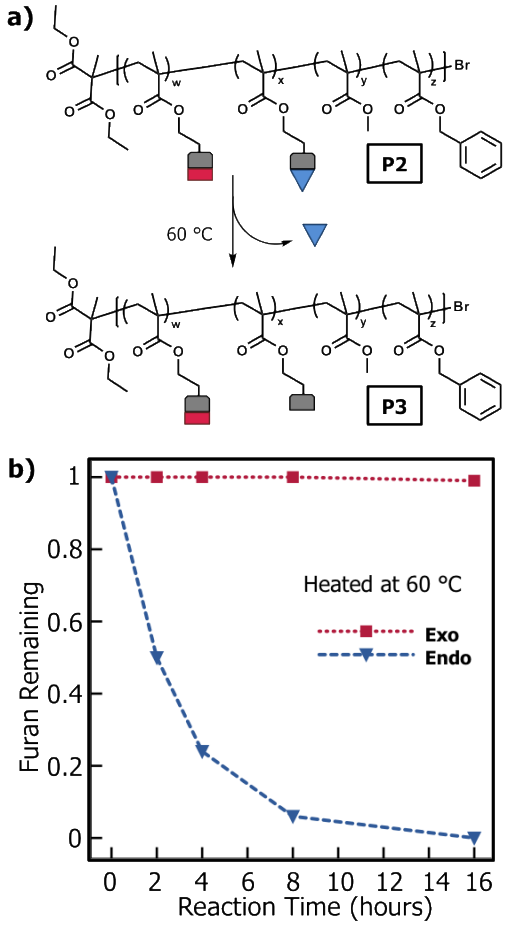

Figure 3.5 (a) Copolymer P2 (synthesized using 6a, 6b, MMA and BnMA, with PhenO and 380 nm light) is heated to selectively deprotect the *endo* isomer to yield P3 (b) Plot depicting stability of the *exo* isomer and quantitative deprotection of *endo* isomer at 60 °C over 16 h.

We then envisioned the preparation of a multi-functional copolymer, wherein one isomer is incorporated on the chain-end and the other as a pendant group along the backbone. Using **5a**, MMA was successfully copolymerized with **6b** to furnish a functional copolymer (**P5**) with good control. Having successfully demonstrated thiol-Michael addition after selective deprotection of the *endo* isomer, we performed selective deprotection at the α terminus and trapped the *in situ* generated maleimide with an irreversible DA cycloaddition with cyclopentadiene (Cp) end-capped poly(ethylene glycol) (**P4**). Inspired by recent reports from Barner-Kowollik and coworkers, Cp end-capped polymers represent a powerful strategy for highly efficient polymer functionalization.[25–27] Indeed when **P4** and **P5** were heated

together in solution, a facile and catalyst-free preparation of diblock copolymer (**P6**), with retention of the *exo* functionality, was achieved (**Figure 3.6**). While *exo* protected maleimides can undergo deprotection to reveal a reactive maleimide, they can also be used for ring opening metathesis polymerization (ROMP),[28] radical thiol-ene 'click',[29] and inverse electron-demand DA (IEDDA) reactions.[30] The IEDDA reaction with tetrazines has found widespread use in polymer conjugation and chemical biology due to the ability to achieve bioorthogonal, catalyst-free conjugation under mild conditions.[31–33] Significantly, in a one-pot fashion, 3,6-bis(methoxycarbonyl)-1,2,4,5-tetrazine was added to **P6**, resulting in quantitative consumption of the remaining *exo* isomer as evidenced by ^{1}H NMR and SEC-UV analysis. Importantly, in a similar fashion to the dual functionalizetion of the small molecule heterodimer (**3**), **P5** can be heated to 60 °C in the presence of *n*-dodecanethiol to give the selective *endo* chain-end functionalized product without deprotection of the pendant *exo* groups. Further heating of the chain-end functionalized polymer at 110 °C in toluene resulted in quantitative deprotection of the *exo*-isomer and the resulting maleimide was reacted with 4-trifluorobenzyl mercaptan in a one pot fashion to yield the dual thiol-Michael addition product. Analysis of the starting polymer and the final dual addition polymer by SEC-RI indicates no observable change of the molar mass distribution or overall dispersity. Furthermore, the versatility of this method also enables synthetic access to the inverse orientation of **P5**, with *exo* on the chain-end and *endo* as pendant groups (**P8**).

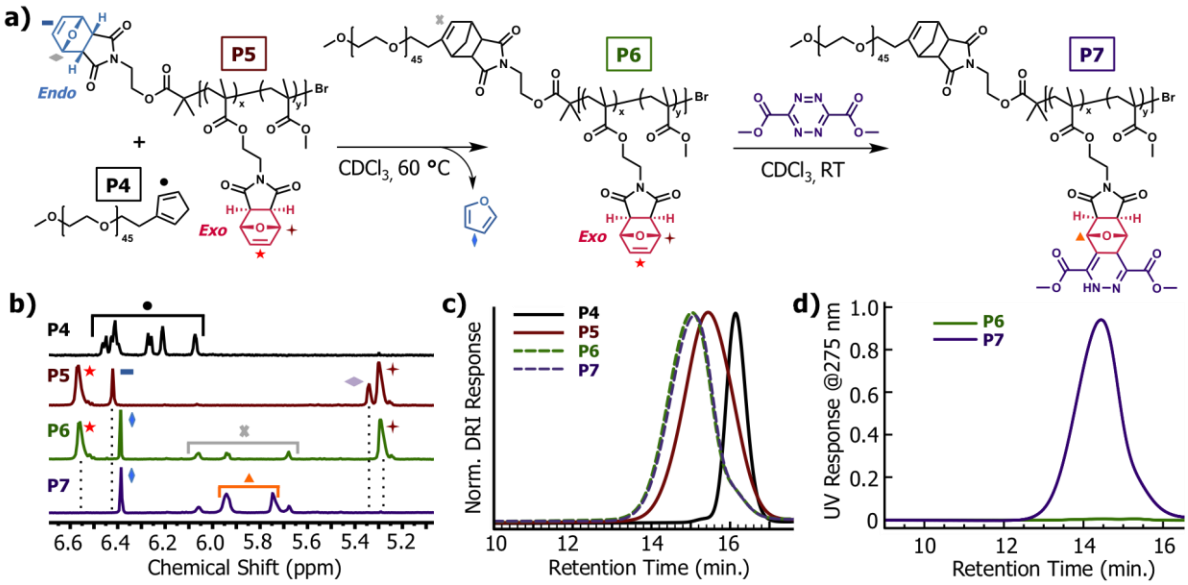

Figure 3.6 (a) Representative schematic of one-pot selective *endo* deprotection and DA cycloaddition conjugation with PEG-Cp followed by functionalization of remaining pendant *exo* functionality through IEDDA with 3,6-bis(methoxycarbonyl)-1,2,4,5-tetrazine. (b) Crude ^{1}H NMR overlay confirming successful conversion after each reaction. (c) SEC-RI overlay showing shift to higher molar mass following diblock formation after heating P4 and P5 at 60 °C for 18 h. (d) SEC-UV @275 nm overlay of P6 and P7 confirming conjugation with bis(methoxycarbonyl)-1,2,4,5-tetrazine after 1 h at room temperature.

3.3 Towards Genetically Encoded *Endo*-Protected Maleimide

Maleimide derivatives are generally considered toxic,[34] as they react quickly with essential endogenous thiols in proteins, glutathione, and cysteine. While the thiol–maleimide adduct, thiosuccinimide, is a commonly used non-toxic linker, maleimide derivatives such as showdomycin or maleimycin are investigated for their cytotoxicity.[35,36] While maleimide's toxicity precludes its use *in vivo*, a protected form could be genetically encoded into proteins. After isolation of this protein, the protecting group could be removed to reveal a maleimide for further conjugation to cyclopentadienes or thiols. As discussed above, *exo* furan-maleimide adducts are often used to protect maleimides, but the high deprotection temperatures (~100 °C) are not compatible with many proteins as they will denature. While *exo* furan-protected maleimide in a non-canonical amino acid (ncAA) may still find use in the radical thiol-ene reaction or in the ROMP reaction, a lower temperature adduct is needed to

furnish the maleimide. The maleimide, now incorporated site-selectively, could be reacted with thiol payloads such as emtansine (**Figure 3.7**).

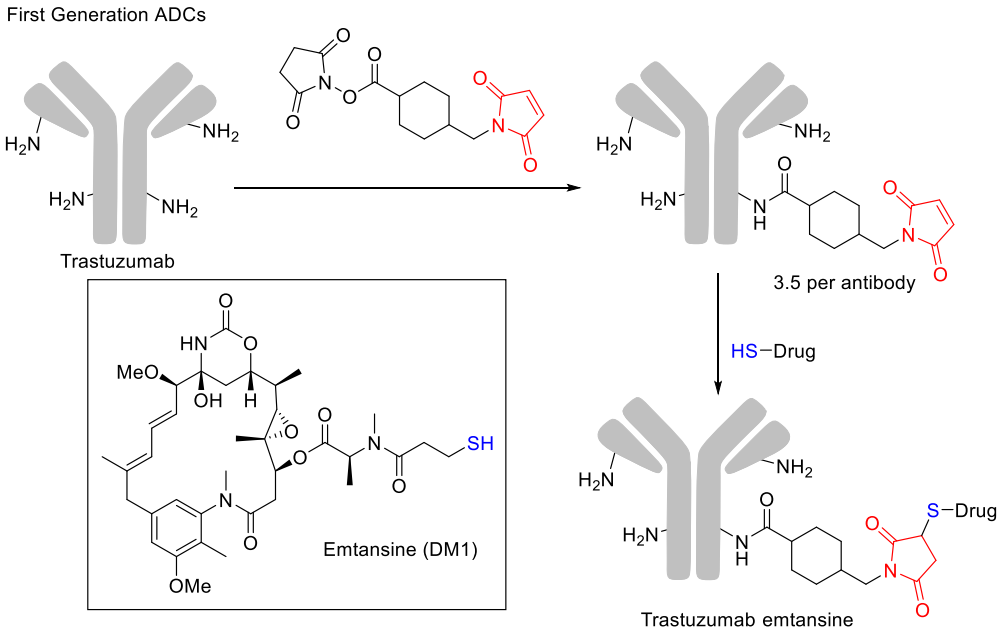

Figure 3.7 Synthesis of first generation ADC trastuzumab entansine through random lysine conjugation.

We began the synthesis with the *endo* alcohol building block **4**, forming the activated carbonate **7** (**Figure 3.8**). Unlike our cyclopentadiene work, we were able to use the Boc-protected lysine for our synthesis, as protected maleimides are stable to acidic conditions. With **8** in hand, a simple deprotection furnished **9** in good yield.

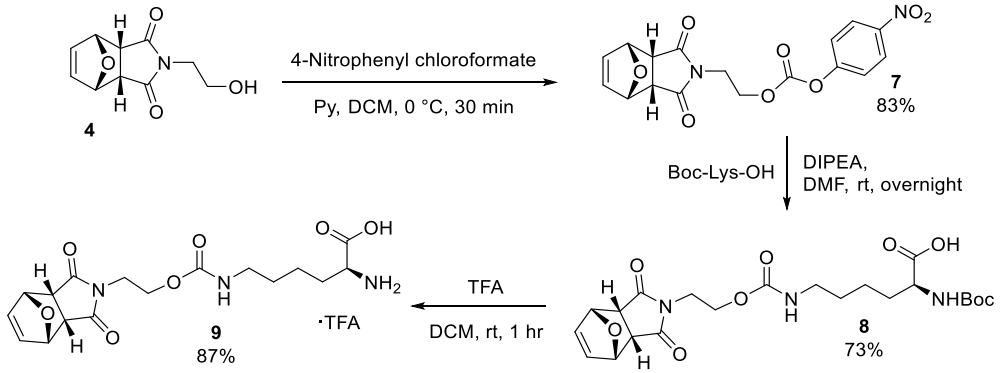

Figure 3.8 Synthesis of *endo* furan-protected ncAA 9.

With ncAA **9** in hand, we sought to incorporate the *endo* protected maleimide into antibodies (**Figure 3.9**) using genetic encoding. An amber stop codon is inserted at the desired

mutation site in the plasmid and the *Methanosarcina mazei* pyrrolysine tRNA synthetase (PylRS)/tRNA(Pyl) pair is transiently infected into a Chinese hamster ovary (CHO) cell expression system. After expression and purification of the protein, mild heating (50 to 70 °C) would furnish a maleimide for conjugation with a thiol (such as commercially available emtansine) or a cyclopentadiene-containing drug or protein. We predict that the mild deprotection with heat would be compatible with the thiol-maleimide Michael addition or cyclopentadiene-maleimide DA reaction, producing the conjugates in one-pot.

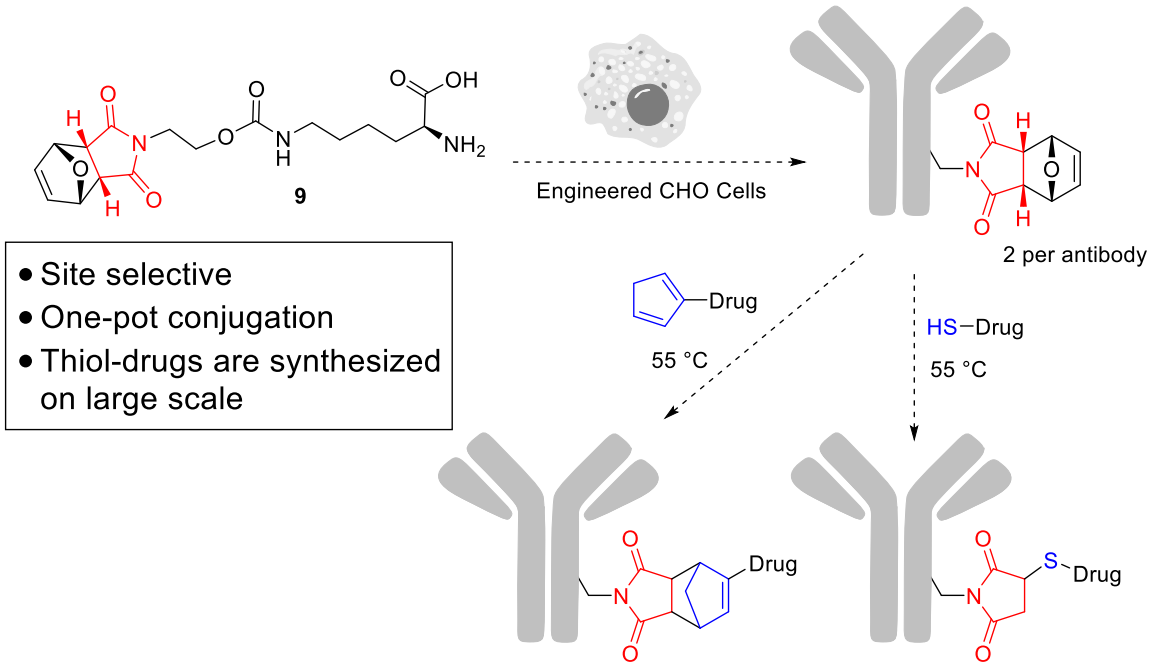

Figure 3.9 Synthesis of antibodies with site-specific *endo*-protected maleimides and their use in the production of ADCs.

In **Chapter 2**, we incorporated dienes into antibodies using genetically encoded ncAAs. We used a transient Chinese hamster ovary (CHO) cell expression system that required 10 day incubation times at 34 °C – conditions that may cause small amounts of deprotection. This may cause toxicity in the cells, misfolding of the antibodies, or antibodies conjugated to endogenous thiols making this strategy unsuitable for antibody production. There are other expression systems that may be required, such as *E. coli*, that can express proteins such as

green fluorescent protein in only 6 h.[37] There is also a concern that temperatures and reaction times required for deprotection of the *endo* adduct will cause denaturing in more sensitive proteins such as antibodies – if this occurs we could investigate a thermophilic enzyme such as *Taq* polymerase as a proof-of-concept.[38]

We have also considered an NHS-ester of *endo*-protected maleimide that would allow us to quickly produce protein-*endo* maleimides to study the deprotection. The DA reaction of maleimide is known to be accelerated in water, partially due to hydrogen bonding.[39,40] We could use model compounds to investigate the effect of water on the rDA reaction.

After optimization of the expression of these "*endo*-proteins" and their deprotection, we will have access to the first genetically encoded maleimides. We envision forming conjugates with Cp- or thiol-containing peptides/proteins, fluorophores, polymers, and drugs.

Overall, there are still experiments required for this project: the synthesis of an *endo*-protected maleimide NHS ester and model compounds, and expression of the genetic encoding machinery, expression of protein, and formation of conjugates. Beyond the protein-small molecule conjugates we will have access to, we envision using this strategy in conjunction with our genetically-encoded cyclopentadiene technology (**Chapter 2**) to produce site-selective and stable protein-protein adducts through the DA reaction.

3.4 *Exo* Furan-Protected Maleimides

Maleimides are a privileged moiety for bioconjugation and polymer conjugation; the usefulness of this conjugation moiety has led to the commercial availability of approximately 4,500 maleimide derivatives (SciFinder, August 2018). Examples of commercially available maleimides include fluorophores,[41] chemical probes (biotin), or polymer crosslinkers such as 1,1′-(methylenedi-4,1-phenylene)bismaleimide, known as bismaleimide in polymer journals.

Despite their wide-spread use, the synthesis of maleimide derivatives requires a 3-step process. For example, protection of maleimide's highly reactive olefin is required. This is often achieved through an *exo* DA-adduct with furan. Subsequently, removal of furan protecting group is required, which proceeds through a retro-DA (rDA).

Although the first part of this Chapter focused on the utility of the *endo* furan–maleimide adduct, these *exo* furan-maleimide adducts are also useful in their own right. The somewhat electron-rich olefin of the furan has a reactivity similar to norbornene, and has been shown by our group[1] and others[30] to react in the IEDDA reaction with tetrazine. Also, like norbornene, it is an effective monomer for ring-opening metathesis polymerization.[28] A third reactivity mode is through a photo-initiated radical thiol–ene reaction, which is favoured for these electron-rich olefins.[29,42] Finally, the olefin of *exo* furan–maleimides can be hydrogenated to produce norcantharimides, a class of drugs similar to cantharidin – a blister agent produced by blister beetles. These norcantharimides are being investigated for their anti-cancer properties.[43]

With the four aforementioned uses of *exo* furan–maleimide adducts, a simple synthesis from the wealth of commercially available maleimides is desirable. Compared to the kinetic *endo* DA adduct,[1] synthesis of the thermodynamic *exo* product from this reversible reaction could be achieved between the *endo* and *exo* rDA temperatures – the *endo* adduct undergoes a rDA reaction while the *exo* adduct accumulates (**Figure 3.10**). Another benefit of this synthetic strategy is that there are no catalysts, side-products, or byproducts – theoretically the product could be obtained by removing the excess furan and solvent *in vacuo*. Two groups, Grandas and Finn, have independently used this strategy to obtain quantitative yields: Grandas' conditions ($CHCl_3$, 38 °C, 5 days)[44] and Finn's conditions (benzene, reflux, 1 day).[45]

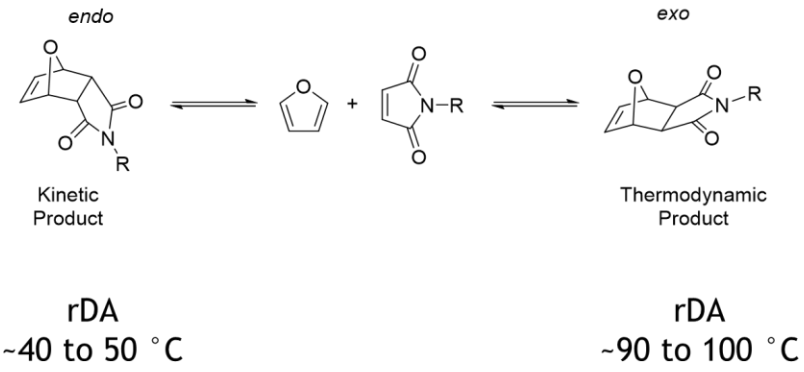

Figure 3.10 The kinetic and thermodynamic products from the reaction of furan and maleimide.

Given the wide-spread use of *exo* furan–maleimide adducts we sought to modify Finn's conditions (1 mmol maleimide, 10 mmol furan, sealed vessel, benzene, 80 °C, 18 hr) to enable quantitative yields of *exo* protected furan-maleimides (**Figure 3.11**). We hypothesized that these reaction conditions, followed by removal of the volatiles, would give quantitative yield of the *exo* DA adducts. To test this hypothesis we initially examined unsubstituted, alkyl, and alcohol functionalized-maleimides. To our gratification, all reacted to completion after 18 hours (**10**–**12**). The solubility of the propionic acid derivative (**13**) in benzene was low and the reaction did not proceed to completion; changing the solvent to MeCN and increasing the reaction time to 22 hr we obtained quantitative yield. The ADC linker succinimidyl 4-(N-maleimidomethyl) cyclohexane-1-carboxylate (SMCC, **14**) was also used (0.1 mmol), producing a norcantharimide with an NHS ester for further functionalization. α-Bromoisobutyryl maleimide **15**, a common ATRP initiator motif, worked well under our conditions. A biotin derivative (**16**) was also used, but due to the cost of the maleimide the reaction was performed in DMSO-d_6 and the conversion is reported.

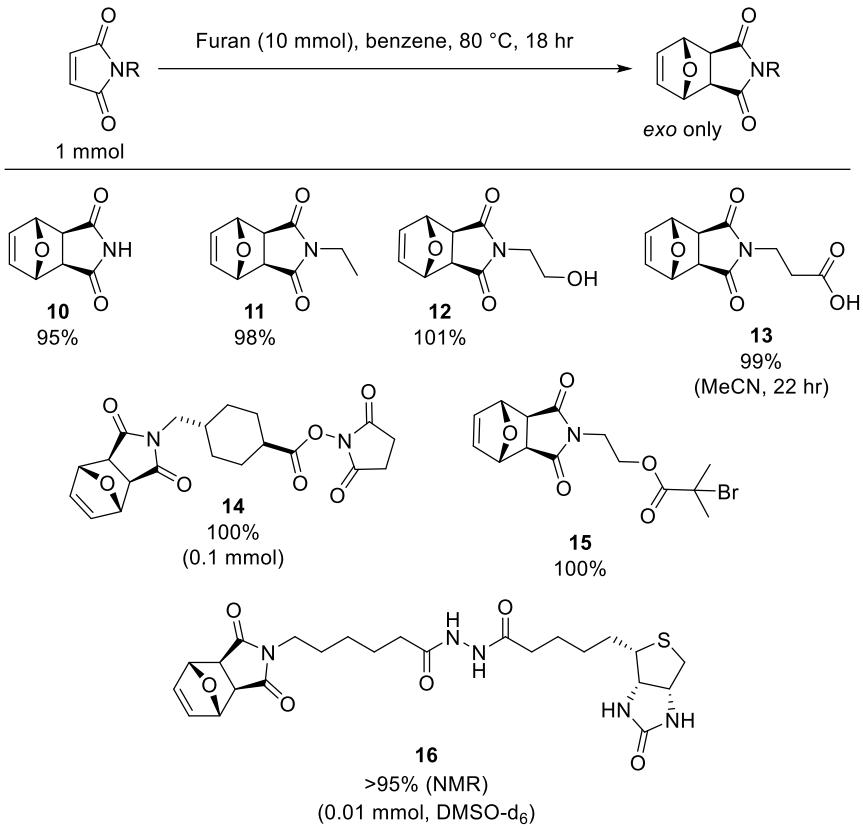

Figure 3.11 Conversion of *N*-alkyl maleimides to *exo* furan–maleimide adducts.

Next, we explored the synthesis of *N*-aryl maleimides as these maleimides are commercially available and widely used, including fluorophores and polymer crosslinkers (**Figure 3.12**). We found that when subjected to our *N*-alkyl maleimide reaction conditions the reaction went to completion in only 3 hr. We hypothesize that this is due to lower rDA temperatures, allowing the reaction to reach equilibrium faster. Mono- and disubstituted phenyl derivatives (**17**, **20**, and **21**) proceeded in quantitative yield. The pyrene derivative **18** produced the *exo* adduct as a mixture of slowly interconverting rotamers. The fluorescein derivative **19** was also used but, due to cost of the starting material, the reaction was performed in DMSO-d_6 and the conversion was measured by ^{1}H NMR.

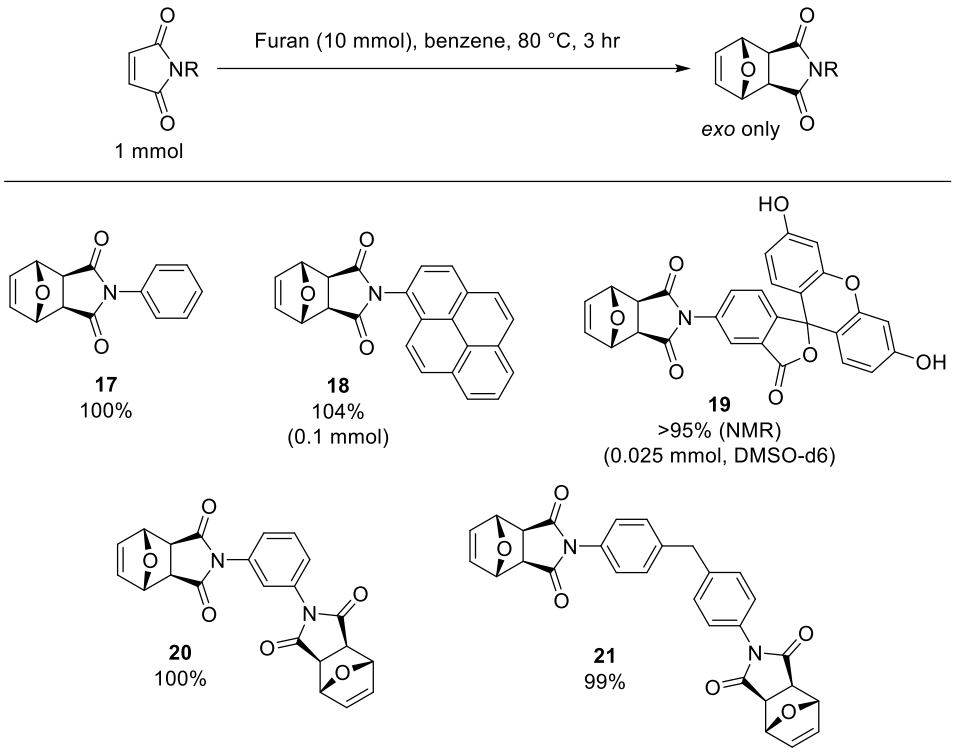

Figure 3.12 Conversion of *N*-aryl maleimides to *exo* furan–maleimide adducts

With a library *exo* furan–maleimides in hand, we wanted to explore the reactivity of these 7-oxanorbornene derivatives in the inverse electron-demand DA (IEDDA) for bioorthogonal conjugation (**Figure 3.13**). There is one example of an IEDDA reaction with these derivatives,[30] but the kinetics of the reaction have not been explored. The reaction rate of several 7-oxanorbornenes were explored by the Carell group in a H_2O/MeOH (95:5) mixture with dipyridyltetrazine (DpTz).[46] We measured the reaction rate in $CDCl_3$ by NMR for the *exo* furan-adduct of *N*-ethylmaleimide and DpTz (**11**) and found the rate to be approximately 0.012 $M^{-1}s^{-1}$, comparable to norbornene but much slower than the trans-cyclooctene dienophile developed by the Fox group (up to 10^6 $M^{-1}s^{-1}$).[47] Although the bioorthogonality of these derivatives is not known, we expect they will have a similar stability *in vivo* as norbornene.

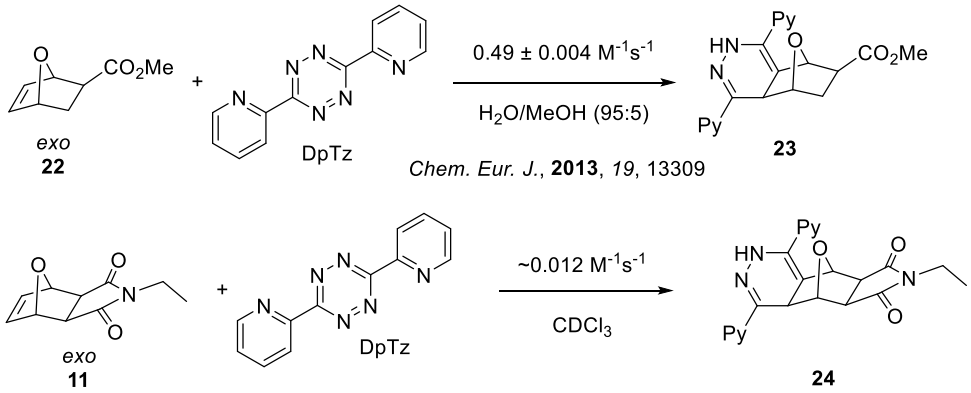

Figure 3.13 Preliminary results of the IEDDA between *exo* furan–maleimide adducts and DpTz.

3.5 Normal-Electron Demand DA Reaction with Tetrazine

The IEDDA reaction has grown to become one of the most important "click" reactions due to its fast kinetics and biorthogonality.[48] Tetrazine has been an essential component for the development of this reaction, as it can be easily synthesized and is a sterically unhindered and electron-deficient dienophile. Modification of tetrazines has focused on increasing the reactivity through electron-withdrawing groups[49] or tuning the sterics/electronics to balance reactivity with serum stability for bioorthogonal conjugation.[50]

The Beck-Sickinger group reported the reaction between tetrazine reacting with maleimide (**Figure 3.14**).[51] Given the electron withdrawn nature of tetrazine and maleimide, this reactivity is unexpected. Although the reaction described by Beck-Sickinger is too slow for many applications, we hypothesized the conjugation reaction can be accelerated by adding electron-donating groups to tetrazine to raise the highest occupied molecular orbital (HOMO).

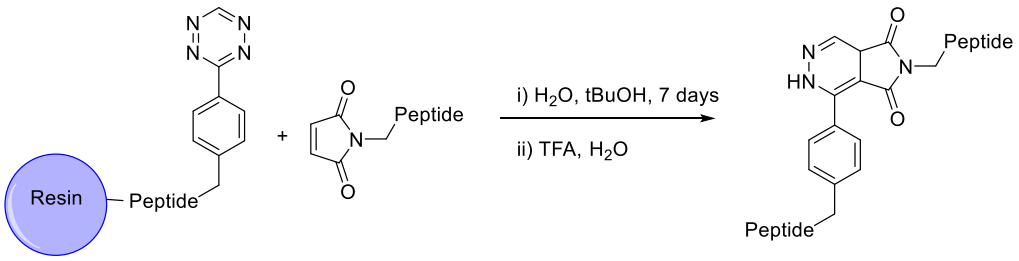

Figure 3.14 Reaction of tetrazine with maleimide.

To evaluate this hypothesis, we synthesized an electron-rich dimethoxytetrazine (**26**)[52] and evaluated the reaction with *N*-ethylmaleimide (**Figure 3.15**). Unfortunately, in $CDCl_3$, we found that there was no appreciable reaction with *N*-ethylmaleimide. Despite this disappointing result, it is worth noting that further optimization (solvents, temperature, extra) were not pursued due to limited time.

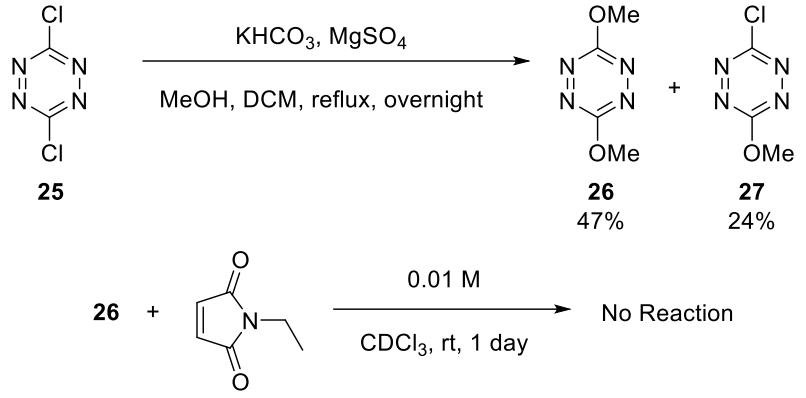

Figure 3.15 Attempted normal-electron demand DA reaction between an electron-rich tetrazine and maleimide.

3.6 Conclusion

In conclusion, we have developed a straightforward and scalable synthesis for an *endo* furan-protected maleimide functional building block and demonstrated its facile incorporation into two distinct systems - a di-functional small molecule *endo-exo* heterodimer and a multifunctional synthetic polymer with control over chain ends and backbone groups. By implementing metal-free ATRP and co-incorporating the *exo* isomer, we highlight key advantages of using a mild CRP for the design of materials with tunable functionalities that undergo selective deprotection based on temperature. Furthermore, we have demonstrated the utility of this chemistry through a series of site-specific and quantitative modifications using established and commonly implemented 'click' reactions including thiol-Michael addition, DA, and IEDDA conjugation chemistries. We envision that the ability to selectively introduce

functionality based on external temperature regulation will pave new pathways forward for efficient and precise small molecule and polymer modifications.

We also synthesized an *endo* furan-protected maleimide ncAA for the site-specific incorporation of maleimide into proteins. We developed a facile synthesis of *exo*-furan protected maleimides, with potential applications in medicinal chemistry, the radical thiol–ene reaction, ROMP, and the IEDDA. An attempt was made towards an electron-rich tetrazine partner for a normal electron-demand DA with maleimide. Further development of different maleimide derivatives and investigation into additional synthetic polymer applications is currently underway.

3.7 Experimental

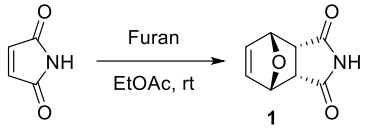

1

23 to 24%

(3a*R*,4*R*,7*S*,7a*S*)-3a,4,7,7a-tetrahydro-1*H*-4,7-epoxyisoindole-1,3(2*H*)-dione (1):

Maleimide (10.0 g, 103 mmol, 1 eq) and furan (20.0 mL, 275 mmol, 2.7 eq) were added to ethyl acetate (20 mL) and the solution was stirred at room temperature for 20 h. The resulting reaction mixture is approximately 1.6:1:0.1, 1:*exo*-adduct:maleimide via NMR. The solvent was removed, DCM (900 mL) was added, and the solution was warmed to the boiling point. The solution was hot filtered through Celite® into a 2 L round-bottomed flask, warmed slightly to ensure complete dissolution, and seed crystals of pure 1 were added to aid in the recrystallization (seed crystals were obtained from the slow evaporation of a saturated solution in DCM). The solution was left at room temperature for 4 hours then in a fridge (5 °C) for 1 to 3 days. The mother liquor was decanted and the crystals were washed with 10 mL of hexane before being dried under high vacuum, yielding **1** (3.8 to 4.0 g, 23 to 24%) as white crystals.

Spectral data matched that of literature reported data.[53] **1**: R_f (EtOAc): 0.50; ^{1}H NMR (500 MHz, DMSO-d_6) δ 10.85 (br. s., 1 H), 6.49 (t, *J* = 1.0 Hz, 2 H), 5.25 (tdd, *J* = 1.0, 1.8, 3.7 Hz, 2 H), 3.55 - 3.39 (m, 2 H) ppm; ^{13}C NMR (125 MHz, DMSO-d_6) δ 176.5, 134.5, 78.5, 47.1 ppm; IR (ATR) 3200 , 3087, 3003, 2956, 2765, 1767, 1707 cm^{-1}; HRMS (ES-) Exact mass cald. for $C_8H_6NO_3$ $[M-H]^-$: 164.0353, found: 164.0347.

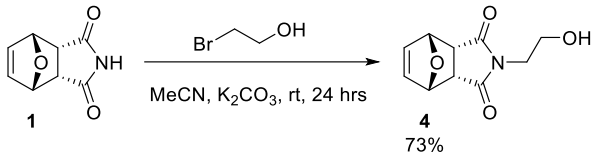

(3a*R*,4*R*,7*S*,7a*S*)-2-(2-hydroxyethyl)-3a,4,7,7a-tetrahydro-1*H*-4,7-epoxyisoindole-1,3(2*H*)-dione (4):

1 (3.75 g, 22.7 mmol, 1 eq) was added to MeCN (150 mL). K_2CO_3 (12.5 g, 90.4 mmol, 4 eq) and bromoethanol (3.3 mL, 47 mmol, 2 eq) were added and the reaction mixture was stirred at rt for 24 h. Brine (200 mL) was added and extracted with DCM (5 x 100 mL). The combined organic layers were dried over sodium sulfate, filtered, the solvent removed, and the residue subjected to flash column chromatography (EtOAc) to yield **4** (3.7 g, 73%) as a white powder. **4**: R_f (EtOAc): 0.37; ^{1}H NMR (400 MHz, $CDCl_3$) δ 6.44 (s, 2 H), 5.45 - 5.25 (m, 2 H), 3.68 (q, *J* = 5.3 Hz, 2 H), 3.61 - 3.48 (m, 4 H), 1.91 (t, *J* = 5.9 Hz, 1 H) ppm; ^{13}C NMR (100 MHz, $CDCl_3$) δ 175.5, 134.4, 79.4, 60.3, 46.0, 41.2 ppm; IR (ATR): 3371, 3083, 2971, 2953, 1795, 1755, 1673 cm^{-1}; HRMS (ES+) Exact mass cald. for $C_{10}H_{11}NO_4Na$ $[M+Na]^+$: 232.0580, found: 232.0596. CIF file was deposited at the CCDC database (CCDC 1821820).

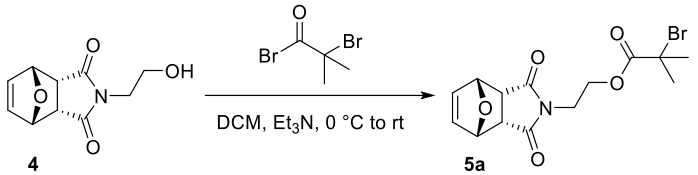

4 5a 84%

2-((3a*R*,4*R*,7*S*,7a*S*)-1,3-dioxo-1,3,3a,4,7,7a-hexahydro-2*H*-4,7-epoxyisoindol-2-yl)ethyl 2-bromo-2-methylpropanoate (5a):

4 (0.42 g, 2.0 mmol, 1 eq), triethylamine (0.56 mL, 4.0 mmol, 2 eq) were added to DCM (10 mL) and cooled to 0 ˚C. α-Bromoisobutyryl bromide (0.31 mL, 3.0 mmol, 1.5 eq), was added drop-wise, the reaction solution was stirred at 0 ˚C for 2 h then a further 36 h at rt. A saturated solution of $NaHCO_{3(aq)}$ (50 mL) was added then extracted with DCM (2 x 100 mL). The combined organic layers were dried over anhydrous sodium sulfate, the solution filtered, and the solvent removed. The residue was subjected to flash column chromatography (Hexanes:EtOAc, 2:1) to yield **5a** (0.60 g, 84%) as a clear and colorless oil that solidified when stored in the freezer. **5a**: R_f 0.30 (2 hexane: 1 EtOAc); ^{1}H NMR (400 MHz, $CDCl_3$) δ 6.45 (s, 2 H), 5.38 - 5.31 (m, 2 H), 4.21 (t, *J* = 5.3 Hz, 2 H), 3.66 (t, *J* = 5.3 Hz, 2 H), 3.58 - 3.51 (m, 2 H), 1.91 (s, 6 H) ppm; ^{13}C NMR (100 MHz, $CDCl_3$) δ 174.5, 171.4, 134.5, 79.3, 62.5, 55.4, 46.0, 37.3, 30.6 ppm; IR (ATR): 3073, 2996, 2981, 1765 cm^{-1}, 1685 cm^{-1}; HRMS (ES+) Exact mass cald. for $C_{14}H_{16}BrNO_5Na$ $[M+Na]^+$: 380.0104, found: 380.0122.

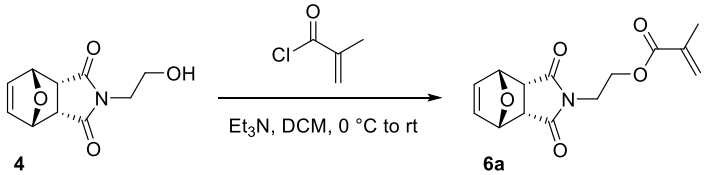

4 6a 80%

2-((3a*R*,4*R*,7*S*,7a*S*)-1,3-dioxo-1,3,3a,4,7,7a-hexahydro-2*H*-4,7-epoxyisoindol-2-yl)ethyl methacrylate (6a):

4 (1.0 g, 4.8 mmol, 1 eq) and triethylamine (1.4 mL, 9.6 mmol, 2 eq) were added to DCM (25 mL) and cooled to 0 ˚C. Methacryloyl chloride (0.7 mL, 7 mmol, 1.5 eq) was added

dropwise over 3 min. The reaction was stirred at 0 ˚C for 30 min then at rt for 4 h. Water (0.5 mL) was added and the reaction stirred a further 30 min. The solvent was removed, and the residue subjected to flash column chromatography (Hexanes:EtOAc, 1:1). The fractions were combined and several drops of an inhibitor solution (1 mg/mL MEHQ in DCM) and DMA (3.5 mL) were added. Removal of most of the volatile solvents yielded 2.63 g of a 38% (m/m, determined by NMR) solution of **6a** in DMA (1.0 g, 80%). **6a**: R_f (Hexanes:EtOAc, 1:1) 0.35; ^{1}H NMR (500 MHz, $CDCl_3$) δ 6.34 (t, *J* = 1.0 Hz, 2 H), 6.09 - 6.02 (m, 1 H), 5.59 (quin, *J* = 1.6 Hz, 1 H), 5.35 - 5.25 (m, 2 H), 4.15 (t, *J* = 5.2 Hz, 2 H), 3.65 (t, *J* = 5.2 Hz, 2 H), 3.51 (dd, *J* = 1.8, 3.6 Hz, 2 H), 1.91 (t, *J* = 1.0 Hz, 3 H) ppm; ^{13}C NMR (100 MHz, $CDCl_3$) δ 174.2, 166.3, 135.3, 133.8, 125.7, 78.8, 60.7, 45.4, 36.9, 17.7 ppm; HRMS (ES+) Exact mass cald. for $C_{14}H_{15}NO_5Na$ $[M+Na]^+$: 300.0842, found: 300.0853.

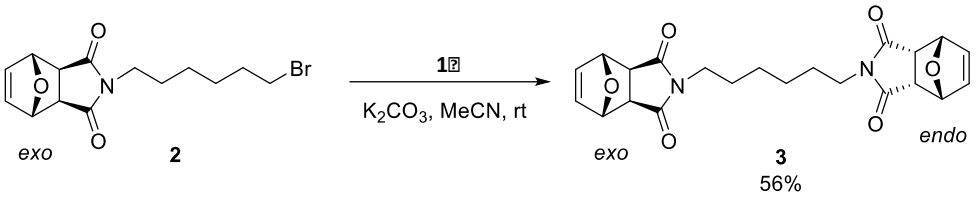

(3aR,4S,7R,7aS)-2-(6-((3aR,4R,7S,7aS)-1,3-dioxo-1,3,3a,4,7,7a-hexahydro-2H-4,7-epoxyisoindol-2-yl)hexyl)-3a,4,7,7a-tetrahydro-1H-4,7-epoxyisoindole-1,3(2H)-dione (3):

1 (0.40 g, 2.4 mmol, 1 eq), **2**[15] (1.2 g, 3.6 mmol, 1.5 eq), and K_2CO_3 (1.7 g, 12 mmol, 5 eq) were added to MeCN (24 mL) and the reaction mixture was stirred at rt for 24 h. The solvent was removed, the residue suspended in EtOAc, and washed with brine. The organic layer was dried over $MgSO_4$, the solution filtered, and the solvent removed. The residue was subjected to flash column chromatography (Hexanes:EtOAc, 1:1 to 1:2) to yield **3** (0.55 g, 1.3 mmol, 56%) as a white solid. **3**: ^{1}H NMR (600 MHz, $CDCl_3$) δ 6.51 (s, 2 H), 6.40 (s, 2H), 5.32 (m, 2H), 5.26 (s, 2H), 3.50 (m, 2H), 3.45 (t, 2H), 3.28 (t, 2H), 2.83 (s, 2H), 1.53 (m, 2H),

1.40 (m, 2H), 1.24 (m, 4H) ppm; ^{13}C NMR (150 MHz, $CDCl_3$) δ 176.4, 175.0, 136.7, 134.6, 81.0, 79.5, 47.5, 46.1, 38.8, 38.5, 27.4, 27.4, 26.4, 26.1 ppm; HRMS (ES+) Exact mass cald. for $C_{22}H_{24}N_2O_6Na$ $[M+Na]^+$: 435.1532, found 435.1343.

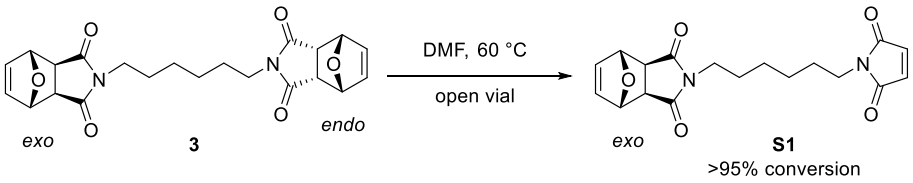

(3aR,4S,7R,7aS)-2-(6-(2,5-dioxo-2,5-dihydro-1H-pyrrol-1-yl)hexyl)-3a,4,7,7a-tetrahydro-1H-4,7-epoxyisoindole-1,3(2H)-dione (S1):

3 (0.010 g, 0.048 mmol) and DMF (2 mL) were added to a 20 ml vial with a magnetic stir bar. The open vial was heated to 60 °C for 22 h (NMR showed >95% conversion). After cooling to room temperature, DMF was evaporated under reduced pressure to afford **S1** as a pale yellow solid which was used directly used in the next step without further purification. Optionally, the residue can be further purified by flash column chromatography (Hexanes:EtOAc, 1:2). **S1**: ^{1}H NMR (600 MHz, $CDCl_3$) δ 6.65 (s, 2H), 6.48 (s, 2H), 5.23 (s, 2H), 3.46 (t, 2H), 3.43 (t, 2H), 2.81 (s, 2H), 1.54-1.51 (m, 4H), 1.32-1.23 (m, 4H) ppm; ^{13}C NMR (150 MHz, $CDCl_3$) δ 176.4, 170.9, 136.6, 134.1, 81.0, 47.5, 38.8, 37.8, 28.4, 27.4, 26.2, 26.1 ppm; HRMS (ES+) Exact mass cald. for $C_{18}H_{20}N_2O_5Na$ $[M+Na]^+$: 367.1270, found 367.1871.

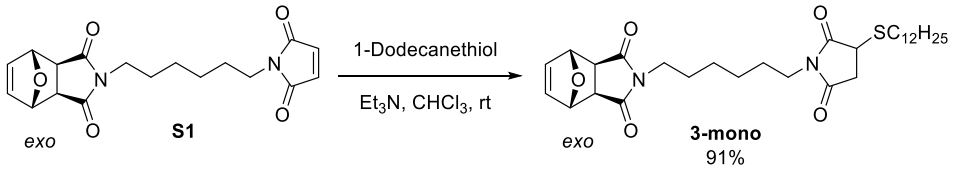

(3aR,4S,7R,7aS)-2-(6-(3-(dodecylthio)-2,5-dioxopyrrolidin-1-yl)hexyl)-3a,4,7,7a-tetrahydro-1H-4,7-epoxyisoindole-1,3(2H)-dione (3-mono):

S1 (0.035 g, 0.10 mmol, 1 eq) was dissolved in $CHCl_3$ (0.4 mL). The solution was purged with argon for 5 minutes, then 1-dodecanethiol (27 μL, 0.11 mmol, 1.1 eq) and triethylamine

(28 μL, 0.2 mmol, 2 eq) were added. The reaction was stirred at room temperature for 15 h. The crude reaction mixture was evaporated under reduced pressure and the residue was subjected to flash column chromatography (Hexanes:EtOAc, 1:1) to yield **3-mono** (0.050 g, 0.091 mmol, 91%) as a white solid. **3-mono**: ^{1}H NMR (600 MHz, $CDCl_3$) δ 6.48 (s, 2H), 5.23 (s, 2H), 3.68 (dd, *J* = 9.0, 3.6 Hz, 1H), 3.52 – 3.34 (m, 4H), 3.09 (dd, *J* = 18.6, 9.0 Hz, 1H), 2.84 (m, 1H), 2.80 (s, 2H), 2.75 – 2.67 (m, 1H), 2.48 (dd, *J* = 18.6, 3.6 Hz, 1H), 1.68 – 1.56 (m, 2H), 1.53 (m, 4H), 1.43 – 1.32 (m, 2H), 1.32 – 1.13 (m, 20H), 0.85 (t, *J* = 7.0 Hz, 3H) ppm; ^{13}C NMR (150 MHz, $CDCl_3$) δ 176.8, 176.3, 174.9, 136.6, 81.0, 81.0, 47.5, 39.1, 38.9, 38.8, 36.2, 32.0, 31.8, 29.7, 29.7, 29.7, 29.6, 29.4, 29.2, 29.1, 28.9, 27.4, 27.4, 26.2, 26.1, 22.8, 14.2 ppm; HRMS (ES+) Exact mass cald. for $C_{30}H_{46}N_2O_5SNa$ $[M+Na]^+$: 569.3025, found 569.4085.

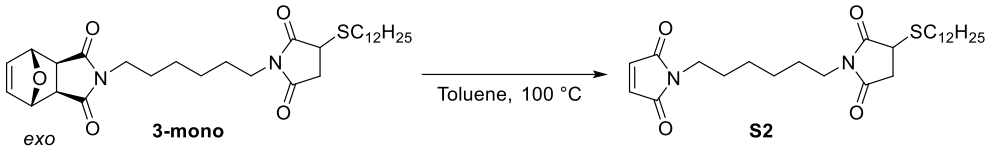

exo **3-mono** **S2**

1-(6-(3-(dodecylthio)-2,5-dioxopyrrolidin-1-yl)hexyl)-1H-pyrrole-2,5-dione (S2):

3-mono (0.012 g, 0.022 mmol) was dissolved in toluene (1.2 mL) in a 20 ml vial with a magnetic stir bar. The solution was purged with argon for 5 minutes and then allowed to stir at 100 °C for 17 h (TLC monitoring indicated complete conversion). After cooling to room temperature, the solvent was removed to yield **S2** as a pale yellow solid which was used directly used in the next step without further purification. **S2**: ^{1}H NMR (600 MHz, $CDCl_3$) δ 6.67 (s, 2H), 3.70 (dd, *J* = 9.0, 3.5 Hz, 1H), 3.56 – 3.40 (m, 4H), 3.11 (dd, *J* = 18.6, 9.0 Hz, 1H), 2.92 – 2.81 (m, 1H), 2.81 – 2.67 (m, 1H), 2.50 (dd, *J* = 18.6, 3.5 Hz, 1H), 1.70 – 1.50 (m, 6H), 1.45 – 1.34 (m, 2H), 1.33 – 1.14 (m, 20H), 0.87 (t, *J* = 6.9 Hz, 3H) ppm; ^{13}C NMR

(150 MHz, $CDCl_3$) δ 176.8, 175.0, 171.0, 134.2, 39.2, 39.0, 37.8, 36.2, 32.1, 31.9, 29.8, 29.8, 29.7, 29.6, 29.5, 29.3, 29.2, 29.0, 28.4, 27.5, 26.3, 26.3, 22.8, 14.3 ppm.

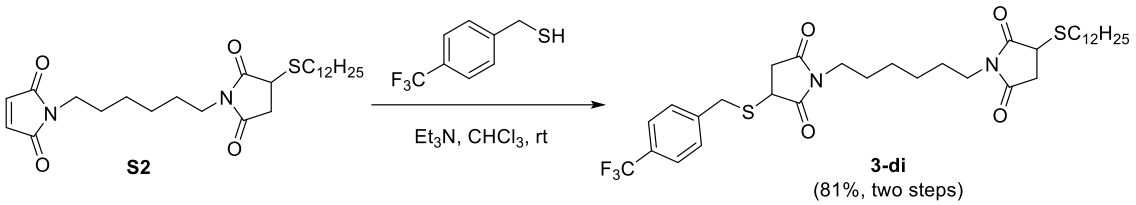

1-(6-(2,5-dioxo-3-((4-(trifluoromethyl)benzyl)thio)pyrrolidin-1-yl)hexyl)-3-(dodecylthio)pyrrolidine-2,5-dione (3-di):

S2 (0.0105 g, 0.022 mmol, 1 eq) was dissolved in $CHCl_3$ (0.3 mL). The vial was purged with argon for 5 minutes. 4-Trifluoromethylbenzyl mercaptan (0.0047 g, 0.024 mmol, 1.1 eq) and triethylamine (1.5 μL, 0.011 mmol, 0.5 eq) were added. The reaction was stirred at rt for 4 h. The solvent was removed and the residue was subjected to flash column chromatography (Hexanes:EtOAc, 2:1) to yield **3-di** (0.012 g, 0.018 mmol, 81% over two steps from **3-mono**) as a white solid. **3-di**: ^{1}H NMR (600 MHz, $CDCl_3$) δ 7.60 (d, *J* = 8.1 Hz, 2H), 7.55 (d, *J* = 8.0 Hz, 2H), 4.32 (d, *J* = 13.7 Hz, 1H), 3.88 (d, *J* = 13.7 Hz, 1H), 3.70 (dd, *J* = 9.0, 3.4 Hz, 1H), 3.56 – 3.46 (m, 4H), 3.43 (dd, *J* = 9.1, 3.4 Hz, 1H), 3.11 (dd, *J* = 18.6, 9.0 Hz, 1H), 2.99 (dd, *J* = 18.7, 9.2 Hz, 1H), 2.93 – 2.82 (m, 1H), 2.74 (m, 1H), 2.50 (dd, *J* = 18.6, 3.5 Hz, 1H), 2.39 (dd, *J* = 18.7, 3.5 Hz, 1H), 1.69 – 1.51 (m, 6H), 1.44 – 1.35 (m, 2H), 1.33 – 1.20 (m, 20H), 0.88 (t, *J* = 7.0 Hz, 3H) ppm; ^{13}C NMR (151 MHz, $CDCl_3$) δ 176.8, 175.0, 174.6, 141.2, 129.7, 125.8, 124.0, 39.2, 39.2, 39.0, 37.0, 36.3, 35.5, 35.2, 32.1, 31.9, 29.8, 29.8, 29.8, 29.7, 29.6, 29.5, 29.3, 29.2, 29.0, 27.5, 27.4, 26.2, 26.2, 22.8, 14.3 ppm; ^{19}F NMR (564 MHz, $CDCl_3$) δ -62.59 ppm; HRMS (ES+) Exact mass cald. for $C_{34}H_{49}F_3N_2O_4S_2Na$ $[M+Na]^+$: 693.2984, found 693.4252.

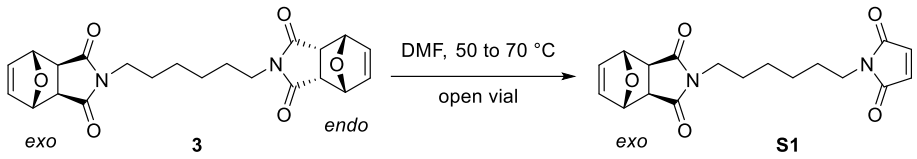

Kinetic profile for the mono-deprotection of *endo* and *exo*-protected maleimide model compound 3:

3 (0.010 g, 0.048 mmol) and 1,3,5-trimethoxybenzene (1 mg) were dissolved in DMF (2 mL) in a 20 ml vial with a magnetic stir bar. The open vial was stirred at 50, 55, 60, or 70 °C. Aliquots were taken intermittently taken to determine the percent deprotection of furan protecting groups by ^{1}H NMR spectroscopy using 1,3,5-trimethoxybenzene as an internal standard.

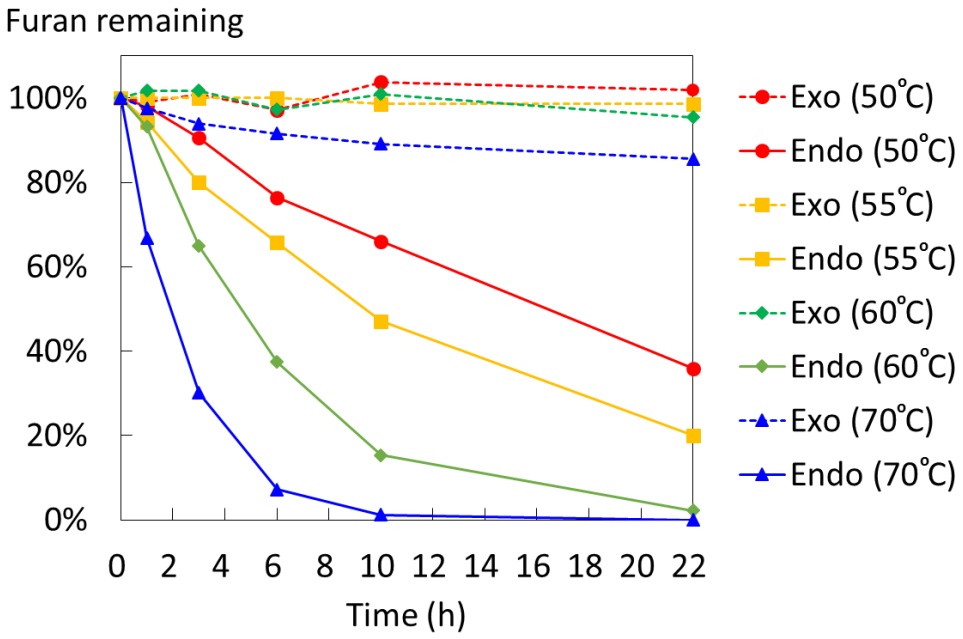

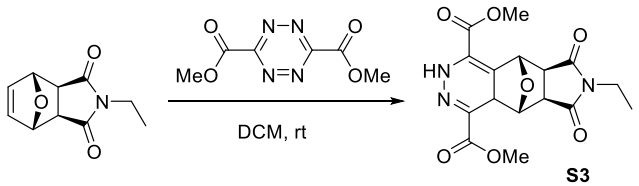

S3
83%

Dimethyl-(5S,5aR,8aS,9S)-7-ethyl-6,8-dioxo-4a,5,5a,6,7,8,8a,9-octahydro-2H-5,9-epoxypyrrolo[3,4-g]phthalazine-1,4-dicarboxylate (S3):

(3aR,4S,7R,7aS)-2-ethyl-3a,4,7,7a-tetrahydro-1H-4,7-epoxyisoindole-1,3(2H)-dione (0.0232 g, 0.12 mmol, 1 eq) was dissolved in DCM (1 mL) in a vial with a vent needle. 3,6-Bis(methoxycarbonyl)-1,2,4,5-tetrazine (35.7, 0.18 mmol, 1.5 eq) was added and the reaction stirred overnight or until the complete consumption of the starting material. The solvent was removed and the residue subjected to flash column chromatography (EtOAc:Hexanes, 3:1) to yield **S3** (0.036 g, 83%) as a white solid. **S3**: R_f (EtOAc:Hexanes, 3:1): 0.35; ^{1}H NMR (600 MHz, $CDCl_3$) δ 8.65 (s, 1 H), 5.96 (s, 1 H), 5.73 (s, 1 H), 3.99 (s, 3 H), 3.90 (s, 3 H), 3.59 (q, J = 7.1 Hz, 2 H), 3.22 (d, J = 7.0 Hz, 1 H), 3.07 (d, J = 7.0 Hz, 1 H), 2.54 (s, 1 H), 1.18 (t, J = 7.1 Hz, 3 H) ppm; ^{13}C NMR (100 MHz, $CDCl_3$) δ 175.5, 175.2, 163.3, 160.5, 126.6, 123.6, 119.4, 79.6, 78.8, 53.3, 52.8, 49.4, 47.8, 41.4, 34.3, 12.9 ppm; IR (ATR): 3285, 2950, 2920, 1735, 1687, 1275, 1144, 1098, 768, 749, 700 cm^{-1}; UV-Vis (DCM) λ: 263, 314 nm; HRMS (ES+) Exact mass cald. for $C_{16}H_{17}N_3O_7Na$ $[M+Na]^+$: 386.0959, found: 386.0954.

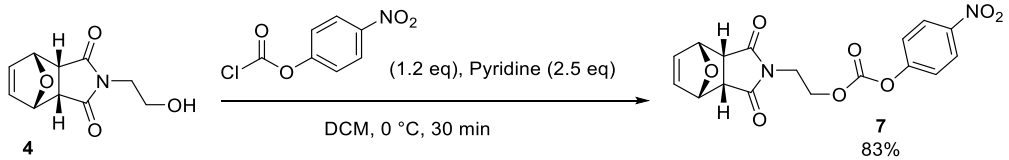

4 **7**
83%

2-((3aR,4R,7S,7aS)-1,3-dioxo-1,3,3a,4,7,7a-hexahydro-2H-4,7-epoxyisoindol-2-yl)ethyl (4-nitrophenyl) carbonate (7):

4 (1.89 g, 9.03 mmol, 1 eq) was added to DCM (50 mL) and cooled to 0 °C. Pyridine (1.84 mL, 22.6 mmol, 2.5 eq) was added, followed by 4-nitrophenyl chloroformate (2.18 g, 10.84

mmol, 1.2 eq). The reaction was stirred at 0 °C until consumption of the starting material (TLC, 30 min). The reaction was poured into a separatory funnel containing a saturated solution of NH_4Cl in H_2O (50 mL) and the layers separated. The aqueous layer was extracted with DCM (2 x 50 mL). The organic layers were combined, washed with brine (50 mL), dried over Na_2SO_4, filtered, and the solvent removed. The residue was subjected to flash column chromatography (Hexane:EtOAc, 1:1 to EtOAc) to yield **7** (2.80 g, 83%) as a tan powder. **7**: Rf (Hexane:EtOAc, 1:1): 0.32; ^{1}H NMR (400 MHz, $CDCl_3$) δ 8.34 - 8.25 (m, 2 H), 7.46 - 7.38 (m, 2 H), 6.47 (s, 2 H), 5.41 - 5.33 (m, 2 H), 4.29 (t, J = 5.1 Hz, 2 H), 3.76 (t, J = 5.1 Hz, 2 H), 3.59 (dd, J = 1.8, 3.7 Hz, 2 H) ppm; ^{13}C NMR (100 MHz, $CDCl_3$) δ 174.8, 155.3, 152.3, 145.6, 134.4, 125.3, 122.0, 79.4, 65.2, 46.0, 36.7 ppm.

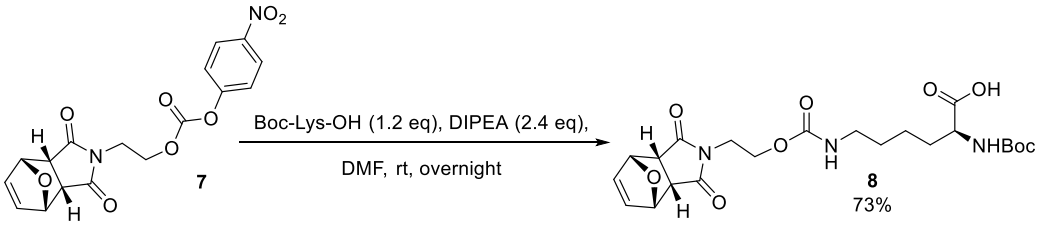

N2-(tert-butoxycarbonyl)-N6-((2-((3aR,4R,7S,7aS)-1,3-dioxo-1,3,3a,4,7,7a-hexahydro-2H-4,7-epoxyisoindol-2-yl)ethoxy)carbonyl)-L-lysine (8):

7 (2.80 g, 7.47 mmol, 1 eq) was added to DMF (30 mL), followed by Boc-Lys-OH (2.21 g, 8.96 mmol, 1.2 eq) and DIPEA (3.12 mL, 17.9 mmol, 2.4 eq). The reaction was stirred at rt overnight, then poured into EtOAc (150 mL) and H_2O (150 mL). The aqueous layer was acidified to pH ~2 with HCl (1 M, ~60 mL), poured into a separatory funnel, and the layers separated. The aqueous layer was extracted with EtOAc (150 mL). The organic layers were combined, washed with brine (100 mL), dried over Na_2SO_4, filtered, and the solvent removed. The residue was subjected to flash column chromatography (DCM:MeOH:AcOH 95:5:1) and the solvent removed. The residue was dissolved in benzene and the solvent removed (3 times)

then repeated with DCM (3 times). The product is a thick foam with residual solvent that does not affect the next reaction. Drying the compound under vacuum yielded **8** (2.64 g, 73%) as a white foam. **8**: Rf (DCM:MeOH, 9:1): 0.14; ^{1}H NMR (400 MHz, $CDCl_3$) δ 7.78 (br. s., 1 H), 6.39 (s, 2 H), 5.40 - 5.31 (m, 3 H), 4.36 - 4.04 (m, 3 H), 3.68 - 3.50 (m, 4 H), 3.16 (q, J = 6.3 Hz, 1 H), 1.92 - 1.79 (m, 1 H), 1.79 - 1.65 (m, 1 H), 1.59 - 1.36 (m, 14 H) ppm; ^{13}C NMR (100 MHz, $CDCl_3$) δ 176.1, 175.0, 156.1, 155.8, 134.4, 80.1, 79.4, 62.2, 61.3, 54.4, 53.2, 45.9, 40.4, 38.0, 31.7, 29.2, 28.3, 22.1 ppm.

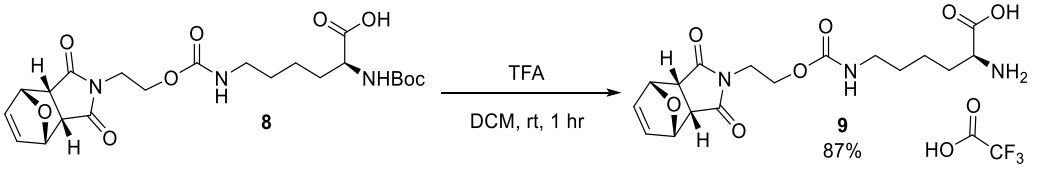

N6-((2-((3aR,4R,7S,7aS)-1,3-dioxo-1,3,3a,4,7,7a-hexahydro-2H-4,7-epoxyisoindol-2-yl)ethoxy)carbonyl)-L-lysine · TFA (9):

TFA (25 mL) was added to a solution of **8** (2.50 g, 5.20 mmol, 1 eq) in DCM (50 mL). The reaction was stirred at rt until consumption of the starting material (TLC, 60 min) then the solvent was removed. The residue was redissolved in DCM (50 mL) then the solvent was removed (repeat a total of 3 times). The residue was suspended in Et_2O (50 mL), sonicated (5 min), filtered, then rinsed with Et_2O (100 mL). The solid was dissolved in H_2O (50 mL) then lyophilized to yield **9** (2.23 g, 87%) as a deliquescent white foam. **9**: Rf (DCM:MeOH, 90:10): 0.06; ^{1}H NMR (400 MHz, D_2O) δ 6.36 (s, 2 H), 5.33 (d, J = 3.5 Hz, 2 H), 4.03 - 3.92 (m, 3 H), 3.68 - 3.59 (m, 2 H), 3.53 (t, J = 4.7 Hz, 2 H), 3.02 (t, J = 6.5 Hz, 2 H), 1.96 - 1.76 (m, 2 H), 1.48 - 1.25 (m, 4 H) ppm; ^{13}C NMR (100 MHz, D_2O): 177.5, 171.9, 157.8, 134.0, 79.1, 61.4, 52.6, 45.3, 39.6, 37.6, 29.2, 28.3, 21.3 ppm; ^{19}F NMR (376 MHz, D_2O) δ = -75.8 ppm.

General Procedure A: *Exo* Furan–Maleimide DA Adducts: Maleimide (1 mmol) was placed in a pressure tube with benzene (1 mL) and furan (250 ppm BHT, 0.73 mL, 10 mmol, 10 eq). The tube was sealed and heated to 80 °C for 3 hr (aryl series) or 18 hr (alkyl series). The volatiles were removed and residual solvent was removed through co-evaporation with DCM. The compounds obtained have BHT (~180 μg) as a contaminant, but were pure enough for most purposes without further purification.

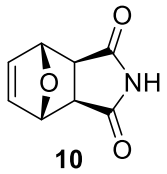

10

(3aR,4S,7R,7aS)-3a,4,7,7a-tetrahydro-1H-4,7-epoxyisoindole-1,3(2H)-dione (10):

Maleimide (1 mmol) was subjected to General Procedure A to afford **10** (157 mg, 95%) as a white powder. **10**: ^{1}H NMR (400 MHz, $CDCl_3$) δ 7.79 (br. s., 1 H), 6.53 (s, 2 H), 5.33 (s, 2 H), 2.90 (s, 2 H) ppm; ^{13}C NMR (100 MHz, $CDCl_3$) δ 176.0, 136.6, 81.0, 48.7 ppm.

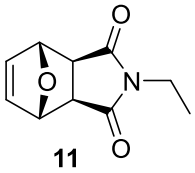

11

(3aR,4S,7R,7aS)-2-ethyl-3a,4,7,7a-tetrahydro-1H-4,7-epoxyisoindole-1,3(2H)-dione (11):

N-Ethylmaleimide (1 mmol) was subjected to General Procedure A to afford **11** (189 mg, 98%) as a white powder. **11**: ^{1}H NMR (400 MHz, $CDCl_3$) δ 6.51 (t, J = 1.0 Hz, 2 H), 5.27 (t, J = 1.0 Hz, 2 H), 3.53 (q, J = 7.0 Hz, 2 H), 2.83 (s, 1 H), 1.16 (t, J = 7.0 Hz, 3 H) ppm; ^{13}C NMR (100 MHz, $CDCl_3$) δ 176.1, 136.5, 80.8, 47.4, 33.9, 12.9 ppm.

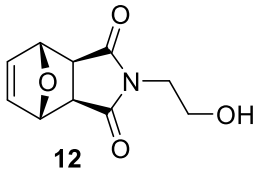

12

(3aR,4S,7R,7aS)-2-(2-hydroxyethyl)-3a,4,7,7a-tetrahydro-1H-4,7-epoxyisoindole-1,3(2H)-dione (12):

1-(2-Hydroxyethyl)-1H-pyrrole-2,5-dione (1 mmol) was subjected to General Procedure A to afford **12** (211 mg, 101%) as a white powder. **12**: ^{1}H NMR (400 MHz, $CDCl_3$) δ 6.53 (s, 2 H), 5.29 (s, 2 H), 3.83 - 3.73 (m, 2 H), 3.70 (t, J = 5.5 Hz, 2 H), 2.90 (s, 2 H), 2.32 (t, J = 4.7 Hz, 1 H) ppm; ^{13}C NMR (100 MHz, $CDCl_3$) δ 176.8, 136.5, 80.9, 60.3, 47.4, 41.7 ppm.

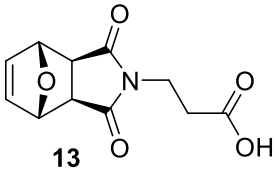

13

3-((3aR,4S,7R,7aS)-1,3-dioxo-1,3,3a,4,7,7a-hexahydro-2H-4,7-epoxyisoindol-2-yl)propanoic acid (13):

3-Maleimidopropionic acid (1 mmol) was subjected to General Procedure A with MeCN (1 mL) to afford **13** (234 mg, 99%) as a white powder. **13**: ^{1}H NMR (400 MHz, DMSO-d_6) 12.47 (br. s, 1 H), 6.54 (s, 2 H), 5.12 (s, 2 H), 3.55 (t, J = 7.6 Hz, 2 H), 2.92 (s, 2 H), 2.42 (t, J = 7.6 Hz, 2 H) ppm; ^{13}C NMR (100 MHz, DMSO-d_6) δ 176.2, 171.8, 136.5, 80.3, 47.2, 33.9, 31.7 ppm.

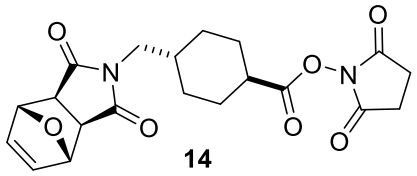

14

2,5-dioxopyrrolidin-1-yl (1R,4r)-4-(((3aR,4S,7R,7aS)-1,3-dioxo-1,3,3a,4,7,7a-hexahydro-2H-4,7-epoxyisoindol-2-yl)methyl)cyclohexane-1-carboxylate (14):

SMCC (0.1 mmol) was subjected to General Procedure A to afford **14** (40.5 mg, 100%) as a white solid. **14**: ^{1}H NMR (400 MHz, $CDCl_3$) δ 6.52 (s, 2 H), 5.27 (s, 2 H), 3.36 (d, J = 7.0 Hz, 2 H), 2.85 (s, 2 H), 2.82 (d, J = 2.7 Hz, 4 H), 2.56 (tt, J = 3.5, 12.1 Hz, 1 H), 2.14 (d, J = 11.3 Hz, 2 H), 1.83 - 1.70 (m, 3 H), 1.53 (dq, J = 3.3, 13.0 Hz, 2 H), 1.04 (dt, J = 2.7, 13.3 Hz, 2 H) ppm; ^{13}C NMR (100 MHz, $CDCl_3$) δ 176.5, 170.6, 169.1, 136.5, 80.9, 47.3, 44.4, 40.3, 35.2, 29.1, 28.0, 25.6 ppm.

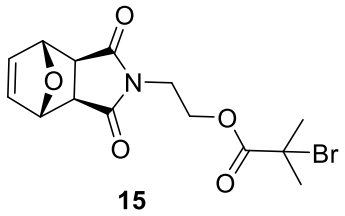

15

2-((3aR,4S,7R,7aS)-1,3-dioxo-1,3,3a,4,7,7a-hexahydro-2H-4,7-epoxyisoindol-2-yl)ethyl 2-bromo-2-methylpropanoate (15):

2-(2,5-dioxo-2,5-dihydro-1H-pyrrol-1-yl)ethyl 2-bromo-2-methylpropanoate (1 mmol) was subjected to General Procedure A to afford **15** (360 mg, 100%) as a white solid. **15**: ^{1}H NMR (400 MHz, $CDCl_3$) δ 6.52 (s, 2 H), 5.27 (s, 2 H), 4.33 (t, J = 5.3 Hz, 2 H), 3.82 (t, J = 5.3 Hz, 2 H), 2.87 (s, 2 H), 1.89 (s, 6 H) ppm; ^{13}C NMR (100 MHz, $CDCl_3$) δ 175.9, 171.4, 136.5, 80.8, 62.2, 55.7, 47.4, 37.6, 30.5 ppm.

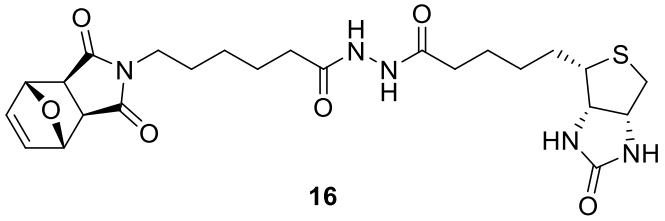

16

6-((3aR,4S,7R,7aS)-1,3-dioxo-1,3,3a,4,7,7a-hexahydro-2H-4,7-epoxyisoindol-2-yl)-N'-(5-((3aS,4S,6aR)-2-oxohexahydro-1H-thieno[3,4-d]imidazol-4-yl)pentanoyl)hexanehydrazide (16):

N-Biotinoyl-*N'*-(6-maleimidohexanoyl)hydrazide (≥95% purity by TLC, 0.01 mmol) was subjected to General Procedure A with DMSO-d_6 (1 mL). The furan was removed to afford **16** (>95% conversion of the maleimide by NMR) as a solution in DMSO-d_6. **16**: ^{1}H NMR (400 MHz, DMSO-d_6) δ 9.66 (s, 2 H), 6.55 (s, 2 H), 6.44 (s, 1 H), 6.37 (s, 1 H), 5.12 (s, 2 H), 4.35 - 4.26 (m, 1 H), 4.18 - 4.08 (m, J = 5.5 Hz, 1 H), 3.34 - 3.28 (m, 1 H), 3.13 - 3.04 (m, 1 H), 2.91 (s, 2 H), 2.82 (dd, J = 5.1, 12.1 Hz, 1 H), 2.57 (d, J = 12.1 Hz, 1 H), 2.14 - 2.02 (m, 4 H), 1.67 - 1.56 (m, 1 H), 1.56 - 1.38 (m, 6 H), 1.34 - 1.12 (m, 5 H), 0.90 - 0.82 (m, 1 H) ppm.

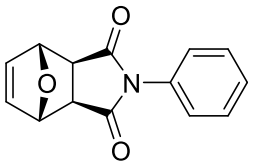

17

(3aR,4S,7R,7aS)-2-phenyl-3a,4,7,7a-tetrahydro-1H-4,7-epoxyisoindole-1,3(2H)-dione (17):

N-Phenylmaleimide (1 mmol) was subjected to General Procedure A to afford **17** (241 mg, 100%) as a white powder. **17**: ^{1}H NMR (400 MHz, $CDCl_3$) δ 7.48 (tt, J = 2.0, 7.4 Hz, 2 H), 7.41 (tt, J = 2.0, 7.4 Hz, 1 H), 7.29 (td, J = 2.0, 7.0 Hz, 2 H), 6.58 (s, 2 H), 5.41 (s, 2 H),

3.03 (s, 2 H) ppm; ^{13}C NMR (100 MHz, $CDCl_3$) δ 175.3, 136.7, 131.6, 129.1, 128.8, 126.5, 81.4, 47.5 ppm.

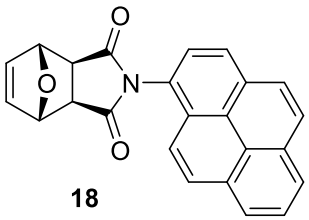

18

(3aR,4S,7R,7aS)-2-(pyren-1-yl)-3a,4,7,7a-tetrahydro-1H-4,7-epoxyisoindole-1,3(2H)-dione (18):

N-(1-Pyrenyl)maleimide (0.1 mmol) was subjected to General Procedure A to afford **18** (38 mg, 104%) as a light yellow powder. **18**: Mixture of rotamers (~3:1); ^{1}H NMR (400 MHz, $CDCl_3$) δ 8.30 - 8.02 (m, 8 H), 7.91 (d, J = 9.4 Hz, 0.75 H), 7.83 (d, J = 7.8 Hz, 1 H), 7.79 (d, J = 9.0 Hz, 0.25 H), 6.66 (s, 1.5 H), 6.64 (s, 0.5 H), 5.61 (s, 1.5 H), 5.54 (s, 0.5 H), 3.25 (s, 0.5 H), 3.21 (s, 1.5 H) ppm; ^{13}C NMR (125 MHz, $CDCl_3$) δ 176.0, 136.8, 136.7, 132.3, 132.2, 131.0, 130.9, 130.8, 130.7, 129.5, 129.0, 128.6, 128.5, 127.8, 127.5, 127.1, 127.0, 126.4, 126.1, 125.9, 125.6, 125.3, 125.19, 125.15, 125.0, 124.4, 124.3, 121.4, 121.1, 81.7, 81.6, 48.0, 47.9 ppm.

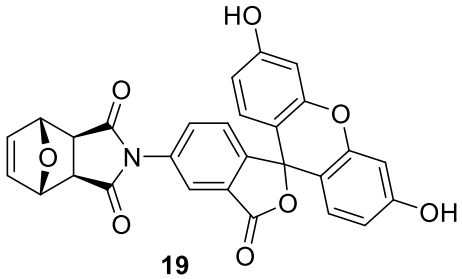

19

(3aR,4S,7R,7aS)-2-(3',6'-dihydroxy-3-oxo-3H-spiro[isobenzofuran-1,9'-xanthen]-5-yl)-3a,4,7,7a-tetrahydro-1H-4,7-epoxyisoindole-1,3(2H)-dione (19):

Fluorescein-5-Maleimide (0.025 mmol) was subjected to General Procedure A with DMSO-d_6 (1 mL). The furan was removed to afford **19** (>95% conversion of the maleimide

by NMR) as a solution in DMSO-d_6. **19**: ^{1}H NMR (400 MHz, DMSO-d_6) δ 10.19 (br. s., 2 H), 7.85 (d, J = 1.6 Hz, 1 H), 7.65 (dd, J = 2.0, 8.2 Hz, 1 H), 7.41 (d, J = 8.2 Hz, 1 H), 6.70 - 6.56 (m, 8 H), 5.30 (s, 2 H), 3.16 (s, 2 H) ppm; ^{13}C NMR (125 MHz, DMSO-d_6) δ 175.5, 167.8, 159.6, 151.9, 151.8, 136.7, 133.6, 133.4, 129.2, 126.8, 124.9, 122.2, 112.8, 109.0, 102.3, 83.4, 81.0, 47.6 ppm.

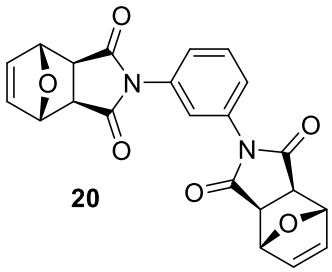

20

(3aR,3a'R,4S,4'S,7R,7aS,7'R,7a'S)-2,2'-(1,3-phenylene)bis(3a,4,7,7a-tetrahydro-1H-4,7-epoxyisoindole-1,3(2H)-dione) (20):

N,*N*′-(1,3-Phenylene)dimaleimide (1 mmol) was subjected to General Procedure A to afford **20** (405 mg, 100%) as a white powder. **20**: ^{1}H NMR (400 MHz, $CDCl_3$) δ 7.59 - 7.52 (m, 1 H), 7.42 - 7.33 (m, 3 H), 6.57 (s, 4 H), 5.39 (s, 4 H), 3.00 (s, 4 H) ppm; ^{13}C NMR (100 MHz, $CDCl_3$) δ 174.8, 136.7, 132.2, 129.4, 126.4, 124.2, 81.4, 47.5 ppm.

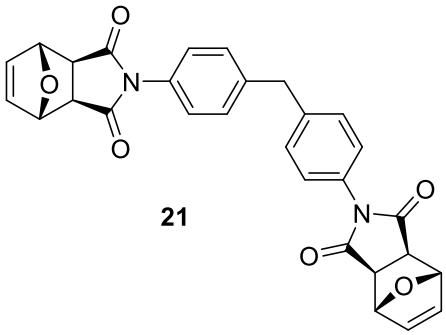

21

(3aR,3a'R,4S,4'S,7R,7aS,7'R,7a'S)-2,2'-(methylenebis(4,1-phenylene))bis(3a,4,7,7a-tetrahydro-1H-4,7-epoxyisoindole-1,3(2H)-dione) (21):

1,1′-(Methylenedi-4,1-phenylene)bismaleimide (1 mmol) was subjected to General Procedure A to afford **21** (491 mg, 99%) as a white powder. **21**: ^{1}H NMR (400 MHz, $CDCl_3$)

δ 7.28 (d, J = 8.6 Hz, 4 H), 7.21 (d, J = 8.2 Hz, 4 H), 6.57 (s, 4 H), 5.40 (s, 4 H), 4.04 (s, 2 H), 3.01 (s, 4 H) ppm; ^{13}C NMR (100 MHz, $CDCl_3$) δ 175.4, 141.1, 136.7, 129.9, 129.7, 126.6, 81.4, 47.5, 41.1 ppm.

3.8 References

(1) Discekici, E. H.; St. Amant, A. H.; Nguyen, S. N.; Lee, I. H.; Hawker, C. J.; Read De Alaniz, J. Endo and Exo Diels-Alder Adducts: Temperature-Tunable Building Blocks for Selective Chemical Functionalization. *J. Am. Chem. Soc.* **2018**, *140* (15), 5009–5013.

(2) Moses, J. E.; Moorhouse, A. D. The Growing Applications of Click Chemistry. *Chem. Soc. Rev.* **2007**, *36* (8), 1249–1262.

(3) Hall, D. J.; Van Den Berghe, H. M.; Dove, A. P. Synthesis and Post-Polymerization Modification of Maleimide-Containing Polymers by "thiol-Ene" Click and Diels-Alder Chemistries. *Polym. Int.* **2011**, *60* (8), 1149–1157.

(4) Chen, G.-Q.; Wu, Z.-Q.; Wu, J.-R.; Li, Z.-C.; Li, F.-M. Synthesis of Alternating Copolymers of N-Substituted Maleimides with Styrene via Atom Transfer Radical Polymerization. *Macromolecules* **2000**, *33* (2), 232–234.

(5) Robin, M. P.; Jones, M. W.; Haddleton, D. M.; O'Reilly, R. K. Dibromomaleimide End Functional Polymers by RAFT Polymerization Without the Need of Protecting Groups. *ACS Macro Lett.* **2012**, *1* (1), 222–226.

(6) Dispinar, T.; Sanyal, R.; Sanyal, A. A Diels-Alder/Retro Diels-Alder Strategy to Synthesize Polymers Bearing Maleimide Side Chains. *J. Polym. Sci. Part A Polym. Chem.* **2007**, *45* (20), 4545–4551.

(7) Mantovani, G.; Lecolley, F.; Tao, L.; Haddleton, D. M.; Clerx, J.; Cornelissen, J. J. L.

M.; Velonia, K. Design and Synthesis of N-Maleimido-Functionalized Hydrophilic Polymers via Copper-Mediated Living Radical Polymerization: A Suitable Alternative to PEGylation Chemistry. *J. Am. Chem. Soc.* **2005**, *127* (9), 2966–2973.

(8) Pelegri-O'Day, E. M.; Maynard, H. D. Controlled Radical Polymerization as an Enabling Approach for the Next Generation of Protein-Polymer Conjugates. *Acc. Chem. Res.* **2016**, *49* (9), 1777–1785.

(9) Bays, E.; Tao, L.; Chang, C.-W.; Maynard, H. D. Synthesis of Semitelechelic Maleimide Poly(PEGA) for Protein Conjugation By RAFT Polymerization. *Biomacromolecules* **2009**, *10* (7), 1777–1781.

(10) Onbulak, S.; Tempelaar, S.; Pounder, R. J.; Gok, O.; Sanyal, R.; Dove, A. P.; Sanyal, A. Synthesis and Functionalization of Thiol-Reactive Biodegradable Polymers. *Macromol. (Washington, DC, United States)* **2012**, *45* (3), 1715–1722.

(11) Hizal, G.; Tunca, U.; Sanyal, A. Discrete Macromolecular Constructs via the Diels-Alder "Click" Reaction. *J. Polym. Sci. Part A Polym. Chem.* **2011**, *49* (19), 4103–4120.

(12) Tolstyka, Z. P.; Kopping, J. T.; Maynard, H. D. Straightforward Synthesis of Cysteine-Reactive Telechelic Polystyrene. *Macromol. (Washington, DC, United States)* **2008**, *41* (3), 599–606.

(13) Froidevaux, V.; Borne, M.; Laborbe, E.; Auvergne, R.; Gandini, A.; Boutevin, B. Study of the Diels-Alder and Retro-Diels-Alder Reaction between Furan Derivatives and Maleimide for the Creation of New Materials. *RSC Adv.* **2015**, *5* (47), 37742–37754.

(14) Dolci, E.; Michaud, G.; Simon, F.; Boutevin, B.; Fouquay, S.; Caillol, S. Remendable Thermosetting Polymers for Isocyanate-Free Adhesives: A Preliminary Study. *Polym. Chem.* **2015**, *6* (45), 7851–7861.

(15) Binder, W. H.; Kluger, C. Combining Ring-Opening Metathesis Polymerization (ROMP) with Sharpless-Type “Click” Reactions: An Easy Method for the Preparation of Side Chain Functionalized Poly(Oxynorbornenes). *Macromolecules* **2004**, *37* (25), 9321–9330.

(16) Anastasaki, A.; Nikolaou, V.; Nurumbetov, G.; Wilson, P.; Kempe, K.; Quinn, J. F.; Davis, T. P.; Whittaker, M. R.; Haddleton, D. M. Cu(0)-Mediated Living Radical Polymerization: A Versatile Tool for Materials Synthesis. *Chem. Rev. (Washington, DC, United States)* **2016**, *116* (3), 835–877.

(17) Discekici, E. H.; Pester, C. W.; Treat, N. J.; Lawrence, J.; Mattson, K. M.; Narupai, B.; Toumayan, E. P.; Luo, Y.; McGrath, A. J.; Clark, P. G.; et al. Simple Benchtop Approach to Polymer Brush Nanostructures Using Visible-Light-Mediated Metal-Free Atom Transfer Radical Polymerization. *ACS Macro Lett.* **2016**, *5* (2), 258–262.

(18) Chen, M.; Zhong, M.; Johnson, J. A. Light-Controlled Radical Polymerization: Mechanisms, Methods, and Applications. *Chem. Rev. (Washington, DC, United States)* **2016**, *116* (17), 10167–10211.

(19) Pan, X.; Fang, C.; Fantin, M.; Malhotra, N.; So, W. Y.; Peteanu, L. A.; Isse, A. A.; Gennaro, A.; Liu, P.; Matyjaszewski, K. Mechanism of Photoinduced Metal-Free Atom Transfer Radical Polymerization: Experimental and Computational Studies. *J. Am. Chem. Soc.* **2016**, *138* (7), 2411–2425.

(20) Theriot, J. C.; Lim, C.-H.; Yang, H.; Ryan, M. D.; Musgrave, C. B.; Miyake, G. M. Organocatalyzed Atom Transfer Radical Polymerization Driven by Visible Light. *Science (80-.).* **2016**, *352* (6289), 1082 LP-1086.

(21) Pearson, R. M.; Lim, C.-H.; McCarthy, B. G.; Musgrave, C. B.; Miyake, G. M.

Organocatalyzed Atom Transfer Radical Polymerization Using N-Aryl Phenoxazines as Photoredox Catalysts. *J. Am. Chem. Soc.* **2016**, *138* (35), 11399–11407.

(22) McKenzie, T. G.; Fu, Q.; Uchiyama, M.; Satoh, K.; Xu, J.; Boyer, C.; Kamigaito, M.; Qiao, G. G. Beyond Traditional RAFT: Alternative Activation of Thiocarbonylthio Compounds for Controlled Polymerization. *Adv. Sci. (Weinheim, Ger.* **2016**, *3* (9), n/a.

(23) Xu, J.; Shanmugam, S.; Duong, H. T.; Boyer, C. Organo-Photocatalysts for Photoinduced Electron Transfer-Reversible Addition-Fragmentation Chain Transfer (PET-RAFT) Polymerization. *Polym. Chem.* **2015**, *6* (31), 5615–5624.

(24) Lee, I.-H.; Discekici, E. H.; Anastasaki, A.; Read de Alaniz, J.; Hawker, C. J. Controlled Radical Polymerization of Vinyl Ketones Using Visible Light. *Polym. Chem.* **2017**, *8* (21), 3351–3356.

(25) Inglis, A. J.; Sinnwell, S.; Stenzel, M. H.; Barner-Kowollik, C.; Andrew J., I.; Sebastian, S.; Martina H., S.; Christopher, B. Ultrafast Click Conjugation of Macromolecular Building Blocks at Ambient Temperature. *Angew. Chemie Int. Ed.* **2009**, *48* (13), 2411–2414.

(26) Inglis, A. J.; Paulöhrl, T.; Barner-Kowollik, C. Ambient Temperature Synthesis of a Versatile Macromolecular Building Block: Cyclopentadienyl-Capped Polymers. *Macromolecules* **2010**, *43* (1), 33–36.

(27) Yameen, B.; Rodriguez-Emmenegger, C.; Preuss, C. M.; Pop-Georgievski, O.; Verveniotis, E.; Trouillet, V.; Rezek, B.; Barner-Kowollik, C. A Facile Avenue to Conductive Polymer Brushes via Cyclopentadiene-Maleimide Diels-Alder Ligation. *Chem. Commun.* **2013**, *49* (77), 8623–8625.

(28) Hillmyer, M. A.; Lepetit, C.; McGrath, D. V; Novak, B. M.; Grubbs, R. H. Aqueous

Ring-Opening Metathesis Polymerization of Carboximide-Functionalized 7-Oxanorbornenes. *Macromolecules* **1992**, *25* (13), 3345–3350.

(29) Durmaz, H.; Butun, M.; Hizal, G.; Tunca, U. Postfunctionalization of Polyoxanorbornene via Sequential Michael Addition and Radical Thiol-Ene Click Reactions. *J. Polym. Sci. Part A Polym. Chem.* **2012**, *50* (15), 3116–3125, S3116/1–S3116/5.

(30) Warrener, R. N.; Butler, D. N.; Margetic, D. Preparation of the First Isobenzofuran Containing Two Ring Nitrogens: A New Diels-Alder Diene for the Synthesis of Molecular Scaffolds Containing One or More End-Fused 3,6-Di(2-Pyridyl)Pyridazine Ligands. *Aust. J. Chem.* **2003**, *56* (8), 811–817.

(31) Hansell, C. F.; Espeel, P.; Stamenović, M. M.; Barker, I. A.; Dove, A. P.; Du Prez, F. E.; O'Reilly, R. K. Additive-Free Clicking for Polymer Functionalization and Coupling by Tetrazine–Norbornene Chemistry. *J. Am. Chem. Soc.* **2011**, *133* (35), 13828–13831.

(32) Jain, S.; Neumann, K.; Zhang, Y.; Valero, E.; Geng, J.; Bradley, M. Tetrazine-Mediated Postpolymerization Modification. *Macromol. (Washington, DC, United States)* **2016**, *49* (15), 5438–5443.

(33) Barker, I. A.; Hall, D. J.; Hansell, C. F.; Du Prez, F. E.; O'Reilly, R. K.; Dove, A. P. Tetrazine-Norbornene Click Reactions to Functionalize Degradable Polymers Derived from Lactide. *Macromol. Rapid Commun.* **2011**, *32* (17), 1362–1366.

(34) Jensen, L. H.; Renodon-Corniere, A.; Wessel, I.; Langer, S. W.; Søkilde, B.; Carstensen, E. V; Sehested, M.; Jensen, P. B. Maleimide Is a Potent Inhibitor of Topoisomerase II in Vitro and in Vivo: A New Mode of Catalytic Inhibition. *Mol. Pharmacol.* **2002**, *61* (5), 1235 LP-1243.

(35) Nishimura, H.; Mayama, M.; Komatsu, Y.; Kato, H.; Shimaoka, N.; Tanaka, Y. Showdomycin, a New Antibiotic from a Streptomyces Sp. *J. Antibiot. (Tokyo).* **1964**, *17*, 148.

(36) Elstner, E. F.; Carnes, D. M.; Suhadolnik, R. J.; Kreishman, G. P.; Schweizer, M. P.; Robins, R. K. Isolation, Structural Elucidation, Biological Properties, and Biosynthesis of Maleimycin, a New Bicyclic Maleimide Antibiotic Isolated from the Culture Filtrates of Streptomyces Showdoensis. 14. *Biochemistry* **1973**, *12* (24), 4992–4997.

(37) J., S. M.; Daniel, S. Red-Light-Controlled Protein–RNA Crosslinking with a Genetically Encoded Furan. *Angew. Chemie Int. Ed.* **2013**, *52* (17), 4690–4693.

(38) Vieille, C.; Zeikus, G. J. Hyperthermophilic Enzymes: Sources, Uses, and Molecular Mechanisms for Thermostability. *Microbiol. Mol. Biol. Rev.* **2001**, *65* (1), 1–43.

(39) Otto, S.; Engberts Jan, B. F. N. Diels_Alder Reactions in Water. *Pure and Applied Chemistry*. 2000, p 1365.

(40) Rideout, D. C.; Breslow, R. Hydrophobic Acceleration of Diels-Alder Reactions. *J. Am. Chem. Soc.* **1980**, *102* (26), 7816–7817.

(41) Renault, K.; Fredy, J. W.; Renard, P.-Y.; Sabot, C. Covalent Modification of Biomolecules through Maleimide-Based Labeling Strategies. *Bioconjug. Chem.* **2018**.

(42) Yu, F.; Cao, X.; Li, Y.; Chen, X. Diels–Alder Click-Based Hydrogels for Direct Spatiotemporal Postpatterning via Photoclick Chemistry. *ACS Macro Lett.* **2015**, *4* (3), 289–292.

(43) Robertson, M. J.; Gordon, C. P.; Gilbert, J.; McCluskey, A.; Sakoff, J. A. Norcantharimide Analogues Possessing Terminal Phosphate Esters and Their Anti-Cancer Activity. *Bioorg. Med. Chem.* **2011**, *19* (18), 5734–5741.

(44) Sánchez, A.; Pedroso, E.; Grandas, A. Maleimide-Dimethylfuran Exo Adducts: Effective Maleimide Protection in the Synthesis of Oligonucleotide Conjugates. *Org. Lett.* **2011**, *13* (16), 4364–4367.

(45) Keller, K. A.; Guo, J.; Punna, S.; Finn, M. G. A Thermally-Cleavable Linker for Solid-Phase Synthesis. *Tetrahedron Lett.* **2005**, *46* (7), 1181–1184.

(46) Vrabel, M.; Kölle, P.; Brunner, K. M.; Gattner, M. J.; López-Carrillo, V.; de Vivie-Riedle, R.; Carell, T. Norbornenes in Inverse Electron-Demand Diels–Alder Reactions. *Chem. – A Eur. J.* **2013**, *19* (40), 13309–13312.

(47) Selvaraj, R.; Fox, J. M. Trans-Cyclooctene — a Stable, Voracious Dienophile for Bioorthogonal Labeling. *Curr. Opin. Chem. Biol.* **2013**, *17* (5), 753–760.

(48) Sletten, E. M.; Bertozzi, C. R. Bioorthogonal Chemistry: Fishing for Selectivity in a Sea of Functionality. *Angew. Chemie Int. Ed.* **2009**, *48* (38), 6974–6998.

(49) Wang, D.; Chen, W.; Zheng, Y.; Dai, C.; Wang, K.; Ke, B.; Wang, B. 3{,}6-Substituted-1{,}2{,}4{,}5-Tetrazines: Tuning Reaction Rates for Staged Labeling Applications. *Org. Biomol. Chem.* **2014**, *12* (23), 3950–3955.

(50) Devaraj, N. K.; Weissleder, R.; Hilderbrand, S. A. Tetrazine-Based Cycloadditions: Application to Pretargeted Live Cell Imaging. *Bioconjug. Chem.* **2008**, *19* (12), 2297–2299.

(51) Pagel, M.; Meier, R.; Braun, K.; Wiessler, M.; Beck-Sickinger, A. G. On-Resin Diels–Alder Reaction with Inverse Electron Demand: An Efficient Ligation Method for Complex Peptides with a Varying Spacer to Optimize Cell Adhesion. *Org. Biomol. Chem.* **2016**, *14* (21), 4809–4816.

(52) Fan, X.; Ge, Y.; Lin, F.; Yang, Y.; Zhang, G.; Ngai, W. S. C.; Lin, Z.; Zheng, S.; Wang,

J.; Zhao, J.; et al. Optimized Tetrazine Derivatives for Rapid Bioorthogonal Decaging in Living Cells. *Angew. Chemie Int. Ed.* **2016**, *55* (45), 14046–14050.

(53) Rulíšek, L.; Šebek, P.; Havlas, Z.; Hrabal, R.; Čapek, P.; Svatoš, A. An Experimental and Theoretical Study of Stereoselectivity of Furan−Maleic Anhydride and Furan−Maleimide Diels−Alder Reactions. *J. Org. Chem.* **2005**, *70* (16), 6295–6302.

4 Norbornadiene as a Protected Form of Cyclopentadiene for a One-Pot Deprotection and Conjugation with Maleimide

Portions of this chapter are included in a manuscript that is under preparation.[1]

4.1 Introduction

The implementation of small molecule conjugation chemistries to materials science has had a transformative impact on the field of functional polymer synthesis.[2,3] Over the years, innumerable post-polymerization modification strategies have emerged from the concept of "click chemistry", enabling the synthesis of polymers with a diverse array of chain-end and backbone functionality, architecture and unique properties.[4] The Diels–Alder (DA) cycloaddition reaction represents one the most facile "click" platforms in polymer synthesis and has been utilized across a range of applications including the functionalization of nanoparticles, surfaces, and the preparation of antibody drug conjugates.[5] Moreover, the versatility of the DA platform is further exemplified by the capacity to tune reaction rates and reversibility of the resulting bonds through judicious selection of dienes and dienophiles.

Maleimides are among the most commonly utilized dienophiles for normal electron-demand DA due to their highly favorable reaction kinetics and widespread availability. In the area of functional polymer synthesis, typical dienes used in conjunction with maleimides include furan or anthracene-based moieties (**Figure 4.1**). While a useful alternative to metal-catalyzed "click" reactions, polymeric materials prepared using these functionalities are not suitable for high temperature applications. Furthermore, the DA cycloaddition with these dienes are plagued by the necessity for high temperatures and long reaction times to achieve good efficiency. To mitigate the limitations of slow conjugation, previous reports describe the

use water as a solvent,[6] or the addition of catalysts (Lewis acid[7] or catalytic antibody[8]) as ways to promote rate acceleration for DA cycloaddition with maleimides. However, the most straightforward method to ensure high conjugation efficiency is to utilize a highly reactive and electron rich functionality such as cyclopentadiene (Cp) as the diene.[9]

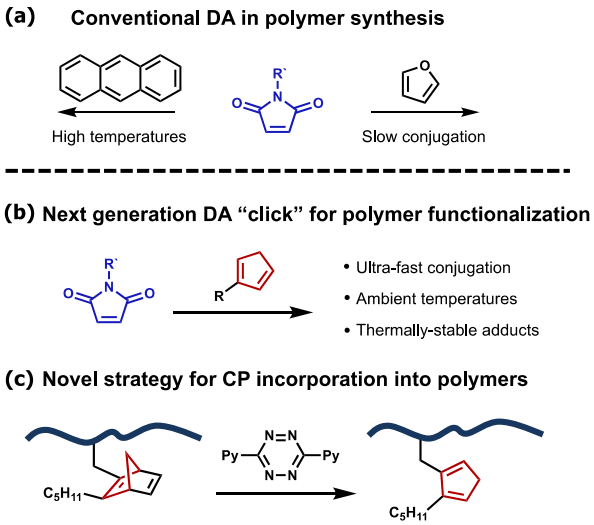

Figure 4.1 (a) Current methods for maleimide-polymer conjugation using anthracene or furan (b) maleimide-polymer conjugation with Cp (c) Strategy reported herein for introducing Cp into polymers

Recognizing the potential of Cp as a polymer "click" platform, Barner-Kowollik and co-workers have developed synthetic routes to access Cp-functionalized polymers (**Figure 4.2a**) for conjugation with maleimides,[10] electron-deficient dithioesters,[11,12] and carbon nanoparticles.[13,14] The synthesis of these Cp-containing polymers is through two main strategies, with the first being nucleophilic substitution using ionic cyclopentadienyl salts (NaCp,[11] LiCp,[15] or Me_2AlCp[16]). This strategy has been used to synthesize Cp chain-end functionalized polystyrene[11] and poly(ethyleneglycol) (PEG).[11] In the case of ester containing polymers, the harsh nature of ionic cyclopentadienyl salts lead to decomposition of the polymer backbone. This prompted the development of an alternative substitution strategy using nickelocene ($NiCp_2$).[12,17,18] Despite the development of these strategies, the ability to

incorporate Cp into controlled polymers has been limited to chain-ends through post-polymerization strategies. This is simply because the high reactivity of Cp renders it incompatible through traditional living polymerization techniques due to general instability[19] and its reactivity towards electron-deficient monomers.[20] We identified these longstanding challenges as an opportunity to develop a novel and exceedingly simple approach for the incorporation of Cp as both chain-end or pendant group functionalities amenable with some of the most commonly utilized "living" polymerization techniques. There are two examples in the literature of post-polymerization incorporation of Cp onto polymer sidechains (a patent using aluminum cyclopentadienyl complexes[16] and the NaCp substitution of a polyketone[15]) forming self-crosslinking gels; as gels are difficult to characterize, it isn't clear if the crosslinking is from DA dimerization or Cp nucleophilically attacking two polymer chains.

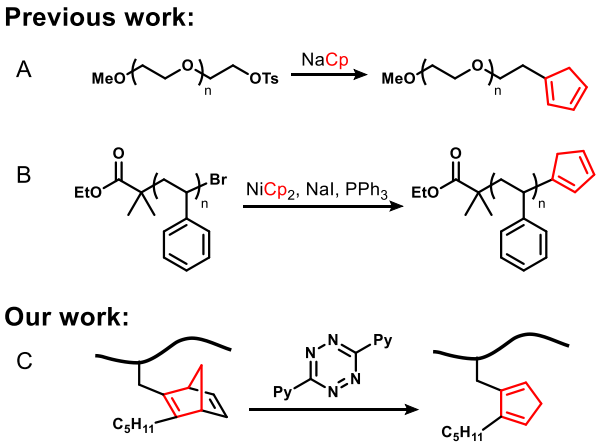

Figure 4.2 Current methods for the synthesis cyclopentadiene-containing polymers: A) Nucleophilic substitution with cyclopentadienyl salts B) Substitution with nickelocene C) Tetrazine deprotection of a polymer-incorporated norbornadiene.

Drawing inspiration from small molecule synthesis,[21,22] we identified norbornadiene (NBD), a strained bicyclic diene, as a potentially well-suited Cp precursor in polymers due to its synthetic simplicity and high bench stability. The McLean group reported a synthesis of cyclopentadiene (**4**) through the reaction of norbornadiene (**1**) with phenylazide (**2**) then thermolysis of **3**, or cyclopentadione (**6**) then thermolysis or photolysis of **7** (**Figure 4.3**).[23]

McLean's application of photolysis towards the production of Cps is to avoid thermal energy that will tautomerize the Cp. Photolysis can also be used in photopatterning to produce advanced materials, such as Barner-Kowollik's application of phencyclone–maleimide adducts towards patterned peptides.[24] It may be possible to produce tetraphenylcyclopentadienone–NBD adducts (similar to **7**) that are attached to a surface. When irradiated with UV, the cascade of reaction will produce surface-patterned Cp for further functionalization.

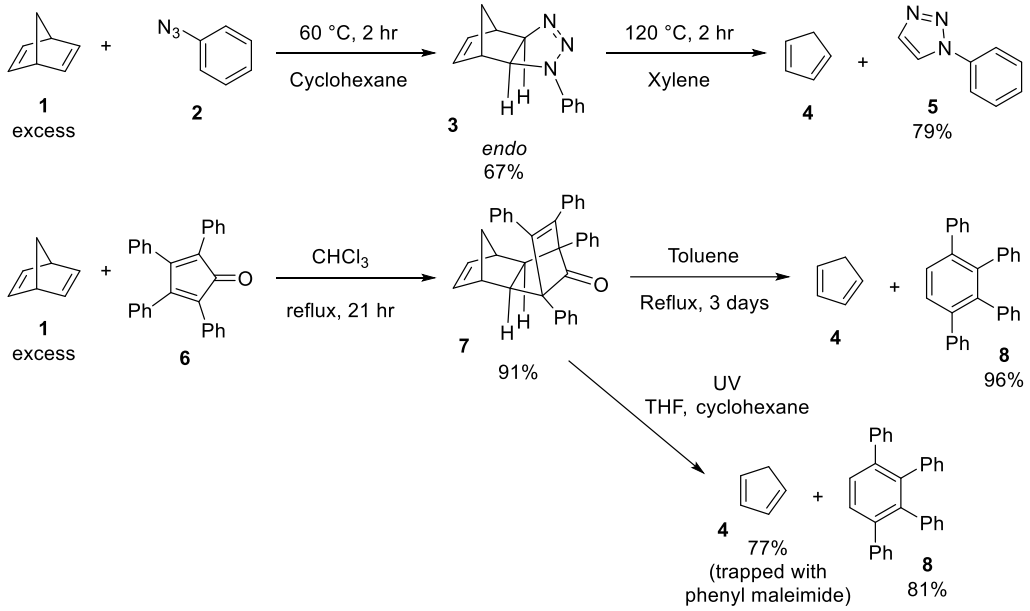

Figure 4.3 McLean's synthesis of cyclopentadiene from norbornadiene using azide or cyclopentadienone.

The high ring strain energy of NBD (32.2 kcal/mol)[25] also facilitates a cascade of rapid cycloaddition reactions when used in conjunction with tetrazine.[26–28] This highly efficient reaction proceeds through an inverse electron-demand DA (IEDDA) reaction that releases N_2, followed by a retro-DA (rDA), to yield pyridazine and Cp as products. This cascade reaction has been utilized for the synthesis of pyridazine ligands[29] and substituted Cps.[21,22] The inspiration for this work came from Daştan's deprotection of norbornadiene (**10**) with

dimethyl 1,2,4,5-tetrazine-3,6-dicarboxylate (**9**, **Figure 4.4**). The fast reaction rate and high yield led makes this strategy applicable to polymer functionalization.

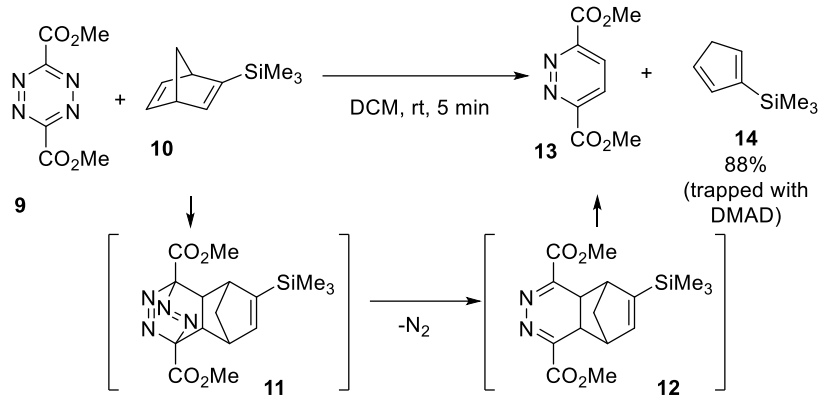

Figure 4.4 Daştan's synthesis of cyclopentadienes through the deprotection of norbornadiene with tetrazine

Interestingly, due to its reversible photoisomerization to quadricyclane,[30] NBD-containing polymers have found utility in a variety of energy storage applications. Typical synthetic routes for NBD-functionalized materials involve post-polymerization modification[31–33] or free radical strategies,[34] with select reports demonstrating the preparation of end functional NBD-macromonomers used for ring opening metathesis polymerization (ROMP).[35,36] Despite the availability of methods to prepare NBD-containing polymers, the concept of using NBD as a precursor to Cp has yet to be explored. We identified this as a unique opportunity to exploit NBD to develop a highly efficient polymer "click" functionalization platform. Herein we report the facile synthesis of a novel NBD polymer building block derived from very inexpensive starting materials and its facile incorporation into polymers using reversible addition−fragmentation chain-transfer (RAFT) and ring-opening polymerization (ROP) strategies. The subsequent reaction of NBD with tetrazine quantitatively produced Cp that can undergo *in situ* conjugation with commercially available maleimides and maleimide-functionalized polymers with high efficiency. This novel "click" platform represents a next-generation methodology in functional polymer synthesis.

4.2 Results and Discussion

Our initial investigation began with the synthesis of NBD derivatives with an alcohol handle as a polymer building block (**Figure 4.5**).

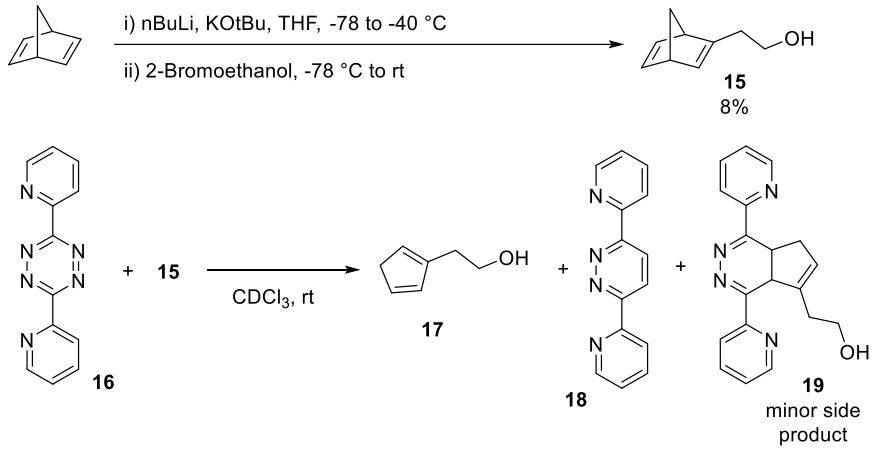

Figure 4.5 Synthesis of NBD model compound and investigation of the deprotection.

The synthesis of **15** begins with the lithiation of norbornadiene using Schlosser's base, then substitution of 2-bromoethanol. The low yield (8%) is due to the unprotected alcohol consuming an equivalent of lithiated norbornene, but provided sufficient material for a model study. The second order kinetics of the IEDDA reaction of DpTz (**16**) and **15** were ~0.006 $M^{-1}s^{-1}$, followed by fast release of N_2, then a slower first order rDA of the adduct to produce **17** and the pyridazine **18**. A minor side-product, where DpTz reacts with the unsubstituted olefin of Cp **17**, was observed. This is not unexpected, as Sauer examined the reaction rate of CpH with electron-withdrawn tetrazines.[37] We believed we could prevent this side-reaction through optimization of the deprotection conditions. We proceeded with a synthesis of a pentylene derivative that would be simpler to synthesize (**Figure 4.6**).

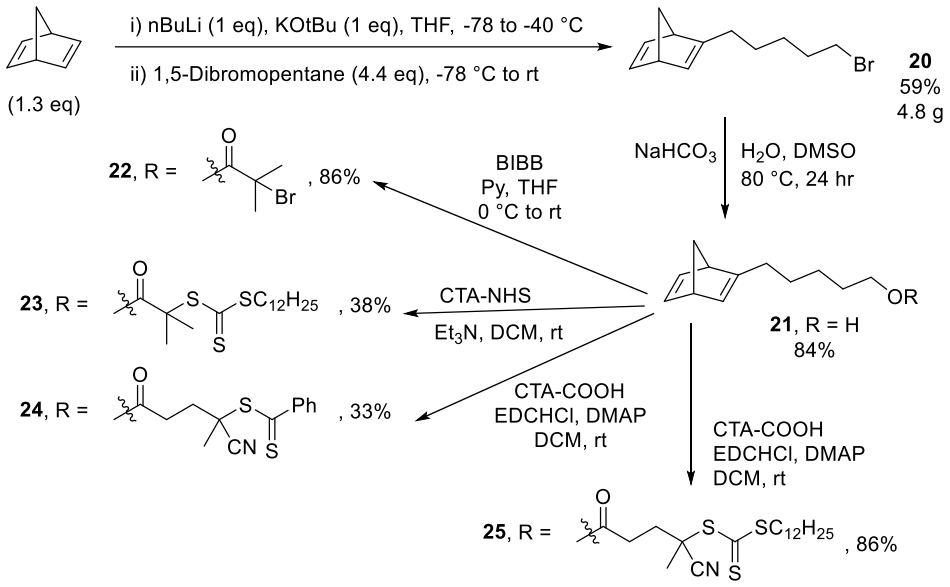

Figure 4.6 Synthesis of a pentylene NBD alcohol.

The lithiated NBD was reacted with an excess of 1,5-dibromopentane, which produced the NBD-bromide **20** in good yield. The hydrolysis proceeded in good yield, producing our NBD building block **21**, a compound with an unpleasant and distinct odour. This building block was used to synthesize ATRP and RAFT initiators **22**-**25** and subjected to polymerization conditions (results not shown), with thermal RAFT conditions giving the best results. After attempts to optimize the deprotection conditions, we found the Cp + DpTz reaction to be unavoidable so an alternative NBD building block was required. We hypothesized that a 2,3-disubtituted NBD would deprotect to produce the 2,3-disubstituted Cp, which would block the side-reaction with tetrazine. Its known that disubstituted Cp will tautomerize through a 1,5-hydride shift, but at room temperature we believed this first order tautomerization would be slower than conjugation to a maleimide. We began the synthesis with the alkyne **27**, as the material was available in house (**Figure 4.7**).

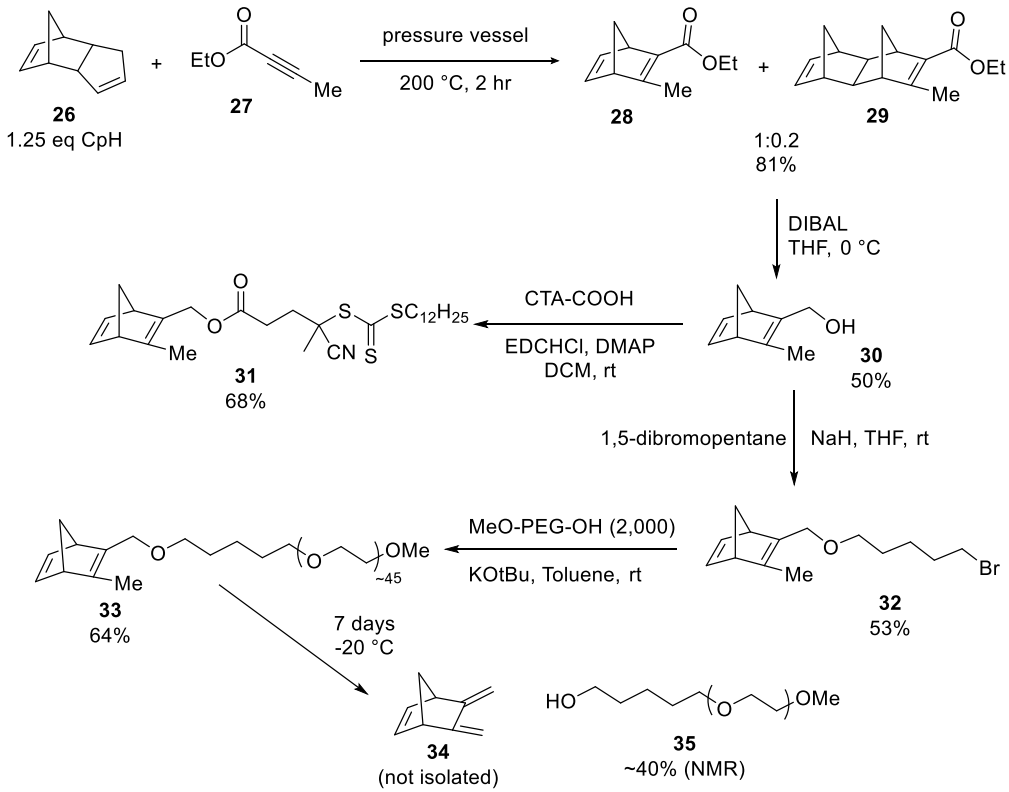

Figure 4.7 Synthesis of the methyl substituted NBD building block.

In a pressure reaction we have diCpH (**26**) (which cracks *in situ*) which undergoes a DA reaction with the electron-withdrawn alkyne. Ester **28** (contaminated with some double DA adduct) is then reduced with DIBAL to produce the building block **30**. RAFT initiator **31** was synthesized along with the alkyl bromide **32** for PEG functionalization. The NBD-PEG **33** was synthesized to be a stable version of Cp-PEG, but we found that it underwent significant decomposition. We suspect the ether bond undergoes an elimination, as ester derivatives (such as in **31**) was found to be stable.

After running out of compound **30**, we had consumed all of the methyl alkyne **27** and its price is ~ $12 per gram. We found that methyl 2-octynoate (**36**), a starting material that would yield the pentyl-NBD, was an inexpensive flavouring agent < $1 per gram. For a scalable synthesis of our NBD building block we used **36** for our synthesis (**Figure 4.8**).

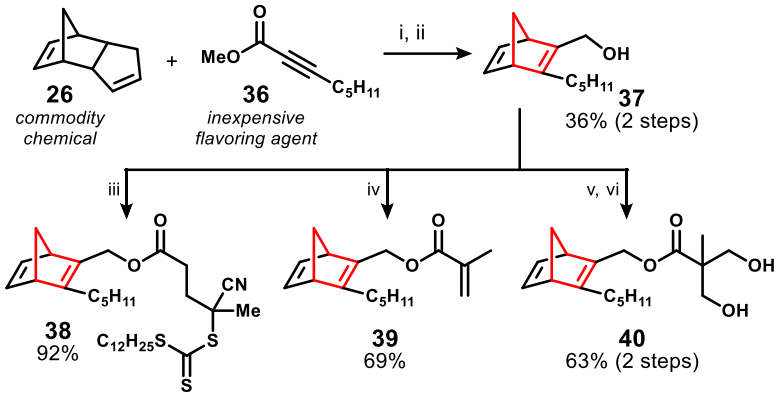

Figure 4.8 Synthesis of norbornadiene polymer building blocks. i) neat, pressure vessel, 200 °C, 5 hr, 50% ii) DIBAL, THF, 0 °C, 30 min, 71% iii) CDTPA, EDC·HCl, DMAP, DCM, rt, 16 hr, 92% iv) Methacryloyl chloride, Et_3N, DCM, 0 °C, 30 min, 69% v) 2,2-Bis(*tert*-butyldimethylsiloxymethyl)propionic acid, EDC·HCl, DMAP, DCM, rt, 2 days, 86% vi) TBAF, THF, rt, 73%.

When **26** and **36** are heated neat in a pressure vessel at 200 °C, the resulting methyl ester compound can be isolated via distillation and subsequently reduced with DIBAL[38] to furnish the NBD alcohol building block **37** in moderate overall yield. Furthermore, the simplicity of this process enables easy access to gram-scale quantities of **37**, which serves as a key precursor for a variety of polymeric building blocks. For instance, **37** can be used directly as a functional ROP initiator or converted to a RAFT chain transfer agent (**38**) in one step from commercial RAFT agents. Additionally, **37** can be utilized to access a novel methacrylate derivative (**39**) that can be incorporated via standard radical polymerization techniques. The diol ROP initiator **40** was also synthesized in two steps from 2,2-bis(*tert*-butyldimethylsiloxymethyl)propionic acid, a widely utilized intermediate for the preparation of dendritic materials.[39]

With access to a variety of polymer building blocks, the ability to integrate NBD via traditional "living" polymerization techniques was investigated. The copolymerization of **39** with methyl methacrylate (MMA) was performed using conventional thermally-initiated RAFT polymerization. RAFT was chosen due to its synthetic simplicity and wide monomer

scope. After 7 h of reaction time at 60 °C, approximately 53% monomer conversion was observed to produce polymer **P1**. Significantly, upon analysis by size exclusion chromatography equipped with a refractive index detector (SEC-RI), a low dispersity (*Đ*) and molar mass in close agreement with theoretical values was confirmed, indicating a well-controlled process. The successful incorporation of NBD was confirmed using ^{1}H NMR analysis (**Figure 4.9**). The versatility of RAFT also permitted incorporation of NBD on the chain-end of methacrylate-based polymers using **38** as the chain transfer agent.

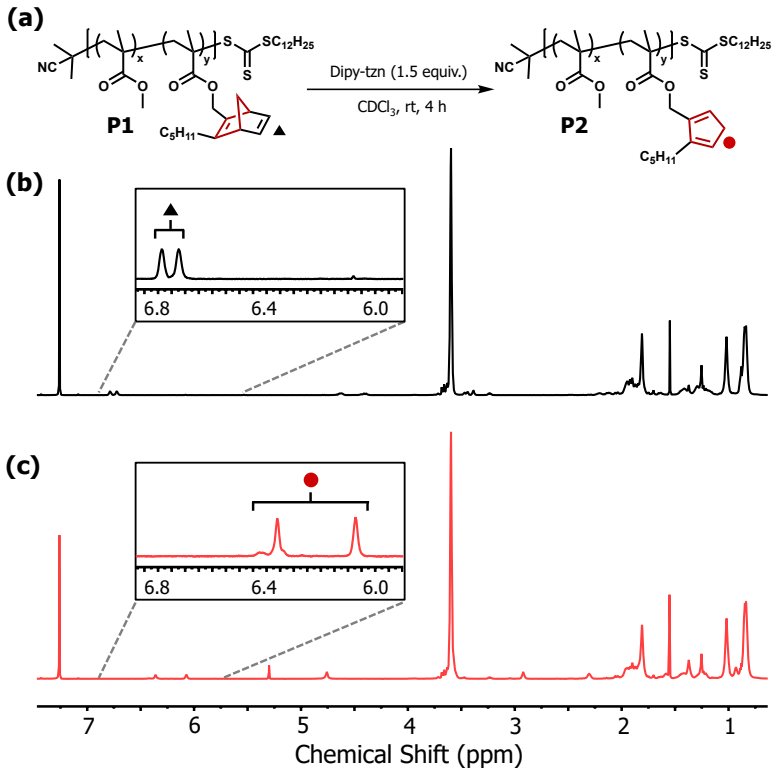

Figure 4.9 (a) NBD deprotection to produce Cp polymer using DpTz. Note: quenched with norbornene after 2 h. ^{1}H NMR of RAFT polymers in $CDCl_3$ (b) Copolymer bearing pendant NBD groups, P1 and (c) Cp-functionalized copolymer, P2.

Following development of a synthetic route to NBD containing polymers, deprotection conditions to convert NBD to Cp were explored. By simply adding 1.5 equivalents of 3,6-di-2-pyridyl-1,2,4,5-tetrazine (DpTz) to **P1** in $CDCl_3$, quantitative conversion to **P2** was observed after 4 h at room temperature as evidenced by ^{1}H NMR analysis (>95% by NMR).

No precaution was taken to ensure an air or moisture-free environment, further exemplifying the simplicity of this strategy. It is important to note that the major Cp isomer formed is the 2,3-disubstituted species. Over time, a [1,5]-hydride shift to a 1,2-disubstituted species can occur[40,37,41] and may result in unwanted reactivity with DpTz. A simple quench of excess DpTz can be performed by adding norbornene after full consumption of NBD. Norbornene reacts rapidly to quench tetrazine, a reaction that has been exploited for polymer conjugation.[42,43] Furthermore, this quenching step enables more facile precipitation of the resulting polymers due to the greater solubility of DpTz-norbornene adducts relative to DpTz. SEC-RI analysis of the polymer before and after the deprotection step indicated no change in the shape of the molar mass distribution (i.e. higher MW shoulders), suggesting good stability of the resulting Cp-functionalized material.

The significance behind the facile introduction of Cp into polymeric systems is the ability to perform metal-free and room temperature "click" post-functionalization with commercial maleimides. We envisioned that this process could proceed through sequential deprotection and traditional DA cycloaddition pathways, wherein the maleimide lies dormant until the Cp is revealed. The orthogonality of these cycloaddition processes combined with the metal-free and user-friendly nature of the reaction set-up points toward the possibility for developing a next-generation "click" functionalization strategy. To demonstrate this concept, **P1** was subject to standard deprotection conditions along with *N*-(1-pyrenyl)maleimide (PyrM) to promote rapid trapping of the released Cp. Interestingly, quantitative incorporation of the PyrM was observed as evidenced by ^{1}H NMR analysis. Thus, the ability to add maleimides at the beginning of the reaction *in situ* enables a one-pot deprotection-conjugation strategy and significantly simplifies reaction set-up.

To further demonstrate the versatility of this process, compound **37** was utilized as an initiator for the base-catalyzed ROP of D,L-lactide to obtain end-functional polylactic acid (PLA) **P3** (**Figure 4.10**). The resulting polymer was determined to have an M_n of 42,000 g/mol and a $Đ$ = 1.04, representing a new class of Cp functional polymers using traditional ROP conditions. To validate the ability to perform highly efficient conjugation on a different polymeric system, **P3** was subject to a solution of DpTz (2.4 equiv) and PyrM (1.2 equiv) in $CDCl_3$ and allowed to react at room temperature for 24 h with a quenching step using norbornene performed at the 4 h mark. Following purification by precipitation, pyrene-functionalized **P4** was obtained in high efficiency. The incorporation of pyrene was determined to be >95% as evidenced by ^{1}H NMR. The pyrene incorporation was confirmed quantitatively by UV-Vis spectroscopy using a calibration curve prepared from known concentrations of PyrM. Significantly, SEC characterization before and after functionalization confirmed no change in molar mass distribution, further exemplifying the mild nature of this platform. It should be emphasized that this chain-end modification strategy was performed on a high molecular weight system, which highlights the high efficiency and "click" nature of this chemistry.

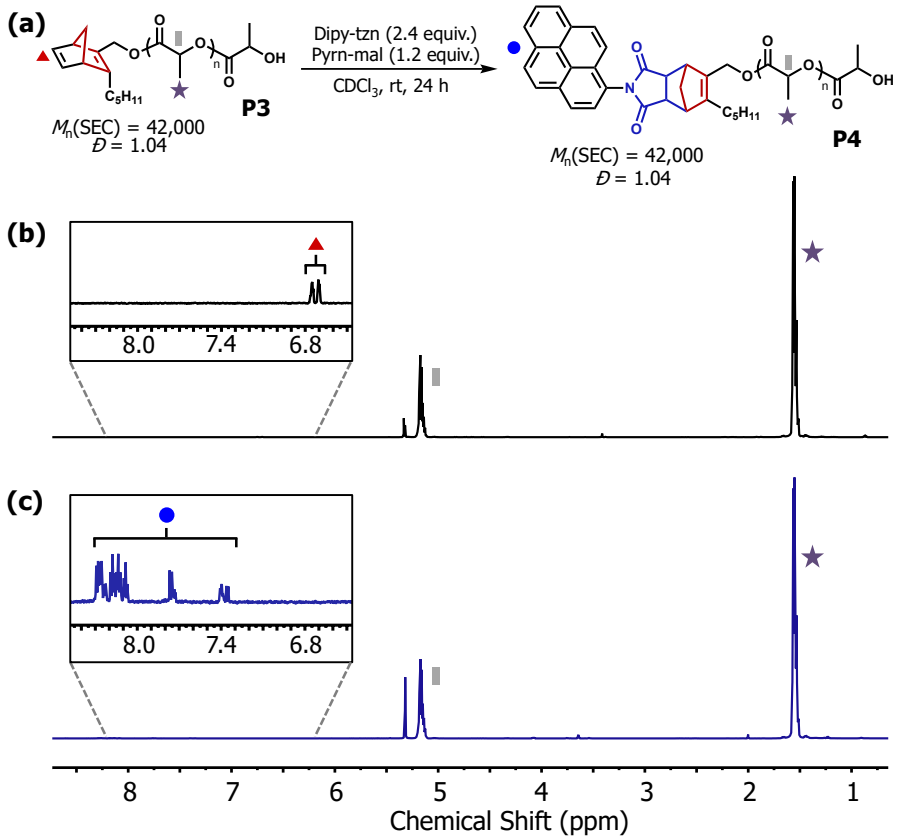

Figure 4.10 (a) One-pot deprotection of NBD and conjugation with maleimide. Note: quenched with norbornene after 4 h. ^{1}H NMR of PLA in dichloromethane-d_2 (b) NBD-functionalized PLA, P3 and (c) PyrM-functionalized PLA, P4.

The extension of this platform to enable access to unique architectures is essential to demonstrate the versatility of this system. With this in mind, we drew inspiration from the dendrimer literature and synthesized NBD-containing diol **40** to produce two-armed polymers. Using standard ROP of lactide, a two-armed B_2 precursor (**Figure 4.11**) was obtained. In addition to highlighting facile reactivity with commercial small molecule maleimides, we envisaged that this synthetic platform would provide access to AB_2 miktoarm star polymers when paired with linear maleimide-terminated polymers. Based on a previously reported preparation of maleimide-terminated poly(methacrylates) from our groups,[44] we synthesized poly(*n*-butyl methacrylate) (PnBMA) **P5** using metal-free ATRP to serve as the conjugation partner. Indeed, when **P5** was used in slight excess (1.5 equiv.) in the presence of

P6 and DpTz, the corresponding AB_2 $(PLA)_2$-*b*-PnBMA miktoarm **P7** was obtained after only 24 h. It is important to note that excess **P5** was simply removed by precipitation of the crude reaction mixture into a 50:50 mixture of methanol:isopropanol. SEC-RI analysis confirmed the expected shift in retention time indicating the successful formation of a higher molar mass species. ^{1}H NMR analysis of **P7** after precipitation also confirmed the presence of PnBMA and PLA blocks. To provide additional evidence for successful conjugation, the self-assembly behavior of **P7** was investigated using small-angle x-ray scattering (SAXS). After annealing **P7** at 120 °C for 4 h, Bragg reflections corresponding to well-ordered lamellae were observed, further confirming the formation of the AB_2 architecture. As an additional demonstration of the modularity of this platform, a second AB_2 miktoarm star was prepared using polymer precursors of different molar masses. Upon annealing, the polymer exhibited microphase separation to hexagonally packed cylinders as evidenced by SAXS characterization. The ability to quickly and efficiently link polymer precursors promotes a more facile avenue to tune chemical composition and volume fraction of blocks through this "mix and match" approach. We envision this strategy will enable easy access to a myriad of interesting polymeric architectures.

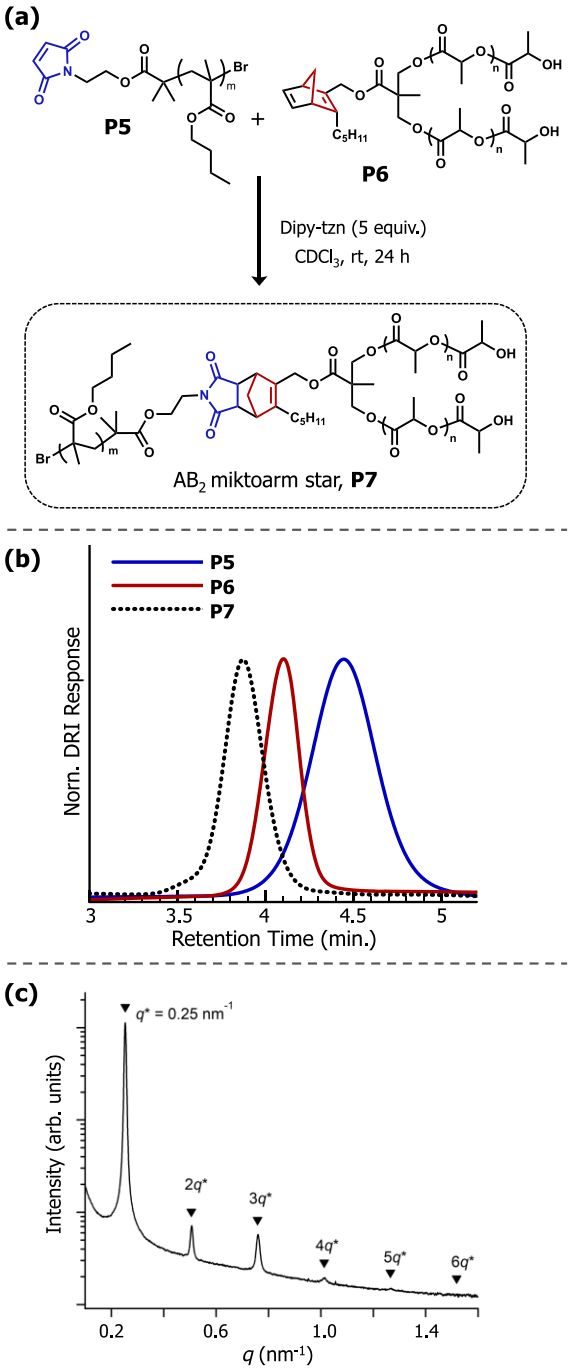

Figure 4.11 (a) Chemical schematic for one-pot AB_2 miktoarm star formation using sequential deprotection-conjugation strategy between maleimide-terminated PnBuMA (P5) and two-arm NBD-functionalized PLA (P6) to yield P7. Note: quenched with norbornene after 5 h (b) SEC-RI overlay of polymer precursors and purified AB_2 miktoarm star (P7) (c) SAXS data confirming self-assembly of P7 to well-ordered lamellae.

4.3 Conclusion

In conclusion, we have disclosed a novel, yet synthetically accessible strategy to introduce Cp functionalities in a range of polymeric systems. The general compatibility of the NBD building block with common polymerization techniques (i.e. RAFT, ROP) was demonstrated, highlighting the versatility and simplicity of this building block. Importantly, upon addition of DpTz, highly efficient deprotection of NBD to release Cp is observed via a rapid cascade of DA reactions. In the presence of maleimide functionalities, a subsequent *in situ* "click" reaction with Cp ensues via a traditional DA process resulting in the desired adduct. This process is metal-free, highly efficient, requires no heating or precaution for an air- or moisture-free environment, and is amenable across an array of functional maleimides. The ability to introduce Cp into macromolecules in an on-demand manner represents a new paradigm in synthetic "click" functionalization. Moreover, the simple synthesis and exceptionally low cost of starting materials facilitates gram-scale quantities of the key NBD building block, making this strategy accessible to non-synthetic experts. Understanding the true potential of this "click" platform via the synthesis of progressively complex polymeric materials is currently underway.

4.4 Experimental

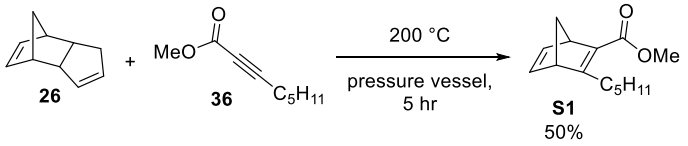

Methyl 3-pentylbicyclo[2.2.1]hepta-2,5-diene-2-carboxylate (S1):

Methyl 2-octynoate (6.7 mL, 40 mmol, 1 eq), dicyclopentadiene (3.2 mL, 24 mmol, 1.2 eq of cyclopentadiene), and hydroquinone (100 mg) were added to a pressure vessel and sealed under an atmosphere of N_2. The vessel was heated to 200 °C for 5 hr (63% conversion by

NMR). The crude product was distilled twice (100–120 °C, ~200 mTorr) to afford racemic **S1** (4.4 g, 50%) as a clear and colorless liquid.

S1: ^{1}H NMR (400 MHz, $CDCl_3$) δ 6.88 (dd, *J* = 3.1, 4.7 Hz, 1 H), 6.70 (dd, *J* = 3.3, 4.5 Hz, 1 H), 3.88 (br. s., 1 H), 3.72 (s, 3 H), 3.51 (br. s., 1 H), 2.75 - 2.60 (m, 2 H), 2.00 (tdd, *J* = 1.6, 6.3, 25.4 Hz, 2 H), 1.55 - 1.21 (m, 6 H), 0.89 (t, *J* = 7.0 Hz, 3 H) ppm; ^{13}C NMR (100 MHz, $CDCl_3$) δ 173.9, 166.3, 143.7, 140.7, 138.0, 71.0, 56.0, 51.0, 50.8, 31.5, 30.2, 26.4, 22.4, 13.9 ppm; IR (ATR) 2957, 2931, 2863, 1705, 1625, 1433, 1338, 1294, 1235, 1100, 1079, 714 cm^{-1}; HRMS (EI+) Exact mass cald. for $C_{14}H_{20}O_2^+$ $[M]^+$: 220.1458, found: 220.1466.

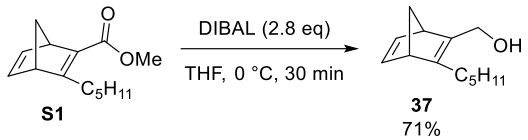

S1 **37** 71%

(3-Pentylbicyclo[2.2.1]hepta-2,5-dien-2-yl)methanol (37):

A solution of **S1** (1.76 g, 8.01 mmol, 1 eq) in THF (100 mL) was cooled to 0 °C. A solution of DIBAL in hexanes (1 M, 22.4 mL, 22.4 mmol, 2.8 eq) was added dropwise over 10 min. The solution was maintained at 0 °C until complete consumption of the starting material (TLC, 30 min). The reaction was carefully quenched at 0 °C with water (0.8 mL), then an aqueous solution of NaOH (1 M, 1.6 mL), then water (0.8 mL). The reaction mixture was removed from the ice bath and stirred a further 30 min. The reaction mixture was dried with $MgSO_4$, stirred a further 10 min, then filtered and rinsed with Et_2O (150 mL). The solvent was removed and the residue subjected to flash column chromatography (Hexane:EtOAc, 6:1) to yield racemic **37** (1.09 g, 71%) as a clear and colorless oil. Spectral data matched that of literature reported data.[38]

37: R_f (Hexane:EtOAc, 6:1): 0.29; ^{1}H NMR (400 MHz, $CDCl_3$) δ 6.81 (dd, *J* = 2.7, 5.1 Hz, 1 H), 6.73 (dd, *J* = 3.1, 5.1 Hz, 1 H), 4.26 (dd, *J* = 5.5, 12.1 Hz, 1 H), 4.14 (dd, *J* = 4.7, 12.1 Hz, 1 H), 3.55 (br. s., 1 H), 3.38 (br. s., 1 H), 2.27 - 2.17 (m, 1 H), 2.17 - 2.07 (m, 1 H),

1.92 (dd, *J* = 5.9, 15.7 Hz, 2 H), 1.47 - 1.24 (m, 4 H), 1.24 - 1.12 (m, 2 H), 0.98 (t, *J* = 5.5 Hz, 1 H), 0.88 (t, *J* = 7.2 Hz, 3 H) ppm; ^{13}C NMR (100 MHz, $CDCl_3$) δ 152.9, 145.1, 143.0, 142.2, 71.4, 58.9, 53.7, 51.8, 31.4, 28.2, 27.0, 22.5, 14.0 ppm; IR (ATR) 3324, 2959, 2928, 2860, 1457, 1378, 1304, 1230, 1209, 1016, 987 cm^{-1}; HRMS (EI+) Exact mass cald. for $C_{13}H_{18}^{+}$ [M-H_2O]$^{+}$: 174.1403, found: 174.1408.

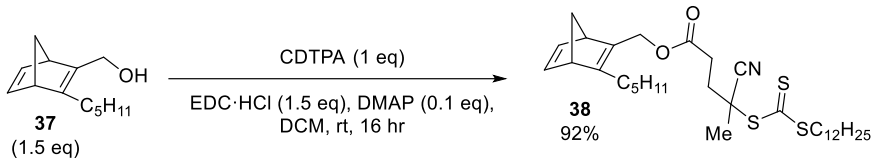

(3-pentylbicyclo[2.2.1]hepta-2,5-dien-2-yl)methyl 4-cyano-4-(((dodecylthio)carbonothioyl)thio)pentanoate (38):

To a solution of 4-cyano-4-[(dodecylsulfanylthiocarbonyl)sulfanyl]pentanoic acid (202 mg, 0.50 mmol, 1 eq) in DCM (1 mL) in a vial was added **37** (144 mg, 0.75 mmol, 1.5 eq), EDC·HCl (144 mg, 0.75 mmol, 1.5 eq), and DMAP (6 mg, 0.05 mmol, 0.1 eq). The reaction was capped under an atmosphere of air and stirred at rt for 16 hr (the starting material was consumed by NMR). The reaction mixture was adsorbed to silica gel (2 g) and subjected to flash column chromatography (Hexane:EtOAc, 15:1) to yield diastereomeric **38** (266 mg, 92%) as a yellow oil.

38: R_f (Hexane:EtOAc, 15:1): 0.21; ^{1}H NMR (400 MHz, $CDCl_3$) δ 6.77 (dd, *J* = 3.0, 5.1 Hz, 1 H), 6.72 (dd, *J* = 2.9, 4.7 Hz, 1 H), 4.75 (dd, *J* = 1.0, 12.2 Hz, 1 H), 4.61 (d, *J* = 11.9 Hz, 1 H), 3.45 (br. s., 1 H), 3.39 (br. s., 1 H), 3.34 (t, *J* = 7.4 Hz, 2 H), 2.68 - 2.57 (m, 2 H), 2.57 - 2.48 (m, 1 H), 2.42 - 2.34 (m, 1 H), 2.24 (ddd, *J* = 6.5, 8.0, 14.1 Hz, 1 H), 2.15 (ddd, *J* = 6.5, 8.0, 14.1 Hz, 1 H), 1.96 (td, *J* = 1.6, 6.0 Hz, 1 H), 1.91 (td, *J* = 1.6, 6.0 Hz, 1 H), 1.88 (s, 3 H), 1.70 (quin, *J* = 7.5 Hz, 2 H), 1.45 - 1.14 (m, 24 H), 0.89 (dt, *J* = 3.1, 7.1 Hz, 6 H) ppm; ^{13}C NMR (125 MHz, $CDCl_3$) δ 216.9, 171.5, 156.1, 142.8, 142.0, 140.6, 119.0, 71.4,

61.3, 53.8, 52.2, 46.4, 37.0, 33.9, 31.9, 31.4, 29.8, 29.6, 29.5, 29.4, 29.3, 29.0, 28.9, 28.4, 27.7, 26.8, 24.8, 22.7, 22.5, 14.1, 14.0 ppm; IR (ATR) 2954, 2923, 2853, 1737, 1645, 1456, 1378, 1291, 1176, 1068, 861, 806 cm^{-1}; HRMS (ES+) Exact mass cald. for $C_{32}H_{51}NNaO_2S_3^+$ $[M+Na]^+$: 600.2974, found: 600.3001.

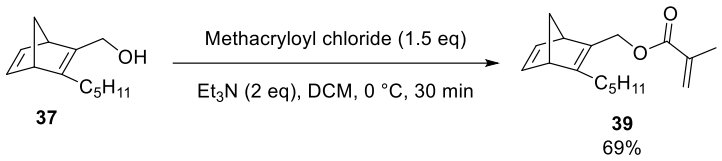

37 **39**
69%

(3-pentylbicyclo[2.2.1]hepta-2,5-dien-2-yl)methyl methacrylate (39):

A solution of **37** (481 mg, 2.5 mmol, 1 eq) and Et_3N (0.70 mL, 5.0 mmol, 2 eq) in DCM (12 mL) was cooled to 0 °C. Methacryloyl chloride (0.37 mL, 3.75 mmol, 1.5 eq) was added dropwise and the solution maintained at 0 °C until complete consumption of the starting material (TLC, 30 min). The reaction was quenched with water (0.1 mL) and allowed to warm to rt. Silica gel (1 g) was added, the solvent removed, and the mixture was subjected to flash column chromatography (Hexane:EtOAc, 15:1). The fractions containing product were combined, several drops of an inhibitor solution (MEHQ, 1 mg/mL in DCM) were added, and the solvent removed to yield racemic **39** (450 mg, 69%) as a clear and colorless oil.

39: R_f (Hexane:EtOAc, 15:1): 0.43; ^{1}H NMR (400 MHz, $CDCl_3$) δ 6.79 - 6.74 (m, 1 H), 6.74 - 6.69 (m, 1 H), 6.09 (s, 1 H), 5.55 (d, *J* = 1.2 Hz, 1 H), 4.79 (d, *J* = 12.1 Hz, 1 H), 4.66 (d, *J* = 12.5 Hz, 1 H), 3.48 (br. s., 1 H), 3.38 (br. s., 1 H), 2.30 - 2.12 (m, 2 H), 2.01 - 1.86 (m, 5 H), 1.47 - 1.23 (m, 4 H), 1.23 - 1.12 (m, 2 H), 0.87 (t, *J* = 7.2 Hz, 3 H) ppm; ^{13}C NMR (100 MHz, $CDCl_3$) δ 167.5, 155.2, 142.9, 141.9, 141.0, 136.5, 125.2, 71.3, 60.9, 53.8, 52.2, 31.3, 28.3, 26.8, 22.5, 18.4, 14.0 ppm; IR (ATR) 2961, 2930, 2864, 1716, 1638, 1453, 1293, 1157, 1010, 937, 814 cm^{-1}; HRMS (ES+) Exact mass cald. for $C_{17}H_{24}NaO_2^+$ $[M+Na]^+$: 283.1669, found: 283.1671.

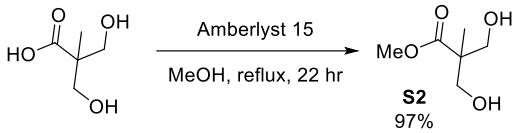

Methyl 3-hydroxy-2-(hydroxymethyl)-2-methylpropanoate (S2):[45]

2,2-Bis(hydroxymethyl)propionic acid (10.0 g, 74.6 mmol, 1 eq) and Amberlyst 15 hydrogen form (3.5 g) were added to MeOH (75 mL) and the mixture was heated to reflux for 22 hr (the reaction was complete by NMR). The reaction was cooled to rt, filtered through Celite, rinsed with MeOH (25 mL), and the solvent removed. The residue was dissolved in DCM (25 mL), filtered through Celite, and the solvent removed to yield **S2** (10.7 g, 97%) as an amber oil that solidifies on standing. The purity was sufficient for the next reaction. Spectral data matched that of literature reported data.[45]

S2: ^{1}H NMR (600 MHz, $CDCl_3$) δ 3.90 (d, J = 11.1 Hz, 2 H), 3.76 (s, 3 H), 3.71 (d, J = 11.5 Hz, 2 H), 3.00 (br. s., 2 H), 1.07 (s, 3 H) ppm.

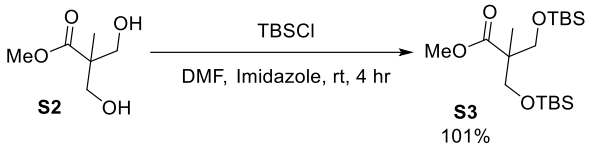

Methyl 3-((tert-butyldimethylsilyl)oxy)-2-(((tert-butyldimethylsilyl)oxy)methyl)-2-methylpropanoate (S3):

To a solution of **S2** (2.25 g, 15.2 mmol, 1 eq) and imidazole (2.48 g, 36.5 mmol, 2.4 eq) in DMF (20 mL) was added TBSCl (5.04 g, 33.4 mmol, 2.2 eq) in portions. After 2 hr the reaction did not go to completion (NMR) and a further imidazole (0.414 g, 6.08 mmol, 0.4 eq) and TBSCl (0.916 g, 6.08 mmol, 0.4 eq) was added. After 2 hr the reaction was deemed complete (NMR) the reaction was poured into an aqueous solution of HCl (1 M, 100 mL) and extracted with Et_2O (2x100 mL). The combined organic layers were washed with brine (2x50 mL), dried over $MgSO_4$, and the solvent removed to yield **S3** (5.80 g, 101%) as a clear and colorless oil that was used directly in the next reaction.

S3: ^{1}H NMR (400 MHz, $CDCl_3$) δ 3.73 (d, J = 9.4 Hz, 2 H), 3.69 - 3.61 (m, 5 H), 1.10 (s, 3 H), 0.87 (s, 18 H), 0.03 (s, 12 H) ppm; ^{13}C NMR (100 MHz, $CDCl_3$) δ 175.6, 64.2, 51.3, 50.3, 25.8, 18.2, 17.0, -5.61, -5.64 ppm.

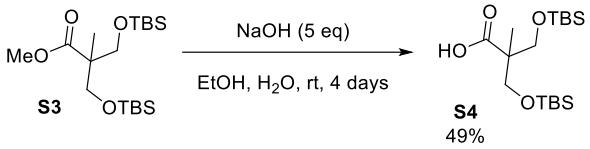

3-((tert-Butyldimethylsilyl)oxy)-2-(((tert-butyldimethylsilyl)oxy)methyl)-2-methylpropanoic acid (S4):

S3 (1.88 g, 5 mmol, 1 eq) was dissolved in EtOH (50 mL). An aqueous solution of NaOH (1 M, 25 mL, 25 mmol, 5 eq) was added and the biphasic mixture was stirred vigorously for 4 days. The reaction mixture, now homogeneous, was poured into an aqueous solution of HCl (1 M, 50 mL) and extracted with EtOAc (2x100 mL). The combined organic layers were washed with brine (50 mL), dried over $MgSO_4$, and the solvent removed. The residue was subjected to flash column chromatography (Hexanes:EtOAc, 9:1) to yield **S4** (897 mg, 49%) as a white solid. Spectral data matched that of literature reported data.[39]

S4: R_f (Hexanes:EtOAc, 9:1): 0.28; ^{1}H NMR (400 MHz, $CDCl_3$) δ 11.12 (br. s., 1 H), 3.75 (d, J = 9.8 Hz, 2 H), 3.70 (d, J = 9.4 Hz, 2 H), 1.15 (s, 3 H), 0.90 (s, 18 H), 0.07 (s, 12 H) ppm; ^{13}C NMR (100 MHz, $CDCl_3$) δ 178.4, 64.5, 49.4, 25.8, 18.2, 17.1, -5.6 ppm.

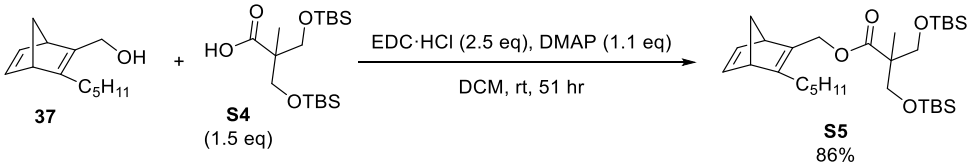

(3-pentylbicyclo[2.2.1]hepta-2,5-dien-2-yl)methyl 3-((tert-butyldimethylsilyl)oxy)-2-(((tert-butyldimethylsilyl)oxy)methyl)-2-methylpropanoate (S5):

To a solution of **37** (192 mg, 1 mmol, 1 eq) and **S4** (544 mg, 1.5 mmol, 1.5 eq) in DCM (1 mL) in a vial was added EDC·HCl (288 mg, 1.5 mmol, 1.5 eq), and DMAP (12 mg, 0.10

mmol, 0.1 eq). The reaction was capped under an atmosphere of air and stirred 23 hr at rt. The conversion was low (~18% by NMR), a further DMAP (110 mg, 0.90 mmol, 0.9 eq) was added, and the reaction mixture stirred 20 hr. A further EDC·HCl (192 mg, 1 mmol, 1 eq) was added, the reaction mixture stirred for 8 hr, and the reaction was deemed complete (NMR). The mixture was adsorbed to silica gel (1.5 g) and subjected to flash column chromatography (Hexane:EtOAc, 1:0 → 15:1) to yield racemic **S5** (460 mg, 86%) as a clear and colorless oil.

S5: R_f (Hexane:EtOAc, 15:1): 0.61; ^{1}H NMR (400 MHz, $CDCl_3$) δ 6.78 - 6.73 (m, 1 H), 6.73 - 6.67 (m, 1 H), 4.70 (d, *J* = 12.5 Hz, 1 H), 4.54 (d, *J* = 12.5 Hz, 1 H), 3.75 (dd, *J* = 4.7, 9.4 Hz, 2 H), 3.64 (d, *J* = 9.4 Hz, 2 H), 3.45 (br. s., 1 H), 3.37 (br. s., 1 H), 2.28 - 2.08 (m, 2 H), 1.98 - 1.85 (m, 2 H), 1.45 - 1.24 (m, 4 H), 1.24 - 1.14 (m, 2 H), 1.10 (s, 3 H), 0.91 - 0.85 (m, 21 H), 0.03 (s, 12 H) ppm; ^{13}C NMR (100 MHz, $CDCl_3$) δ 175.1, 154.7, 142.9, 141.9, 141.2, 71.2, 64.2, 60.4, 53.7, 52.0, 50.4, 31.4, 28.3, 26.9, 25.8, 22.5, 18.2, 17.1, 14.0, -5.6 ppm; IR (ATR) 2955, 2929, 2884, 2857, 1732, 1471, 1250, 1083, 833, 774 cm^{-1}; HRMS (ES+) Exact mass cald. for $C_{30}H_{56}NaO_4Si_2$ $[M+Na]^+$: 559.3609, found: 559.3629.

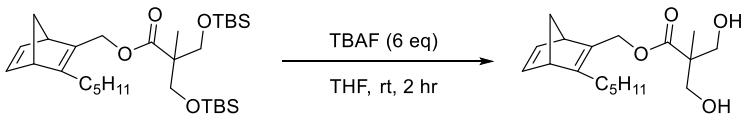

S5 **40** 73%

(3-pentylbicyclo[2.2.1]hepta-2,5-dien-2-yl)methyl 3-hydroxy-2-(hydroxymethyl)-2-methylpropanoate (40):

To a solution of **S5** (440. mg, 0.819 mmol, 1 eq) in THF (12 mL) was added a solution of TBAF in THF (1 M, 4.9 mL, 4.9 mmol, 6 eq). After 2 hr the reaction was deemed complete by NMR and the solvent was removed. The residue was suspended in Et_2O (100 mL), washed with a saturated solution of NH_4Cl (50 mL), then brine (50 mL). The organic layer was dried over $MgSO_4$ and the solvent removed. The residue was subjected to flash column

chromatography (Hexane:EtOAc, 1:1) to yield racemic **40** (185 mg, 73%) as a clear and colorless oil.

40: R_f (Hexane:EtOAc, 1:1): 0.31; ^{1}H NMR (400 MHz, $CDCl_3$) δ 6.80 - 6.74 (m, 1 H), 6.74 - 6.68 (m, 1 H), 4.84 (d, *J* = 12.1 Hz, 1 H), 4.70 (d, *J* = 12.1 Hz, 1 H), 3.88 (dd, *J* = 6.1, 11.2 Hz, 2 H), 3.77 - 3.67 (m, 2 H), 3.46 (br. s., 1 H), 3.39 (br. s., 1 H), 2.79 (t, *J* = 6.5 Hz, 2 H), 2.30 - 2.12 (m, 2 H), 1.98 - 1.89 (m, 2 H), 1.48 - 1.24 (m, 4 H), 1.24 - 1.12 (m, 2 H), 1.06 (s, 3 H), 0.87 (t, *J* = 7.2 Hz, 3 H) ppm; ^{13}C NMR (100 MHz, $CDCl_3$) δ 175.9, 156.3, 142.8, 142.0, 140.6, 71.6, 68.39, 68.37, 61.1, 53.8, 52.2, 49.3, 31.4, 28.4, 26.8, 22.5, 17.2, 14.0 ppm; IR (ATR) 3420, 2959, 2930, 2864, 1717, 1460, 1378, 1293, 1219, 1118, 1035, 909, 730 cm^{-1}; HRMS (ES+) Exact mass cald. for $C_{18}H_{28}NaO_4^+$ $[M+Na]^+$: 331.1880, found: 331.1884.

4.5 References

(1) St. Amant, A. H.; Discekici, E. H.; Zayas, M. S.; Shankel, S. L.; Schulze, M. W.; Anastasaki, A.; Hawker, C. J.; Read de Alaniz, J. Norbornadiene as a Protected Form of Cyclopentadiene: Next Generation "Click" Chemistry for Functional Polymer Synthesis.

(2) Arda, G. K.; Patrick, T.; Harm-Anton, K. Standing on the Shoulders of Hermann Staudinger: Post-polymerization Modification from Past to Present. *J. Polym. Sci. Part A Polym. Chem.* **2012**, *51* (1), 1–28.

(3) Lunn, D. J.; Discekici, E. H.; Read de Alaniz, J.; Gutekunst, W. R.; Hawker, C. J. Established and Emerging Strategies for Polymer Chain-End Modification. *J. Polym. Sci. Part A Polym. Chem.* **2017**, *55* (18), 2903–2914.

(4) Blasco, E.; Sims, M. B.; Goldmann, A. S.; Sumerlin, B. S.; Barner-Kowollik, C. 50th

Anniversary Perspective: Polymer Functionalization. *Macromolecules* **2017**, *50* (14), 5215–5252.

(5) St Amant, A. H.; Lemen, D.; Florinas, S.; Mao, S.; Fazenbaker, C.; Zhong, H.; Wu, H.; Gao, C.; Christie, R. J.; Read De Alaniz, J. Tuning the Diels-Alder Reaction for Bioconjugation to Maleimide Drug-Linkers. *Bioconjug. Chem.* **2018**, *29* (7), 2406–2414.

(6) Rideout, D. C.; Breslow, R. Hydrophobic Acceleration of Diels-Alder Reactions. *J. Am. Chem. Soc.* **1980**, *102* (26), 7816–7817.

(7) Aversa, M. C.; Barattucci, A.; Bonaccorsi, P.; Giannetto, P.; Panzalorto, M.; Rizzo, S. Diels–Alder Reactions of (RS)-3-[(1S)-Isoborneol-10-Sulfinyl]-1-Methoxybuta-1,3-Dienes with Electron-Deficient Carbodienophiles. The Effects of Lewis Acid Catalysis. *Tetrahedron: Asymmetry* **1998**, *9* (9), 1577–1587.

(8) Hilvert, D.; Hill, K. W.; Nared, K. D.; Auditor, M. T. M. Antibody Catalysis of the Diels-Alder Reaction. *J. Am. Chem. Soc.* **1989**, *111* (26), 9261–9262.

(9) Sauer, J.; Lang, D.; Mielert, A. The Order of Reactivity of Dienes towards Maleic Anhydride in the Diels-Alder Reaction. *Angew. Chemie Int. Ed. English* **1962**, *1* (5), 268–269.

(10) Yameen, B.; Rodriguez-Emmenegger, C.; Preuss, C. M.; Pop-Georgievski, O.; Verveniotis, E.; Trouillet, V.; Rezek, B.; Barner-Kowollik, C. A Facile Avenue to Conductive Polymer Brushes via Cyclopentadiene-Maleimide Diels-Alder Ligation. *Chem. Commun.* **2013**, *49* (77), 8623–8625.

(11) Inglis, A. J.; Sinnwell, S.; Stenzel, M. H.; Barner-Kowollik, C.; Andrew J., I.; Sebastian, S.; Martina H., S.; Christopher, B. Ultrafast Click Conjugation of

Macromolecular Building Blocks at Ambient Temperature. *Angew. Chemie Int. Ed.* **2009**, *48* (13), 2411–2414.

(12) Yameen, B.; Zydziak, N.; Weidner, S. M.; Bruns, M.; Barner-Kowollik, C. Conducting Polymer/SWCNTs Modular Hybrid Materials via Diels–Alder Ligation. *Macromolecules* **2013**, *46* (7), 2606–2615.

(13) Nebhani, L.; Barner-Kowollik, C. Functionalization of Fullerenes with Cyclopentadienyl and Anthracenyl Capped Polymeric Building Blocks via Diels–Alder Chemistry. *Macromol. Rapid Commun.* **2010**, *31* (14), 1298–1305.

(14) Zydziak, N.; Hübner, C.; Bruns, M.; Barner-Kowollik, C. One-Step Functionalization of Single-Walled Carbon Nanotubes (SWCNTs) with Cyclopentadienyl-Capped Macromolecules via Diels−Alder Chemistry. *Macromolecules* **2011**, *44* (9), 3374–3380.

(15) Claudio, T.; Stephan, B.; Augustinus, B. A.; Francesco, P. Cyclopentadiene-functionalized Polyketone as Self-cross-linking Thermo-reversible Thermoset with Increased Softening Temperature. *J. Appl. Polym. Sci.* **2015**, *133* (4).

(16) Kennedy, J. P.; Castner, K. F. Synthesis of Substituted Cyclopentadienes and Cyclopentadiene-Functionalized Polymers. Google Patents July 1, 1980.

(17) Hughes, R. P.; Trujillo, H. A. Selective Solubility of Organometallic Complexes in Saturated Fluorocarbons. Synthesis of Cyclopentadienyl Ligands with Fluorinated Ponytails. *Organometallics* **1996**, *15* (1), 286–294.

(18) Inglis, A. J.; Paulöhrl, T.; Barner-Kowollik, C. Ambient Temperature Synthesis of a Versatile Macromolecular Building Block: Cyclopentadienyl-Capped Polymers. *Macromolecules* **2010**, *43* (1), 33–36.

(19) Wilson, P. J.; Wells, J. H. The Chemistry and Utilization of Cyclopentadiene. *Chem. Rev.* **1944**, *34* (1), 1–50.

(20) Gonzalez, A.; Holt, S. L. Effect of Microemulsions on the Diels-Alder Reaction: Endo/Exo Ratios in the Reaction of Cyclopentadiene and Methyl Methacrylate. *J. Org. Chem.* **1982**, *47* (16), 3186–3188.

(21) Dalkılıç, E.; Güney, M.; Daştan, A.; Saracoglu, N.; Lucchi, O. De; Fabris, F. Novel and Versatile Protocol for the Preparation of Functionalized Benzocyclotrimers. *Tetrahedron Lett.* **2009**, *50* (17), 1989–1991.

(22) Dalkılıç, E.; Daştan, A. Synthesis of Cyclopentadiene Derivatives by Retro-Diels–Alder Reaction of Norbornadiene Derivatives. *Tetrahedron* **2015**, *71* (13), 1966–1970.

(23) Findlay, D. M.; Roy, M. L.; McLean, S. Thermal Routes to Substituted Cyclopentadienes. *Can. J. Chem.* **1972**, *50* (19), 3186–3195.

(24) Pauloehrl, T.; Welle, A.; Bruns, M.; Linkert, K.; Börner, H. G.; Bastmeyer, M.; Delaittre, G.; Barner-Kowollik, C. Spatially Controlled Surface Immobilization of Nonmodified Peptides. *Angew. Chemie Int. Ed.* **2013**, *52* (37), 9714–9718.

(25) Khoury, P. R.; Goddard, J. D.; Tam, W. Ring Strain Energies: Substituted Rings, Norbornanes, Norbornenes and Norbornadienes. *Tetrahedron* **2004**, *60* (37), 8103–8112.

(26) Sauer, J.; Heinrichs, G. Kinetik Und Umsetzungen von 1.2.4.5-Tetrazinen Mit Winkelgespannten Und Elektronenreichen Doppelbindungen. *Tetrahedron Lett.* **1966**, *7* (41), 4979–4984.

(27) Wilson, W. S.; Warrener, R. N. A Mild Retro-[[Small Pi]4s+[Small Pi]2s] Cleavage Route to Furans and Fulvenes. *J. Chem. Soc. Chem. Commun.* **1972**, No. 4, 211–212.

(28) Barlow, M. G.; Haszeldine, R. N.; Pickett, J. A. Heterocyclic Polyfluoro-Compounds. Part 26. Synthesis of 3,6-Bis-Trifluoromethyl-Pyridazines and -Dihydropyridazines. *J. Chem. Soc. Perkin Trans. 1* **1978**, No. 4, 378–380.

(29) Oxtoby, N. S.; Blake, A. J.; Champness, N. R.; Wilson, C. Structural Influence of Cis and Trans Coordination Modes of Multi-Modal Ligands upon Coordination Polymer Dimensionality. *Dalt. Trans.* **2003**, No. 20, 3838–3839.

(30) Dubonosov, A. D.; Bren, V. A.; Chernoivanov, V. A. Norbornadiene–quadricyclane as an Abiotic System for the Storage of Solar Energy. *Russ. Chem. Rev.* **2002**, *71* (11), 917.

(31) Nishikubo, T.; Sahara, A.; Shimokawa, T. Syntheses of Polymers Containing Pendant Norbornadiene Derivatives by a Phase Transfer Catalysis and Their Photochemical Valence Isomerization. *Polym. J.* **1987**, *19*, 991.

(32) Nishikubo, T.; Shimokawa, T.; Sahara, A. Successful Synthesis of Polymers Containing Pendant Norbornadiene Moieties and Norbornadiene Photochemical Valence Isomerization. *Macromolecules* **1989**, *22* (1), 8–14.

(33) Tadatomi, N.; Tatsuo, K.; Sadayuki, W. Synthesis of Polymers Bearing Pendant Norbornadiene Moieties by Addition Reaction of Poly(Glycidyl Methacrylate-co-methyl Methacrylate)s with 2,5-norbornadiene-2-carboxylic Acids. *J. Polym. Sci. Part A Polym. Chem.* **1993**, *31* (7), 1659–1665.

(34) Kamogawa, H.; Yamada, M. Synthesis of Photosensitive Poly(2,5-Norbornadien-7-Yl Acrylate and Methacrylate). *Bull. Chem. Soc. Jpn.* **1986**, *59* (5), 1501–1504.

(35) Koji, M.; Akinori, K.; Kazuaki, O.; Yoshiaki, K.; Hideki, M.; Hiroshi, H.; Masahiro, H.; Kouichi, O. High-Contrast Fluorescence Imaging of Tumors In Vivo Using

Nanoparticles of Amphiphilic Brush-Like Copolymers Produced by ROMP. *Angew. Chemie Int. Ed.* **2011**, *50* (29), 6567–6570.

(36) Koji, M.; Kazuaki, O.; Akinori, K.; Yoshiaki, K.; Hideki, M.; Hiroshi, H.; Masahiro, H.; Kouichi, O. Influence of Side Chain Length on Fluorescence Intensity of ROMP-Based Polymeric Nanoparticles and Their Tumor Specificity in In-Vivo Tumor Imaging. *Small* **2011**, *7* (24), 3536–3547.

(37) Thalhammer, F.; Wallfahrer, U.; Sauer, J. Reaktivität Einfacher Offenkettiger Und Cyclischer Dienophile Bei Diels-Alder-Reaktionen Mit Inversem Elektronenbedarf. *Tetrahedron Lett.* **1990**, *31* (47), 6851–6854.

(38) Tuktarov, A. R.; Akhmetov, A. R.; Khuzin, A. A.; Dzhemilev, U. M. Synthesis and Properties of Energy-Rich Methanofullerenes Containing Norbornadiene and Quadricyclane Moieties. *J. Org. Chem.* **2018**, *83* (7), 4160–4166.

(39) Hedrick, J. L.; Trollsås, M.; Hawker, C. J.; Atthoff, B.; Claesson, H.; Heise, A.; Miller, R. D.; Mecerreyes, D.; Jérôme, R.; Dubois, P. Dendrimer-like Star Block and Amphiphilic Copolymers by Combination of Ring Opening and Atom Transfer Radical Polymerization. *Macromolecules* **1998**, *31* (25), 8691–8705.

(40) Mironov, V. A.; Sobolev, E. V; Elizarova, A. N. Some General Characteristic Properties of Substituted Cyclopentadienes. *Tetrahedron* **1963**, *19* (12), 1939–1958.

(41) Kotschy, A.; Smith, D. M.; Bényei, A. C. Tandem 'Inverse Electron-Demand' Diels-Alder Reactions of Dienamines with a 1,2,4,5-Tetrazine. A New Azo-Bridged Ring System. *Tetrahedron Lett.* **1998**, *39* (9), 1045–1048.

(42) Fiore, G. L.; Jing, F.; Young Victor G., J.; Cramer, C. J.; Hillmyer, M. A. High Tg Aliphatic Polyesters by the Polymerization of Spirolactide Derivatives. *Polym. Chem.*

2010, *1* (6), 870–877.

(43) Hansell, C. F.; Espeel, P.; Stamenović, M. M.; Barker, I. A.; Dove, A. P.; Du Prez, F. E.; O'Reilly, R. K. Additive-Free Clicking for Polymer Functionalization and Coupling by Tetrazine–Norbornene Chemistry. *J. Am. Chem. Soc.* **2011**, *133* (35), 13828–13831.

(44) Discekici, E. H.; St. Amant, A. H.; Nguyen, S. N.; Lee, I. H.; Hawker, C. J.; Read De Alaniz, J. Endo and Exo Diels-Alder Adducts: Temperature-Tunable Building Blocks for Selective Chemical Functionalization. *J. Am. Chem. Soc.* **2018**, *140* (15), 5009–5013.

(45) Jishkariani, D.; MacDermaid, C. M.; Timsina, Y. N.; Grama, S.; Gillani, S. S.; Divar, M.; Yadavalli, S. S.; Moussodia, R.-O.; Leowanawat, P.; Berrios Camacho, A. M.; et al. Self-Interrupted Synthesis of Sterically Hindered Aliphatic Polyamide Dendrimers. *Proc. Natl. Acad. Sci.* **2017**, *114* (12), E2275 LP-E2284.

5 A One-Pot Synthesis of Anilines and Nitrosobenzenes from Phenols

Parts of this chapter were originally published in a manuscript.[1] Adapted from Ref. 1 with permission from The Royal Society of Chemistry.

5.1 Introduction

Anilines are found in many biologically active compounds, and their synthesis is of continuing interest to chemists.[2] They are typically synthesized through the nitration, then reduction of aromatic compounds, reactions that come with many drawbacks.[3] For example, aryl nitrations and reductions are energy intensive, require expensive industrial equipment for safety, and can have low functional group compatibility.

An attractive alternative to avoid these problems is to use phenols as the starting material;[4–6] phenols are a diverse class of compounds, with many commercially available as commodity chemicals, and they are often less expensive than their corresponding aniline analogues. Industrially, the synthesis of unsubstituted anilines are performed in the silica-alumina catalyzed reaction of phenol and ammonia at 370 °C and 1.7 MPa pressure.[3] Several milder methods exist to perform the reaction in an academic setting and they can be applied to substituted phenols (**Figure 5.1**).

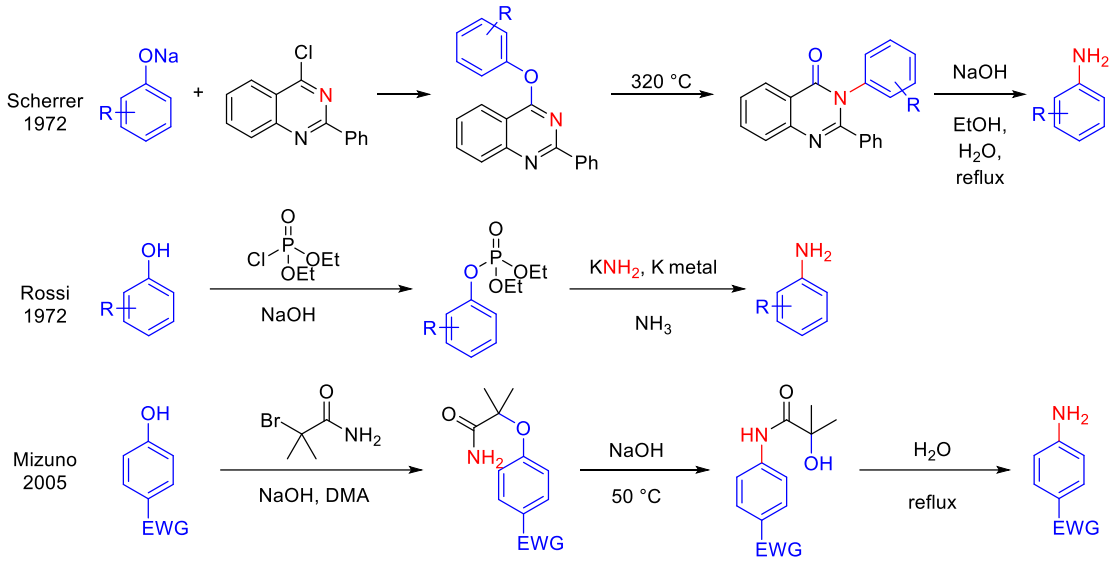

Figure 5.1 Current syntheses of anilines from phenols.

The first phenol-to-aniline method applicable to a broad range of phenols was reported by Scherrer in 1972, and utilized an O→N migration as the key step.[5] However, base (sodium salt), heat (320 °C), and strong base and heat (KOH, EtOH, H_2O, reflux) were required to perform the transformation, which limits the synthetic utility of this methodology. Inspired by Scherrer's work, Rossi,[6] utilized diethyl chlorophosphate. In this case, rather than use a migration, the phosphate was cleaved in a radical reaction with potassium amide and potassium metal in ammonia. The state of the art is a one-pot reaction developed by Mizuno,[7] which utilizes 2-bromo-2-methylpropion-amide as the nitrogen source. After alkylation, the compound undergoes a Smiles rearrangement[8] with sodium hydroxide, which can be hydrolyzed to the corresponding aniline. Compared to the methodology developed by Scherrer and Rossi, this reaction is milder (i.e. lower temperature and milder base). However, the Smiles rearrangement requires phenols bearing electron withdrawing groups, again limiting the synthetic utility.

An attractive alternative to convert phenols to anilines was reported by Taylor[9] in 1978 (**Figure 5.2**). This method proceeds through the dearomatization of phenol to quinone **2**,

condensation with a nitrogen-containing nucleophile to furnish **3**, and rearomatization to synthesize nitrogen-containing aromatics **4-6**. While the synthesis of aryl amine, nitroso and diazo compounds are desirable, the drawback of this method is the use of highly toxic thallium (III) nitrate as an oxidant. Based on our interest in C-N bond forming reactions[10–13] and inspired by Taylor's work, we sought to develop a safe and practical synthesis of anilines and aryl nitroso compounds from phenols.

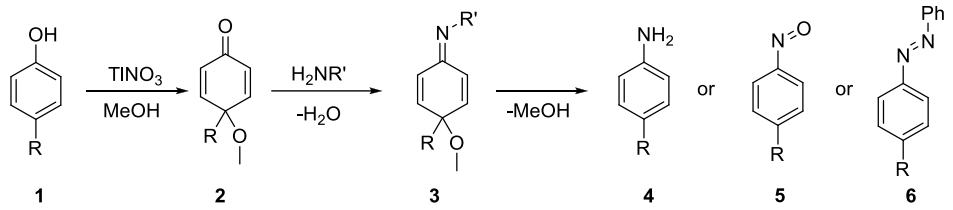

Figure 5.2 Taylor's synthesis of aniline, aryl nitroso, or aryl dizaonium compounds from phenol.

5.2 Results and Discussion

Initially we focused on replacing toxic thallium (III) nitrate as the oxidant and expanding the scope of Taylor's work beyond the single example reported. Since Taylor's report, several oxidants with excellent phenol selectivity have been developed. We chose to investigate phenyliodoso diacetate (PIDA), which has excellent literature precedent with broad substrate scope, is mild, and operationally simple.[14] With *para*-methoxy substituted phenol **9**, the PIDA oxidation in methanol proceeds in excellent yields to produce the quinone monoketal **10** (**Figure 5.3**). When the phenol *para* position is unsubstituted (**7**), two equivalents of the oxidant are consumed to give the same quinone **10** in a lower yield. The byproducts to this reaction are iodobenzene and acetic acid, which we predicted to be innocuous in the following step, leading us to develop a highly efficient, one-pot method.

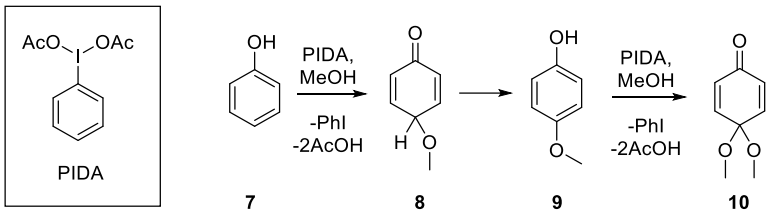

Figure 5.3 Synthesis of quinone monoketals from phenol using PIDA.

We used 4-methoxyphenol for our reaction optimization because of its high yielding oxidation. We screened several nitrogen sources and found that Taylor's ethyl glycinate produced the best results. After condensation with carbonyl **11**, there is a long-range methanol elimination restoring aromaticity to the ring (**Figure 5.4**). The condensation and Schiff base intermediates **11** and **12** are not observed, presumably reacting quickly to yield the aniline **13**. An acidic extraction, then basification furnished the aniline in sufficient purity for subsequent transformations, which eliminates the need for column chromatography.

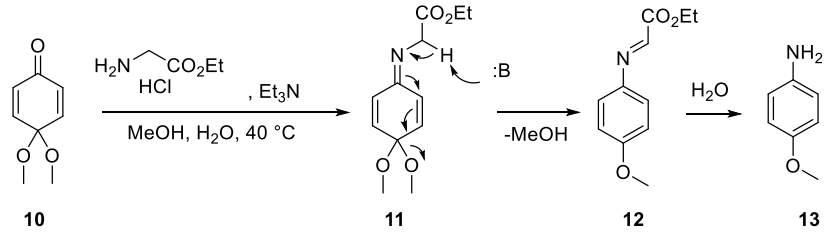

Figure 5.4 Conversion of a quinone monoketal to aniline.

With a general procedure in hand, we began to examine the scope of the reaction (**Figure 5.5**). In general, the compounds that are readily oxidized with PIDA provided the best yields. For example, phenols with a *para* alkoxy group oxidize in higher yields than *para* unsubstituted phenols (65–93% vs 44–65%), and were used through much of the scope.

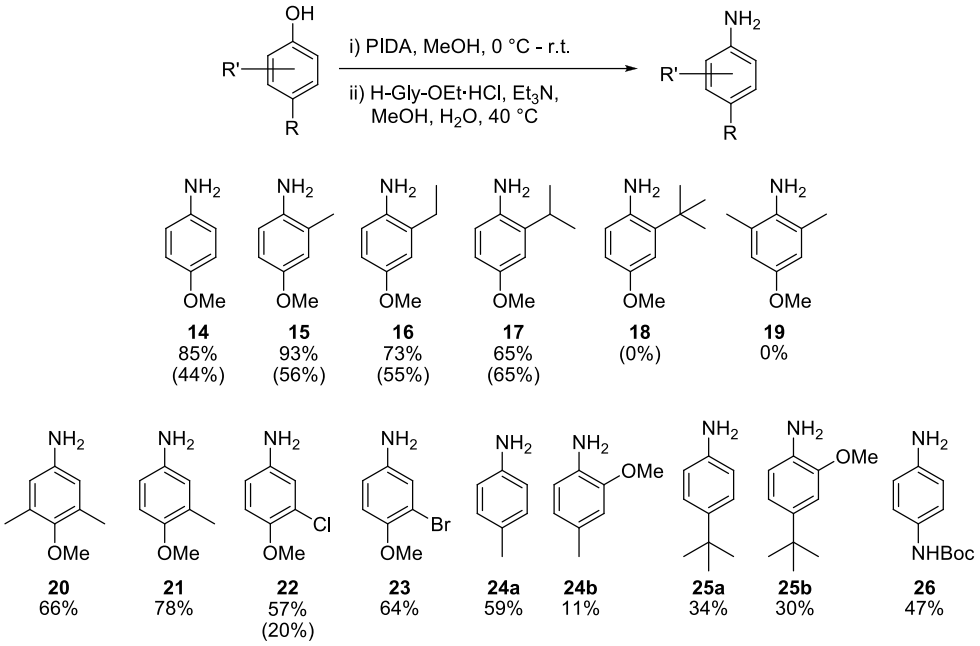

Figure 5.5 Scope of phenol to aniline reaction. Yields in parentheses are obtained from the *para*-unsubstituted phenol.

The method tolerates a range of functional groups including chloro, bromo, alkyl, and carbamate. The steric requirements of the reaction were analyzed by increasing the size at the *ortho* position (**14**-**18**). Through these experiments we discovered that isopropyl (**17**) is the largest alkyl group tolerated at the *ortho* position, with *tert*-butyl oxidizing to the quinone, but not forming the aniline in the second step (**18**). 2,6-Dimethylphenol (**19**) also oxidized to the quinone, but failed to produce the aniline in the second step. It's unclear whether the steric bulk is preventing the condensation of ethyl glycinate or the long-range methanol elimination. 4-Alkyl substituted anilines (**24** & **25**) oxidize to the 4-methoxy-4-alkylquinones, which react to produce the anilines **24a** and **25a**. Some *ortho* methoxylation is seen as a byproduct of the PIDA oxidation, producing **24b** and **25b**. Surprisingly, *N*-Boc-4-aminophenol produces aniline **26** in a modest yield, presumably proceeding through the *p*-quinonimine rather than the hemiaminal.

We next explored the scope at the ketal position (**Table 5.1**). All of the examples discussed thus far have used ketals of methanol; we also found that ethoxy monoketal worked well, performing the reaction in ethanol (**Entry 3**). The oxidation of 4-methoxyphenol in ethanol gives the mixed ketal as an intermediate (**Table 5.1**, **Key Step**), which yields a ~4:1 ratio of 4-ethoxyaniline to 4-methoxyaniline (**Entry 2**). It wasn't clear if 4-ethoxyaniline was the major product due to the solvent ethanol exchanging with the mixed ketal to produce the diethoxy monoketal. To test this, the same mixed ketal was synthesized through reaction of 4-ethoxyphenol in methanol (**Entry 4**). Surprisingly, it gave the same ratio of products indicating that the mixed ketal is not exchanging with the solvent and the ratio of products is determined at the alcohol elimination step.

Table 5.1 Mixed ketal reaction. Insert illustrates the key step in the formation of product A or B.

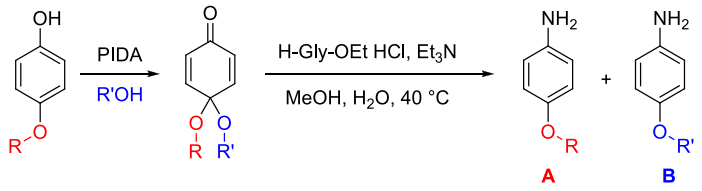

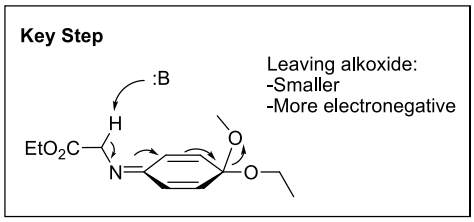

Entry	4-Alkoxy Phenol (R)	Solvent (R'OH)	Aniline 4-Alkoxy Substitution	
			A	B
1	Me	MeOH	Me (85%)	N/A
2	Me	EtOH	Me (16%)	Et (67%)
3	Et	EtOH	Et (82%)	N/A
4	Et	MeOH	Et (72%)	Me (21%)
5	iPr	MeOH	iPr (75%)	Me (10%)
6	Me	iPrOH	Me (5%)	iPr (11%)
7	Bn	MeOH	Bn (33%)	Me (52%)
8	Bn	TFE	Bn (44%)	CH_2CF_3 (0%)
9	CH_2CF_3	MeOH	CH_2CF_3 (0%)	Me (76%)
10	Me	TFE	Me (43%)	CH_2CF_3 (0%)
11	Ac	MeOH	Ac (0%)	Me (21%)

We hypothesize that the ratio of products formed is due to the nature of the alkoxides in the alcohol elimination step. The larger alkoxides, such as isopropanol (**Entry 5 & 6**) are more likely to stay in the plane of the ring and therefore be incorporated in the product.

The electronic nature of the alkoxides plays a factor as well. The most electron withdrawn alkoxide, 2,2,2-trifluoroethoxide, was the best leaving group giving 4-methoxyaniline as the only product (**Entry 9** and **10**). The electron poor acetoxy group (**Entry 11**) reacted similarly but gave a lower yield, perhaps being too reactive and leading to byproducts. The trend from these studies is such that when a mixed ketal is formed, the larger and more electron rich alkoxide will be retained in the aniline product. These results are useful if the phenol being oxidized cannot yield a monoketal or if exchange of the *para* alkoxy group is desired.

After the optimization and examination of the scope of our phenol to aniline reaction, we wanted to apply this strategy to other nitrogen containing aromatic compounds. Based on our interest in nitroso chemistry, we also sought to explore the direct synthesis of aryl nitroso compounds from phenols. Taylor demonstrated one example where 4-methoxyphenol was oxidized with thallium (III) nitrate, then condensed with hydroxylamine in one pot, yielding 4-methoxy-nitrosobenzene in good yield (70%). Encouraged by this precedent we adapted our one-pot aniline synthesis method using PIDA as the oxidant (**Figure 5.6**). The best substrate for this reaction is 4-methoxyphenol, which our one pot method yields 4-methoxynitrosobenzene **27** in 79% yield. Many of the nitrosobenzenes synthesized contain a 4-alkoxy group, whose electron donating nature reduces the dimerization and lower yields seen in electron poor or electron neutral aryl nitroso compounds.[15] Interestingly, no *ortho* substitution was tolerated for this reaction (0%, **28**), which highlights a limitation for this methodology. The method works for chloro, bromo, and 4-alkyl phenols in similar yields to

our aniline methodology (**31**-**33**). The mixed ketal formed from 4-isopropoxyphenol and methanol gives a 5:1 ratio of 4-isopropoxynitrosobenzene to 4-methoxynitrosobenzene (**34**), a similar ratio to our aniline reaction (7.5:1).

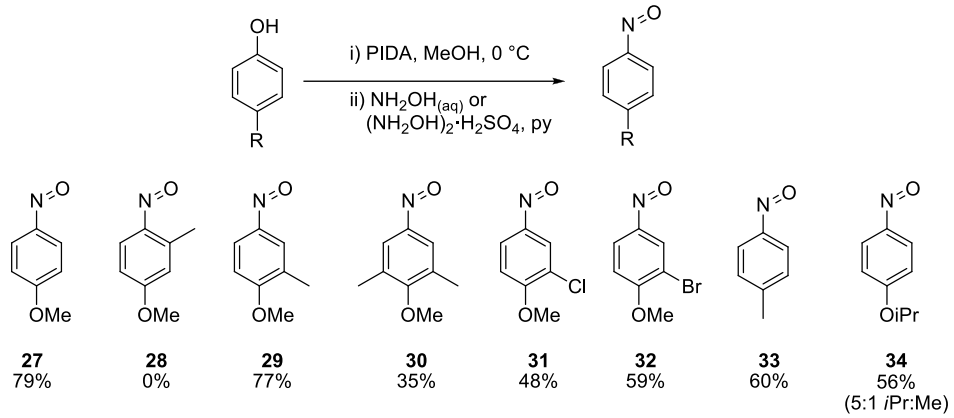

Figure 5.6 Scope of our phenol to nitrosobenzene reaction. Yields are isolated after column chromatography.

With a robust method in hand, we wanted to highlight the potential synthetic utility using a tyrosine derivative (**35**, **Figure 5.7**). Using the protected 4-hydroxyphenylalanine, we synthesized and isolated the quinone derivative **36**. The amino acid 4-aminophenylalanine **37** and the 4-nitrosophenylalanine **38** were synthesized using our methods, albeit in low yields. These materials are unstable on silica gel, with much of the material being lost during column chromatography, and experiments are underway to improve the isolated yields of these reactions. The unnatural amino acid 4-aminophenylalanine is used in the synthesis of VLA-4 antagonists,[16] and 4-nitrosophenylalanine has been used to make a photoswitch to cyclize peptides using click chemistry.[17]

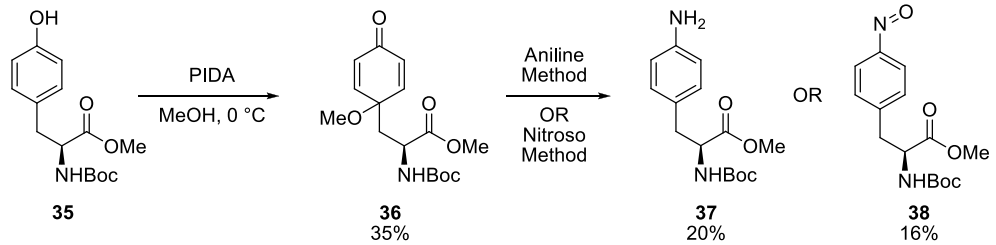

Figure 5.7 The synthesis of phenylalanine analogues for use in biological studies.

5.3 Conclusion

In conclusion, we have developed a method to synthesize electron rich or electron neutral anilines from phenols that complements the existing literature for electron poor anilines. The transformation, originally conceived by Taylor, is now operationally simple (one-pot) and more accessible by replacing thallium (III) nitrate with the safer and inexpensive PIDA oxidant. The strategy was also applied to synthesize aryl nitroso compounds, and phenylalanine derivatives that can be used in biological studies. We envision our mild, one-pot transformation being used to access a variety of anilines and aryl nitroso compounds from the wealth of commercially available phenols. The small library of nitrosobenzenes we have synthesized is currently being used in our group as a substrate for a copper catalyzed radical reaction.[18,19]

5.4 Experimental

General Procedure A: Reaction with 4-substituted phenols

PIDA (0.71 g, 2.2 mmol, 1.1 equiv) was suspended in MeOH (10 mL) and cooled on an ice bath. The phenol (2.0 mmol, 1 equiv) was dissolved in MeOH (10 mL) and added dropwise over 1 min. The ice bath was removed and the reaction mixture was stirred for 30 min or until consumption of the starting material. The reagents Et_3N (2.5 mL, 18 mmol, 9 equiv), H_2O (1 mL), and ethyl glycinate hydrochloride (1.95 g, 14 mmol, 7 equiv) were added sequentially and the reaction mixture was stirred at 40 °C overnight or until consumption of the quinone. The solvent was evaporated, DCM (100 mL) was added then transferred to a separatory funnel. The organic layer was extracted with $HCl_{(aq)}$ (1 M, 6 x 10 mL). The aqueous layers were combined, neutralized with saturated $NaHCO_{3(aq)}$ (140 mL), and extracted with DCM (3

x 50 mL). The organic layers were combined, dried over Na_2SO_4, filtered, and the solvent removed.

General Procedure B: Reaction with 4-unsubstituted phenols

PIDA (1.35 g, 4.2 mmol, 2.1 equiv) was suspended in MeOH (10 mL) and cooled on an ice bath. The phenol (2.0 mmol, 1 equiv) was dissolved in MeOH (10 mL) and added dropwise over 1 min. The ice bath was removed and the reaction mixture was stirred for 30 min or until consumption of the starting material. The reagents Et_3N (2.5 mL, 18 mmol, 9 equiv), H_2O (1 mL), and ethyl glycinate hydrochloride (1.95 g, 14 mmol, 7 equiv) were added sequentially and the reaction mixture was stirred at 40 °C overnight or until consumption of the quinone. The solvent was evaporated, DCM (100 mL) was added then transferred to a separatory funnel. The organic layer extracted with $HCl_{(aq)}$ (1 M, 6 x 10 mL). The aqueous layers were combined, neutralized with saturated $NaHCO_{3(aq)}$ (140 mL), and extracted with DCM (3 x 50 mL). The organic layers were combined, dried over Na_2SO_4, filtered, and the solvent removed.

General Procedure C:

PIDA (81 mg, 0.25 mmol, 1 equiv) was suspended in MeOH (2.5 mL) and cooled on an ice bath. Phenol (0.25 mmol, 1 equiv) was added and the reaction mixture stirred at room temperature until consumption of the starting material (~30 min). Pyridine (40 μL, 0.50 mmol, 2 equiv) then hydroxylammonium sulfate (41 mg, 0.25 mmol, 1 equiv) were added and the reaction was stirred until complete consumption of the quinone (overnight to 70 hr). The reaction was quenched with a saturated ammonium chloride solution and extracted with Et_2O (3 x 10 mL). The organic layers were combined, dried over $MgSO_4$, filtered, and the solvent removed. The residue was subjected to flash column chromatography (Hexane:EtOAc, 15:1

to 1:1) to yield the nitrosobenzene. Note: some of the nitrosobenzenes were found to be volatile, and care must be taken while removing solvent.

General Procedure for obtaining NMR Yield:

A known amount of dimethyl terephthalate (DMT) was weighed and added to the crude product. The mixture was dissolved in $CDCl_3$ and a ^1H NMR experiment was performed (relaxation delay set to 40 s). To determine the yield the integration for DMT's aromatic peak (8.09 ppm, 4H) is set to:

[4 * (mass DMT in mg) / 194.18] / (scale of reaction in mmol)

Gram-scale synthesis of 14:

PIDA (6.76 g, 21.0 mmol, 1.05 equiv) was suspended in MeOH (90 mL) and cooled on an ice bath. 4-Methoxyphenol (2.48 g, 20.0 mmol, 1 equiv) was dissolved in MeOH (10 mL) and added dropwise over 2 min. The ice bath was removed and the reaction mixture was stirred for 30 min. The reagents Et_3N (11 mL, 80. mmol, 4 equiv), H_2O (5 mL), and ethyl glycinate hydrochloride (5.6 g, 40. mmol, 2 equiv) were added sequentially and the reaction mixture was stirred at 40 °C overnight. The solvent was evaporated until ~20 mL remained. DCM (50 mL) and H_2O (50 mL) were added and the pH was adjusted to 1-2 with $HCl_{(conc)}$ (~7 mL). The mixture was transferred to a separatory funnel and the layers separated. The aqueous layer's pH was adjusted to 7-8 with solid Na_2CO_3 then extracted with DCM (2 x 50 mL). The organic layers were combined, dried over $MgSO_4$, filtered, and the solvent removed. The residue was subjected to flash column chromatography (Hexane:EtOAc, 2:1 → 1:1, with 2% Et_3N) to yield **14** (1.41 g, 57%) as a flaky orange solid.

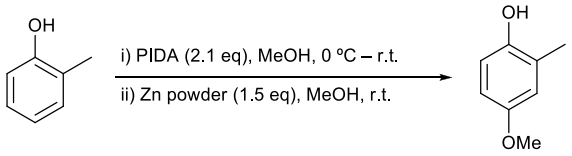

SI-1

4-Methoxy-2-methylphenol (**SI-1**): PIDA (6.8 g, 21 mmol, 2.1 eq) was added to MeOH (90 mL) and cooled on an ice bath. *o*-Cresol (1.08 g, 10.0 mmol, 1 eq) was dissolved in MeOH (10 mL) and added dropwise over 2 min with vigorous stirring. The ice bath was removed and the reaction mixture was stirred 30 min. The reaction mixture was cooled on an ice bath and zinc powder (0.98 g, 15 mmol, 1.5 eq) was added in one portion. The reaction mixture was taken off of the ice bath and stirred 1 hr. The solvent was removed, Et_2O (100 mL) was added, and the solution was transferred to a separatory funnel. The solution was washed with water (50 mL), then extracted with $NaOH_{(aq)}$ (3 M, 2 x 20 mL). The combined basic layers were acidified with $HCl_{(aq)}$ (1 M, 140 mL), then extracted with DCM (3 x 50 mL). The organic layers were combined, dried over Na_2SO_4, filtered, and the solvent removed. The residue was subjected to flash column chromatography (Hexane:EtOAc, 6:1 → 4:1) to yield **SI-1** (0.546 g, 40%) as white solid. Spectral data matched that of literature reported data.[20] Rf (Hexane:EtOAc, 4:1): 0.34; ^{1}H NMR (400 MHz, $CDCl_3$) δ 6.74 - 6.68 (m, 2 H), 6.64 (dd, *J* = 2.7, 8.6 Hz, 1 H), 4.35 (br. s., 1 H), 3.76 (s, 3 H), 2.25 (s, 3 H) ppm.

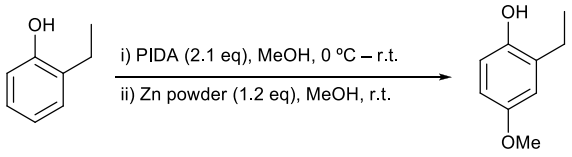

SI-2

2-Ethyl-4-methoxyphenol (**SI-2**): PIDA (2.1 g, 6.6 mmol, 1.1 eq) was added to MeOH (55 mL) and cooled on an ice bath. 2-Ethylphenol (0.72 mL, 6.0 mmol, 1 eq) was dissolved in MeOH (5 mL) and added dropwise over 5 min with vigorous stirring. The reaction mixture was taken off of the ice bath, stirred for 1 hr, a second portion of PIDA (1.9 g, 6.0 mmol, 1

eq) was added and stirring continued for 30 min. The reaction mixture was cooled on an ice bath and zinc powder (0.47 g, 7.2 mmol, 1.2 eq) was added in one portion. The reaction mixture was taken off of the ice bath and stirred 1 hr. The reaction mixture was filtered through Celite® and the solvent removed. EtOAc (50 mL) and $HCl_{(aq)}$ (1 M, 50 mL) were added, the solution was transferred to a separatory funnel and the layers separated. The aqueous layer was extracted again with EtOAc (50 mL). The organic layers were combined, dried over Na_2SO_4, filtered, and the solvent removed. The residue was subjected to flash column chromatography (Hexane:EtOAc, 6:1) to yield **SI-2** (0.517 g, 57%). Spectral data matched that of literature reported data.[21] Rf (Hexane:EtOAc, 4:1): 0.41; ^{1}H NMR (500 MHz, $CDCl_3$) δ 6.75 - 6.68 (m, 2 H), 6.67 - 6.61 (m, 1 H), 4.59 (br. s, 1 H), 3.77 (s, 3 H), 2.62 (q, *J* = 7.6 Hz, 2 H), 1.25 (t, *J* = 7.5 Hz, 3 H) ppm.

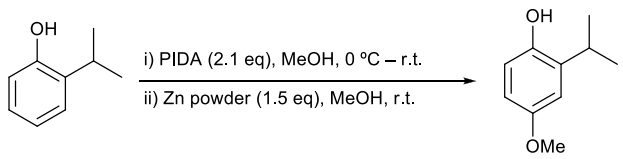

SI-3

2-Isopropyl-4-methoxyphenol (**SI-3**): PIDA (5.4 g, 17 mmol, 2.1 eq) was added to MeOH (70 mL) and cooled on an ice bath. 2-Isopropylphenol (1.1 mL, 8.0 mmol, 1 eq) was dissolved in MeOH (10 mL) and added dropwise over 2 min with vigorous stirring. The reaction mixture was taken off of the ice bath, stirred for 30 min. The reaction mixture was cooled on an ice bath and zinc powder (0.79 g, 12 mmol, 1.5 eq) was added in one portion. The reaction mixture was taken off of the ice bath and stirred 1 hr. The solvent was removed, Et_2O (50 mL) and $HCl_{(aq)}$ (1 M, 50 mL) were added, the solution was transferred to a separatory funnel, and the layers separated. The aqueous layer was extracted again with Et_2O (50 mL). The organic layers were combined and extracted with $NaOH_{(aq)}$ (1 M, 4 x 20 mL). The basic aqueous layers were combined, acidified with $HCl_{(aq)}$ (1 M, 100 mL), and extracted with DCM (2 x 50 mL).

The organic layers were combined, dried over Na_2SO_4, filtered, and the solvent removed. The residue was subjected to flash column chromatography (Hexane:EtOAc, 6:1) to yield **SI-3** (0.50 g, 38%) as a peach oil. Spectral data matched that of literature reported data.[22] Rf (Hexane:EtOAc, 4:1): 0.42; ^{1}H NMR (600 MHz, $CDCl_3$) δ 6.78 (d, *J* = 2.8 Hz, 1 H), 6.70 (d, *J* = 8.7 Hz, 1 H), 6.62 (dd, *J* = 2.8, 8.7 Hz, 1 H), 4.37 (br. s., 1 H), 3.78 (s, 3 H), 3.19 (spt, *J* = 6.9 Hz, 1 H), 1.26 (d, *J* = 6.6 Hz, 6 H) ppm.

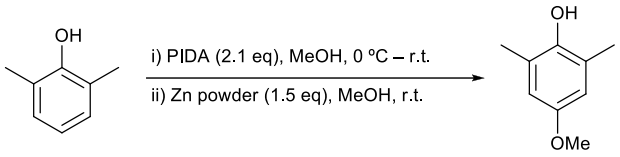

SI-4

4-Methoxy-2,6-dimethylphenol (**SI-4**): PIDA (5.4 g, 17 mmol, 2.1 eq) was added to MeOH (70 mL) and cooled on an ice bath. 2,6-Dimethylphenol (0.98 g, 8.0 mmol, 1 eq) was dissolved in MeOH (10 mL) and added dropwise over 2 min with vigorous stirring. The reaction mixture was taken off of the ice bath, stirred for 30 min. The reaction mixture was cooled on an ice bath and zinc powder (0.79 g, 12 mmol, 1.5 eq) was added in one portion. The reaction mixture was taken off of the ice bath and stirred 1 hr. The solvent was removed, Et_2O (50 mL) and $HCl_{(aq)}$ (1 M, 50 mL) were added, the solution was transferred to a separatory funnel, and the layers separated. The aqueous layer was extracted again with Et_2O (50 mL). The organic layers were combined and extracted with $NaOH_{(aq)}$ (1 M, 2 x 20 mL). The basic aqueous layers were combined, acidified with $HCl_{(aq)}$ (1 M, 50 mL), and extracted with DCM (2 x 50 mL). The organic layers were combined, dried over Na_2SO_4, filtered, and the solvent removed. The residue was subjected to flash column chromatography (Hexane:EtOAc, 15:1 → 9:1) to yield **SI-4** (0.40 g, 33%) as a white powder. Spectral data matched that of literature reported data.[23] Rf (Hexane:EtOAc, 9:1): 0.23; ^{1}H NMR (400 MHz, $CDCl_3$) δ 6.56 (s, 2 H), 4.23 (br. s, 1 H), 3.75 (s, 3 H), 2.24 (s, 6 H) ppm.

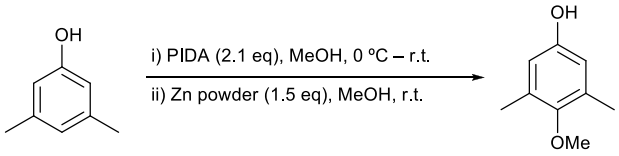

SI-5

4-Methoxy-3,5-dimethylphenol (**SI-5**): PIDA (5.4 g, 17 mmol, 2.1 eq) was added to MeOH (70 mL) and cooled on an ice bath. 3,5-Dimethylphenol (0.98 g, 8.0 mmol, 1 eq) was dissolved in MeOH (10 mL) and added dropwise over 2 min with vigorous stirring. The reaction mixture was taken off of the ice bath, stirred for 30 min. The reaction mixture was cooled on an ice bath and zinc powder (0.79 g, 12 mmol, 1.5 eq) was added in one portion. The reaction mixture was taken off of the ice bath and stirred 1 hr. The solvent was removed, Et_2O (50 mL) and water (50 mL) were added, the solution was transferred to a separatory funnel, and the layers separated. The organic layer was extracted with $NaOH_{(aq)}$ (1 M, 2 x 40 mL). The basic aqueous layers were combined, acidified with $HCl_{(aq)}$ (1 M, 100 mL), and extracted with DCM (3 x 50 mL). The organic layers were combined, dried over Na_2SO_4, filtered, and the solvent removed. The residue was subjected to flash column chromatography (Hexane:EtOAc, 6:1) to yield **SI-5** (0.54 g, 44%). Spectral data matched that of literature reported data.[24] Rf (Hexane:EtOAc, 4:1): 0.31; ^{1}H NMR (400 MHz, $CDCl_3$) δ 6.49 (s, 2 H), 4.45 (br. s., 1 H), 3.68 (s, 3 H), 2.24 (s, 6 H) ppm.

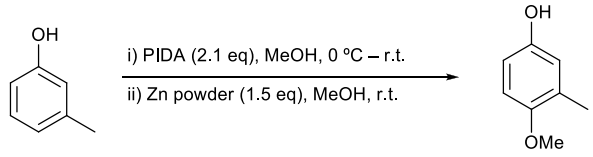

SI-6

4-Methoxy-3-methylphenol (SI-6): PIDA (6.8 g, 21 mmol, 2.1 eq) was added to MeOH (100 mL) and cooled on an ice bath. *m*-Cresol (1.05 g, 10.0 mmol, 1 eq) was added dropwise over 2 min with vigorous stirring. The reaction mixture was taken off of the ice bath and stirred 30 min. The reaction mixture was cooled on an ice bath and zinc powder (0.98 g, 15 mmol, 1.5

eq) was added in one portion. The reaction mixture was taken off of the ice bath and stirred 1 hr. The solvent was removed, Et_2O (100 mL) was added, and the solution was transferred to a separatory funnel. The solution was washed with water (50 mL), then extracted with $NaOH_{(aq)}$ (3 M, 2 x 20 mL). The combined basic layers were acidified with $HCl_{(aq)}$ (1 M, 140 mL) and extracted with DCM (3 x 50 mL). The organic layers were combined, dried over Na_2SO_4, filtered, and the solvent removed. The residue was subjected to flash column chromatography (Hexane:EtOAc, 4:1) to yield **SI-6** (0.77 g, 56%). Spectral data matched that of literature reported data.[25] Rf (Hexane:EtOAc, 4:1): 0.26; ^{1}H NMR (400 MHz, $CDCl_3$) δ 6.73 - 6.59 (m, 3 H), 4.37 (br. s., 1 H), 3.79 (s, 3 H), 2.19 (s, 3 H) ppm.

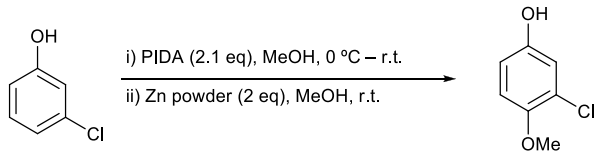

SI-7

3-Chloro-4-methoxyphenol (SI-7): PIDA (5.4 g, 17 mmol, 2.1 eq) was added to MeOH (70 mL) and cooled on an ice bath. 3-Chlorophenol (1.03 g, 8.00 mmol, 1 eq) was dissolved in MeOH (10 mL) and added dropwise over 2 min with vigorous stirring. The reaction mixture was taken off of the ice bath, stirred for 30 min. The reaction mixture was cooled on an ice bath and zinc powder (0.79 g, 12 mmol, 1.5 eq) was added in one portion. The reaction mixture was taken off of the ice bath and stirred 1 hr. Another portion of zinc powder (0.26 g, 4.0 mmol, 0.5 eq) was added and the reaction stirred for 30 min. The solvent was removed, Et_2O (50 mL) and water (50 mL) were added, the solution was transferred to a separatory funnel, and the layers separated. The organic layer was extracted again with Et_2O (50 mL). The organic layers were combined and extracted with $NaOH_{(aq)}$ (1 M, 2 x 40 mL). The basic aqueous layers were combined, acidified with $HCl_{(aq)}$ (1 M, 100 mL), and extracted with DCM (2 x 50 mL). The organic layers were combined, dried over Na_2SO_4, filtered, and the solvent

removed. The residue was subjected to flash column chromatography (Hexane:EtOAc, 6:1 → 4:1) to yield **SI-7** (0.30 g, 24%). Spectral data matched that of literature reported data.[26] Rf (Hexane:EtOAc, 4:1): 0.24; ^{1}H NMR (500 MHz, $CDCl_3$) δ 6.92 (d, *J* = 3.1 Hz, 1 H), 6.82 (d, *J* = 8.8 Hz, 1 H), 6.71 (dd, *J* = 3.1, 8.8 Hz, 1 H), 4.50 (br. s., 1 H), 3.85 (s, 3 H) ppm.

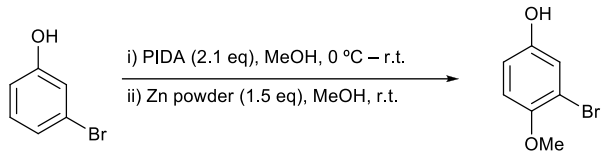

SI-8

3-Bromo-4-methoxyphenol (SI-8): PIDA (5.4 g, 17 mmol, 2.1 eq) was added to MeOH (70 mL) and cooled on an ice bath. 3-Bromophenol (1.38 g, 8.00 mmol, 1 eq) was dissolved in MeOH (10 mL) and added dropwise over 2 min with vigorous stirring. The reaction mixture was taken off of the ice bath, stirred for 30 min. The reaction mixture was cooled on an ice bath and zinc powder (0.79 g, 12 mmol, 1.5 eq) was added in one portion. The reaction mixture was taken off of the ice bath and stirred 1 hr. The solvent was removed, Et_2O (50 mL) and water (50 mL) were added, the solution was transferred to a separatory funnel, and the layers separated. The organic layer was extracted with $NaOH_{(aq)}$ (1 M, 2 x 40 mL). The basic aqueous layers were combined, acidified with $HCl_{(aq)}$ (1 M, 100 mL), and extracted with DCM (2 x 50 mL). The organic layers were combined, dried over Na_2SO_4, filtered, and the solvent removed. The residue was subjected to flash column chromatography (Hexane:EtOAc, 6:1 → 4:1) to yield **SI-8** (0.42 g, 26%). Spectral data matched that of literature reported data.[27] Rf (Hexane:EtOAc, 4:1): 0.23; ^{1}H NMR (400 MHz, $CDCl_3$) δ 7.09 (d, *J* = 2.7 Hz, 1 H), 6.83 - 6.74 (m, 2 H), 4.57 (br. s., 1 H), 3.85 (s, 3 H) ppm.

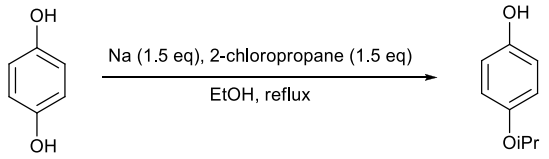

SI-9

4-Isopropoxyphenol (SI-9): Sodium metal (0.69 g, 30. mmol, 1.5 eq) was added to EtOH (50 mL). The solution was stirred until complete reaction of the sodium (40 min). Hydroquinone (2.2 g, 20. mmol, 1 eq) and 2-chloropropane (2.7 mL, 30. mmol, 1.5 eq) were added and the reaction was heated to reflux overnight. The solvent was removed, DCM (100 mL) was added, and the solution was transferred to a separatory funnel. The organic layer was washed with $HCl_{(aq)}$ (0.4 M, 100 mL) then brine (2 x 50 mL). The organic layer was extracted with $NaOH_{(aq)}$ (1 M, 3 x 10 mL). The basic aqueous layers were combined, washed with DCM (30 mL), acidified with $HCl_{(aq)}$ (1 M, 40 mL), and extracted with DCM (2 x 50 mL). The organic layers were combined, dried over Na_2SO_4, filtered, and the solvent removed to yield **SI-9** (0.89 g, 29%). Spectral data matched that of literature reported data.[28] Rf (Hexane:EtOAc, 2:1): 0.53; ^{1}H NMR (500 MHz, $CDCl_3$) δ 6.82 - 6.78 (m, 2 H), 6.78 - 6.73 (m, 2 H), 4.49 (s, 1 H), 4.41 (spt, *J* = 6.1 Hz, 1 H), 1.31 (d, *J* = 6.3 Hz, 6 H) ppm.

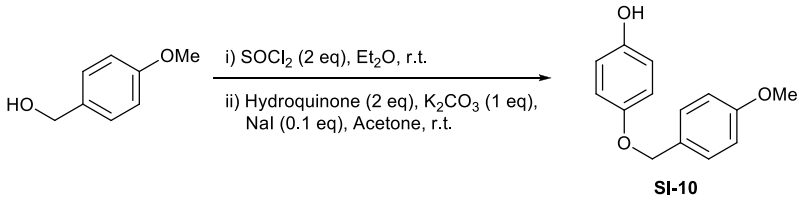

SI-10

4-(4-Methoxybenzyloxy)phenol (SI-10): To a solution of 4-methoxybenzyl alcohol (1.25 mL, 10.0 mmol, 1 eq) in Et_2O (20 mL) was added thionyl chloride (1.5 mL, 20. mmol, 2 eq) dropwise. The reaction mixture was stirred for 5 hr. Water (20 mL) was added carefully and the reaction mixture was stirred for 5 min then transferred to a separatory funnel. The layers were separated then the aqueous layer was extracted again with DCM (2 x 20 mL). The organic layers were combined, washed with water (20 mL), then brine (20 mL). The organic

layers was dried over $MgSO_4$, filtered, and the solvent removed to yield 4-methoxybenzyl chloride (1.52 g, 97%) as a clear and colorless oil.

The intermediate was suspended in acetone (20 mL), then hydroquinone (2.2 g, 20. mmol, 2 eq), K_2CO_3 (1.4 g, 10 mmol, 1 eq), and NaI (0.15 g, 1.0 mmol, 0.1 eq) were added. The reaction mixture was stirred overnight, filtered through Celite® with acetone, and then the solvent was removed. EtOAc (50 mL) was added then transferred to a separatory funnel. The organic layer was washed with water and brine (3 x 50 mL). The organic layer was dried over Na_2SO_4, filtered, and the solvent removed. The residue was subjected to flash column chromatography (Hexane:EtOAc, 3:1) to yield **SI-10** (0.89 g, 39% from 4-methoxybenzyl alcohol) as a crystalline peach solid. Spectral data matched that of literature reported data.[29] Rf (Hexane:EtOAc, 2:1): 0.38; ^{1}H NMR (400 MHz, DMSO) δ 8.90 (s, 1 H), 7.36 - 7.30 (m, 2 H), 6.96 - 6.89 (m, 2 H), 6.84 - 6.76 (m, 2 H), 6.72 - 6.61 (m, 2 H), 4.89 (s, 2 H), 3.75 (s, 3 H) ppm; ^{13}C NMR (100 MHz, DMSO) δ 158.8, 151.2, 151.2, 129.4, 129.3, 115.8, 115.7, 113.7, 69.5, 55.0 ppm.

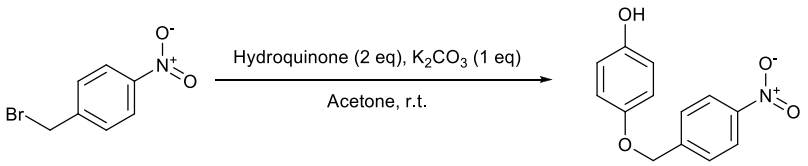

4-(4-Nitrobenzyloxy)phenol (**SI-11**): Hydroquinone (2.2 g, 20. mmol, 2 eq) and K_2CO_3 (1.4 g, 10 mmol, 1 eq) were added to acetone (20 mL). 4-Nitrobenzyl bromide (2.16 g, 10.0 mmol, 1 eq) was added in portions and the reaction mixture was stirred overnight. The reaction mixture was filtered through Celite® with acetone, and then the solvent was removed. EtOAc (50 mL) was added then transferred to a separatory funnel. The organic layer was washed with water (3 x 50 mL). The organic layer was dried over Na_2SO_4, filtered, and the solvent removed. The residue was subjected to flash column chromatography (Hexane:EtOAc, 2:1 →

1:1) to yield **SI-11** (0.91 g, 37%) as a yellow powder. Rf (Hexane:EtOAc, 1:1): 0.51; ^{1}H NMR (600 MHz, $CDCl_3$) δ 8.25 (d, *J* = 8.7 Hz, 2 H), 7.60 (d, *J* = 8.7 Hz, 2 H), 6.88 - 6.84 (m, 2 H), 6.81 - 6.77 (m, 2 H), 5.13 (s, 2 H), 4.44 (s, 1 H) ppm; ^{1}H NMR (400 MHz, DMSO) δ 9.00 (br. s., 1 H), 8.23 (d, *J* = 8.6 Hz, 2 H), 7.67 (d, *J* = 8.6 Hz, 2 H), 6.84 (d, *J* = 9.0 Hz, 2 H), 6.69 (d, *J* = 9.0 Hz, 2 H), 5.15 (s, 2 H) ppm; ^{13}C NMR (100 MHz, DMSO) δ 151.7, 150.7, 146.9, 145.6, 128.1, 128.0, 123.5, 115.8, 68.6 ppm; HRMS (EI) Exact mass cald. for $C_{13}H_{11}NO_4$ $[M]^+$: 245.0688, found: 245.0679.

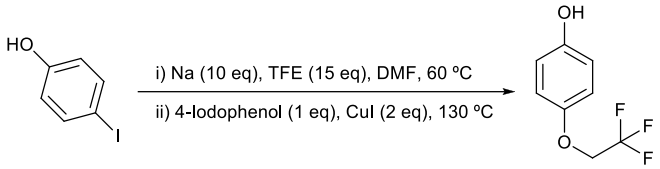

SI-12

4-(2,2,2-Trifluoroethoxy)phenol (**SI-12**): Sodium metal (2.3 g, 0.10 mol, 10 eq) was added to DMF (100 mL). 2,2,2-Trifluoroethanol (7.3 mL, 0.10 mol, 10 eq) was added slowly, keeping the temperature ~20 °C with an ice bath. The solution was stirred for 1 hr, and then another portion of 2,2,2-trifluoroethanol (3.7 mL, 50. mmol, 5 eq) was added slowly. The solution was stirred at 60 °C until complete reaction of the sodium (20 min). CuI (3.8 g, 20. mmol, 2 eq), and 4-iodophenol (2.2 g, 10. mmol, 1 eq) were added and the reaction mixture was stirred at 130 °C for 6 hours. Most of the solvent was removed (< 30 mL remained) and water (100 mL) was added. The solution was filtered through Celite®, acidified (pH ~1-2) with $HCl_{(aq)}$ (1 M, ~100 mL), and extracted with DCM (3 x 50 mL). The organic layers were combined, dried over Na_2SO_4, filtered, and the solvent removed. The residue was subjected to flash column chromatography (Hexane:EtOAc, 4:1 → 3:1) to yield **SI-12** (0.14 g, 7%). Spectral data matched that of literature reported data.[30] Rf (Hexane:EtOAc, 4:1): 0.25; ^{1}H NMR (400 MHz, $CDCl_3$) δ 6.90 - 6.83 (m, 2 H), 6.83 - 6.75 (m, 2 H), 4.58 (br. s., 1 H), 4.30 (q, *J* = 8.2 Hz, 2 H) ppm.

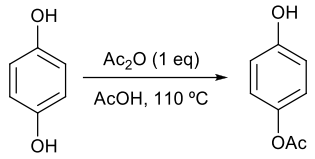

SI-13

4-Hydroxyphenyl acetate (SI-13): Hydroquinone (2.2 g, 20. mmol, 2 eq) was added to AcOH (5 mL). Ac_2O (0.47 g, 5.0 mmol, 0.5 eq) was added dropwise, the reaction mixture stirred for 30 min at 110 °C, Ac_2O (0.47 g, 5.0 mmol, 0.5 eq) was added dropwise and the reaction mixture was stirred a further 1.5 hr at 110 °C. The solvent was removed and toluene (10 mL) was added. The solution was sonicated for 2 min, stirred for 5 min, filtered, and the solvent removed to yield **SI-13** (1.3 g, 85%). Spectral data matched that of literature reported data.[31] ^{1}H NMR (500 MHz, $CDCl_3$) δ 6.95 - 6.90 (m, 2 H), 6.80 - 6.75 (m, 2 H), 5.04 (br. s., 1 H), 2.29 (s, 3 H) ppm.

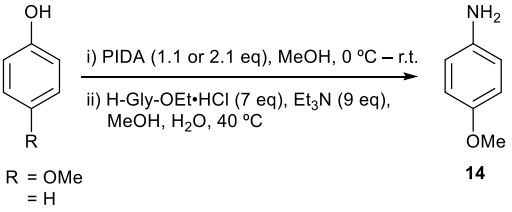

14

4-Methoxyaniline (14): Obtained using General Procedure **A** from 4-methoxyphenol (85%) or General Procedure **B** from phenol (44%). Spectral data matched that of literature reported data.[32] ^{1}H NMR (500 MHz, $CDCl_3$) δ 6.68 (td, *J* = 3.4, 8.8 Hz, 2 H), 6.56 (td, *J* = 3.4, 8.8 Hz, 2 H), 3.66 (s, 3 H), 3.34 (br. s., 2 H) ppm; ^{13}C NMR (125 MHz, $CDCl_3$) δ 152.1, 139.9, 115.9, 114.3, 55.1 ppm.

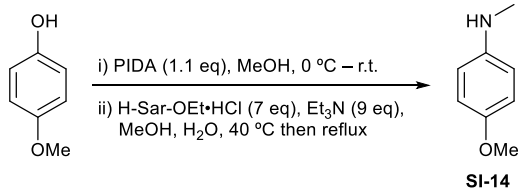

SI-14

4-Methoxy-N-methylaniline (SI-14): Obtained using General Procedure **A** from 4-methoxyphenol using sarcosine ethyl ester hydrochloride (44%). The second step was stirred

at 40 °C overnight, then at reflux for 5 hr. Spectral data matched that of literature reported data.[33] ^{1}H NMR (400 MHz, $CDCl_3$) δ 6.71 (d, *J* = 9.0 Hz, 2 H), 6.50 (d, *J* = 9.0 Hz, 2 H), 3.66 (s, 3 H) 3.16 (br. s., 1 H), 2.71 (s, 3 H) ppm; ^{13}C NMR (100 MHz, $CDCl_3$) δ 151.6, 143.4, 114.5, 113.2, 55.4, 31.2 ppm.

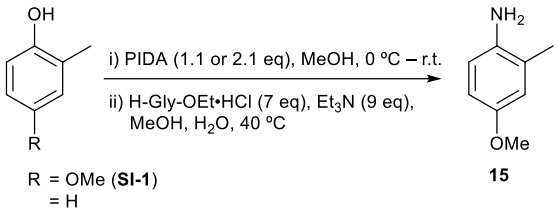

4-Methoxy-2-methylaniline (**15**): Obtained using General Procedure **A** from **SI-1** (93%) or General Procedure **B** from 2-methylphenol (56%). Spectral data matched that of literature reported data.[34] ^{1}H NMR (400 MHz, $CDCl_3$) δ 6.68 - 6.53 (m, 3 H), 3.69 (s, 3 H), 3.35 (br. s., 2 H), 2.11 (s, 3 H) ppm; ^{13}C NMR (100 MHz, $CDCl_3$) δ 152.0, 138.0, 123.4, 115.8, 115.5, 111.6, 55.1, 17.1 ppm.

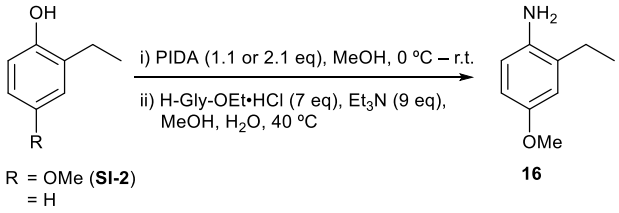

2-Ethyl-4-methoxyaniline (**16**): Obtained using General Procedure **A** from **SI-2** (73%) or General Procedure **B** from 2-ethylphenol (55%). Spectral data matched that of literature reported data.[35] ^{1}H NMR (400 MHz, $CDCl_3$) δ 6.67 (s, 1 H), 6.62 - 6.56 (m, 2 H), 3.72 (s, 3 H), 3.40 (br. s., 2 H), 2.47 (q, *J* = 7.4 Hz, 2 H), 1.22 (t, *J* = 7.6 Hz, 3 H) ppm; ^{13}C NMR (100 MHz, $CDCl_3$) δ 152.5, 137.4, 129.4, 116.0, 114.1, 111.3, 55.2, 23.9, 12.7 ppm.

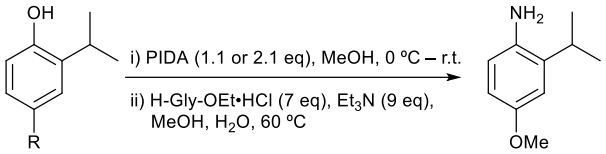

R = OMe (**SI-3**)
= H

17

2-Isopropyl-4-methoxyaniline (17): Obtained using General Procedure **A** from **SI-3** (65 %) or General Procedure **B** from 2-isopropylphenol (65%). The second step was performed at 60 °C. Spectral data matched that of literature reported data.[36] ^{1}H NMR (400 MHz, $CDCl_3$) δ 6.70 (d, *J* = 2.3 Hz, 1 H), 6.60 - 6.51 (m, 2 H), 3.68 (s, 3 H), 3.52 (br. s., 2 H), 2.86 (spt, *J* = 6.8 Hz, 1 H), 1.19 (d, *J* = 7.0 Hz, 6 H) ppm; ^{13}C NMR (125 MHz, $CDCl_3$) δ 152.8, 136.8, 133.6, 116.5, 111.7, 110.9, 55.3, 27.6, 22.0 ppm.

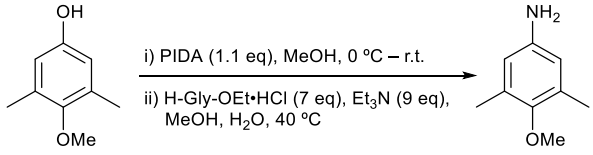

SI-5 **20**

4-Methoxy-3,5-dimethylaniline (20): Obtained using General Procedure **A** from **SI-5** (66%). The second step required 2 days to react to completion. Spectral data matched that of literature reported data.[37] ^{1}H NMR (400 MHz, $CDCl_3$) δ 6.33 (s, 2 H), 3.65 (s, 3 H), 3.46 (br. s., 2 H), 2.20 (s, 6 H) ppm; ^{13}C NMR (100 MHz, $CDCl_3$) δ 149.2, 142.0, 131.0, 115.0, 59.6, 15.8 ppm.

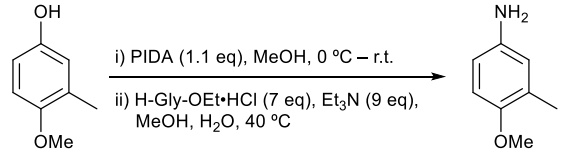

SI-6 **21**

4-Methoxy-3-methylaniline (21): Obtained using General Procedure **A** from **SI-6** (78%). Spectral data matched that of literature reported data.[38] ^{1}H NMR (400 MHz, $CDCl_3$) δ 6.63 (d, *J* = 8.6 Hz, 1 H), 6.51 - 6.43 (m, 2 H), 3.72 (s, 3 H), 3.32 (br. s., 2 H), 2.15 (s, 3 H) ppm; ^{13}C NMR (100 MHz, $CDCl_3$) δ 150.4, 139.5, 126.9, 118.0, 112.6, 111.1, 55.4, 15.8 ppm.

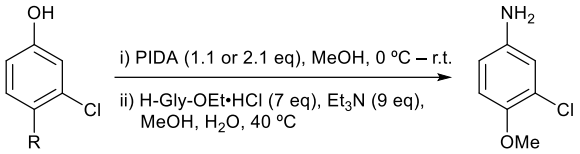

R = OMe (**SI-7**)
= H

22

3-Chloro-4-methoxyaniline (22): Obtained using General Procedure **A** at 1 mmol scale from **SI-7** (57 %) or General Procedure B from 3-chlorophenol (20%). Spectral data matched that of literature reported data.[39] ^{1}H NMR (400 MHz, $CDCl_3$) δ 6.72 - 6.63 (m, 2 H), 6.48 (dd, *J* = 2.5, 8.8 Hz, 1 H), 3.73 (s, 3 H), 3.38 (br. s., 2 H) ppm; ^{13}C NMR (100 MHz, $CDCl_3$) δ 147.6, 140.8, 122.6, 116.9, 114.0, 113.7, 56.6 ppm.

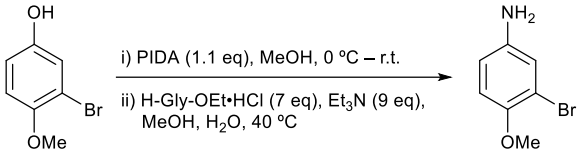

SI-8 **23**

3-Bromo-4-methoxyaniline (23): Obtained using General Procedure **A** from **SI-8** (64%). Spectral data matched that of literature reported data.[40] ^{1}H NMR (400 MHz, $CDCl_3$) δ 6.77 (d, *J* = 2.3 Hz, 1 H), 6.60 (d, *J* = 8.6 Hz, 1 H), 6.46 (dd, *J* = 2.3, 8.6 Hz, 1 H), 3.65 (s, 3 H), 3.33 (br. s., 2 H) ppm; ^{13}C NMR (100 MHz, $CDCl_3$) δ 148.1, 141.1, 119.5, 114.5, 113.2, 111.6, 56.4 ppm.

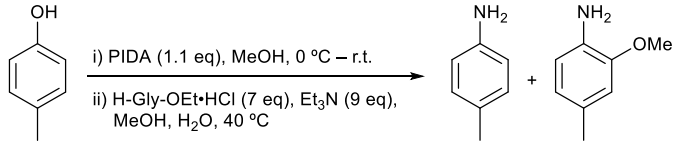

24a **24b**

***p*-Toluidine (24a) and 2-methoxy-4-methylaniline (24b):** Obtained using General Procedure **A** from *p*-cresol giving **24a** (59%) and **24b** (11%). The second step required 2 days to react to completion. Spectral data matched that of literature reported data.[41,42] **24a**: ^{1}H NMR (400 MHz, $CDCl_3$) δ 6.97 (d, *J* = 7.8 Hz, 2 H), 6.59 (d, *J* = 8.2 Hz, 2 H), 3.69 (br. s., 2 H), 2.26 (s, 3 H) ppm; ^{13}C NMR (100 MHz, $CDCl_3$) δ 143.7, 129.3, 126.9, 114.8, 20.0 ppm.

24b: ^{1}H NMR (400 MHz, $CDCl_3$) δ 6.65 - 6.61 (m, 3 H, overlaps with **24a**), 3.81 (s, 3 H), 3.69 (br. s., 2 H, overlaps with **24a**), 2.30 (s, 3 H) ppm; ^{13}C NMR (100 MHz, $CDCl_3$) δ 146.9, 133.2, 127.4, 120.8, 114.6, 111.1, 54.9, 20.5 ppm.

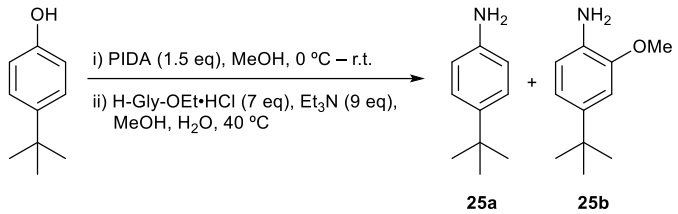

25a **25b**

4-*tert*-Butylaniline (25a) and 4-*tert*-butyl-2-methoxyaniline (25b): Obtained using General Procedure **A** with 1.5 equivalents of PIDA from 4-*tert*-butylphenol. The residue was subjected to flash column chromatography (Hexane:EtOAc, 4:1, with 1% Et_3N) yielding **25a** (20 %) as a clear and colorless oil and **25b** (19%) as a white solid. Spectral data matched that of literature reported data.[43,44] **25a**: Rf (Hexane:EtOAc, 4:1): 0.30; ^{1}H NMR (600 MHz, $CDCl_3$) δ 7.25 - 7.21 (m, 2 H), 6.70 - 6.66 (m, 2 H), 3.60 (s., 2 H), 1.33 (br. s., 9 H) ppm; ^{13}C NMR (151 MHz, $CDCl_3$) δ 143.7, 141.3, 126.0, 114.9, 33.8, 31.5 ppm. **25b**: Rf (Hexane:EtOAc, 4:1): 0.36; ^{1}H NMR (600 MHz, $CDCl_3$) δ 6.87 (d, *J* = 2.1 Hz, 1 H), 6.85 (dd, *J* = 2.1, 8.2 Hz, 1 H), 6.69 (d, *J* = 8.2 Hz, 1 H), 3.89 (s, 3 H), 3.72 (br. s., 2 H), 1.33 (s, 9 H) ppm; ^{13}C NMR (150 MHz, $CDCl_3$) δ 147.0, 141.8, 133.6, 117.6, 114.7, 108.2, 55.5, 34.2, 31.6 ppm.

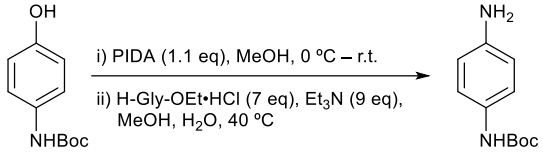

26

***tert*-Butyl 4-aminophenylcarbamate (26):** Obtained using General Procedure **A** from *tert*-butyl 4-hydroxyphenylcarbamate. The residue was subjected to flash column chromatography (Hexane:EtOAc, 2:1, with 1% Et_3N) to yield **26** (34%) as a flaky white solid. Spectral data matched that of literature reported data.[45] Rf (Hexane:EtOAc, 2:1): 0.16; ^{1}H NMR (500 MHz, $CDCl_3$) δ 7.14 (br. d, *J* = 7.8 Hz, 2 H), 6.67 - 6.61 (m, 2 H), 6.26 (br. s., 1 H), 3.57 (br. s., 2

H), 1.51 (s, 9 H) ppm; ^{13}C NMR (125 MHz, $CDCl_3$) δ 153.3, 142.3, 129.6, 120.9, 115.5, 79.9, 28.3 ppm.

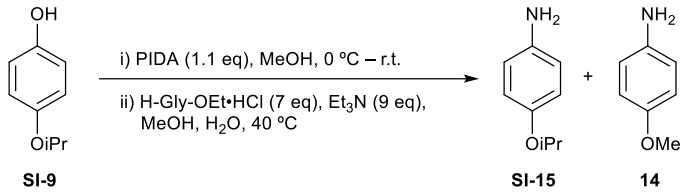

SI-9 **SI-15** **14**

Entry 1: 4-Isopropoxyaniline (SI-15) and 4-methoxyaniline (14): Obtained using General Procedure **A** from **SI-9** giving a mixture of **SI-15** (75%)[46] and **14** (10%). Spectral data matched that of literature reported data. **SI-15**: ^{1}H NMR (400 MHz, $CDCl_3$) δ 6.72 - 6.63 (m, 2 H, overlaps with **14**), 6.59 - 6.48 (m, 2 H, overlaps with **14**), 4.29 (spt, *J* = 6.1 Hz, 1 H), 3.39 (br. s., 2 H, overlaps with **14**), 1.22 (d, *J* = 6.3 Hz, 6 H) ppm; ^{13}C NMR (100 MHz, $CDCl_3$) δ 150.0, 140.1, 117.3, 115.8, 70.5, 21.7 ppm.

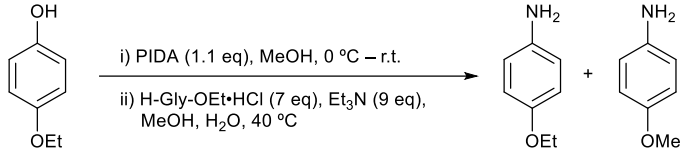

SI-16 **14**

Entry 2: 4-Ethoxyaniline (SI-16) and 4-methoxyaniline (14): Obtained using General Procedure **A** from 4-ethoxyphenol giving a mixture of **SI-16** (72%)[47] and 14 (21%). Spectral data matched that of literature reported data. **SI-16**: ^{1}H NMR (400 MHz, $CDCl_3$) δ 6.70 (d, *J* = 8.6 Hz, 2 H, overlaps with **14**), 6.57 (d, *J* = 8.6 Hz, 2 H, overlaps with **14**), 3.90 (q, *J* = 7.0 Hz, 2 H), 3.43 (br. s., 2 H, overlaps with **14**), 1.33 (t, *J* = 7.0 Hz, 3 H) ppm; ^{13}C NMR (100 MHz, $CDCl_3$) δ 151.5, 139.8, 115.9, 115.2, 63.6, 14.6 ppm.

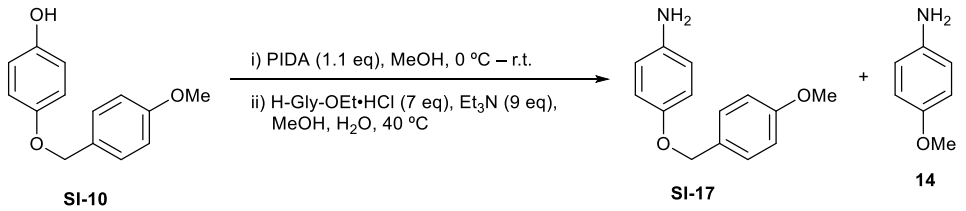

Entry 3: 4-(4-Methoxybenzyloxy)aniline (SI-17) and 4-methoxyaniline (14): Obtained using General Procedure **A** from **SI-10** giving a mixture of **SI-17** (37%)[48] and **14** (45%). Spectral data matched that of literature reported data. **SI-17**: ^{1}H NMR (400 MHz, $CDCl_3$) δ 7.34 (d, *J* = 8.2 Hz, 2 H), 6.91 (d, *J* = 8.6 Hz, 2 H), 6.75 (d, *J* = 8.6 Hz, 2 H), 6.67 - 6.60 (m, 2 H, overlaps with **14**), 4.90 (s, 2 H), 3.80 (s, 3 H), 3.32 (br. s., 2 H, overlaps with **14**) ppm; ^{13}C NMR (100 MHz, $CDCl_3$) δ 159.1, 151.7, 139.8, 129.3, 129.1, 116.2, 115.8, 113.7, 70.3, 55.1 ppm.

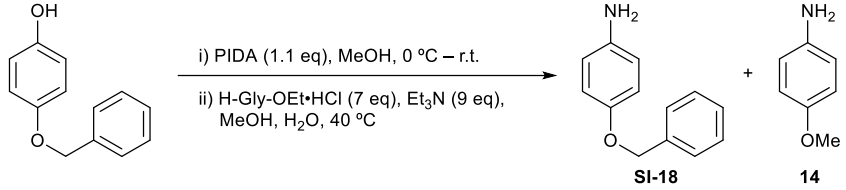

Entry 4: 4-(Benzyloxy)aniline (SI-18) and 4-methoxyaniline (14): Obtained using General Procedure **A** from 4-benzyloxyphenol giving a mixture of **SI-18** (33%)[49] and **14** (52%). Spectral data matched that of literature reported data. **SI-18**: ^{1}H NMR (400 MHz, $CDCl_3$) δ 7.41 - 7.23 (m, 5 H), 6.78 (d, *J* = 9.0 Hz, 2 H), 6.56 (d, *J* = 9.0 Hz, 2 H, overlaps with **14**), 4.92 (s, 2 H), 3.33 (br. s., 2 H, overlaps with **14**) ppm; ^{13}C NMR (100 MHz, $CDCl_3$) δ 151.2, 140.1, 137.1, 128.0, 127.3, 127.0, 115.8, 115.5, 70.1 ppm.

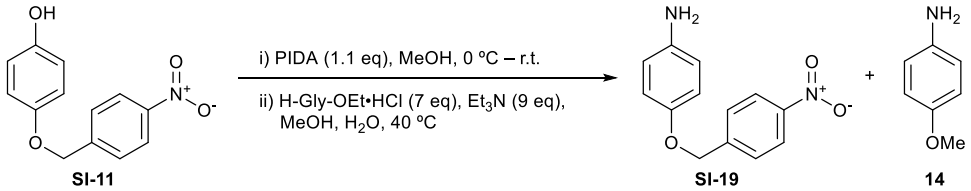

Entry 5: 4-(4-Nitrobenzyloxy)aniline (SI-19) and 4-methoxyaniline (14): Obtained using General Procedure **A** from **SI-11** giving a mixture of **SI-19** (5%)[50] and **14** (57%). Spectral

data matched that of literature reported data. **SI-19**: ^{1}H NMR (400 MHz, $CDCl_3$) δ 8.22 (d, *J* = 8.2 Hz, 2 H), 7.59 (d, *J* = 8.2 Hz, 2 H), 6.79 (d, *J* = 8.6 Hz, 2 H), 6.65 (d, *J* = 8.6 Hz, 2 H), 5.09 (s, 2 H), 3.18 (br. s., 2 H, overlaps with **14**) ppm; ^{1}H NMR (400 MHz, DMSO) δ 8.23 (d, *J* = 8.6 Hz, 2 H), 7.67 (d, *J* = 8.6 Hz, 2 H), 6.74 (d, *J* = 8.6 Hz, 2 H), 6.54 - 6.49 (m, 2 H, overlaps with **14**), 5.11 (s, 2 H), 4.64 (s, 2 H) ppm; ^{13}C NMR (100 MHz, $CDCl_3$) δ 151.2, 148.4, 145.0, 140.6, 127.5, 123.7, 116.4, 115.9, 69.3 ppm.

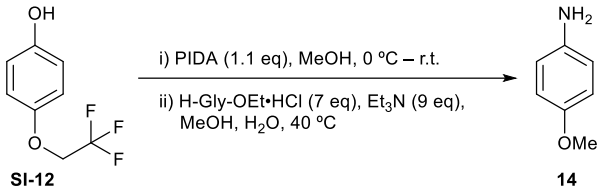

SI-12 **14**

Entry 6: 4-Methoxyaniline (14): Obtained using General Procedure **A** from **SI-12** at 0.5 mmol scale giving **14** (76%) as the sole product. Spectral data matched that of literature reported data.

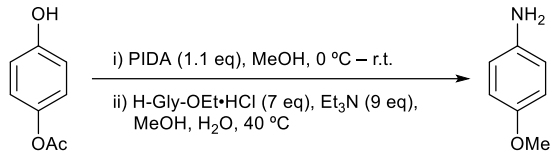

SI-13 **14**

Entry 7: 4-Methoxyaniline (14): Obtained using General Procedure **A** from **SI-13** giving **14** (21%) as the sole product. Spectral data matched that of literature reported data.

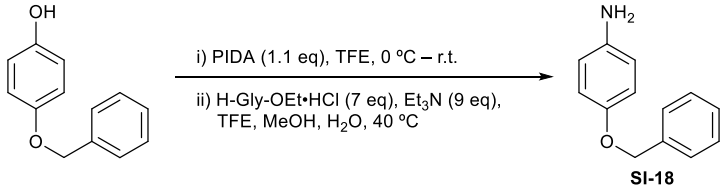

SI-18

Entry 8: 4-(Benzyloxy)aniline (SI-18): Obtained using General Procedure **A** from 4-benzyloxyphenol at 0.5 mmol scale. The first step was performed in 2,2,2-trifluoroethanol (TFE), the second step was performed in TFE:methanol (1:1) at room temperature, giving **SI-18** (44 %) as the sole product. Spectral data matched that of literature reported data.

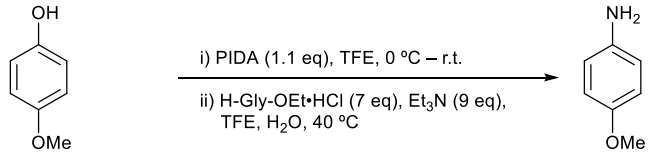

14

Entry 9: 4-Methoxyaniline (14): Obtained using General Procedure **A** from 4-methoxyphenol at 0.5 mmol scale. Both steps of the reaction were performed in TFE, giving **14** (43%) as the sole product. Spectral data matched that of literature reported data.

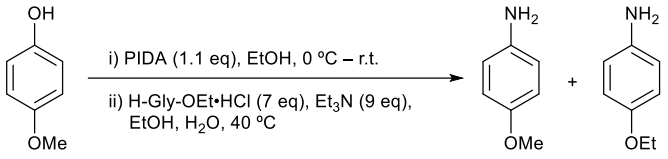

14 SI-16

Entry 10: 4-Methoxyaniline (**14**) & 4-Ethoxyaniline (**SI-16**)**:** Obtained using General Procedure **A** from 4-methoxyphenol with the reaction performed in ethanol giving a mixture of **14** (16%) and **SI-16** (67 %). Spectral data matched that of literature reported data.

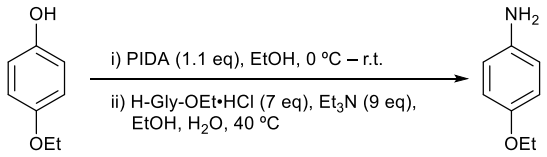

SI-16

Entry 11: 4-Ethoxyaniline (SI-16): Obtained using General Procedure **A** from 4-ethoxyphenol with the reaction performed in ethanol giving **SI-16** (82%). Spectral data matched that of literature reported data.

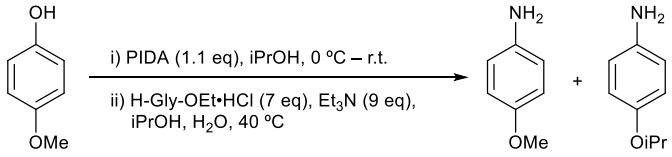

14 SI-15

Entry 12: 4-Methoxyaniline (14) and 4-isopropoxyaniline (SI-15): Obtained using General Procedure **A** from 4-methoxyphenol with the reaction performed in isopropanol giving a mixture of **SI-15** (11%) and **14** (5%). There were significant solubility issues in both steps of the reaction. Spectral data matched that of literature reported data.

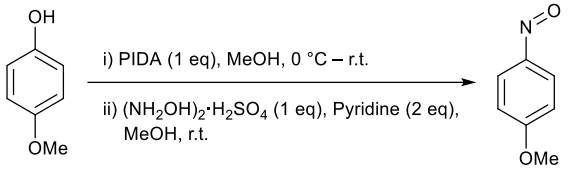

27

1-Methoxy-4-nitrosobenzene (27): Obtained using General Procedure **C** from 4-methoxyphenol giving **27** (79%). Spectral data matched that of literature reported data.[51] ^{1}H NMR (500 MHz, $CDCl_3$) δ 7.92 (d, *J* = 5.7 Hz, 2 H), 7.03 (d, *J* = 9.1 Hz, 2 H), 3.95 (s, 3 H) ppm; ^{13}C NMR (125 MHz, $CDCl_3$) δ 165.6, 164.0, 124.4, 113.9, 56.0 ppm.

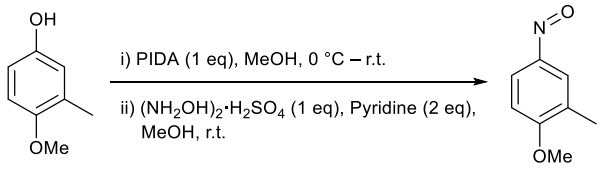

SI-6 **29**

1-Methoxy-2-methyl-4-nitrosobenzene (29): Obtained using General Procedure **C** from **SI-6** giving **29** (77%). The second step required 70 hr to react to completion. Spectral data matched that of literature reported data.[52] ^{1}H NMR (500 MHz, $CDCl_3$) δ 8.17 (br. d, *J* = 6.0 Hz, 1 H), 7.39 (br. s., 1 H), 7.01 (d, *J* = 8.6 Hz, 1 H), 4.00 - 3.96 (m, 3 H), 2.28 (s, 3 H) ppm; ^{13}C NMR (125 MHz, $CDCl_3$) δ 164.1, 163.8, 127.5, 127.0, 120.1, 109.1, 56.1, 16.2 ppm; HRMS (EI) Exact mass cald. for $C_8H_9NO_2$ $[M]^+$: 151.0633, found: 151.0632.

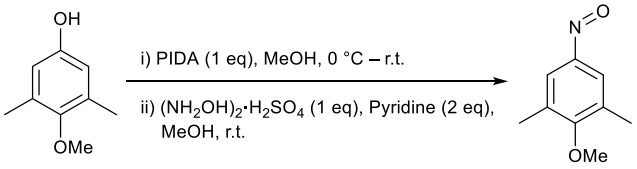

SI-5 **30**

2-Methoxy-1,3-dimethyl-5-nitrosobenzene (30): Obtained using General Procedure **C** from **SI-5** giving **30** (35%). The second step required 48 hr to react to completion. Spectral data matched that of literature reported data.[52] ^{1}H NMR (400 MHz, $CDCl_3$) δ 7.59 (s, 2 H), 3.80

(s, 3 H), 2.39 (s, 6 H) ppm; ^{13}C NMR (100 MHz, $CDCl_3$) δ 163.9, 163.6, 132.0, 122.5, 59.7, 16.3 ppm; HRMS (EI) Exact mass cald. for $C_9H_{11}NO_2$ $[M]^+$: 165.0790, found: 165.0788.

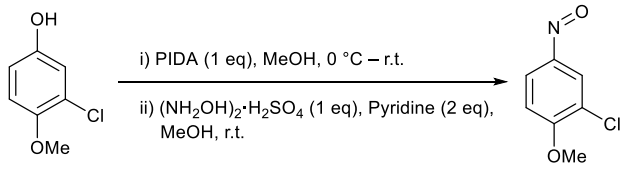

SI-7 **31**

2-Chloro-1-methoxy-4-nitrosobenzene (31): Obtained using General Procedure **C** from **SI-7** giving **31** (48%). ^{1}H NMR (500 MHz, $CDCl_3$) δ 8.31 (br. d, *J* = 8.0 Hz, 1 H), 7.59 (br. s., 1 H), 7.18 (d, *J* = 8.8 Hz, 1 H), 4.07 (s, 3 H) ppm; ^{13}C NMR (125 MHz, $CDCl_3$) δ 162.3, 160.7, 127.1, 124.3, 119.5, 111.0, 56.9 ppm; HRMS (EI) Exact mass cald. for $C_7H_6ClNO_2$ $[M]^+$: 171.0087, found: 171.0091.

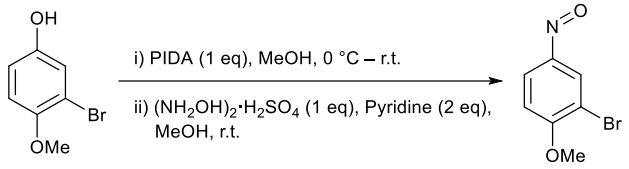

SI-8 **32**

2-Bromo-1-methoxy-4-nitrosobenzene (32): Obtained using General Procedure **C** from **SI-8** giving **32** (59%). The second step required 29 hr to react to completion. Spectral data matched that of literature reported data.[52] ^{1}H NMR (400 MHz, $CDCl_3$) δ 8.31 (br. d, *J* = 8.2 Hz, 1 H), 7.73 (s, 1 H), 7.11 (d, *J* = 9.0 Hz, 1 H), 4.03 (s, 3 H) ppm; ^{13}C NMR (100 MHz, $CDCl_3$) δ 162.7, 161.4, 127.5, 122.9, 113.3, 110.9, 57.0 ppm; HRMS (EI) Exact mass cald. for $C_7H_6BrNO_2$ $[M]^+$: 214.9582, found: 214.9584.

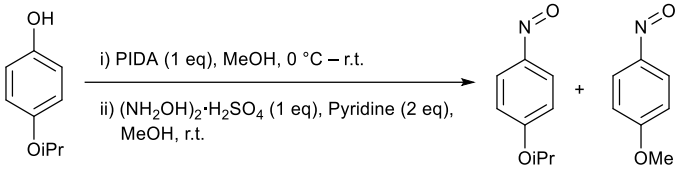

SI-9 **34** **27**

1-Isopropoxy-4-nitrosobenzene (34) and 1-methoxy-4-nitrosobenzene (27): Obtained using General Procedure **C** from **SI-9** giving a mixture of **34** (47%)[51] and **27** (9%). Spectral data matched that of literature reported data for **34**. ^{1}H NMR (500 MHz, $CDCl_3$) δ 7.91 (br. s., 2 H, overlaps with **27**), 6.98 (d, *J* = 9.3 Hz, 2 H), 4.74 (spt, *J* = 6.1 Hz, 1 H), 1.41 (d, *J* = 6.2 Hz, 6 H) ppm; ^{13}C NMR (125 MHz, $CDCl_3$) δ 164.3, 163.9, 124.4, 115.0, 71.0, 21.9 ppm.

5.5 References

(1) St. Amant, A. H.; Frazier, C. P.; Newmeyer, B.; Fruehauf, K. R.; de Alaniz, J. R.; Amant, A. H. S.; Frazier, C. P.; Newmeyer, B.; Fruehauf, K. R.; de Alaniz, J. R. Direct Synthesis of Anilines and Nitrosobenzenes from Phenols. *Org. Biomol. Chem.* **2016**, *14* (24), 5520–5524.

(2) Travis, A. S. Manufacture and Uses of the Anilines: A Vast Array of Processes and Products. In *PATAI'S Chemistry of Functional Groups*; John Wiley & Sons, Ltd, 2009.

(3) Downing, R. S.; Kunkeler, P. J.; van Bekkum, H. Catalytic Syntheses of Aromatic Amines. *Catal. Today* **1997**, *37* (2), 121–136.

(4) Kahl, T.; Schröder, K.-W.; Lawrence, F. R.; Marshall, W. J.; Höke, H.; Jäckh, R. Aniline. In *Ullmann's Encyclopedia of Industrial Chemistry*; Wiley-VCH Verlag GmbH & Co. KGaA, 2000.

(5) Scherrer, R. A.; Beatty, H. R. General Conversion of Phenols to Anilines. *J. Org. Chem.* **1972**, *37* (11), 1681–1686.

(6) Rossi, R. A.; Bunnett, J. F. General Conversion of Phenols to Anilines. *J. Org. Chem.*

1972, *37* (22), 3570–3570.

(7) Mizuno, M.; Yamano, M. A New Practical One-Pot Conversion of Phenols to Anilines. *Org. Lett.* **2005**, *7* (17), 3629–3631.

(8) Truce, W. E.; Kreider, E. M.; Brand, W. W. The Smiles and Related Rearrangements of Aromatic Systems. In *Organic Reactions*; John Wiley & Sons, Inc., 2004.

(9) Taylor, E. C.; Jagdmann, G. E.; McKillop, A. Thallium in Organic Synthesis. 53. Simple Procedures for the Replacement of a Phenolic OH Group by N = NAr, N = O, H, NH2, and C Substituents. *J. Org. Chem.* **1978**, *43* (22), 4385–4387.

(10) Veits, G. K.; Wenz, D. R.; Read de Alaniz, J. Versatile Method for the Synthesis of 4-Aminocyclopentenones: Dysprosium(III) Triflate Catalyzed Aza-Piancatelli Rearrangement. *Angew. Chemie Int. Ed.* **2010**, *49* (49), 9484–9487.

(11) Palmer, L. I.; Read de Alaniz, J. Direct and Highly Diastereoselective Synthesis of Azaspirocycles by a Dysprosium(III) Triflate Catalyzed Aza-Piancatelli Rearrangement. *Angew. Chemie Int. Ed.* **2011**, *50* (31), 7167–7170.

(12) Wenz, D. R.; Read de Alaniz, J. Aza-Piancatelli Rearrangement Initiated by Ring Opening of Donor–Acceptor Cyclopropanes. *Org. Lett.* **2013**, *15* (13), 3250–3253.

(13) Yu, D.; Thai, V. T.; Palmer, L. I.; Veits, G. K.; Cook, J. E.; Read de Alaniz, J.; Hein, J. E. Importance of Off-Cycle Species in the Acid-Catalyzed Aza-Piancatelli Rearrangement. *J. Org. Chem.* **2013**, *78* (24), 12784–12789.

(14) Moriarty, R. M.; Om, P. Oxidation of Phenolic Compounds with Organohypervalent Iodine Reagents. In *Organic Reactions*; John Wiley & Sons, Inc., 2004.

(15) Biljan, I.; Cvjetojevic, G.; Smrecki, V.; Novak, P.; Mali, G.; Plavec, J.; Babic, D.; Mihalic, Z.; Vancik, H. Nitrosobenzene Cross-Dimerization: Structural Selectivity in

Solution and in Solid State. *J. Mol. Struct.* **2010**, *979* (1–3), 22–26.

(16) Doherty, G. A.; Yang, G. X.; Borges, E.; Tong, S.; McCauley, E. D.; Treonz, K. M.; Van Riper, G.; Pacholok, S.; Si, Q.; Koo, G. C.; et al. N-Isonicotinoyl-(l)-4-Aminophenylalanine Derivatives as Tight Binding VLA-4 Antagonists. *Bioorg. Med. Chem. Lett.* **2003**, *13* (11), 1891–1895.

(17) Hoppmann, C.; Schmieder, P.; Heinrich, N.; Beyermann, M. Photoswitchable Click Amino Acids: Light Control of Conformation and Bioactivity. *ChemBioChem* **2011**, *12* (17), 2555–2559.

(18) Fisher, D. J.; Burnett, G. L.; Velasco, R.; Read de Alaniz, J. Synthesis of Hindered α-Amino Carbonyls: Copper-Catalyzed Radical Addition with Nitroso Compounds. *J. Am. Chem. Soc.* **2015**, *137* (36), 11614–11617.

(19) Fisher, D. J.; Shaum, J. B.; Mills, C. L.; Read de Alaniz, J. Synthesis of Hindered Anilines: Three-Component Coupling of Arylboronic Acids, Tert-Butyl Nitrite, and Alkyl Bromides. *Org. Lett.* **2016**, *18* (19), 5074–5077.

(20) Mori, T.; Grimme, S.; Inoue, Y. A Combined Experimental and Theoretical Study on the Conformation of Multiarmed Chiral Aryl Ethers. *J. Org. Chem.* **2007**, *72* (18), 6998–7010.

(21) Eisch, J. J.; Galle, J. E.; Piotrowski, A.; Tsai, M. R. Rearrangement and Cleavage of [(Aryloxy)Methyl]Silanes by Organolithium Reagents: Conversion of Phenols into Benzylic Alcohols. *J. Org. Chem.* **1982**, *47* (26), 5051–5056.

(22) Chang, J.; Wang, S.; Shen, Z.; Huang, G.; Zhang, Y.; Zhao, J.; Li, C.; Fan, F.; Song, C. Ethylene Glycol as Hydrogen Donor for the Syntheses of Thymol Analogues via Hydrolysis of 4-Methylcoumarins. *Tetrahedron Lett.* **2012**, *53* (50), 6755–6757.

(23) Punna, S.; Meunier, S.; Finn, M. G. A Hierarchy of Aryloxide Deprotection by Boron Tribromide. *Org. Lett.* **2004**, *6* (16), 2777–2779.

(24) Nakamura, R.; Obora, Y.; Ishii, Y. Selective One-Pot Synthesis of Various Phenols from Diarylethanes. *Chem. Commun.* **2008**, No. 29, 3417–3419.

(25) Vyvyan, J. R.; Loitz, C.; Looper, R. E.; Mattingly, C. S.; Peterson, E. A.; Staben, S. T. Synthesis of Aromatic Bisabolene Natural Products via Palladium-Catalyzed Cross-Couplings of Organozinc Reagents†. *J. Org. Chem.* **2004**, *69* (7), 2461–2468.

(26) Chuang, K. V; Navarro, R.; Reisman, S. E. Benzoquinone-Derived Sulfinyl Imines as Versatile Intermediates for Alkaloid Synthesis: Total Synthesis of (-)-3-Demethoxyerythratidinone. *Chem. Sci.* **2011**, *2* (6), 1086–1089.

(27) Zhu, X.; Plunkett, K. N. Controlled Regioregularity in Oligo(2-Methoxy-5-(2′-Ethylhexyloxy)-1,4-Phenylenevinylenes. *J. Org. Chem.* **2014**, *79* (15), 7093–7102.

(28) Gu, Y. G.; Weitzberg, M.; Clark, R. F.; Xu, X.; Li, Q.; Zhang, T.; Hansen, T. M.; Liu, G.; Xin, Z.; Wang, X.; et al. Synthesis and Structure−Activity Relationships of N-{3-[2-(4-Alkoxyphenoxy)Thiazol-5-Yl]-1- Methylprop-2-Ynyl}carboxy Derivatives as Selective Acetyl-CoA Carboxylase 2 Inhibitors. *J. Med. Chem.* **2006**, *49* (13), 3770–3773.

(29) Sajiki, H.; Hirota, K. Pd/C-Catalyzed Chemoselective Hydrogenation in the Presence of a Phenolic MPM Protective Group Using Pyridine as a Catalyst Poison. *Chem. Pharm. Bull. (Tokyo).* **2003**, *51* (3), 320–324.

(30) Dichiarante, V.; Salvaneschi, A.; Protti, S.; Dondi, D.; Fagnoni, M.; Albini, A. The β Effect of Silicon in Phenyl Cations. *J. Am. Chem. Soc.* **2007**, *129* (51), 15919–15926.

(31) Belyanin, M. L.; Stepanova, E. V; Ogorodnikov, V. D. First Total Chemical Synthesis

of Natural Acyl Derivatives of Some Phenolglycosides of the Family Salicaceae. *Carbohydr. Res.* **2012**, *363*, 66–72.

(32) Maddani, M. R.; Moorthy, S. K.; Prabhu, K. R. Chemoselective Reduction of Azides Catalyzed by Molybdenum Xanthate by Using Phenylsilane as the Hydride Source. *Tetrahedron* **2010**, *66* (1), 329–333.

(33) Zou, Q.; Wang, C.; Smith, J.; Xue, D.; Xiao, J. Alkylation of Amines with Alcohols and Amines by a Single Catalyst under Mild Conditions. *Chem. – A Eur. J.* **2015**, *21* (27), 9656–9661.

(34) Jiang, L.; Lu, X.; Zhang, H.; Jiang, Y.; Ma, D. CuI/4-Hydro-l-Proline as a More Effective Catalytic System for Coupling of Aryl Bromides with N-Boc Hydrazine and Aqueous Ammonia. *J. Org. Chem.* **2009**, *74* (12), 4542–4546.

(35) WO, 030469, 2009.

(36) Bartoli, G.; Bosco, M.; Dal Pozzo, R.; Petrini, M. One-Pot Chemoselective Reductive Alkylation of Nitroarenes: A New General Method of Synthesis of Alkylanilines. *Tetrahedron* **1987**, *43* (18), 4221–4226.

(37) Cheemala, M. N.; Knochel, P. New P,N-Ferrocenyl Ligands for the Asymmetric Ir-Catalyzed Hydrogenation of Imines. *Org. Lett.* **2007**, *9* (16), 3089–3092.

(38) Knölker, H.-J.; Bauermeister, M.; Pannek, J.-B.; Wolpert, M. Transition Metal-Diene Complexes in Organic Synthesis, Part 22.The Iron-Mediated Quinone Imine Cyclization: A General Route to 3-Hydroxycarbazoles. *Synthesis (Stuttg).* **1995**, *1995* (04), 397–408.

(39) Http://Sdbs.Db.Aist.Go.Jp/Sdbs/Cgi-Bin/Direct_frame_disp.Cgi?Sdbsno=21784 (National Institute of Advanced Industrial Science and Technology, Accessed on

November 30, 2015).

(40) Mitchell, H.; Leblanc, Y. Amination of Arenes with Electron-Deficient Azodicarboxylates. *J. Org. Chem.* **1994**, *59* (3), 682–687.

(41) Cantillo, D.; Baghbanzadeh, M.; Kappe, C. O. In Situ Generated Iron Oxide Nanocrystals as Efficient and Selective Catalysts for the Reduction of Nitroarenes Using a Continuous Flow Method. *Angew. Chemie Int. Ed.* **2012**, *51* (40), 10190–10193.

(42) Okuyama, M.; Laman, H.; Kingsbury, S. R.; Visintin, C.; Leo, E.; Eward, K. L.; Stoeber, K.; Boshoff, C.; Williams, G. H.; Selwood, D. L. Small-Molecule Mimics of an [Alpha]-Helix for Efficient Transport of Proteins into Cells. *Nat Meth* **2007**, *4* (2), 153–159.

(43) Shen, Q.; Hartwig, J. F. Palladium Catalyzed Coupling of Ammonia and Lithium Amide with Aryl Halides. *J. Am. Chem. Soc.* **2006**, *128* (31), 10028–10029.

(44) Buckingham, F.; Calderwood, S.; Checa, B.; Keller, T.; Tredwell, M.; Collier, T. L.; Newington, I. M.; Bhalla, R.; Glaser, M.; Gouverneur, V. Oxidative Fluorination of N-Arylsulfonamides. *J. Fluor. Chem.* **2015**, *180*, 33–39.

(45) Schulze Isfort, C.; Kreickmann, T.; Pape, T.; Fröhlich, R.; Hahn, F. E. Helical Complexes Containing Diamide-Bridged Benzene-o-Dithiolato/Catecholato Ligands. *Chem. – A Eur. J.* **2007**, *13* (8), 2344–2357.

(46) Stylianides, N.; Danopoulos, A. A.; Pugh, D.; Hancock, F.; Zanotti-Gerosa, A. Cyclometalated and Alkoxyphenyl-Substituted Palladium Imidazolin-2-Ylidene Complexes. Synthetic, Structural, and Catalytic Studies. *Organometallics* **2007**, *26* (23), 5627–5635.

(47) Kim, J. H.; Park, J. H.; Chung, Y. K.; Park, K. H. Ruthenium Nanoparticle-Catalyzed, Controlled and Chemoselective Hydrogenation of Nitroarenes Using Ethanol as a Hydrogen Source. *Adv. Synth. Catal.* **2012**, *354* (13), 2412–2418.

(48) Cui, H.; Carrero-Lérida, J.; Silva, A. P. G.; Whittingham, J. L.; Brannigan, J. A.; Ruiz-Pérez, L. M.; Read, K. D.; Wilson, K. S.; González-Pacanowska, D.; Gilbert, I. H. Synthesis and Evaluation of α-Thymidine Analogues as Novel Antimalarials. *J. Med. Chem.* **2012**, *55* (24), 10948–10957.

(49) Cheung, C. W.; Surry, D. S.; Buchwald, S. L. Mild and Highly Selective Palladium-Catalyzed Monoarylation of Ammonia Enabled by the Use of Bulky Biarylphosphine Ligands and Palladacycle Precatalysts. *Org. Lett.* **2013**, *15* (14), 3734–3737.

(50) Servinis, L.; Henderson, L. C.; Andrighetto, L. M.; Huson, M. G.; Gengenbach, T. R.; Fox, B. L. A Novel Approach to Functionalise Pristine Unsized Carbon Fibre Using in Situ Generated Diazonium Species to Enhance Interfacial Shear Strength. *J. Mater. Chem. A* **2015**, *3* (7), 3360–3371.

(51) Prakash, G. K. S.; Gurung, L.; Schmid, P. C.; Wang, F.; Thomas, T. E.; Panja, C.; Mathew, T.; Olah, G. A. Ipso-Nitrosation of Arylboronic Acids with Chlorotrimethylsilane and Sodium Nitrite. *Tetrahedron Lett.* **2014**, *55* (12), 1975–1978.

(52) Bosch, E.; Kochi, J. K. Direct Nitrosation of Aromatic Hydrocarbons and Ethers with the Electrophilic Nitrosonium Cation. *J. Org. Chem.* **1994**, *59* (19), 5573–5586.

6 Towards a Total Synthesis of (±)-Desmethoxy Cephalotaxine using the Aza-Piancatelli Reaction

6.1 Introduction

Omacetaxine mepesuccinate **1** (OM, or homoharringtonine), an ester of cephalotaxine **2**, is an FDA approved compound for the treatment of chronic myeloid leukemia (**Figure 6.1**). The compound is naturally occurring in the *Cephalotaxus* genus, where it was first isolated.[1] On a large scale, OM is made through a semisynthesis beginning from naturally derived cephalotaxine.[2] The complexity of cephalotaxine's five fused rings and its medicinal importance has led to over 30 formal and total syntheses, racemic and stereospecific, over the past 40 years.

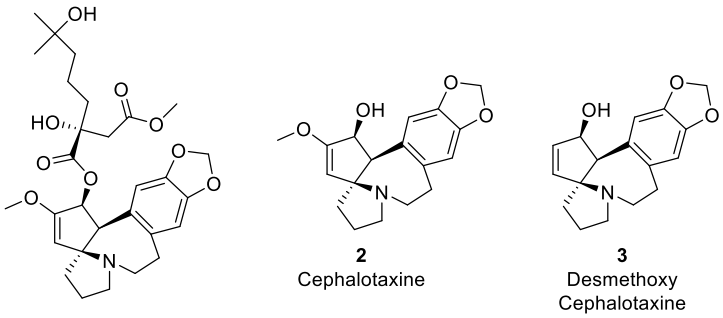

Figure 6.1 Cephalotaxine and related structures.

While cephalotaxine is biologically inactive, esters have been synthesized and tested for antitumour properties, with OM being the best candidate.[3] However, a structure activity relationship (SAR) for the cephalotaxine core has not been examined, presumably due to the amount of synthetic effort each modification would require.

We wanted to apply aza-Piancatelli chemistry our group has developed[4] towards the synthesis of (±)-desmethoxy cephalotaxine **(±)-3**, a previously undescribed compound. The

methoxy group of OM sits outside of the drug's binding pocket and doesn't appear to make positive interactions with the ribosome (**Figure 6.2**);[5] removing it will increase our understanding of OM's action and could impart better antitumour properties.

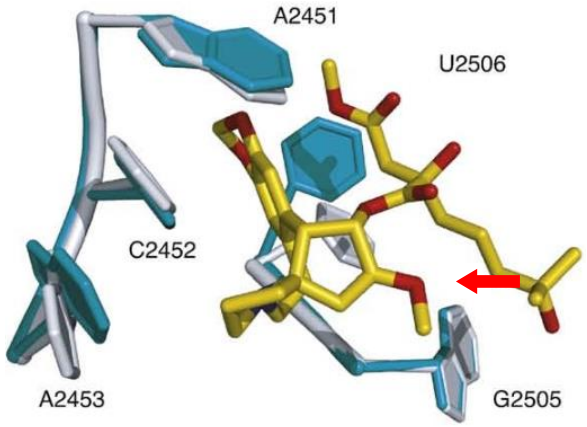

Figure 6.2 Crystal structure of OM in binding pocket of ribosome. Apo conformation in grey, drug-bound conformation in cyan. Figure reproduced (Gürel, 2009), the methoxy group is indicated with an arrow.

6.2 Retrosynthetic Analysis

The spirocyclic core in cephalotaxine is similar to the products of the tethered aza-Piancatelli rearrangement developed in our laboratory,[6] which we sought out to use in the synthesis of **(±)-3**. Our retrosynthesis (**Figure 6.3**) relies on the manipulation of the N-O bond in compound **4**, which can be traced back to the aryliodide **5** using chemistry developed by Semmelhack.[7] The spirocycle **5** will be synthesized through the aza-Piancatelli rearrangement of furan **6**. Using a tethered hydroxylamine as a nucleophile, the reaction would follow the Piancatelli rearrangement mechanism: leaving group formation of oxonium **7a**, nucleophilic attack to form **7b**, the opening of furan **7c**, and the 4π electron conrotatory Nazarov cyclization of **7d**.

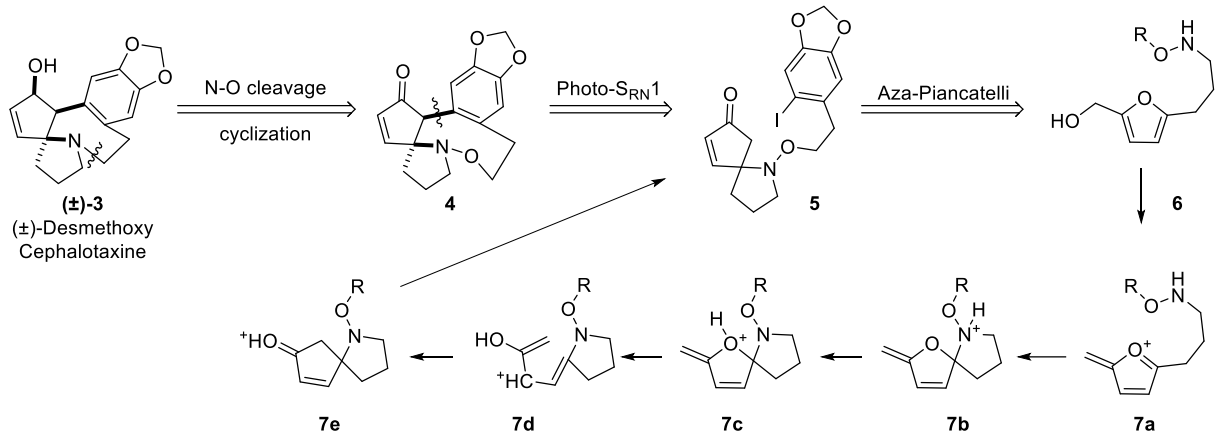

Figure 6.3 The retrosynthesis of (±)-demethoxy cephalotaxine and the mechanism of the aza-Piancatelli rearrangement mechanism.

6.3 Results and Discussion

We began the synthesis of the furan/aldehyde portion **11** (**Figure 6.4**) from **8**,[8] which was produced through the formylation of the inexpensive flavouring agent ethyl 2-furanpropionate (which smells like the trees north of Phelps Hall). Protecting the aldehyde as the dimethyl or diethyl acetal was not stable in the later steps, so **8** was protected as dioxolane **9**. After LAH reduction and DMP oxidation, aldehyde **11** was obtained.

The aromatic/hydroxylamine component (**17**) was synthesized from 3,4-(methylenedioxy) phenylacetic acid **12**. The acid was reduced with LAH and the aromatic ring was iodinated to produce the alcohol **14**. The alcohol was mesylated and displaced with the protected hydroxylamine *N*-hydroxyphthalimide to produce **16**. After deprotection with hydrazine, *O*-substituted hydroxylamine **17** was produced. The condensation of **11** and **17** in MeOH proceeded quickly, but the reduction with $NaCNBH_3$, HCl, and methyl orange (as an indicator) unexpectedly reduced the protected acetal. The acid may have protonated the acetal to produce a furan-stabilized carbocation that underwent reduction to ether **18**. If the acetal had survived the reductive amination, we would deprotect/reduce the acetal to the alcohol; with ether **18** in hand we attempted to develop aza-Piancatelli reaction conditions that would

be suitable. When the reduction was performed on small scale in MeOH a mixture of **18** and the methyl ether was obtained; when the reaction was scaled up, the solvent was changed to ethylene glycol to avoid production of the methyl ether and obtain a better yield of **18**.

Following the synthetic route described we could access hundreds of milligrams of **18**. Unfortunately, despite a number of Lewis acid conditions screened, we have not been able to successfully demonstrate the aza-Piancatelli rearrangement on this advanced substrate. In most cases the starting material was recovered or the hydroxylamine decomposed to aldehyde **19**. This was surprising because we have previously shown that *O*-protected hydroxylamines are good nucleophiles for the aza-Piancatelli rearrangement.[4] Due to the instability of the N-O bond it was clear we had to revaluate our synthesis.

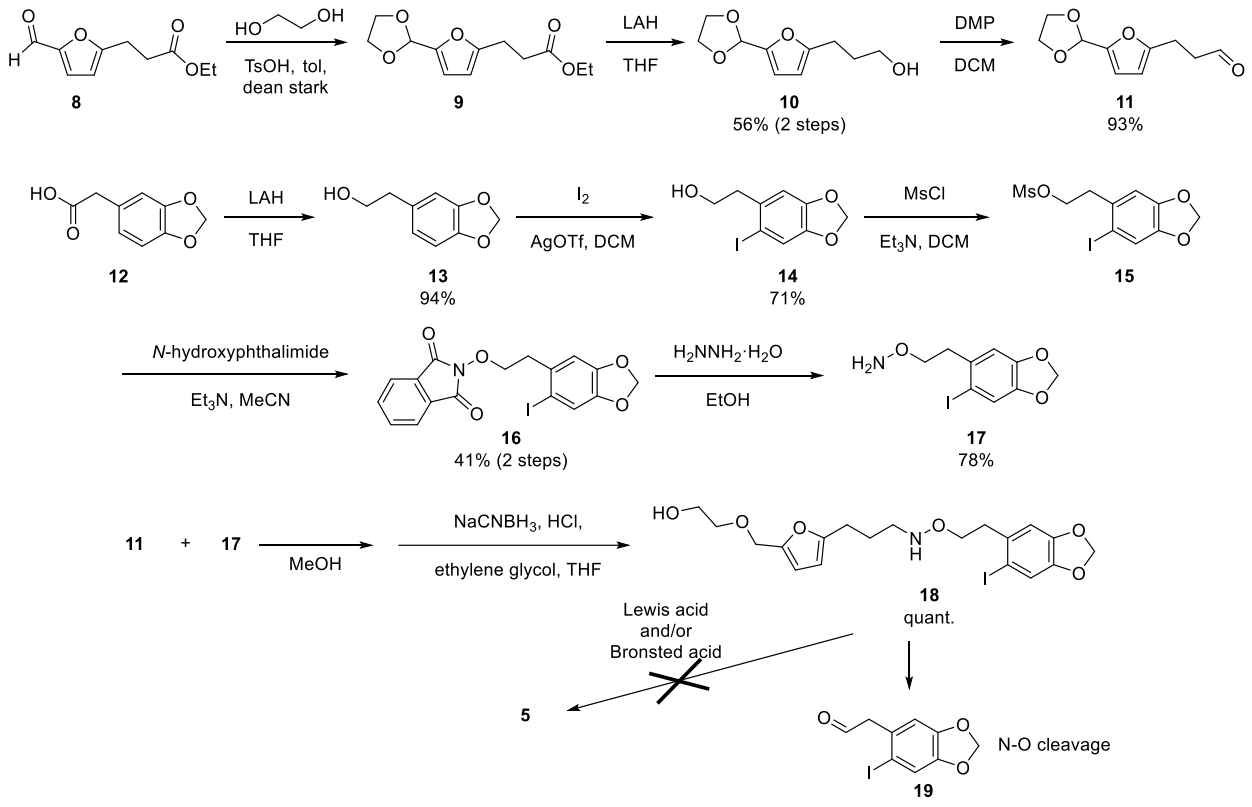

Figure 6.4 First generation attempt at the synthesis of desmethoxy cephalotaxine.

Unpublished results in our laboratory suggested a secondary amine could also be used as a nucleophile when tethered to the furan. The replacement of the hydroxylamine with the secondary amine (**20**, **Figure 6.5**) would be ideal, as an N-O bond cleavage to aldehyde **19** would not be possible. Before beginning the lengthy synthesis of compound **20**, the model compound **21** was synthesized to test the aza-Piancatelli reaction with the tethered secondary amine. Several conditions were attempted but the spirocyclic cyclopentenone **22** was not produced, yielding either starting material or decomposition of the furan. Primary furylcarbinols are less reactive than aryl substituted compounds and more prone to side reactions, and while working on this reaction in 2015, optimized conditions eluded us. This reactivity was later disclosed in 2017 by the Jiang group where, rather than using a Lewis acid catalyst, they used Mitsunobu-like conditions (PPh_3, DEAD).[9] We believe these conditions could be applied towards the synthesis of desmethoxy cephalotaxine, but this line of reactivity was not pursued further.

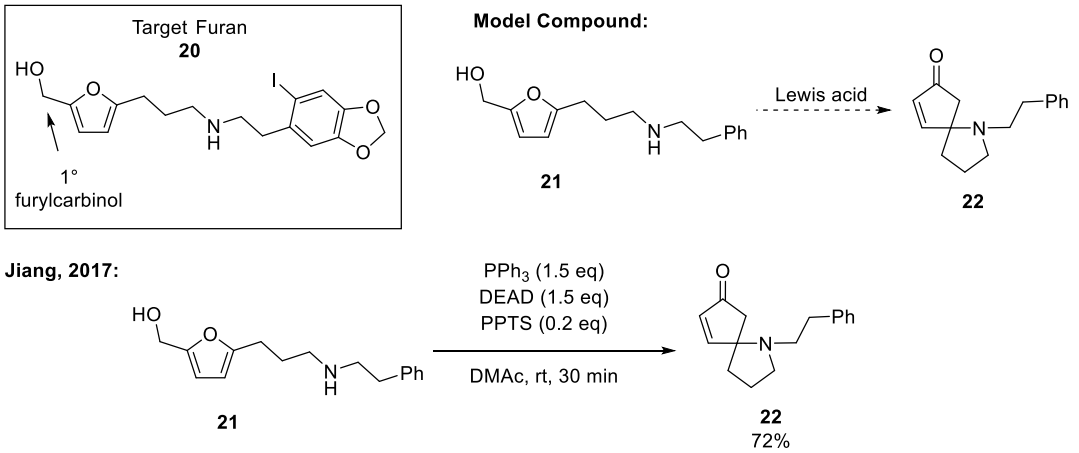

Figure 6.5 Target furan for the second generation synthesis of (±)-desmethoxy cephalotaxine, its model compound, and Jiang's conditions.

Before the disclosure of Jiang's Mitsunobu-like conditions, one more attempt was made towards the synthesis of **3**. As previously mentioned, at the time of our attempts, 1° furylcarbinols were poor substrates for the aza-Piancatelli rearrangement and their yields were

modest. One way to circumvent this problem is to use an aryl-substituted furylcarbinol, which led us to the third synthetic scheme using macrocycle **29** (**Figure 6.6**). Aryl substitution on the furylcarbinol typically gives better yields in the aza-Piancatelli rearrangement compared to unsubstituted or alkyl substituted analogues, possibly through the stabilization of the carbocation intermediates. The aza-Piancatelli rearrangement within a macrocycle has no precedent, but if conditions could be developed it would streamline the synthesis of the aza-spirocycle **30**, which only requires a simple 1,2-reduction to yield (±)-desmethoxy cephalotaxine (**3**). The synthesis of **30** began with the benzyl protection of homopiperonylamine (**23**). The Duff reaction was used to formylate **24** in low yield. 2-Furanpropanol, obtained from the LAH reduction of ethyl 2-furanpropionate, was dilithiated (**26**) and added into the aldehyde **25**. The primary alcohol was mesylated to **28**, but attempts to deprotect the dibenzyl amine proceeded in very low yields with Pd/C and Pearlman's catalyst, and the advanced intermediate **28** was depleted. If deprotection and macrocyclization conditions could be developed, the aza-Piancatelli rearrangement within a macrocycle to produce **30** could be explored.

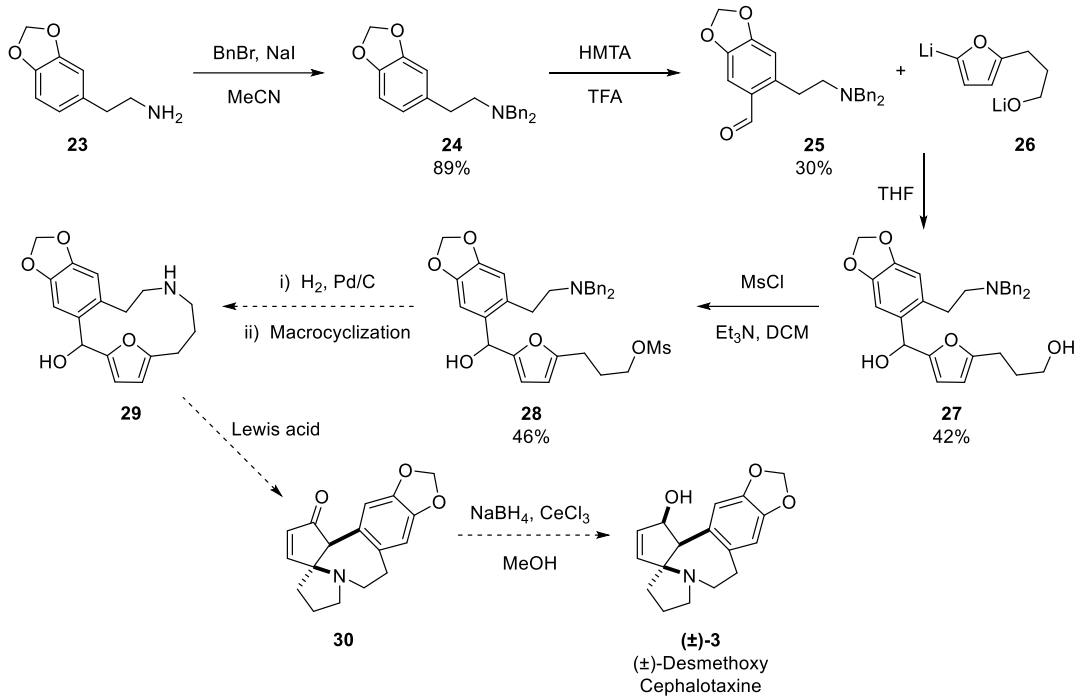

Figure 6.6 Third generation synthesis towards (±)-desmethoxy cephalotaxine

6.4 Conclusion

When the synthesis of (±)-desmethoxy cephalotaxine is completed, we envision using the chemistry developed to synthesize other cephalotaxine analogues for antitumour studies. The aza-Piancatelli reaction's strengths and limitations were revealed in the course of this synthesis, allowing it to be used more effectively in the future.

6.5 References

(1) Paudler, W. W.; Kerley, G. I.; McKay, J. The Alkaloids of Cephalotaxus Drupacea and Cephalotaxus Fortunei. *J. Org. Chem.* **1963**, *28* (9), 2194–2197.

(2) Ding, H. X.; Leverett, C. A.; Kyne Jr, R. E.; Liu, K. K. C.; Sakya, S. M.; Flick, A. C.; O'Donnell, C. J. Synthetic Approaches to the 2012 New Drugs. *Bioorg. Med. Chem.* **2014**, *22* (7), 2005–2032.

(3) Mikolajczak, K. L.; Smith, C. R.; Weisleder, D. Synthesis of Cephalotaxine Esters and Correlation of Their Structures with Antitumor Activity. *J. Med. Chem.* **1977**, *20* (3),

328–332.

(4) Veits, G. K.; Wenz, D. R.; Palmer, L. I.; Amant, A. H. S.; Hein, J. E.; de Alaniz, J. R. Cascade Rearrangement of Furylcarbinols with Hydroxylamines: Practical Access to Densely Functionalized Cyclopentane Derivatives. *Org. Biomol. Chem.* **2015**, *13* (31), 8465–8469.

(5) Gürel, G.; Blaha, G.; Moore, P. B.; Steitz, T. A. U2504 Determines the Species Specificity of the A-Site Cleft Antibiotics:: The Structures of Tiamulin, Homoharringtonine, and Bruceantin Bound to the Ribosome. *J. Mol. Biol.* **2009**, *389* (1), 146–156.

(6) Palmer, L. I.; Read de Alaniz, J. Direct and Highly Diastereoselective Synthesis of Azaspirocycles by a Dysprosium(III) Triflate Catalyzed Aza-Piancatelli Rearrangement. *Angew. Chemie Int. Ed.* **2011**, *50* (31), 7167–7170.

(7) Semmelhack, M. F.; Chong, B. P.; Stauffer, R. D.; Rogerson, T. D.; Chong, A.; Jones, L. D. Total Synthesis of the Cephalotaxus Alkaloids. Problem in Nucleophilic Aromatic Substitution. *J. Am. Chem. Soc.* **1975**, *97* (9), 2507–2516.

(8) Zhu, L.; Song, L.; Tong, R. Diastereoselective Reductive Ring Expansion of Spiroketal Dihydropyranones to Cis-Fused Bicyclic Ethers. *Org. Lett.* **2012**, *14* (23), 5892–5895.

(9) Xu, Z.-L.; Xing, P.; Jiang, B. Intramolecular Aza-Piancatelli Rearrangement of Alkyl- or Arylamines Promoted by PPh3/Diethyl Azodicarboxylate. *Org. Lett.* **2017**, *19* (5), 1028–1031.